Investigation of macrophages response to infection with Crohn's disease associated Adherent-invasive *Escherichia coli*

Xiang Li

BSc, MSc

A thesis submitted to the University of Glasgow for the degree of Doctor of Philosophy (PhD)

School of infection and immunity
College of Medical, Veterinary and Life Sciences
University of Glasgow
Glasgow
G12 8QQ

September, 2022

Abstract

Adherent-invasive *Escherichia coli* (AIEC) have been implicated in the aetiology of Crohn's Disease (CD). CD is believed to be caused by a complex interaction between genetics, microbiome, the immune system and the environment. AIEC are characterised by an ability to survive and replicate intracellularly in macrophages with increased secretion of pro-inflammatory cytokines, which may contribute to further dissemination of the pathogen. Bacterial persistence within cells is thought to lead to immune evasion and chronicity of infections. Understanding the maintenance of AIEC in macrophages may elucidate methods of targeting AIEC colonization as a potential therapeutic intervention strategy for patients with CD.

A histopathological hallmark of CD is aggregation of intestinal macrophages, referred to as granulomas, which may result from fusion of monocytes and macrophages giving rise to the formation of multinucleated giant cells (MGCs). However, cell-cell interactions are highly heterogeneous. Therefore, image-based technologies such as imaging flow cytometry (IFC) and fluorescent microscopy were employed on macrophages during AIEC infection. IFC employs a traditional flow cytometer equipped with a fluorescent camera capable of imaging over different wavelengths. With real high-resolution images of AIEC-infected macrophages, images of mono- and bi-nucleated cells as well as polynucleated cells were observed. In addition, the morphologic features and of cell-cell interaction could be monitored. As a result, significantly more multi-nucleated cells were found in AIEC-infected macrophages when compared to uninfected macrophages. AIEC infection induced an enhanced connection between cells as a result of increased cellular adhesion, phagocytosis, and cell fusion. Therefore, it is possible that the formation of MGCs may result from phagocytosis or cell fusion.

The use of IFC for examining host-pathogen interactions is well established, so we applied it to identifying the role of specific host proteins in bacterial infection. Little is known about how macrophage-killing of AIEC is impeded. We used an *in vitro* infection model to identify macrophage proteins associated with AIEC intracellular replication. Phosphorylated proline-rich tyrosine kinase 2 (p-PYK2) levels were identified as being significantly altered during AIEC infection.

The pPyk2 inhibitor PF-431396 significantly decreased intramacrophage replication of AIEC as determined by viable colony count, fluorescence immunostaining and imaging flow cytometry. Meanwhile, Pyk2 inhibition also decreased TNFα secretion from AIEC-infected macrophages. Pyk2 has previously been identified as a risk locus in inflammatory bowel diseases through genome-wide association studies and is overexpressed in patients with intestinal and colorectal cancer (CRC), the latter a major long-term complication of CD. In this thesis, we have outlined that Pyk2 inhibition could be a potential strategy for CD treatment via controlling intracellular AIEC levels within macrophages.

To better understand host-pathogen interactions, it is important to take into account the extreme heterogeneity of the host response after an infection. Infection is a dynamic process and modelling the outcomes of the infectious process has always proved challenging. Using an *in vitro* infection model, IFC found that less than 50% of RAW 264.7 cells were actually infected by AIEC strain LF82 after 24 hours. In this thesis, using high-throughput RNA-sequencing combined with FACS sorting, infected cells from these heterogeneous populations were sorted into populations based on their intracellular pathogen burden. This allowed a greater understanding of what benefit AIEC bacteria could gain from resisting killing by mucosal macrophages and to what extent the expression of host gene expression affects AIEC intramacrophage replication. Based on this transcriptomic analysis of infected macrophages, I identified specific chemical inhibitors targeting proteins identified as highly expressed in infected cells with heavy bacterial burdens. The ubiquitin E3 ligase Itch, involved in the ubiquitin-proteasome system, was targeted by the drug clomipramine significantly reducing intracellular bacterial burden in macrophages. This finding suggests the possibility that AIEC could manipulate the ubiquitin-proteasome system during infection, allowing AIEC to survive within macrophages.

The discovery of potent chemical inhibitors, identified as targeting proteins with a novel role in AIEC infection, will hopefully open up new avenues of research and opportunities for the development of new intervention strategies in infection and CD.

Table of Contents

List of Tables

List of Figures

List of Appendices

Acknowledgement

Four-year PhD life seems like a long time, time pasts quickly and I still vividly remember the scene of the first day I started my PhD, and the people I met. The people I met during my 4-year PhD, I am really thankful to.

Dr Dónal Wall, my primary supervisor, I can't imagine how I could finish my PhD on time without your help. You let me run wild and encourage and support every idea I have. When I am not very confident in my research ability, you always tell me I am doing a good job. It is thanks to you that I have gained confidence in my academic journey.

I would like to express my heartfelt thanks to my supervisors Prof Daniel Waller, Dr Michael Ormsby and Dr Damo Xu, for giving me a great deal of support and assistance for my PhD project and for their excellent supervision. I would like to extend my sincere thanks to my assessors Dr Gillian Douce and Prof Andrew Roe for their guidance and research assistance, giving me useful advice in my research area.

Dr Michael Ormsby, your assistance with my experiments has been invaluable. My journey to scientific research was greatly influenced by the lessons you taught me. Dr Khedidja Mosbahi helped me a lot in the research. When I'm having problems, whether at work or at home, I always bother you. You always bring sunshine and joy to my life. Dr Andreas Haag gave me huge assistance, you are a genius, giving me a lot of useful advice for my research field. I appreciate your willingness and your time to answer any of my tiny questions.

My colleagues, Ghaith Fallata and Maya Kamat, we started our PhD at the same year. Throughout 4 years, we experienced joys and sorrows together. I sincerely hope that we can graduate successfully together. Najla Qalit A Alfaqeer, Clio Dritsa, Lauren Adams and Katja Muecklisch, because of you, our office is full of happiness. Deborah Sym, we have benefited from a good experimental environment created by you. I enjoy every time I work out with you and had lunch together.

In the Wall Lab and the bacteriology department, I really enjoyed the time spending with everyone and those who have come and gone over the years.

A big thanks to all of the people who gave me technical assistance over the years. Thank Fiona McMonagle for the histology. A big thank to Diane Vaughan for FACS. Thank Leandro Lemgruber Soares and Susan Gannon in imaging stuff for their guidance and assistance. A special thanks to John Cole for his talented bioinformative skills.

Here, I really appreciate every friend I met in Glasgow. It is you who make life fulfilled with colourful in Glasgow. Whether we develop in different cities in the future, I hope we will remain in touch and share our daily lives. Especially, Ming Lin and Shiqian Wang, are “stumbling blocks” on my way to completing my PhD thesis. Because of them, my wish list for having fun in France Disneyland was fulfilled. Yixin Huang, really grateful to meet you in Glasgow. You are the treasure of my life. Having you by my side has given me huge courage to go through tough times. I look forward to creating more common memories with you in the future.

Special thanks to my friends in China, it has been over fifteen years since we first met in elementary school. More than friends, you are my family. Yinbo and Yuan, I am so lucky to have you in Glasgow! Thank you for putting up with me, spoiling and feeding me. Being with you, I feel like a child never grows up. Finally, the biggest thanks really have to go to my Dad and Mom, who always support my any choices. Thank you for supporting me in my 4-year PhD mentally and finically. It is because of you that I am who I am today! What I really say at here is: I love you!

Author's Declaration

I hereby declare that this thesis is the result of my own work and has been composed for the degree of PhD at the University of Glasgow. This work has not been submitted for any other degree at this or any other institution. All work presented was performed by myself unless otherwise stated. All sources of information and contributions to the work have been specifically acknowledged in the text.

Xiang Li

September 2022

Abbreviations

7-AAD	7-aminoactinomycin D
AP-1	Activator protein 1
AIEC	Adherent invasive *Escherichia coli*
AOPPs	Advanced oxidation protein products
ATCC	American type culture collection
APCs	Antigen-presenting cells
AhR	Aryl hydrocarbon receptor
ATG16L1	Autophagy-related 16-like 1
BMDMs	Bone marrow-derived macrophages
BSA	Bovine serum albumin
CO_2	Carbon dioxide
CEACAM6	Carcinoembryonic antigen-related cell-adhesion molecule 6
CARD9	Caspase recruitment domain-containing protein 9
CCL2	CC-chemokine ligand 2
CCR6	Chemokine receptor 6
CFU	Colony forming units
CD	Crohn's disease
°C	Degrees Celsius
DCs	Dendritic cells
DEGs	Differentially expressed genes
DAEC	Diffusely adherent *E. coli*
DMSO	Dimethyl sulfoxide
DPBS	Dulbecco's Phosphate-Buffered Saline
EAEC	Enteroaggregative *E. coli*
EIEC	Enteroinvasive *E. coli*
EPEC	Enteropathogenic *E. coli*
ETEC	Enterotoxigenic *E. coli*
ELISA	Enzyme linked immunosorbent assay
et al.	*et alios* (and others)
EDTA	Ethylenediaminetetraacetic acid
FFU	Fluorescence focus units
FACS	Fluorescence-activated cell sorting
FP	Fluorescent protein
FCS	Foetal calf serum
FSC	Forward scatter
GO-BP	Gene Ontology-Biological Processes
Gp2	Glycoprotein 2
g	Gram(s)
GFP	Green fluorescent protein
HR	Hazard ratio
h	Hour(s)
Hpi	Hours post infection
HMOs	Human milk oligosaccharides
IL12R	IL12 receptor
IFC	Imaging flow cytometry

IRGM	Immunity-related GTPase M
IBD	Inflammatory bowel diseases
IκBs	Inhibitory κB protein
ILCs	Innate lymphoid cells
IFN-γ	Interferon-gamma
IL	Interleukin
IECs	Intestinal epithelial cells
JAK2	Janus kinase 2
LDH	Lactate dehydrogenase
LRRK2	Leucine-rich repeat kinase 2
LPS	Lipopolysaccharide
LB	Lysogeny-broth
MIP-1α	Macrophage inflammatory protein-1α
MLN	Mesenteric lymph nodes
µg	Microgram
µl	Microlitre
µm	Micrometre
µM	Micromolar
mg	Milligram
MAPK	Mitogen-activated protein kinases
M	Molar
MGCs	Multinucleated giant cells
MOI	Multiplicity of infection
Moi	Multiplicity of infection
MAP	*Mycobacterium avium paratuberculosis*
NLRC4	Nod-like receptor family member 4
NLRs	Nod-like receptors
NF-κB	Nuclear factor kappa B
NOD2	Nucleotide oligomerisation domain 2
OD_{600}	Optical density at 600 nm
OMP	Outer membrane porin
OMVs	Outer membrane vesicles
PFA	Paraformaldehyde
PAMPs	pathogen-associated molecular patterns
PRRs	pattern recognition receptors
PBS	Phosphate-Buffered Saline
pPyk2	Phosphorylation of Pyk2
PCR	Polymerase chain reaction
PVDF	Polyvinylidene fluoride
PCA	Principal component analysis
Pyk2	Proline Tyrosine Kinase 2
RIPA	Radioimmunoprecipitation assay
RT-PCR	Reverse transcriptase polymerase chain reaction
rpm	Revolutions per minute
RIN	RNA integrity numbers
RNA-seq	RNA-sequencing
RMS	Root mean square
RPMI	Roswell Park Memorial Institute 1640 medium

SEM	Scanning electron microscopy
SIgA	Secretory immunoglobulin A
STEC	Shiga toxin-producing *E. coli*
SCFAs	Short-chain fatty acids
SSC	Side scatter
STAT1	Signal transducer and activator of transcription 1
SDS-PAGE	Sodium dodecyl sulphate-polyacrylamide gel electrophoresis
SPON2	Spondin 2
SD	Standard deviation
TH1	T helper 1
TH17	T helper 17
TH2	T helper 2
TLRs	Toll-like receptors
TNF-α	Tumour necrosis factor
FimH	Type 1 pili
UC	Ulcerative colitis
Vat	Vacuolating autotransporter toxin

Chapter 1 General Introduction

1.1 Crohn's Disease

Crohn's disease (CD) was first described by three doctors Burrill Crohn, Leon Ginsberg and Gordon D. Oppenheimer in 1932, as belonging to a major form of distinct chronic relapsing inflammatory intestinal disorders, known as inflammatory bowel diseases (IBD) (Crohn, Ginzburg and Oppenheimer, 1932). IBD consists of two subtypes: ulcerative colitis (UC) and CD and these are characterised by chronic, uncontrolled and relapsing inflammation of the gastrointestinal tract. The prevalence and incidence of CD are on the rise, with the highest frequency in North America, the United Kingdom and northern Europe (Cosnes *et al.*, 2011). Nowadays, it has become a global healthcare problem with a steady increase. Patients with CD most often see symptoms begin in young adulthood and last throughout life (Roda *et al.*, 2020). CD can cause transmural inflammation affecting any part of the gastrointestinal tract in a non-continuous type, predominantly the terminal ileum and adjacent colon, and presents with segmental, asymmetric distribution of granulomatous inflammation (Thia *et al.*, 2010). The main clinical symptoms are chronic diarrhoea often accompanied by abdominal pain, weight loss, faecal blood, and systemic symptoms of different severity in the body (Sands, 2004). About 6.0% of patients have extraintestinal manifestations within the skin, eyes, liver and joints (Bernstein *et al.*, 2001). The pathogenesis of CD reflects a disturbed intestinal mucosal immune system, along with remarkably increased secretion of the pro-inflammatory cytokine tumour necrosis factor (TNF-α) (Brandtzaeg, 2009). Although the definitive causes of CD remain largely unknown, recent research have indicated that a dysregulated immune system, individual's genetic susceptibility, external environment, and an altered intestinal microbial flora are all contributing to risk of disease onset and progression (Figure 1-1) (Torres *et al.*, 2017). Current therapeutic strategies aim for deep and prolonged remission, with the goal of preventing complications and halting the progressive course of disease.

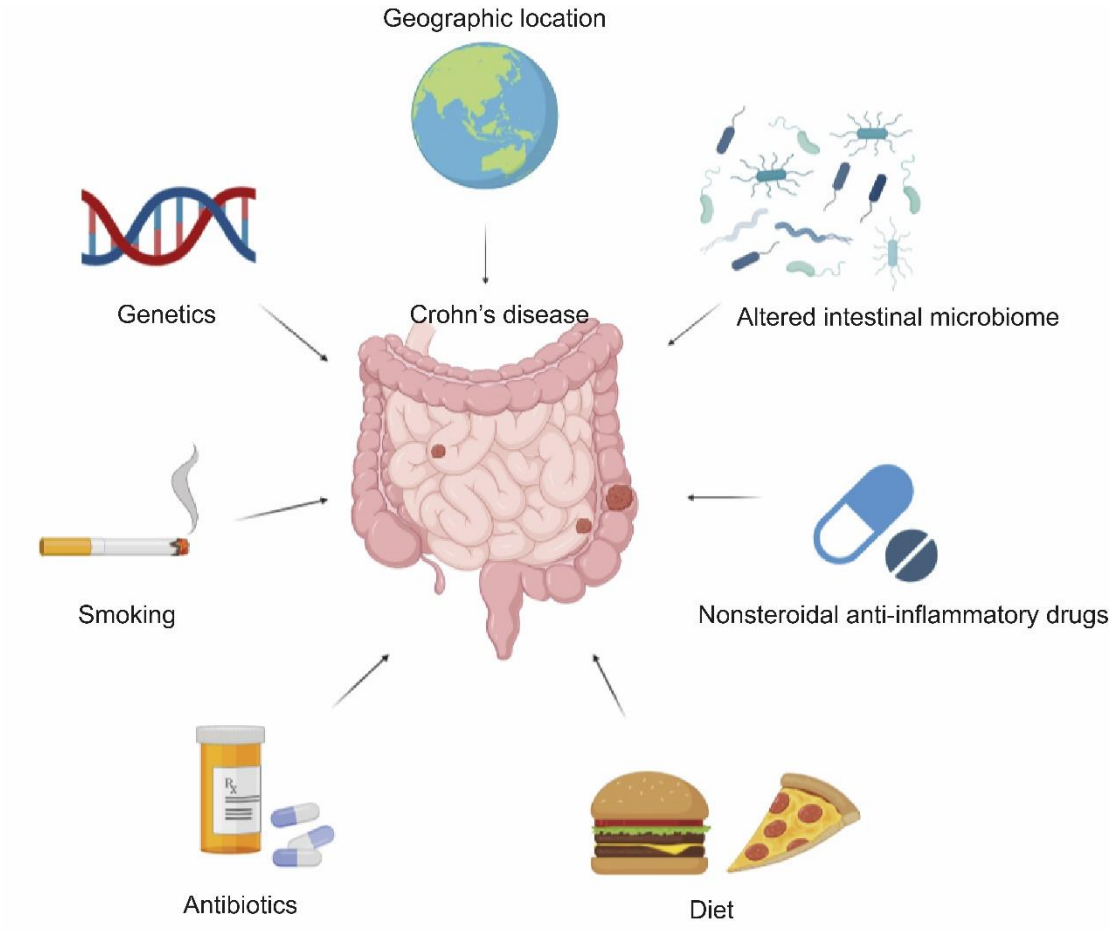

Figure 1-1 Schematic representation of risk factors contributing to CD.

CD develops at the interaction of genetics, dysbiosis of the gut microbiota and environmental influences.

1.1.1 Epidemiology

The prevalence of CD has not been demonstrated to be sex-specific, as 59 CD studies reported the female to male ratio ranged from 0.34 to 1.65 (Molodecky et al., 2012). The age for CD patients presents a bimodal distribution with the highest rate seen in adolescents and young adults ranging from 15 to 30 years old and a second peak in later years occurring at 40 to 60 years old (Cosnes et al., 2011). The incidence of CD differs by region. The higher occurrence of CD in Western countries may indicate that a common etiologic feature exists, with many environmental factors of importance related mainly to a Western lifestyle. CD is more prominent in the industrialised world, particularly in North America, northern Europe and New Zealand. New Zealand has among the highest incidence of CD (16.5 cases per 100,000 people) (Gearry *et al.*, 2006). In the UK, the incidence of CD was 14.3 per 100,000 per year from 2000 to 2018 and was

forecast to increase by 11% by the year 2025 (King *et al.*, 2020). The prevalence of CD has an annual incidence of 0.3 to 12.7 cases per 100,000 in Europe; 0.04 to 5 cases per 100,000 in Asia and the Middle East; and 0 to 20.2 cases per 100,000 in North America (Molodecky *et al.*, 2012). The highest reported prevalence of CD was in Europe (322 cases per 100,000 person in Germany) and North American (319 cases per 100,000 person in Canada) (Bernstein *et al.*, 2006). Since the turn of the twenty-first century, outside of Western countries, CD is increasingly emerging in newly industrialised countries in Asia, Africa and South America in which it had rarely been previously reported (Yang *et al.*, 2000; Sood *et al.*, 2006; Thia *et al.*, 2008). Asia, where some countries are undergoing fast urbanisation, is witnessing an increase in annual incidence of CD (0·54 per 100 000) (Ng *et al.*, 2013). In China, there has been a change in the incidence of CD from being a rare condition to one that requires more hospitalisations (1.4 per 100,000). In South Korea, studies reported an annual incidence increasing from 0.5 per 100,000 between the years of 1986-1990 to 1.3 cases per 100,000 between 2001- 2005.

Epidemiologic studies of migrant populations indicate that genetic and environmental factors interact to determine risk for IBD early in life. The prevalence of IBD in ethnic groups changes with their migration; studies of these changes might lead to identification of environmental factors that contribute to development of CD and UC. A study of IBD in immigrants to Canada found a younger age at time of arrival in Canada increases the risk for development of IBD (Benchimol *et al.*, 2015).

1.1.2 Environmental Factors

Environmental factors for the development of CD are trigged by altered gut microbiome or disruption in the intestinal mucosa, which is related to a large number of environmental factors including geography, diet, lifestyle and exposure to medication.

Smoke

Smoking is a well-recognised risk factor in CD, conferring a two-fold increase in the risk of developing CD (odds ratio [OR] 1.76; 95% confidence interval CI 1.40-

2.22) (Piovani *et al.*, 2019). It is considered a modifiable risk factor for CD, as the effect is attenuated on cessation of smoking (S. Mahid *et al.*, 2006; Higuchi *et al.*, 2012). This risk is increased in both current and former smokers. Although the pathogenic mechanism behind the effect of smoking is yet to be firmly established, it is thought to influence IBD aetiology through epigenetic alterations affecting adaptive immune responses, autophagy and gut microbiota composition, and through immunosuppression.

Diet

The higher frequency of incidence and prevalence of CD emerged in developed countries over the last 15 years indicates a role for environment in disease pathogenesis. As the lifestyle of low-risk countries such as Japan, China and South Keara has become more westernised, the incidence of CD has increased sharply in the last 2 decades (Asakura *et al.*, 2008; Ananthakrishnan, Cagan, *et al.*, 2013). The main characteristics of these changes are; a reduction in dietary fibre, low intake of fruits and vegetables, as well as an increase in saturated fat and sugar intake. A recently published meta-analysis examination identified significant inverse relationships between dietary fibre, fruit and vegetable consumption and risk of CD (Amre *et al.*, 2007; Milajerdi *et al.*, 2021). Research has identified that dietary fibre is beneficial to maintain the intestinal flora and it provides a substrate for bacteria to depolymerise and ferment dietary polysaccharides into host absorbable short-chain fatty acids (SCFAs) such as butyrate, propionate and acetate, which are a primary energy source for colonic epithelial cells (Michaudel and Sokol, 2020). SCFAs exert anti-inflammatory effects by inhibiting nuclear factor kappa B (NF-κB), a proinflammatory transcription factor (Ananthakrishnan, Khalili, *et al.*, 2013). Additionally, fibre intake may reduce translocation of potentially pathogenic bacteria such as the enteroinvasive *Escherichia coli* across M cells stopping development of CD (Roberts *et al.*, 2010). Moreover, dietary fibre may also activate the aryl hydrocarbon receptor (AhR) which is widely expressed in intestinal lymphocytes, influencing formation of intestinal lymphoid follicles and protecting against environmental antigens (Kiss *et al.*, 2011; Monteleone *et al.*, 2012).

Medication exposure

Exposure to medication has been associated with an increased risk of CD. Medications including nonsteroidal anti-inflammatory drugs, antibiotics and oral contraceptive agents have all been implicated in the development of IBD (Ponder and Long, 2013). Nonsteroidal anti-inflammatory drugs are the most commonly used medications for the treatment of various inflammatory conditions. However, the main factor limiting nonsteroidal anti-inflammatory drug use is the concern for the induction of IBD via direct damage to the mucosa of the bowel or reduction in prostaglandin synthesis (Wolfe, Lichtenstein and Singh, 1999; Cipolla *et al.*, 2002). Prostaglandins play a pivotal role in mucosal defence, maintenance of microcirculation and modulation of the immune system in the colon (Wallace, 2008). Studies have also demonstrated that early or recurrent antibiotic use is associated with an increased risk of developing CD. A meta-analysis found that antibiotic exposure in childhood was clearly correlated with primary CD diagnosis (OR 1.74; 95% CI 1.35-2.23) (Ungaro *et al.*, 2014). Another population-based cohort study of children 2 years of age or older from the UK indicated that IBD incidence rates among subjects exposed to antibiotics against anaerobic bacteria antibiotic, compared to unexposed, were 1.52 and 0.83/10000 person-years, respectively, for an 84% relative risk increase (Kronman *et al.*, 2012). Misuse of antibiotics may therefore lead to an imbalance in normal intestinal microbiota, or alternatively, lead to loss of these protective microorganisms and may have a continuous influence on gastrointestinal immune tolerance and sensitivity to pathogens.

Other medications potentially associated with increased risk include oral contraceptives. In two large prospective cohorts studied in the USA published in 2013, when compared with non-users of oral contraceptives, past and current users of oral contraceptives had a higher risk of developing CD (Khalili *et al.*, 2013). The multivariate adjusted hazard ratio (HR) of CD for women who currently used contraceptive was 2.82 (95% CI 1.65 to 4.82), and that for past users was 1.39 (95% CI 1.05 to 1.85) (Khalili *et al.*, 2013). The proposed mechanism of oral contraceptive use linked to development of IBD is thought to be related to exogenous oestrogen which decreased colonic paracellular permeability, enhanced pro-inflammatory responses and enhanced macrophages

cell proliferation (Shoenfeld *et al.*, 2008; Looijer-van Langen *et al.*, 2011; Khalili, 2016).

Zinc, Calcium and Vitamin D

The role of micronutrients (zinc and calcium) and vitamin D in IBD development and exacerbation is emerging. A large prospective cohort study of females revealed that higher incidence of IBD for women living in northern latitudes when compared to those residing in southern latitudes, suggesting a greater incidence in areas associated with reduced exposure to UV light (Khalili, Talasaz and Salarifar, 2012). Patients with both previously diagnosed, and new onset IBD, have been found to be vitamin D deficient. It is possible that vitamin D affects the immune system through T cells, B cells, and antigen-presenting cells, impacting disease development (De Silva and Ananthakrishnan, 2012). The oral supplementation of zinc has been shown to ameliorate colonic inflammation in experimental colitis (Luk *et al.*, 2002; Tran *et al.*, 2007; Barollo *et al.*, 2011). In human and mouse models, increased levels of intracellular zinc led to clearance of bacteria through autophagy in macrophages (Lahiri and Abraham, 2014). Although the effect of zinc supplementation on IBD has been investigated, the influence of zinc on colitis remains unclear.

There is intense interest in understanding the role environmental factors may play in the pathogenesis and management of IBD, which may enable modification of the environment to influence or prevent disease, or improve outcomes in patients with CD.

1.1.3 Genetic Factors

Genetic factors have been widely considered a major risk factor for the onset of CD. So far, genome-wide association studies in cohorts of 70,000 European individuals identified more than 200 loci associated with CD risk (Jimmy Z. Liu *et al.*, 2015; Huang *et al.*, 2017). Genetic associations identified in CD have highlighted the key role of autophagy pathway. Much of the genetic variation associated with CD is related to immune pathways, specifically, interactions between the immune system and the microbiome. Recently, a novel autoimmune IBD susceptibility gene, *PTPN2*, was identified and this gene modulates the gut

microbiome to protect against a novel pathogen (Shawki *et al.*, 2020). In a *Ptpn2* deficient mice model, increased abundance of adherent invasive *Escherichia coli* (AIEC) were detected as it functions by clearance of AIEC by integrating bacterial phagocytosis and lysosomal defence (Shawki *et al.*, 2020; Lei *et al.*, 2022). The genes involved in CD pathogenesis function via different mechanisms, such as defective intracellular bacteria killing, dysregulated intestinal epithelium barrier function, defective in autophagy and deregulated innate immunity and adaptive immune responses (Khor, Gardet and Xavier, 2011; Torres *et al.*, 2017).

NOD2

The first locus identified as a risk factor for CD was the nucleotide oligomerisation domain 2 (*NOD2*) locus on chromosome 16 (Hugot *et al.*, 2001; Ogura *et al.*, 2001). *NOD2* is a member of NOD-like receptor, primarily acting as an intracellular sensor defence mechanism to pathogens or microbes through binding peptidoglycan found in both Gram-positive and Gram-negative bacterial cell membranes, and releasing a number of protective cytokines by triggering NF-κB-dependent and mitogen-activated protein kinases (MAPK)-dependent gene transcription (Strober and Watanabe, 2011; Dickson, 2016). In addition, *NOD2* functions in maintenance of the intestinal epithelial barrier integrity, in the regulation of immune homeostasis and in the balance of the mucosal microbiota (Kobayashi *et al.*, 2005; Petnicki-Ocwieja *et al.*, 2009; Al Nabhani *et al.*, 2016). Three *NOD2* variants (L1007fsinsC, R702W and G908R) have been consistently linked to CD onset (Hugot *et al.*, 2001; Ogura *et al.*, 2001; Cuthbert *et al.*, 2002; Li *et al.*, 2004; Couturier-Maillard *et al.*, 2013). They are located within microbe-associated molecular recognition region of the *NOD2* proteins (Homer *et al.*, 2010). In murine models, *NOD2*-deficient mice have increased susceptibility to colitis along with an altered microbiome, are defective in mucosal barrier function and have decreased expression of inflammatory cytokines (Couturier-Maillard *et al.*, 2013; Ramanan *et al.*, 2014). CD patients with *NOD2* mutations have decreased anti-inflammatory cytokine interleukin (IL)-10 expression and alterations in mucosa-associated bacteria, with increased abundance of *Escherichia* species and decreased *Faecalibacterium* species (Swidsinski *et al.*, 2002; Al Nabhani *et al.*, 2017).

ATG16L1

Autophagy-related 16-like 1 (*ATG16L1*) contributes to regulation of autophagy, a complex degradation mechanism where cells generate double-membrane vacuoles ultimately fusing with lysosomes, leading to the degradation of intracellular proteins or the clearance of infecting bacteria by inducing cellular stress responses (Cadwell *et al.*, 2008; Bel *et al.*, 2017). This results in antigen presentation during the immune response (Vazeille *et al.*, 2015). *ATG16L1* mutations in patients with CD impair bacterial clearance and antigen presentation (Cohen *et al.*, 2019). A variant of *ATG16L1*, amino acid change T300A, is most commonly associated with developing CD (Levin *et al.*, 2016; Cohen *et al.*, 2019). Three potential mechanisms of *ATG16L1* mutation T300A inducing defective autophagy are the; (1) enhanced the degradation of caspase-3 in response to stress signals (Murthy *et al.*, 2014), (2) impact on the ability of ATG16L1 interact with transmembrane protein 59 (TMEM59) to induce autophagy in response to bacterial infection (Boada-Romero *et al.*, 2016), (3) a defect in the interaction between *NOD2* and *ATG16L1*, where NOD2 recruits ATG16L1 to the plasma membrane at the entry site of invasive bacteria and promotes MHC class II-mediated antigen presentation by dendritic cells (DCs) (Lapaquette, M. A. Bringer and Darfeuille-Michaud, 2012; Nguyen *et al.*, 2013). Human immune cells expressing the T300A variant of *ATG16L1* exhibit impaired clearance of intracellular bacteria; defects in regulatory T-lymphocyte development and increased pro-inflammatory cytokine production (Chu *et al.*, 2016; Lapaquette, Nguyen and Faure, 2017).

IRGM

Immunity-related GTPase M (*IRGM*) is a member of the p47 immunity-related guanosine triphosphatase family and its mutations have been also implicated in CD pathogenesis (Palomino-Morales *et al.*, 2009). Depletion of *IRGM* in human intestinal epithelial cells and macrophages prevents autophagy induction, elimination of invasive pathogens and antigen presentation (Singh *et al.*, 2006; McCarroll *et al.*, 2008; Nguyen *et al.*, 2013). A subsequent study has shown that *IRGM* modulates *TFEB*, a transcriptional activator of lysosomal system, in a positive regulate lysosomal gene expression (Kumar *et al.*, 2020). Similarly, mutations in caspase recruitment domain-containing protein 9 (*CARD9*) and

leucine-rich repeat kinase 2 (*LRRK2*) have also been identified as CD susceptibility loci and are involved in bacterial recognition, phagocytosis function and ROS pathway-dependent immune responses (Parkes *et al.*, 2007; McGovern *et al.*, 2010; Tawfik, Flanagan and Campbell, 2014).

1.1.4 Altered intestinal microbiome

The gut microbiome comprises different organisms including bacteria, fungi, viruses, parasite and protozoa, residing in niches adjacent to epithelial surfaces colonising the intestine (Nishida *et al.*, 2018). Human intestinal bacteria include *Firmicutes*, *Bacteroidetes*, *Proteobacteria*, and *Actinomycetes* (Jandhyala *et al.*, 2015). In healthy adults, *Firmicutes* and *Bacteroidetes* predominate in the gut (Jandhyala *et al.*, 2015). The intestinal epithelium as a primarily defensive line protects homeostasis of the gut microbiota by detecting and destroying translocated bacteria and loss of these functions contributes to bacterial changes resulting in disrupted mucosal homeostasis, increased intestinal inflammation and development of colitis (Gallo and Hooper, 2012; Buttó and Haller, 2016).

Intestinal microbiome dysbiosis is characterised as an alteration or disturbance in the normal observed diversity of gut microbiota, which is associated with numerous diseases including CD (Casén *et al.*, 2015). Normally, the microbiome is beneficial to the host, through modulation of immune system, the maintenance of mucosal homeostasis, and defence against intestinal pathogens, while under conditions of dysbiosis, the microbial communities can be harmful to the host (Cerf-Bensussan and Gaboriau-Routhiau, 2010; Chu *et al.*, 2016; Brun, 2019). CD is strongly associated with dysbiosis; a reduction in the overall biodiversity of the gut microbiome and an increase in the proportion of harmful proteobacteria (Morgan *et al.*, 2012; Quévrain *et al.*, 2016). More specifically, the most defined changes encompass a decrease in beneficial bacteria, such as those of the *Bifidobacterium* (*Bifidobacterium adolescentis*), *Firmicutes* phylum (*Faecalibacterium prausnitzii*) and *Clostridium* clusters (XIVa and IV), and an increase in certain members of *Enterobacteriaceae* (Fava and Danese, 2011; Joossens *et al.*, 2011; Loh and Blaut, 2012; Fujimoto *et al.*, 2013; Kostic, Xavier and Gevers, 2014). Approximately a third of patients with CD have an increased abundance of mucosa-associated AIEC, while a commensal bacterium with anti-

inflammatory properties, *Faecalibacterium prausnitzii* is reduced in CD patients (Darfeuille-Michaud, Boudeau, Bulois, Neut, A. L. Glasser, *et al.*, 2004; Sokol *et al.*, 2008; Lapaquette *et al.*, 2010; Quévrain *et al.*, 2016). Although the literature surrounding these changes in CD is evolving, the exact mechanism by which microbiome alterations may contribute to pathogenesis of CD is still not fully understood.

The mucosal immune system involves both the innate (macrophage, neutrophil and DCs) and acquired (T and B cell) immune systems to detect bacteria and antigens at the mucosal surface and to drive an appropriate response (Balfour Sartor, 2006; Hooper, Littman and Macpherson, 2012; Alexander, Targan and Elson III, 2014; Kayama and Takeda, 2016). Pathogenic bacteria can activate innate immune cells via binding with toll-like receptors (TLRs), Nod-like receptors (NLRs), C-type lectin-like molecules, or b-glucan receptors resulting in further activation of NF-kB or MAPKs, key intracellular signalling enzymes for pro-inflammatory gene transcription (Hruz et al., 2009; Pandey et al., 2015; Christophi et al., 2012). In response to receptor activation, innate immune cells such as intestinal DCs and macrophages, produce IL-1β, TNF-α, IL-12 and IL-23, which contribute to development of intestinal inflammation and colitis in mice model (Mahida, 2000; Kamada *et al.*, 2005; Niess and Reinecker, 2005; Becker *et al.*, 2006; Kullberg *et al.*, 2006; Zareie *et al.*, 2006; Zoeten and Fuss, 2013). High levels of these pro-inflammatory molecules promote trafficking and migration of the circulating innate immune cells including neutrophils, macrophages and DCs into the intestinal mucosa (Reaves, Chin and Parkos, 2005; Griffith, Sokol and Luster, 2014; Peterson and Artis, 2014). Recruitment of activated immune cells also result in granuloma formation in states of chronic intestinal inflammation (Balfour Sartor, 2006; Mizoguchi *et al.*, 2007; Fournier and Parkos, 2012; Brazil, Louis and Parkos, 2013). Thus, the bacterial contribution to CD pathogenesis can be described as a dysregulated gut microbiota filled with immunostimulatory bacteria and depleted of immunosuppressive immune cells.

1.2 Immunobiology in Crohn's Disease

The biggest compartment of the immune system is located underneath gastrointestinal epithelial cells, having essential housekeeping functions in both

recognition and clearance of dangerous agents. The gut epithelium is protected by both the innate and adaptive immune systems. The major components of the former are neutrophils, DCs, monocytes, macrophages and innate lymphoid cells (ILCs). The latter is the population of B-cells producing secretory immunoglobulin A (SIgA) antibodies, which functions as an anti-inflammatory first line of defence performing “immune exclusion” (Thomas and Baumgart, 2012). Adaptive immunity is also strictly dependent on T cells. Naïve T cells to be primed against pathogen-associated antigen by encountering antigen-presenting cells (APCs), resulting in massive proliferation of T cells and the acquisition of T cell effector functions. Effector T cells produce long-lived memory T cells that protect the body against re-infection (O’Leary *et al.*, 2006). The main immune response in the development of CD is summarised in Figure 1-2. In this process both low-affinity and high-affinity antibody functions at the mucosal surface, which is intended to prevent both microbial invasion and penetration of foreign antigens through the epithelial barrier (Brandtzaeg, 2007; Corthésy, 2010). The pathogenesis of CD is believed to occur when immune tolerance to the commensal microflora breaks down in genetically susceptible individuals (Baumgart and Sandborn, 2012). Several genes, such as *NOD2*, *ATG16L1*, *LRRK2*, *XBP1* and *IRGM*, are altered, as a result of which, Paneth cells show altered survival and function, including abnormal secretion of antibacterial protein (Ouellette, 2010).

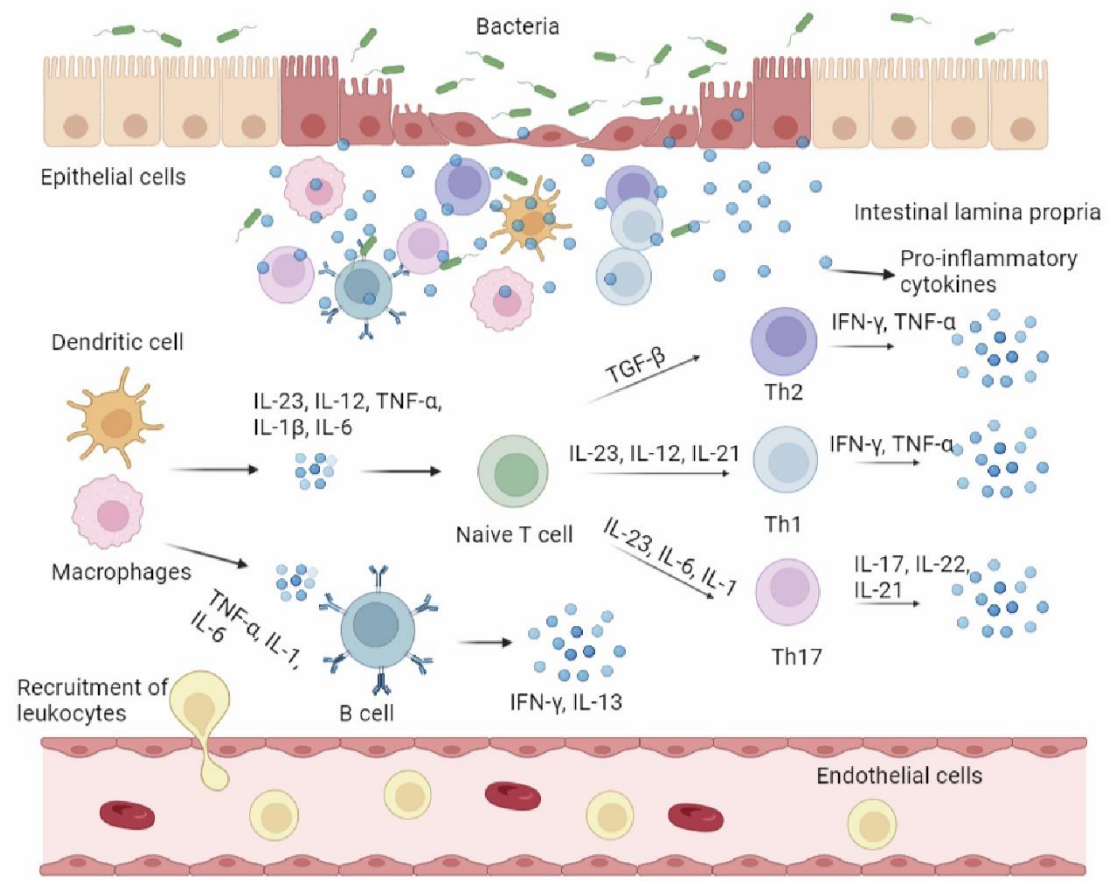

Figure 1-2 Immune response in CD.

CD develops via epithelial barrier dysfunction that leads to a process involving bacterial translocation and subsequent activation of immune cells. The activation of DCs and macrophages in the intestinal lamina propria leads to the production of inflammatory cytokines IL-23, IL-12, TNF-α, IL-1β and IL-6. Antigens delivered to naïve T lymphocytes induces the differentiation to Th2, Th1 and Th17 cells, with the release of inflammatory cytokines. Macrophage-releasing cytokines TNF-α, IL-1 and IL-6 can be recognised by B cells (Roda *et al.*, 2020).

1.2.1 Innate immunity

The immunity of the host depends critically on the recognition and killing of pathogens directly by professional immune cells such as neutrophils, macrophages, and DCs. These cells are capable of warding off invading bacteria by phagocytosis and detecting and responding to microbial stimuli, in conjunction with the production of antimicrobial compounds like reactive oxygen and proteases (Steinbach and Plevy, 2014).

Dendritic Cells (DCs)

It is thought that the initial gut mononuclear phagocyte subpopulations in contact with the microbiome are DCs due to the large dendritic projections

present (Seldenrijk *et al.*, 1989). The accumulation of mucosal DCs has been commonly seen in CD. Immunohistochemical studies in CD patients revealed an increased number of CD83 positive DCs in aggregated lymphoid nodules and in single cells within the lamina propria (Velde *et al.*, 2003; Salim *et al.*, 2009). The inflammatory ileal mucosa of patients with active CD also contains myeloid DCs which are M-DC8+ localised in the T cell area of Peyer's patches (de Baey *et al.*, 2003). There was some correlation of these immunohistochemical findings with functional flow cytometry studies of myeloid DCs using a variety of different marker panels. It has been reported that the inflamed mucosa of CD patients contains an abundance of activated, myeloid DCs expressing CD40, CD83, and/or CD86 (Hart *et al.*, 2005; Baumgart *et al.*, 2009). Researchers using a DC antigen presenting marker (RFD1) identified that macrophages in actively inflamed gastrointestinal segments and pouches phenotypically change from interdigitating to mature macrophages (Allison and Poulter, 1991; De Silva *et al.*, 1991). Further investigation in embryonic aphthoid lesions in the colonic mucosa of CD patients contained a dense cellular aggregate consisting of CD68+ macrophages that were surrounded by a large number of DCs expressing ICAM-1, HLA-DR and ID-1 molecules (Morise *et al.*, 1994).

A number of microbial pattern recognition receptors are expressed by DCs from patients with CD, including TLR2, TLR4, and co-stimulatory receptors (Lindsay *et al.*, 2006; Silva, 2009). In CD, TLR4 expression may correlate positively with disease activity and signal the release of proinflammatory cytokines (Ng *et al.*, 2011). In experiments with human myeloid DCs from IBD patients, lipopolysaccharide produces an exaggerated immune response through primarily binding to TLR4 (Baumgart *et al.*, 2009).

Moreover, neutrophils are also essential for maintaining gut homeostasis and for inflammatory processes to take place. In IBD, neutrophils have been shown to phagocytose pathogens in the gut in order to maintain homeostasis, however, subsequent accumulation of these phagocytes within the gut epithelium impairs the epithelial barrier function and leads to a great production of inflammatory mediators that exert an inflammatory effect (De Souza and Fiocchi, 2016). Gut macrophages have essential housekeeping functions in a healthy gut mucosa and

control tissue remodelling by removing apoptotic or senescent cells (De Souza and Fiocchi, 2016).

Monocytes and Macrophages

As part of the innate immune system, monocytes and macrophages also play important roles. In the intestine, macrophages differentiate from monocytes, undertaking a characteristic functional phenotype dependent on the microenvironmental signals, including intestinal microbiota products (Steinbach and Plevy, 2014). Macrophages can be divided into two broad types as described in the literature in the recent decades: M1 macrophages have easily triggered defence mechanisms that are capable of destroying bacteria and causing inflammation, while M2 macrophages are tolerogenic and promote tissue repair and growth (Italiani and Boraschi, 2014). Within a healthy gastrointestinal tract, macrophages have a tolerogenic phenotype (M2-like) and contribute to preventing inflammation against commensal bacteria; while in IBD, monocytes do not differentiate fully into M2-like macrophages but remain in a M1 phenotypic state (Motwani and Gilroy, 2015). There are many functionally important proteins found in macrophages that carry potential variations that may affect the risk of developing IBD. Species-specific engagement of human NOD2 and TLRs are upregulated during intestinal inflammation (Hausmann *et al.*, 2002; Motwani and Gilroy, 2015). In contrast “normal” intestinal macrophages are irresponsive to lipopolysaccharide (LPS) as these cells are not expressing LPS receptors (TLR4 and CD14). T-cell co-stimulatory molecules are upregulated on intestinal macrophages from IBD mucosa which consequently can induce clonal T-cell reactions; however, this process is silent in the normal intestine (Rogler *et al.*, 1999). Data from these experiments indicates that there are anergic tolerance-inducing macrophages in the normal intestinal mucosa. Understanding the causes for insufficient intestinal macrophage differentiation will provide new insight in IBD pathogenesis and develop effective therapies.

1.2.2Adaptive immunity

Effector T cells

Given the increased number of activated CD4+ T cells in the lamina propria of both inflamed mouse and human intestinal tissues, T cells have been recognized as essential to mucosal inflammation and thought to even be the instigator of disease (Elson *et al.*, 2005; Shale, Schiering and Powrie, 2013). It commonly seems that a dysregulation in the effector T cell response to the commensal microbiota in IBD pathogenesis (Maynard and Weaver, 2009). Based on their cytokine secretion profiles, effective T cells are broadly classified into Th1, Th2, or Th17 cells. Th1 cells produce Interferon-gamma (IFN-γ) and TNF-α; Th2 cells produce IL-4, IL-5, and IL-13; whereas Th17 cells produce IL-17. Th1 cells secrete cytokines in response to intracellular bacteria and viruses while Th2 cells create cytokines in response to parasitic infections. Meanwhile, Th17 cells respond specifically to extracellular bacteria and fungi (Murphy and Reiner, 2002; Ansel *et al.*, 2006; Weaver *et al.*, 2007).

CD was firstly thought to be associated with Th1 cells (Fuss *et al.*, 1996), but recently, CD also has been classified as a Th17-associated disease, since the mucosa of CD patients produces IL-17 along with TNFα and IFNγ (Fujino *et al.*, 2003). Consequently, Th1 and Th17 cells perpetuate inflammation by secreting pro-inflammatory cytokines (IL-17, TNFα and IFN-γ). There is currently some controversy regarding the assumption that altered T cells do not drive inflammation in most IBD patients; but rather that these cells play an essential role in propagating and mediating the disease resulting from aberrant innate immunity (Maynard and Weaver, 2009). To be specific, Th1 and Th17 related cytokines are stimulated by TNF-α, IL-1, IL-6, IL-8, IL-12, and IL-18 production by macrophages, endothelial cells and monocytes (Uhlig and Powrie, 2018). In addition, there is considerable evidence that CD is caused by an excessive Th1 and Th17 cell response to pro-inflammatory cytokines (IL-12, IL-18 and IL-23) which are released by antigen-presenting cells and macrophages (Uhlig and Powrie, 2018).

In light of the fact that IFNγ, IL-17 and IL-13 are expressed in large quantities by CD4+ T cells from patients with CD, these three cytokines have been considered as potential targets for the treatment of IBD (MacDonald *et al.*, 1990; Fujino *et al.*, 2003; Fuss *et al.*, 2004). CD patients have increased serum IFN-γ, but neither UC patients nor control patients did (Beltrán *et al.*, 2010). Early studies

have shown that treatment with an IFN-γ-blocking antibody almost completely abrogated the development of colitis in two models, CD45RBhi T cell transfer and IL-10–deficient models of colitis (Powrie *et al.*, 1994; Berg *et al.*, 1996). Fontolizumab, a humanized antibody against IFN-γ, has been studied by several groups in patients with CD, however, its efficacy remains unclear (Reinisch *et al.*, 2006; Colombel *et al.*, 2010; Cui *et al.*, 2013). Additionally, CD4+ T cells from the lamina propria of CD patients expressed both chains of the IL12 receptor (IL12Rß1 and IL-12Rß) and of the IL-18 receptor, which may account for their enhanced ability to produce IFN-γ when activated with IL-12 and IL-18 *ex vivo* (Okazawa *et al.*, 2002). Although antibody blockade of IFN-γ has shown limited effectiveness in IBD patients, similar to its limited efficacy in established disease in mice, treatment with an IL-12p40 mAb (which neutralizes both IL-12 and IL-23) however, has shown substantial efficacy in active CD (Mannon *et al.*, 2004).

Importantly, adoptive transfers of intestinal bacteria-responding Th17 cells into immunodeficient recipients resulted in severe colitis more often than comparable transfers of Th1 cells, as well as causing disease at far lower cell doses (Elson *et al.*, 2007). In a study by Elson and colleagues (2007), the treatment with a monoclonal antibody against IL-23p19 inhibited colitis development when administered at the time of transfer, but also suppressed ongoing disease and depleted the transferred Th17 effectors, indicating that IL-23 is required to sustain the pathogenic Th17 population (Elson *et al.*, 2007).

B cells

It is likely that B cells, which are predominant in inflammation-prone mucosal surfaces and can recognise microbial ligands, play a role in the pathogenesis of IBD (Strober, Fuss and Mannon, 2007; Abraham and Cho, 2009). In the mucosal immune system, B cells are important for maintaining an epithelial barrier, regulating enteric microflora diversity, and developing an appropriate immune response to enteric antigens and floral antigens. B lymphocytes mature in mucosal lymphoid follicles and mesenteric lymph nodes (MLN) with subsequent migration to the lamina propria before undergoing differentiation to IgA secretion plasma cells. The entry of translocated enteric bacteria or bacterial antigens may activate mature mucosal B cells in a specific phenotype (TLR2+)

(Noronha *et al.*, 2009). Cells isolated from the inflamed mucosa secrete antibodies to strains of *Escherichia coli* which are more often detected in CD patients (Heddle, La Brooy and Shearman, 1982), as well as antibodies against colonic epithelial antigens (Hibi *et al.*, 1990). As several types of circulating antibodies respond to both antigens and self-antigens, it is believed that the primary pathogenic event in IBD is dysregulated immunity to normal enteric microorganisms. These antibodies include anti-*Saccharomyces cerevisiae* antibodies, anti-neutrophilic cytoplasmic antibodies, and antibodies to outer membrane porin (OMP), *Pseudomonas fluorescens*-related sequence I2, and anti-carbohydrate antibodies (Ferrante *et al.*, 2007; Peyrin-Biroulet *et al.*, 2007). Studies of circulating antibodies have focused more on their diagnostic or prognostic value than their role in IBD pathogenesis (Sellin and Shah, 2012; Tesija Kuna, 2013).

The functional characterization of mucosal B cells in human IBD has been the subject of only a limited number of studies so far. A research study showed that B cells in peripheral blood from CD patients express surface TLR2, constitutively secreting copious amounts of proinflammatory IL-8 and contain increased *ex vivo* levels of phosphorylated signalling proteins; however, this cannot be observed in UC patients or healthy controls (Noronha *et al.*, 2009). These findings suggest a positive correlation between TLR2 and IL-8 in B cells and CD disease pathogenesis (Noronha *et al.*, 2009). In another study, increased serum levels of LPS and high mobility group box 1 (HMGB1), an endogenous TLR ligand, were quantified in both CD and UC, which suggested that B cells were modulated towards either pro- or anti-inflammatory activity by TLR4 ligands (LPS or eotaxin-1) (McDonnell *et al.*, 2011; Rehman *et al.*, 2013). Additionally, it has been proposed that the circulating B cell may serve as an important indicator of the amount of LPS lipid A acylation in the IBD patients (McDonnell *et al.*, 2011).

1.2.3 Cytokines in IBD

It was first described in the mid to late 1980s and early 1990s how patients with IBD produce altered patterns of cytokines from their peripheral tissues and lamina propria (Ebert *et al.*, 1984; Mitsuyama *et al.*, 1991). In genetic and immunological studies, cytokines and cytokine-producing immune cells have been implicated in the pathogenesis of IBD, and their control is considered

instrumental in preventing intestinal inflammation its associated symptoms. Genome-wide associated studies (GWAS) have identified several Th cell responses and cytokine/chemokine receptor signalling loci for IBD susceptibility that contain genes encoding signal transducer and activator of transcription 1 (STAT1), STAT3, STAT4, CC-chemokine receptor 6 (CCR6), CC-chemokine ligand 2 (CCL2), CCL13, IL12 receptor (IL12R), IL23R and Janus kinase 2 (JAK2). Additional studies have identified gene loci encoding cytokines as risk factors for IBD (such as IL2, IL21, IFN-γ, IL10, and IL27) indicating that these cytokines may play a key role in disease pathogenesis (Jostins *et al.*, 2012). The modulation of cytokine function can be used as potential targets for treatment of chronic intestinal inflammation (Neurath, 2014). For instance, in the clinic, anti-TNF-α treatment is now a common therapy for IBD (Baumgart and Sandborn, 2012).

The IL-1 family

Lamina propria DCs and macrophages in the inflamed mucosa in IBD, produce a large amount of pro-inflammatory cytokines, such as IL-1β, IL-6, IL-18 and TNF-α following activation by components of the commensal microbiota and TLR signals (Ng *et al.*, 2011). In patients with CD and UC, the ratio of IL-1 receptor antagonist to IL-1 was significantly lower than in controls, indicating higher activation of the IL-1 system in IBD (Casini-Raggi *et al.*, 1995). Multiple murine models of acute and chronic colitis benefited from blocking the IL-18 cytokine, belonging to member of the IL-1 family, primarily expressed in macrophages and epithelial cells in CD patients (Pizarro *et al.*, 1999; Kanai *et al.*, 2001). Researchers also found that deficiency of caspase 1, an enzyme responsible for cleaving IL-1β and IL-18 into active cytokines, prevented mice from developing DSS-induced colitis, indicating that blockage of IL-1 family members may be relevant to the treatment of chronic intestinal inflammation (Siegmund *et al.*, 2001).

IL-6

IL-6 is produced by lamina propria macrophages and CD4+ T cells in experimental colitis as well as in patients with IBD (Atreya and Neurath, 2005; Kai *et al.*, 2005). In the pathogenesis of IBD, IL-6 binds to soluble IL-6R (sIL-6R), then activates intestinal target cells (including APCs, T cells and intestinal

epithelial cells) by binding to gp130 surface molecule (also known as IL-6R subunit ß) (Atreya and Neurath, 2005). As a result, IL-6 can stimulate inflammation by activating targeting cells to produce pro-inflammatory cytokines, preventing programmed cell death of mucosal T cells, as well as stimulating the proliferation and expansion of intestinal epithelial cells (Atreya and Neurath, 2005). It is interesting to note that in mouse models of chronic intestinal inflammation, monoclonal antibodies blocking IL-6 signalling were effective in suppressing inflammation, along with the induction of T cell apoptosis and reduction of pro-inflammatory cytokines, such as IFNγ, TNF-α and IL-1ß, which suggests IL-6 may be a therapeutic target in IBD (Yamamoto *et al.*, 2000). In light of these promising results, an antibody specific to IL6R (Tocilizumab) was designed in clinical therapy to target IL-6 signalling in patients with CD (Ito *et al.*, 2004); in addition, a novel anti-IL-6 antibody (PF-04236921) was clinically used in the phase II trial for CD patients (Danese *et al.*, 2019). However, due to limited usage in a small group of CD patients, the therapeutic potential of this approach in CD requires further investigation (Ito *et al.*, 2004).

TNF-α

Both membrane-bound and soluble TNF-α are produced in greater amounts by lamina propria mononuclear cells in IBD patients, in particular from macrophages, adipocytes, fibroblasts and T cells (Strober, Fuss and Blumberg, 2002; Kamada *et al.*, 2010; Atreya *et al.*, 2011). In colitis, TNF-α may induce pro-inflammatory cytokines production by binding to its receptors TNFR1 and TNFR2, followed by activation of the transcription factor NF-κß. To be specific, TNFR1 signalling are known to trigger cell death by activating receptor-interacting protein kinase 1 (RIPK1) and caspase-3. Furthermore, post-activation of TNFR2, TNF-α promotes a multitude of pro-inflammatory effects in colitis, including increased angiogenesis, necroptosis, the secretion of matrix metalloproteinases by myofibroblasts, the activation of macrophages and effector T cells, and the direct damage to intestinal epithelial cells (IECs) (Di Sabatino *et al.*, 2007; Meijer *et al.*, 2007; Atreya *et al.*, 2011; Günther *et al.*, 2011; Su *et al.*, 2013). Consistent with these effects, the inhibition of TNF-α resulted in T cell apoptosis and suppression of experimental colitis in mice

(Holtmann *et al.*, 2002; Perrier *et al.*, 2013). In clinical trials, using anti-TNF-α antibodies infliximab and adalimumab for treating IBD, the results were highly successful, with T cell apoptosis being demonstrated *in vivo* (Van den Brande *et al.*, 2003, 2007; Atreya *et al.*, 2011; D'Haens *et al.*, 2018).

IL-12 family

IL-12 family members, such as IL-12, IL-23, IL-27 and IL-35, are heterodimeric cytokines that are produced by innate immune cells (such as macrophages, dendritic cells and possibly neutrophils) and have emerged as central drivers of intestinal inflammation and major mediators of inflammation in IBD. Specifically, dendritic cells and macrophages produce elevated amounts of IL-12 and IL-23 in CD, whereas they do not increase in UC (Monteleone *et al.*, 1997; Liu *et al.*, 2009; Ng *et al.*, 2011). IL-12 and IL-23 share the same p40 subunit but pair with p35 and p19 subunits, respectively. In experimental colitis models that are driven by either T cells or innate immune cells, research has demonstrated that IL-23 is of particular importance. Using neutralizing antibodies targeting the above cytokines have been shown to be therapeutic for experimental models of colitis and for clinical trials in IBD (Uhlig *et al.*, 2006; Yen *et al.*, 2006; Izcue *et al.*, 2008; Ahern *et al.*, 2010). Currently, CD treatment involved the use of monoclonal anti-p40 antibody for targeting both IL-12 and IL-23 (briakinumab, ustekinumab), and several anti-p19 antibodies (specifically targeting IL-23) that have completed clinical phase II studies (Mannon *et al.*, 2004; Sandborn *et al.*, 2012; Sands *et al.*, 2017). In patients with CD who fail in respond to anti-TNF-α antibodies, anti-IL-12 and IL-23 antibodies showed a greater clinical response than placebo. These studies suggest new therapeutic options in patients with CD who are resistant to anti-TNF-α treatments.

IFN

Besides IL-12 family members, APCs are also capable of producing a variety of cytokines belonging to the interferon family (including IFN-α and IFN-ß) (Kole *et al.*, 2013). After epithelial damage, intestinal bacteria are shown to activate TLR9 and induce plasmacytoid DCs to produce IFN-α and IFN-ß (Katakura *et al.*, 2005). These cytokines are beneficial for epithelial regeneration or for the induction of IL-10 producing Treg cells. Deficient type I IFN receptors mice

exhibited a more severe colitis than wild-type mice (Katakura *et al.*, 2005). Additionally, in recombination-activating gene 1 (RAG1) deficient mice, TLR9 agonists or recombinant IFN were administered with a result of the suppression of colitis (Katakura *et al.*, 2005). Thereby, taking advantage of these cytokines produced by APCs is crucial for the treatment of IBD.

1.3 Adherent-invasive *E. coli* in Crohn's Disease

With respect to CD aetiology, a member of the *Enterobacteriaceae* family *E. coli* that adheres to the inflamed ileal and colonic mucosa of patients with CD, has attracted the most attention over the last 10-15 years. AIEC is more often found associated with the ileum than the colon in CD patients, with a prevalence range of 21% to 62% in CD versus 0% to 19% in healthy controls (Darfeuille-Michaud, Boudeau, Bulois, Neut, A.-L. Glasser, *et al.*, 2004; Martinez-Medina *et al.*, 2009; Palmela *et al.*, 2018). *E. coli* is frequently able to colonise near the intestinal mucosa due to their relatively higher tolerance of oxygen dispersed by the epithelium (Zeng, Inohara and Nuñez, 2017). According to bacterial genetics and phylogeny, strains of *E. coli* can be distinctly classified as either overtly pathogenic or commensal. Pathogenic *E. coli* have acquired sets of virulence genes subdividing them into 6 major diarrheagenic *E. coli* phenotypes: enteropathogenic *E. coli* (EPEC), Shiga toxin-producing *E. coli* (STEC), enteroinvasive *E. coli* (EIEC), enteroaggregative *E. coli* (EAEC), diffusely adherent *E. coli* (DAEC), enterotoxigenic *E. coli* (ETEC) and adherent-invasive *E. coli* (AIEC) (Boudeau *et al.*, 1999).

In particular, AIEC firstly discovered in the late 1990's, are most notable for being implicated in the pathogenesis of CD and its virulence properties are linked to; (1) the ability of adhere and invade to IECs through the involvement of actin polymerisation and microtubule recruitment (Darfeuille-Michaud, 1998; Boudeau, 1999), (2) the ability to survive and replicate within macrophages without inducing cell death (Glasser *et al.*, 2001), and (3) the induction of secretion of high amounts of TNF-α from infected macrophages (Bringer *et al.*, 2012).

1.3.1 Pathogenetic Features of AIEC

The identification of AIEC is based on their ability to adhere to and to invade IECs, as well as their ability to survive and replicate within macrophages. A schematic of pathogenetic features of AIEC is shown in Figure 1-3.

To adhere and invade

IECs and M cells act as a primary barrier to prevent enteric bacteria entering and translocating to immune cells underlying Peyer's patches or lamina propria (Kagnoff, 2014). Prior to translocation and entrance of the submucosal compartment, AIEC adheres to and colonises IECs, an essential first step in the pathogenicity of infectious gut diseases. Colonisation by AIEC disrupts the mucosal barrier, limiting clearance from the intestine and triggering abnormal expression of epithelial receptors, leading to altered intestinal permeability and activation of intestinal inflammation (Fujimura, Kamoi and Iida, 1996; Wine *et al.*, 2009). Several virulence factors of AIEC promote the initial interactions leading to adhesion and invasion, including flagella, Type 1 fimbriae, outer membrane proteins (OMPs), and outer membrane vesicles (OMVs).

In development of CD, the adherence and colonisation by AIEC type strain LF82 requires flagellar genes and their mutation supresses LF82 motility and reduces colonisation (Rooks *et al.*, 2017). The presence of bacterial flagella is required for AIEC interacting with the epithelial barrier (Martinez-Medina *et al.*, 2009). Flagellin on the AIEC surface activates and upregulates TLR5, Nod-like receptor family member (NLRC4), and flagellin receptors, instigating the innate immune response (Carvalho *et al.*, 2008). The binding of flagellin to TLR5 on IEC initiates the NF-κB pathway and induces IL-8 and TNF-α secretion leading to an increased mucosal inflammatory response and an inhibition of the autophagic process of host cells (Eaves-Pyles *et al.*, 2008; Subramanian *et al.*, 2008; Mimouna *et al.*, 2011).

Adhesion and subsequent translocation of AIEC across IECs and M cells was supported by extracellular receptors glycoprotein 2 (Gp2) and carcinoembryonic antigen-related cell-adhesion molecule 6 (CEACAM6) that can recognise type 1 pili (FimH) expressed on the surface of AIEC strains (Barnich *et al.*, 2007; Hase

et al., 2009; Barnich and Darfeuille-Michaud, 2010). In addition, AIEC OMVs fuse with the endoplasmic reticulum stress response factor Gp96, thus promoting virulence factor release and enabling further invasion (Rolhion, Hofman and Darfeuille-Michaud, 2011). Finally, AIEC crossing of the epithelial barrier through M cells is supported by bacterial FimH binding to M cells through the recognition of apical glycoprotein 2 (Gullberg and Söderholm, 2006; Hase *et al.*, 2009).

To survive and replication within macrophages

Once AIEC cross the mucosal barrier, phagocytosis by immune cells will occur. The AIEC reference strain LF82 are able to persist in macrophages in a phagosome fused with lysosomes, suggesting that AIEC bacteria have the ability to replicate in an environment with acidic pH, oxidative stress, active proteolytic enzymes, and antimicrobial compounds (Alpuche-Aranda *et al.*, 1994; Glasser *et al.*, 2001). In addition, other proteins also contribute to AIEC persistence in macrophages; the HtrA stress protein supports bacteria in acidic pH conditions; a series of Dsb proteins is needed for LF82 to mimic the harsh environment; Hfq protein facilitating integration between the regulatory RNA and mRNA (Bringer *et al.*, 2005; Heras *et al.*, 2009; Vogel and Luisi, 2011). After macrophage stimulation, hypersecretion of proinflammatory cytokines TNF-α and IFN-γ was induced *in vitro* and *in vivo*, which is likely to increase CEACAM6 expression which is associated with AIEC expansion and pathogenesis (Dreux *et al.*, 2013). Meanwhile, intra-macrophages AIEC leads to NF-κB signalling activation that is responsible to immune system, inflammation and cancer, which may play an important role in AIEC pathogenesis (Petersen *et al.*, 2009).

To produce cytokines

In colon biopsy samples from patients with CD, AIEC strains were shown to stimulate increased expression of mRNA for TNF-α, IFN-γ, and IL-8 (Mazzarella *et al.*, 2017). Additionally, LF82 affects the cell cycle in Caco2 cells (Mazzarella *et al.*, 2017). In IECs, LF82 can activate NF-κB signalling via IκB-α phosphorylation, NF-κB p65 nuclear translocation, and the elevation of the production of TNF-α secretion (Jarry *et al.*, 2015). Specifically, AIEC bacteria modulate ubiquitin proteasome system turnover in infected IECs by downregulating the NF-κB regulator CYLD, leading to degradation of inhibitor of κB kinase (IκB) peptides

and subsequent activation of NF-κB (Cleynen *et al.*, 2014). As a result of the proinflammatory property of flagella, these bacteria can promote the secretion of inflammatory cytokines such as IL-8 and CCL20 in polarised IECs, leading to the recruitment of macrophages and dendritic cells to the infection site (Eaves-Pyles *et al.*, 2008; Subramanian *et al.*, 2008). As mentioned above, there is evidence in the literature that IFN-γ and TNF-α secreted by macrophages and lymphocytes are the inducers of CEACAM6 expression, which results in AIEC colonisation (Dreux *et al.*, 2013).

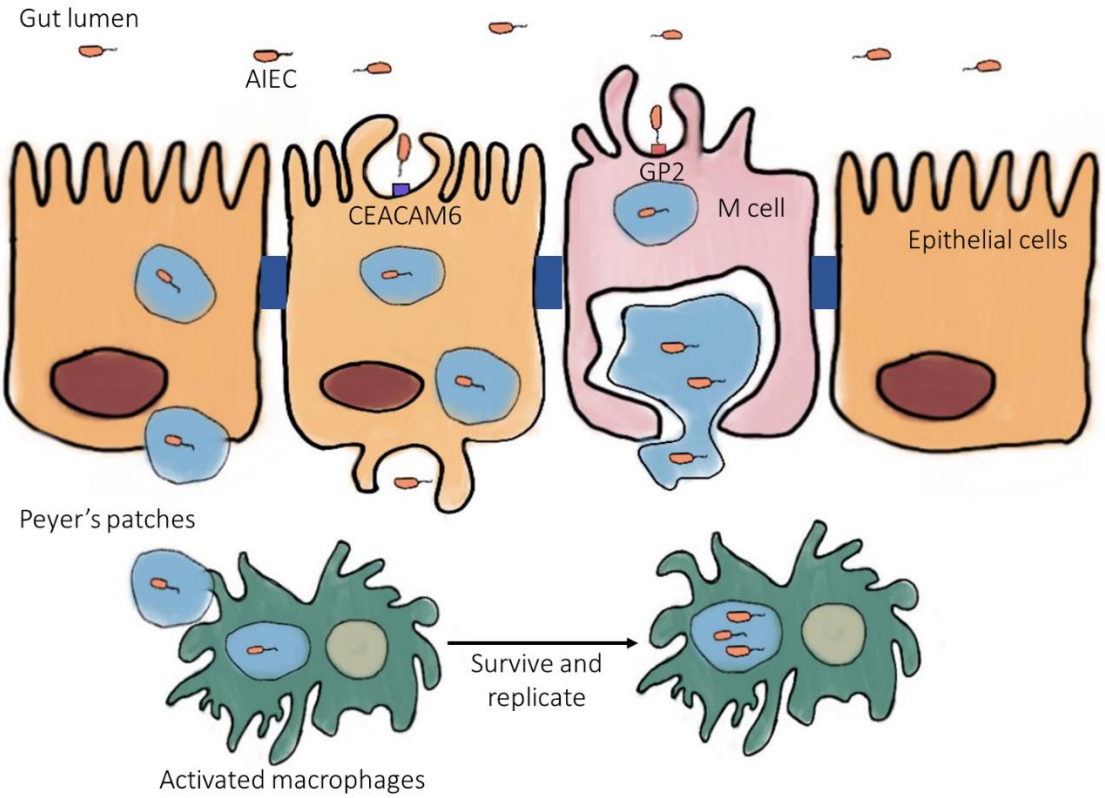

Figure 1-3 AIEC in the pathogenesis of Crohn's disease.

AIEC penetrates the mammalian intestine by either directly invading through the epithelial layer or by entering through the microfold (cells and into the Peyer's patches Surface host receptor, GP2 located on the M cells and glycoprotein CEACAM 6 on epithelial cells, selectively bind the FimH adhesion of type I fimbriae of AIEC, supporting adherence to epithelial barrier and contributing to AIEC invasion. Once AIEC translocate across the mucosal barrier invasion of immune cells such as macrophages occurs AIEC can survive and replicate within underlying mucosal macrophages (Rolhion and Darfeuille-Michaud, 2007).

1.3.2 Common virulence factors in AIEC

The influence of AIEC isolates on CD pathogenesis was extensively studied, and their virulence factors were compared to reference AIEC strain LF82, and non-AIEC strains.

Type 1 fimbriae

Pathogenic strains of *E. coli* possess fimbriae as virulence factors, enabling them to stick to, and colonize, different host epithelia. It is well-known that the *fimH* gene is one of the most highly studied virulence factors in AIEC strains and when expressed, FimH functions in bacterial adherence to glycosylated and non-glycosylated host receptors (Sokurenko *et al.*, 1997). A variety of FimH adhesins are found in the majority of AIEC strains, which makes them more effective at binding to CEACAM6 expressed on human intestinal epithelial cells (Dreux *et al.*, 2013). The *fimH* gene has been detected in AIEC strains and non-AIEC strains alike, finding no significant association with AIEC pathotype; however, AIEC isolates from biopsy samples of patients with UC have been found with a higher occurrence of the *fimH* gene than control patients (Céspedes *et al.*, 2017; Zamani *et al.*, 2017). Among all virulence genes, the *fimH* gene is the only gene detected in all kinds of AIEC strains and primarily in B2 phylogenetic group *E. coli* (O'Brien *et al.*, 2017). Interestingly, *CEABAC10* transgenic mice expressing human CEACAM6 receptors showed a significant reduction in inflammation when AIEC *fimH* was replaced with commensal *E. coli fimH* (Carvalho *et al.*, 2009; Dreux *et al.*, 2013). In addition to this study, mutations in *fimH* enhanced AIEC adhesion. Therefore, *fimH* polymorphisms may provide insights into the mechanisms of AIEC colonization of the gut and give an opportunity to create new therapeutic approaches.

Polysaccharide K capsule gene

The polysaccharide K capsule found in pathogenic *E. coli* strains, including AIEC strains, is a major determinant of resistance and survival during infection due to its effect on bacterial protection from innate immune factors (Jann and Jann, 1992). *In vivo*, early in acute urinary tract infections (UTI), *K1* is responsible for the development of intracellular bacterial communities that resemble biofilms

(Anderson *et al.*, 2010). K1 capsule is made of sialic acid chains that are synthesized by enzymes encoded by genes in region II of the capsule locus (*neuDBACES*) (Troy, 1995). Due to the similarity of this polysaccharide to that found on some human cells, the K1 antigen is considered poorly immunogenic (Troy, 1995). In the AIEC LF82 strain, the genes *k1*, *k5* and *KPSMT II* are involved in the synthesis of capsular materials and have a positive association with paediatric patients with CD (Darfeuille-Michaud, Boudeau, Bulois, Neut, A. L. Glasser, *et al.*, 2004; Dale and Woodford, 2015).

Vacuolating autotransporter toxin

An *E. coli* strain isolated from a septicaemic chicken produces vacuolating autotransporter toxin (Vat), a serine protease autotransporter, responsible for vacuolating activity and encoded on a pathogenicity island (Parreira and Gyles, 2003; Henderson *et al.*, 2004). The AIEC Vat protein is part of the ATPase family which enhances serine proteolysis by catalysing the action of certain serine proteases. By decreasing mucus viscosity, it can promote the penetration of the AIEC into the mucus. The function of Vat is to impair the mucosal barrier function of the intestine and induce severe inflammation by dysfunction in cytokine secretion, thus Vat is regarded as a new component of AIEC virulence (Gibold *et al.*, 2016). The AIEC Vat virulence has been studied little so far, and further research will be needed in order to understand its role in IBD.

1.3.3 Targeting AIEC in CD

Inhibition of FimH adhesin by chemical inhibitors

One of the most studied *FimH-CEACAM6* interactions occurs between the FimH adhesin of AIEC and mannose residues of CEACAM6 expressed at the surface of IECs. In this regard, it is necessary to develop anti-adhesive molecules to competitively bind to the FimH carbohydrate recognition site and inhibit this interaction with a view to limiting AIEC colonisation. Thiazolylaminomannosides and n-heptyl-D-mannose (HM)-based glycopolymers exhibit high affinity for FimH to inhibit LF82 adhesion to IECs *in vitro*, as well as present strong inhibition of LF82 adhesion to colonic tissues of CEABAC10 *in vivo* (Brument *et al.*, 2013; Yan *et al.*, 2015; Chalopin *et al.*, 2016). A study on CEABAC10 mice infected with

AIEC LF82 demonstrated that heptylmannoside derivatives significantly impaired the ability of LF82 to adhere to human T84 IECs; reduced LF82levels both in faeces and within the mucosa of infected mice ; and decreased the severity of colitis and intestinal inflammation (Sivignon *et al.*, 2015). Based on studies *in vitro* and *in vivo*, heptylmannoside derivatives were shown to exhibit strong anti-adhesive effects, suggesting they may be useful for treating CD patients colonized with AIEC. A clinical trial is currently assessing the efficacy of these treatments in 358 participants with CD using the FimH blocker EB8018/TAK-018 molecule, and the results showed that the molecule is safe and well tolerated in human (Chevalier *et al.*, 2021).

Gp96 antagonist

Invasion of host cells by AIEC is facilitated through the interaction of *OmpA* and *Gp96* (Rolhion *et al.*, 2010; Rolhion, Hofman and Darfeuille-Michaud, 2011). The following treatment option may be effective in inhibiting AIEC colonization: synthetic peptide Gp96-II is an antagonist of Gp96 that has protected mice against intestinal inflammation (Nold-Petry *et al.*, 2017). While searching for new Gp96 antagonists at the same time, it could be interesting to test this antagonist in the context of AIEC infection to see if it disrupts OmpA-Gp96 interaction and inhibits AIEC colonization *in vitro* and *in vivo*.

Meprin-producing bacteria: cleavage of type I pili by meprin

To protect the host against bacterial colonization, IECs express multiple types of endo- and exoproteases. Meprin treatment reduced the ability of LF82 to adhere to and invade T84 IECs owing to proteolytic cleavage of type 1 pili of LF82 (Vazeille *et al.*, 2011). CD in the ileum is also associated with low levels of meprin. It may be possible to disrupt the FimH-CEACAM6 interaction by administering probiotic strains that produce meprin to CD patients to limit AIEC adhesion to IECs and thus gut colonisation (Vazeille *et al.*, 2011).

Yeast-based probiotics

A study was conducted on the effect of *Saccharomyces cerevisiae* CNCM I-3856 as a probiotic to inhibit AIEC interaction with IECs (Sivignon *et al.*, 2015) . Bacteria

are able to recognize yeast cell walls by their high concentration of mannose residues. LF82 were strongly inhibited from adhering to IECs and isolated enterocytes from CD patients by *S. cerevisiae* CNCM I-3856 (Sivignon *et al.*, 2015). Yeast and *S. cerevisiae* CNCM I-3856 derivatives decreased AIEC gut colonization and prevented intestinal permeability and pro-inflammatory cytokine production in CEABAC10 mice infected with LF82 (Sivignon *et al.*, 2015; Gayathri *et al.*, 2020). *S. cerevisiae* could therefore be a good therapy option for CD patients who are already colonised with AIEC or at risk of colonisation by AIEC (Sivignon *et al.*, 2021).

1.4 AIEC interactions with Macrophages

In 2001, Glasser, *et al.*, first time found that AIEC type strain LF82 can survive and replicate within J774.1 murine macrophages and human monocyte-derived macrophages (MDMs) without inducing host cell death resulting in high secretion of TNF-α (Glasser *et al.*, 2001; Bringer *et al.*, 2006). There is increasing evidence that, unlike non-pathogenic bacteria that are killed effectively by macrophages, AIEC are able to resist the killing action of macrophages within MDMs isolated from healthy controls, and patients with CD and UC (Elliott *et al.*, 2015; Vazeille *et al.*, 2015). The phagocytosis of LF82 by macrophages was accompanied by a rapid replacement of plasma membrane proteins by early endosomal antigen 1, allowing the AIEC phagosome to mature to the late endosomal stage, where Rab7 GTPase is acquired (Bringer *et al.*, 2006). Furthermore, on the AIEC-containing phagosome, peripheral transmembrane glycoproteins called Lamps were also observed on the peripheral side of the membrane, as well as increased intraluminal concentrations of degradative protease cathepsin D (Bringer *et al.*, 2006). In analysis of these phagosomes containing LF82, cathepsin D was found to be in an active proteolytic form, as well as the phagosome having an acidic pH. As a result of pH-neutralizing agents, such as chloroquine and ammonium chloride, intracellular replication of LF82 was inhibited, suggesting that acidic pH may activate expression of virulence genes that enable AIEC to thrive in this niche. Recently, Demarre *et al.*, found LF82 perform a switch between replicating and not replicating within macrophages, and this shift depends on genotoxic damage, the SOS and stringent responses (Demarre *et al.*, 2019). The adaptation of LF82 to phagolysosomal stress is characterized by a long lag time during which many LF82 cells become antibiotic-tolerant. Simultaneously they

are found to proliferate in vacuoles and multiply into colonies containing dozens of bacteria, indicating that intracellular LF82 forms biofilm-like communities in order to protect itself from phagolysosomal attack (Demarre *et al.*, 2019; Prudent *et al.*, 2021).

1.4.1 Factors involved in facilitating AIEC survival and replication within macrophages

In phagolysosomes that are extremely harsh environments, AIEC might be able to survive and replicate by expressing bacterial virulence factors. Stress present in the phagolysosomes induces the expression of almost all factors that are essential to the intramacrophage survival and/or replication of AIEC. The screening of a transposon mutant library constructed in LF82 suggests that five genes (*htrA*, *dsbA*, *yfgL*, *slyB*, and *yraP*) are involved in the resistance of these bacteria to macrophage degradation (Bringer *et al.*, 2005, 2007; Cieza *et al.*, 2015).

htrA

In acidic pH conditions, the HtrA stress protein is essential for the survival and replication of LF82 within macrophages. A 38-fold increase in *htrA* expression was observed in intramacrophage LF82, but there was no upregulation seen in a non-pathogenic *E. coli* K-12 strain after phagocytosis (Bringer *et al.*, 2005). Similarly, *htrA* is also required for *Salmonella*, *Legionella pneumophila*, and *Brucella abortus* to replicate within macrophages (Bäumler *et al.*, 1994; Elzer *et al.*, 1996; L. *et al.*, 2001; Eriksson *et al.*, 2003).

Hfq

Hfq is a gene regulator that controls the virulence and fitness of several intracellular bacteria by regulating small RNA (sRNA)-based gene expression (Oliva, Sahr and Buchrieser, 2015). Hfq functions by binding to small regulatory RNA molecules, allowing them to more easily interact with their targets, usually mRNAs (Sauer, Schmidt and Weichenrieder, 2012). Deficiency of Hfq prevents AIEC from surviving and replicating in the mouse macrophage cell line J774 (Simonsen *et al.*, 2011). Furthermore, deletion of *Hfq* increased the sensitivity

of LF82 to respond to a range of phagolysosomal stresses such as low pH, reactive oxygen species, and reactive nitrogen species (Sasaki *et al.*, 2007).

ibeA

The invasion of the brain endothelium protein A (*IbeA*) gene contributes to invasion, macrophage survival and inflammatory response (Cieza *et al.*, 2015). It was found that the *ibeA* virulence gene was more common in *E. coli* isolates from patients with CD than those from controls (Conte *et al.*, 2014). In humans, this gene is shown to encode a 50-kDa outer membrane protein with seven predicted transmembrane domains as well as expanded layers passing from the cell membrane to the extracellular space (Cieza *et al.*, 2015).

dsbA

A member of the Dsb protein family is responsible for the formation of disulfide bonds, which play a critical role in protein synthesis, particularly located in periplasms or on the surfaces of Gram-negative bacteria (Heras *et al.*, 2009). The role of *dsbA* in virulence has already been reported for many pathogens. LF82 *dsbA* mutants failed to replicate within macrophages (Bringer *et al.*, 2007).

gipA

A higher proportion of *E. coli* harbouring the gipA gene was found in CD patients (27.3%) than in controls (17.2%) (Vazeille *et al.*, 2016). *gipA* expression is induced by reactive oxygen species, a stress to which bacteria within the intracellular environment are particularly exposed (Vazeille *et al.*, 2016). Furthermore, *gipA* plays a key role in AIEC resistance to oxidative stress and enabling replication within macrophages, and it has been demonstrated in a mouse model that deletion of *gipA* impairs translocation of AIEC to MLN (Vazeille *et al.*, 2016).

1.4.2 Role of Autophagy in AIEC Replication

There is increasing evidence that autophagy is involved in the aetiology of CD, which is in turn linked to susceptibility polymorphisms in autophagy-associated

genes (*ATG16L1*, *NOD2* and *IGRM*) (Singh *et al.*, 2006; Fujita *et al.*, 2008; Cooney *et al.*, 2010). Autophagy is a cellular process conserved in all eukaryotes that destroys cytoplasmic material such as aggregated proteins, damaged mitochondria or invading pathogens inside lysosomes. Phagocytosis or autophagy can be used by macrophages to combat bacterial infections (Glick, Barth and Macleod, 2010). During phagocytosis, *E. coli* are detected via membrane receptors TLR4 and TLR5 (Sanjuan, Milasta and Green, 2009; Underhill and Goodridge, 2012). During infection with LF82, macrophages rapidly recruited the autophagy machinery at the entry site of the bacteria and also restricted their replication (Lapaquette, M. A. Bringer and Darfeuille-Michaud, 2012). Interesting to note that TLR4 has also been shown to be associated with activating autophagy by recruiting the autophagy cargo protein NOD2 and autophagosome marker ATG16L1 to the site of bacterial entry (Lapaquette, M. A. Bringer and Darfeuille-Michaud, 2012; Ungaro *et al.*, 2014). Thus, it would appear that autophagy and phagocytosis have an important regulatory crosstalk to work together. Compared to MDMs from UC patients or healthy controls, MDMs from CD patients contain greater levels of internalised AIEC and are incapable of limiting AIEC intracellular replication, with a consequence of disordered inflammatory responses (Elliott *et al.*, 2015; Vazeille *et al.*, 2015). Nonetheless, an increased number of LF82 replicating within cells, and the secretion of TNF-α and IL-6, was seen when CD-associated genes ATG16L1, IRGM or NOD2 were impaired in macrophages (Lapaquette, M. A. Bringer and Darfeuille-Michaud, 2012; Ungaro *et al.*, 2014). Therefore, autophagosomes in macrophages are effective at killing AIEC, and deficiencies in autophagy are linked to CD and AIEC persistence. Currently, researchers have been linking macrophage dysfunction in CD to autophagy-associated genes IRGM and ULK-1 (Lapaquette, M. A. Bringer and Darfeuille-Michaud, 2012). In CD patients therefore, a possible working hypothesis is that AIEC make use of autophagy deficiency to survive and replicate within macrophages inducing an increased pro-inflammatory response.

1.4.3 Secretion of Cytokines

There has been accumulating research on the sequestration of MDMs from a healthy population and patients with CD or UC in response to infection with AIEC, non-AIEC, or laboratory *E. coli* strains. Vazeille, *et al.*, observed that a higher amount of IL-6 and TNF-α were secreted by AIEC-infected MDM isolated

from patients with CD, as compared to AIEC-infected MDM obtained from UC patients and healthy individuals (Vazeille *et al.*, 2015). Additionally, there was an increase in IL-6 and TNF-α secretion in MDM sourced from CD patients infected with AIEC compared with non-pathogenic *E. coli* (Vazeille *et al.*, 2015). Interestingly, in the murine macrophage cell line J774-A1 as well as in MDM from CD patients, there has been a correlation between the number of intracellular AIEC and the amount of secreted TNF-α (Bringer *et al.*, 2012; Vazeille *et al.*, 2015). Alternatively, *in vitro* experiments have suggested that TNF-α secretion could be required for replication of AIEC within macrophages (Bringer *et al.*, 2012). Macrophages treated with TNF-α were seen to enable AIEC to replicate intracellularly, whereas macrophages incubated with anti-TNF-α antibodies prevented AIEC replication (Bringer *et al.*, 2012). Macrophages infected with AIEC secrete different amounts of TNF-α, thus increasing the number of AIEC residing within macrophages, showing that targeting TNF-α might be an effective way to control the proliferation of AIEC within macrophages. Despite this, the cellular mechanism underlying the action of TNF-α on AIEC replication within macrophages is still not fully understood.

1.4.4 Release of Exosomes

Exosomes, small extracellular vesicles with a diameter of about 30 to 100 nm are produced by most cell types including IECs and macrophages as a result of the fusion of multivesicular bodies with plasma membrane, which cells communicate with each other by transferring bioactive contents such as noncoding RNA and immune regulatory proteins (Carrière *et al.*, 2016). In immune regulation, exosomes play a significant role as they participate in antigen presentation, T-cell activation, and immune suppression, and they have already been implicated in infection (Greening *et al.*, 2015; Larabi, Barnich and Nguyen, 2020a). Recent work has demonstrated that upon infection with AIEC, immune cells and intestinal epithelial cells initiate the release of exosomes that are subsequently taken up by uninfected cells, causing an inflammatory response and poor clearance of intracellular AIEC (Carrière *et al.*, 2016). The amount of exosomes released by AIEC-infected T84 IECs were greater than those released by uninfected or non-pathogenic *E. coli*. Exosomes from AIEC-infected cells were capable of modulating NF-κB and MAPK pathways to activate naive T84 cells and naive THP-1 macrophages to exude pro-inflammatory cytokines (Carrière *et al.*,

2016). Consequently, upon AIEC infection, exosomes were released to trigger a pro-inflammatory response in neighbouring IECs but also in macrophages. *In vitro* experiments have demonstrated that exosomes freed from LF82-infected RAW 264.7 cells or THP-1 cells produced a similar pro-inflammatory response (Carrière *et al.*, 2016; Larabi, Barnich and Nguyen, 2020a). Furthermore, exosomes released from AIEC LF82 infected cells can be involved in the viral replication process. Exosomes released from uninfected IECs or macrophages, inhibited LF82 intracellular replication while those released from infected RAW 264.7 or THP-1 cells increased LF82 replication. *In vivo*, a similar pro-inflammatory response was induced by exosomes released from LF82-infected CEABAC10 mice in the ileum, which suggests that AIEC are able to use exosomes as a tool to replicate and to provoke inflammatory responses in neighbouring cells (Chervy, Barnich and Denizot, 2020). Recent work found that exosomes containing human milk oligosaccharides (HMOs) were taken up by macrophages, which were responsible for the establishment of intestinal immunity. To be specific, mice pre-treated with exosome encapsulated HMOs were observed to be protected from infection by AIEC, as well as LPS-induced inflammation and intestinal damage (He *et al.*, 2021). Similarly, macrophages infected with other intracellular pathogens, such as *Salmonella enterica* serovar Typhimurium, *Toxoplasma gondii*, *Mycobacterium tuberculosis* or *Mycobacterium bovis*, have been reported to secrete exosomes containing bacterial antigens, bacteria- and host-derived nucleic acids, as well as modulating the immune response of uninfected surrounding cells (Bhatnagar *et al.*, 2007; Giri and Schorey, 2008; Giri *et al.*, 2010; Singh *et al.*, 2012; Cheng *et al.*, 2019). Since exosomes are present and highly stable in most bodily fluids, as well as containing various contents under different pathological conditions, they can serve as potential carriers of therapeutic compounds.

1.5 Therapeutic strategies directed at macrophages

Currently, the main treatments used in CD that target macrophages and their activity, are anti-inflammatory medications (corticosteroids and aminosalicylates), immunosuppressants (azathioprine, methotrexate and mercaptopurine), and biologic drugs (anti-TNFα agents such as vedolizumab; IL-12/23 antagonist ustekinumab) (Roda *et al.*, 2020; Greuter *et al.*, 2021).

1.5.1 Immunosuppressive Compounds Targeting Macrophages

In the last two decades, macrophage-targeting therapies have become a more popular treatment option for IBD (Na *et al.*, 2019).

In many clinical practices, corticosteroids such as budesonide and prednisone have been used successfully for CD management for many decades (Khan *et al.*, 2018). It is especially noteworthy that corticosteroids are very effective in inducing remission in most children (Hyams *et al.*, 2006; Markowitz *et al.*, 2006). It is still unclear exactly how they work, despite their widespread use. The anti-inflammatory effects of corticosteroids are primarily attributed to their ability to influence multiple signal transduction pathways through the glucocorticoid receptor. To be specific, they inhibit the expression of inflammatory genes and increase expression of anti-inflammatory genes via transcription factors activator protein 1 (AP-1) and NF-κB (McKay and Cidlowski, 1998). In addition, corticosteroids have a particular effect in attenuating the NF-κB pathway which plays a crucial role in mucosal inflammation (Atreya, Atreya and Neurath, 2008). In macrophages, glucocorticoid receptors are highly expressed, and upon activation by liberated corticosteroids, these receptors suppress NF-κB activity, reduce macrophage activity, and consequently reduce the secretion of pro-inflammatory cytokines, such as TNF-α, IFN-γ, IL-2 and IL-12 (Schwenger, 1998; Berrebi *et al.*, 2003; Elenkov *et al.*, 2005; Glass *et al.*, 2010).

Thiopurines (azathioprine and 6-mercaptopurine) and methotrexate have been used in IBD treatment since the 1960s (Rosen and Dubinsky, 2016). Among immunosuppressive compounds, azathioprine is distinguished by its mechanism of action involving decreased synthesis of purines, which ultimately leads to apoptosis of fast-proliferating cells such as CD4+ T cells (Aguilar *et al.*, 2014). Until recently, the only mechanism thought to account for azathioprine's immunosuppressive properties was the cytotoxic effect (Marshall, 1995). Nevertheless, other studies have shown that thiopurines influence macrophage proliferation and inflammation as well as functions such as phagocytosis and chemotactic responses (Moeslinger, Friedl and Spieckermann, 2006; Marinković *et al.*, 2014). In CD azathioprine inhibits nitric oxide synthase, a specific macrophage activation marker expressed more abundantly in mucosa of active patients. It could also inhibit CD163 expression, a macrophage activation marker

expressed more abundantly in mucosa of CD patients (Moeslinger, Friedl and Spieckermann, 2006; Franze *et al.*, 2013; Marinković *et al.*, 2014; Davis, 2015; Zhang *et al.*, 2015; Brunner *et al.*, 2019).

Another immunosuppressive molecule, 6-mercaptopurine, suppresses macrophages with the mRNA expression of monocyte chemotactic protein-1, which upregulated in CD and it functions in regulation of migration and infiltration of monocytes and macrophages (Grip, Janciauskiene and Lindgren, 2004; Pols *et al.*, 2010). Several *in vitro* studies have demonstrated that methotrexate induces apoptosis in primary murine macrophages and suppresses NF-κB activity at low concentrations, when administered *in vitro* (Lo, Steer and Joyce, 2011). Methotrexate is also thought to have proinflammatory effects, though its mechanisms are not known (Feagan *et al.*, 2014; Olsen, Spurlock and Aune, 2014).

1.5.2 Anti-TNF-α Therapy

The use of anti-TNF-α therapy, such as adalimumab, infliximab and certolizumab has transformed the management of CD on a global scale over the past two decades. There is increasing evidence that these drugs are being used earlier in the disease course, and they are the therapy of choice, particularly for patients who have a high risk of developing the disease. Even though these targeted biologic therapies are major advances in the treatment of CD, they are also associated with significant safety concerns because of intravenous administration and possible immunogenicity (Greuter *et al.*, 2021).

Several mechanisms are thought to mediate the effects of anti-TNF-α antibodies, including neutralisation of TNF-α, reversing signalling, and inducing cell death (Berns and Hommes, 2016). The dysfunction of TNF-α is caused by anti-TNF-α antibodies binding soluble and transmembrane TNF-α or its receptors, resulting in blockage of pro-inflammatory signals. In *in vitro* experiments, anti-TNF-α treatment supresses cytokines release by reverse signalling (Eissner *et al.*, 2000; Eissner, Kolch and Scheurich, 2004). In addition, anti-TNF-α also acts as a ligand when it binds to the cell-surface bound precursor of TNF-α, which leads to stimulation of a multiple biological processes of targeting cells, such as cell activation, cytokines suppression or apoptosis (Berns and Hommes, 2016).

Furthermore, The Fc region of some anti-TNF-α antibodies (such as infliximab and adalimumab, but not certolizumab) can cause antibody-mediated cytotoxicity and complement-mediated cytotoxicity (Mitoma *et al.*, 2018).

Infliximab is a 149 kDa human-murine chimeric monoclonal IgG1 antibody, composed of a 25% murine variable region and a 75% human constant region that are linked by a disulfide bond (Bell and Kamm, 2000). this antibody binds with greater specificity and affinity to membranous TNF-α on activated T cells and possess an Fc region interacting with the Fc receptor on antigen-presenting cells, resulting in a rapid increase in complement activation and subsequent cytotoxicity of CD4+ macrophages and T cells (Scallon *et al.*, 1995; Dige *et al.*, 2014), counteracting the pathological mechanism in CD where mucosal T cells proliferate in excess of T cell apoptosis (Van den Brande *et al.*, 2007). As a consequence of these interactions, blood-derived monocytes differentiate to macrophages that possess a regulatory phenotype (CD206+) harbouring anti-inflammatory properties (Dige *et al.*, 2014). Additionally, infliximab promotes peripheral blood CD4+ and CD8+ T cell production, preventing Th1 lymphocytes from homing into inflamed tissue (Maurice *et al.*, 1999). Anti-TNF-α treatments including infliximab and adalimumab decreased soluble CD163 (a specific biomarker of macrophage activation) levels in CD patients, indicating that anti-TNF-α agents may target macrophage activation directly in CD (Lügering *et al.*, 2001; Shen *et al.*, 2005).

The effect of infliximab treatments on circulating monocyte subsets and macrophages cytokine production in response to bacterial infection also have been analysed. Nazareth and colleagues have found that infliximab treatment increased the production of CD macrophage–induced TNF-α in response to bacteria (AIEC, *Mycobacterium avium paratuberculosis* (MAP) and *M. avium avium*) (Nazareth *et al.*, 2014). Meanwhile, they detected MAP and AIEC DNA from macrophages isolated from CD patients with or without infliximab treatment, and the results have shown that in CD patients, the prevalence of MAP decreases with remission and further with infliximab treatment, but these findings have been not observed with AIEC (Nazareth *et al.*, 2015). To date, the ability of macrophages from CD patients treated with anti-TNF-α to control intramacrophage AIEC infection remains an unknown concern that remains to be

explored since little data have been available (Lapaquette, M. A. Bringer and Darfeuille-Michaud, 2012; Vazeille *et al.*, 2015).

1.5.3 Activation of Autophagy

Autophagy is triggered after AIEC infection in order to limit their intracellular replication and thus prevent their persistence. As noted above, there are CD-associated variants in autophagy-related genes such as *ATG16L1*, *IRGM*, and *NOD2* that their mutations favour AIEC intracellular replication and persistence in the gut. Lapaquette and colleagues demonstrated that physiological (starvation) and pharmacological (rapamycin) induction activating autophagy led to the inhibition of AIEC intracellular replication and pro-inflammatory cytokine (TNF-α and IL-6) release in NOD2 deficit murine macrophages (Lapaquette, M. A. Bringer and Darfeuille-Michaud, 2012). Another *in vitro* experiment, using a current IBD drug azathioprine activated autophagy in THP-1 macrophages, which enhanced the clearance of intracellular AIEC and reduced pro-inflammatory cytokine release (Hooper *et al.*, 2019). This drug also successfully activated autophagy in peripheral blood mononuclear cells from individuals who presents a CD-associated variant for ATG16L1 (Hooper *et al.*, 2019). Thereby, to limit AIEC persistence and slow down inflammation response, activating autophagy with pharmaceutical drugs might be an interesting therapeutic solution in CD patients whose genes are polymorphic in autophagy-associated genes.

1.6 Main Aims

Previous studies found that crossing to the lamina propria, AIEC can be engulfed by innate immune cells such as dendritic cells, neutrophils, and macrophages. Most importantly, they are capable of replication in an environment with an acidic pH, oxidative stress, active proteolytic enzymes, and antimicrobial compounds. Macrophages are key players in the infection process and preventing systemic bacterial circulation in the host. There is still much to be learned about host-pathogen interactions that govern AIEC infection biology. There is a need to develop new therapeutic agents in order to inhibit the survival and replication of these intracellular bacteria. This study aimed to provide novel insights into the role of macrophages in the response to AIEC, eventually screening potential

chemical inhibitors not previously used in CD, to determine their ability to control of AIEC replication within macrophages.

Macrophages are highly heterogenous during AIEC infection and can alter their phenotype and function in response to different intracellular bacterial load. To understand the interaction between host and pathogen, imaging flow cytometry (IFC), which can carry out both fluorescent microscopy and flow cytometry simultaneously, allowed the analysis of thousands of cells and their intracellular bacterial load, identifying different populations of infected cells and their response to infection. For example, using IFC enabled us to identify morphological characteristics of infected macrophages such as being mononucleated, binucleated and multinucleated cells, and to analyse how bacteria influenced this process and how these cell-cell connections could potentially lead to granulomas being formed.

In addition, the growth rate of intracellular AIEC can vary greatly within macrophages, which can have major consequences for infection outcomes. Therefore, it was deemed useful to understand how AIEC-macrophage interactions contribute to this intracellular AIEC growth heterogeneity. To date, there has been a lack of understanding regarding how this heterogeneity arises, why some macrophages kill AIEC while others are unable to do so. In this study, a combination of fluorescent-based cell sorting and RNA-seq were conducted to address this question. Through this transcriptomic approach, novel genes of interest were identified and their role in facilitating intracellular replication by AIEC in macrophages was further investigated by chemical inhibition.

Chapter 2 General Methods and Materials

2.1 Bacterial Strain and Culture Conditions

Strains used in this study are listed in Table 2-1 and these were routinely cultured in lysogeny-broth (LB) at 37ºC with shaking at 180 revolutions per minute (rpm) (Darfeuille-Michaud *et al.*, 1998). Prior to infection, strains were grown overnight in Roswell Park Memorial Institute (RPMI)-1640 media (21875034, Invitrogen) supplemented with 3% heat-inactivated foetal bovine serum (FBS; F9665, Sigma-Aldrich), and 1% L-glutamine (25030024, Invitrogen). *In vitro* infections were carried out using LF82 transformed with a reporter plasmid, pAJR70 expressing enhanced green fluorescent protein (eGFP) under the control of the *rpsM* promoter (Roe *et al.*, 2003). GFP expression was measured in a black 96-well plate (excitation at 485 nm; emission at 550 nm) using a FLUOstar Optima Fluorescence Plate Reader (BMG Labtech).

Escherichia coli strains B94, B115, B122 and B125 are clinical isolates from CD patients with a median age of 13.7 who have participated in the "Bacteria in Inflammatory Bowel Disease in Scottish Children Undergoing Investigation Before Treatment" (BISCUIT) study (Hansen *et al.*, 2013). Histologically, 50 % of the cases were found to have granulomas. Based on Paris criteria (Levine *et al.*, 2011) at diagnosis, phenotypic structure was identified as follows: B94- colonic, non-stricturing/non-penetrating (L2, B1); B115- colonic, non-stricturing/non-penetrating (L2, B1); B122- ileocolonic, stricturing (L3, B2); B125- ileocolonic, non-stricturing/non-penetrating (L3, B1).

Table 2-1 Strain Information

Strain	Description	Reference
LF82	Adherent-invasive *E. coli*	Prof. Daniel Walker, University of Glasgow
LF82 *rpsM*::GFP	LF82 expressing GFP	
F18	Commercial strain	
SL1344	*Salmonella Typhimurium* strain	
B95	Clinical isolate AIEC	
B115	Clinical isolate AIEC	
B122	Clinical isolate AIEC	
B125	Clinical isolate AIEC	

2.2 Cell Culture

The RAW 264.7 murine macrophage-like cell line was obtained from the American Type Culture Collection (ATCC). RAW 264.7 cells were cultured in RPMI-1640 media supplemented with 10% heat-inactivated FBS, 1% penicillin/streptomycin (P/S) (15140122, Invitrogen), and 1% L-glutamine (maintenance media) at 37°C in 5% CO_2.

2.3 Bacterial Infections

RAW 264.7 cells were seeded into a 24-well plate at a density of 2 x 10^5 cells-per-well 24 hours prior to infection. Twelve hours prior to infection, maintenance media was replaced with RPMI-1640 media supplemented with 3% FCS and 1% L-glutamine containing 1 µg/ml lipopolysaccharide (LPS) (L7770, Sigma-Aldrich) for macrophage activation. Cells were infected at a multiplicity of infection (MOI) of 100 and incubated at 37°C /5% CO_2 for 1 hour. After 1 hour the infected RAW 264.7 cells were washed twice with fresh RPMI-1640 cell culture media to remove excess extracellular bacteria and incubated at 37°C /5% CO_2 in maintenance media with 50 µg/ml gentamicin to kill any remaining extracellular bacteria. The infected cells were then incubated for the time specified at 37°C/5% CO_2.

To measure bacterial intra-macrophage survival, infected macrophages were washed with RPMI-1640 media, and lysed using 200 µl of 2% Triton X-100 (93443, Sigma-Aldrich) in phosphate buffered saline (PBS, 14190094, Invitrogen) for 5 min at room temperature. Lysates were removed, serially diluted in PBS, and plated onto LB agar plates to determine the number of colony forming units (CFU) per ml. Total protein concentration was determined using a BCA assay (23227, Thermo Fisher Scientific Life Technologies) and bacterial numbers were normalised to total protein concentration and presented as CFU/g. Normalising CFU to protein concentration, as opposed to expressing CFU numbers per well, meant CFUs could be related to cell density/number in each individual well, especially important if cell numbers differed between wells due to proliferation or cell death during infection or drug treatment. Expressing as CFU per ml would not take this into account.

2.4 Lactate Dehydrogenase Assay to Monitor Cytotoxicity

RAW 264.7 cells were infected at an MOI of 100 and supernatants of LF82 infected and control uninfected macrophages were sampled at different time points post-gentamicin treatment, centrifuged at 10,000 x g for 4 min and assayed for lactate dehydrogenase (LDH) activity (11644793001, Roche). LDH activity is reported as milliunit/ml. One unit of LDH activity is defined as the amount of enzyme that catalyses the conversion of lactate into pyruvate to generate 11.0 µmol of NADH per minute at 37^{o}C.

2.5 Caspase-3 Assay

Caspase-3 activity in cell lysates was measured using the Apo-One Homogenous Caspase-3 Activity Kit (G8091, Promega). Post-measurement caspase-3 activity was corrected for protein concentration (BCA Protein Assay Kit, Pierce) and expressed as caspase-3 activity Fluorescence Focus Units (FFU) per gram of protein. Samples were measured using a FluoStar Optima fluorescent plate reader (BMG Biotech).

2.6 Cell Counting Kit 8 (CCK-8) Assay for Detection of Cell Viability

Cell survival rates were estimated by the CCK-8 assay (ab228554, Abcam). Approximately 1 x 10^4 cells were seeded in 96-well plates with 100 µl medium each well. After 24 h cultivation, different doses of drugs were added for a further time point. Each well was incubated with 10 µl of CCK-8 solution for 2 h away from light before measuring the absorbance at 450 nm by FluoStar Optima fluorescent plate reader (BMG Biotech). The relative viability was expressed by the formula: % of viability = ((Aexp – ABlank)/Acontrol - ABlank)) X 100%.

2.7 Enzyme-linked Immunosorbent Assays (ELISA)

The amount of TNF-α secreted in the supernatants from cell culture and cell lysates was determined by ELISA MAX™ Deluxe Set Mouse TNF-α kit (430904, BioLegend) according to the manufacturer's instructions. TNF-α concentrations were normalised by protein concentration from cell lysates and were reported as ρg of TNF-α/ g of protein.

2.8 Gene Expression Analysis

2.8.1 RNA Extraction and Reverse Transcription

Cells or tissues were harvested post-infection and the RNA was isolated using a PureLink™ RNA Mini Kit (12183018A, Invitrogen) according to the manufacturer's specifications. Contaminating DNA was removed using TURBO DNA-free Kit (AM1907, Invitrogen) according to manufacturer's instructions and then RNA purification was conducted using Phenol:Chloroform:Isoamyl Alcohol 25:24:1 (P3803, Sigma). Purified RNA was solubilised in 30 μl of RNAse-free water and was quantified using a NanoDrop 2000 spectrophotometer (Thermo Fisher Scientific). RNA was reverse transcribed into cDNA using the High-Capacity cDNA reverse transcription kit (Applied Biosystems) according to the manufacturer's guidelines. cDNA was stored at -20ºC until use.

2.8.2 Quantitative real-time PCR (qRT-PCR)

Gene expression was assayed by quantitative reverse transcription PCR (qRT-PCR) using SYBR Green FastMix (Agilent τechnologies) using primers obtained from DNA Oligos (Sigma) as detailed in Table 2-2. Individual cDNA samples were assayed in triplicate within each of the three biological replicates. The *Gapdh* gene was used to normalise the results. RT-PCR reactions were carried out using the CXF Connect Real-Time PCR Detection System (BIO-RAD Laboratories, Inc.). According to manufacturer's specifications and the data were analysed according to the $2^{-\Delta\Delta CT}$ method (Livak and Schmittgen, 2001).

Table 2-2 Primers used in qRT-PCR

Gene	Sense	Anti-Sense
Pyk2	GGACTATGTGGTGGTGGTGA	TCTGCCAGGTCTTTGTTGAG
GapDH	CAACTTTGGCATTGTGGAAGGGCTC	GCAGGGATGATGTTCTGGGCAGC

2.9 Western Blotting

Infected or uninfected cells were washed with PBS 3 times before being lysed for 15 min in radioimmunoprecipitation assay (RIPA) lysis buffer (ThermoFisher) supplemented with cOmplete™ Mini (EDTA) Protease Inhibitor Cocktail

(11836170001, Roche) and PhoSTOP™ phosphatase inhibitor (4906845001, Roche). Lysates were frozen at -80°C until use. Next day, cells were centrifuged at 14,000 X g for 10 min to harvest the protein-containing supernatant. The protein concentration of the cell extracts was determined using the Pierce™ BCA Protein Assay Kit (ThermoFisher Scientific). Protein concentration for lysates was adjusted to 2 µg/µl before adding 4 X NuPAGE® LDS Sample Buffer (NP0007, Invitrogen), heating to 95°C for 10 min and running on a 4-12% Bis-Tris SDS-PAGE gel (NP0321BOX, Invitrogen). Samples were transferred via electrophoretic wet transfer to a polyvinylidene fluoride (PVDF) membrane. The membrane was blocked in 5% non-fat milk in PBS-Tween (PBS-T) (0.05%) for 1 hour and probed with a 1:1,000 dilution of primary antibody overnight at 4°C with sharking. Blots were visualised with HRP-conjugated secondary antibody (1:10,000) (ThermoFisher Scientific) and developed using enhanced chemiluminescence (ECL, 32106, Thermo Fisher Scientific) and imaged using a C-DiGit blot scanner (LI-COR). Membranes were stripped in 0.1 mM glycine, pH 2.2, and re-probed with anti-GAPDH (1:10,000; Abcam) antibody as a loading control. The bands were quantified using ImageJ software (Schneider, Rasband and Eliceiri, 2012). All Western blots were performed in triplicate, with each performed on a biological replicate. The antibodies used for Western blotting are listed in Table 2-3.

Table 2-3 List of antibodies for Western Blot

Antibody	Species	Reference	Manufacturer
Pyk2	Rabbit monoclonal	ab32448	Abcam
phosphorylated Pyk2	Rabbit polyclonal	ab4800	Abcam
GapDH	Rabbit monoclonal	2118	Cell Signalling Technology
Anti-Rabbit antibody (HRP)	Goat	31460	Thermo Fisher Scientific

2.10 Immunofluorescence staining

Images for all experiments were captured using a Leica DMi8 fluorescent microscope. Cells were plated onto glass coverslips in 24-well-plates at 2 x 10^5 cells per well. Cells were fixed with 4% paraformaldehyde (PFA) solution for 15

minutes at 37°C, followed by permeabilization with 0.2% Triton X-100 for 4 minutes for 4°C after rinsing with Dulbecco's Phosphate-Buffered Saline (DPBS). Coverslips were treated with 1% bovine serum albumin (BSA)/DPBS to block non-specific binding for 30 min at 37°C. The primary antibodies were used at a specific dilution and then incubated with secondary antibodies conjugated with specific fluorophore for 2 hours at room temperature. Rhodamine phalloidin (R415, ThermoFisher) and DAPI were used for visualizing F-actin and the nucleus, respectively. Before image acquisition, the samples were incubated with a drop of antifade mounting medium with DAPI (H-1200, Vector Laboratories). Images were processed or analysed using ImageJ.

2.11 Imaging flow cytometry (IFC)

2.11.1 Antibody staining and sample acquisition

Cells were seeded onto 6-well plates with a density of 2 x 10^5 cells per ml. Post-infection, cells were harvested by adding 600 µl Trypsin/1 X EDTA (T3924, Sigma) per well for 5 minutes at 37°C and transferred to a 1.5 ml microfuge tube. Harvested cells were fixed using 250 µl Fix buffer (554655, BD biosciences) for 10 minutes at 37°C water bath, followed by permeabilization with 200 µl of Perm Buffer III (558050, BD biosciences) for 30 minutes on ice. Cells were then washed twice in FACS buffer and incubated with appropriate fluorochrome-conjugated antibodies for 30 minutes at 4°C protected from light. Before the acquisition, cells were resuspended in 50 µl of FACS buffer containing 5 µl 7-aminoactinomycin D (7-AAD; 420403, BioLegend) for staining of nuclei.

2.11.2 Data acquisition

IFC data acquisition was achieved using an ImageStream X MKII (ISX, Amnis) equipped with dual cameras and 405 nm, 488 nm, and 642 nm excitation lasers. All samples were acquired at 60 times magnification giving an optimal 7 µM visual slide through the cell, and a minimum of 10,000 single cell events were collected for each sample. In focus cells were determined by a gradient root mean square (RMS) for image sharpness. Brightfield of greater than 50 and single cells were identified by area versus aspect ratio. Laser wavelength from relevant channels were Channel 01 (Ch01, 374 nm), Ch02 (488 nm), Ch03 (561 nm), Ch04

(bright field), and Ch05 (642 nm). Single colour compensation controls were also acquired, and a compensation file was generated via IDEAS software (Luminex).

2.12 Statistical Analysis

Values are shown as means and standard deviation. All statistical tests were performed with GraphPad Prism software, version 8.3.0. All replicates in this study were biological; that is, repeat experiments were performed with freshly grown bacterial cultures and cells, as appropriate. Technical replicates of individual biological replicates were also conducted. Significance was determined as indicated in the figure legends. Values were considered statistically significant when p-values were $*$ = $p<0.05$; $**$ = $p<0.01$; $***$ = $p<0.001$; $****$ = $p<0.0001$.

2.13 Graphs generation

All illustrations were created with Biorender.com and Adobe illustrator.

Chapter 3 Image-based Approaches for Monitoring Host-Pathogen interactions during AIEC Infection of Macrophages

3.1 Introduction

AIEC have been implicated in the aetiology of Crohn's Disease (CD). AIEC are characterised by an ability to survive and replicate intracellularly in macrophages, which may contribute to dissemination of the pathogen further. Bacterial persistence within cells is thought to lead to immune evasion and chronicity of infections. Intracellular bacteria adherent, invade and live in the host eukaryotic cells, which are integral to the biology, pathology and evolution of infection (Fuchs *et al.*, 2012). *In vitro* bacterial infection models are often used to understand bacterial intracellular growth or host-bacteria interactions. Traditional quantitative measurements (colony-forming unit (cfu) counts) are based on a cellular population level, which quantify the intracellular bacteria load by lysing cell populations and subsequently counting the bacteria (Stevenson, Baillie and Richards, 1984). However, intracellular pathogen populations are heterogeneous. Infection of host cells with a clonal population of intracellular pathogen frequently results in variable numbers of bacterial pathogens in each host cell. Furthermore, these are a product of both replication within cells and killing sustained by the bacteria, and the relative contributions of these processes is difficult to distinguish (Helaine *et al.*, 2010).

A modern approach employs fluorescence-based technologies such as flow cytometry and fluorescent microscopy. However, these techniques have limitations. Microscopic analysis reveals heterogeneity during intracellular pathogen internalization but lacks the capability of quantification of large data sets while flow cytometry, while using a fluorescence signal, lacks the visual confirmation that can provide additional confidence in data sets. Imaging flow cytometry (IFC) is a novel emerging technique that combines the single-cell imaging capabilities of microscopy with the high-throughput capabilities of conventional flow cytometry. This makes it an extremely powerful tool for acquisition and analysis of hundreds of thousands of individual cellular or subcellular events in a single experiment. It allows study of the heterogeneity present during intracellular pathogen internalization and intracellular replication

that is induced by a variety of cell- and pathogen-dependent factors (Haridas *et al.*, 2017). In this investigation, we used IFC to monitor the survival and replication characteristics of the AIEC type strain LF82 in the murine macrophage RAW 264.7 cell line.

It is furthermore possible to use IFC to study the relationship between cells, such as multinucleated cells and cell colocalization. The understanding of multinucleated cells may be one of the most important aspects of CD. A histopathological hallmark of CD is the presence of granulomas. Typical findings from endoscopy in CD patients are granulomatous lesions infiltrating the gut and their discontinuous distribution involving any part of gastrointestinal tract (Lee and Lee, 2016). To date, clinical studies have demonstrated that lymphatic and blood vessels are essential for the formation and maintenance of CD epithelioid cell granulomas (Kodama *et al.*, 2020). Adams and his colleagues elucidated that the difference between granuloma formation and chronic inflammatory aggregation is the characteristic organisation of mature macrophages into dense structures (Adams, 1976). There is strong evidence that multinucleated cell generation is required for the evolution of epithelioid and necrotic granulomas. Multinucleated giant cells (MGCs) were first described by Theodor Langhans over 150 years ago in his studies on tuberculosis and were subsequently named Langhans giant cells in his honour (Helming and Gordon, 2009). The histological appearance of MGCs can be determined by the presence of three or more uniformly shaped nuclei within a large, much larger cell than a mononuclear leukocyte. As a matter of fact, we have little understanding of what causes MGCs. In the past few decades, it was believed that the only mechanism by which MGCs could form was cell fusion (Helming and Gordon, 2009). This fusion can be stimulated by cytokines, myeloid growth factors, as well as by mycobacterial lipids. Macrophages isolated from different tissues can be differentiated into MGCs *in vitro* (McNally and Anderson, 2015). To be specific, macrophages or monocytes can be differentiated into MGCs under several conditions, including culturing with IL-4 or IL-13, GM-CSF plus IL-4, IFN-γ plus IL-3, or mycobacterial glycolipids (DeFife *et al.*, 1997; Yagi *et al.*, 2005; Helming and Gordon, 2009; Miyamoto, 2013; McNally and Anderson, 2015). In summary of Pagán and Ramakrishnan's review, MGC formation is a macrophage-specific, macrophage-intrinsic, evolutionarily ancient program that occurs in response to

persistent extrinsic stimuli as well as developmental cues and intrinsic stimuli (Pagán and Ramakrishnan, 2018).

The granuloma immunological response described by Dalziel in 1913 is a localised accumulation of epithelioid cells, macrophages and lymphocytes (Smith and Wakefield, 1993). Such granulomas are associated with several infectious diseases involving *Mycobacterium tuberculosis*, *Salmonella spp.*, *Shigella spp.*, *Yersinia enterocolitica*, and other pathogenic bacteria able to enter and survive within host cells (Zumla and James, 1996). There is also evidence suggesting that AIEC is involved in the formation of granulomas (Palmela *et al.*, 2018). Like tuberculous granulomas, well-circumscribed granulomas develop during CD by the accumulation of lymphocytes and macrophages, the latter maturing to form epithelioid cells (Cronan *et al.*, 2016). Given the behaviour of AIEC strains within macrophages, it was decided therefore to investigate whether the AIEC type strain, LF82, like the tuberculous bacillus which also persists within macrophages, induces the formation of granulomas using the *in vitro* model of human granulomas developed by Dr. Puissegur in Dr. Altare's laboratory (Puissegur *et al.*, 2004). Previous work has demonstrated that LF82 induces aggregation of infected macrophages and subsequently activates the recruitment of lymphocytes (Meconi *et al.*, 2007). Given that a hypothesis of granulomas is caused by the AIEC induced MGCs. Schematic process of the formation of granulomas driven by bacterial and host factors in the CD patients was shown in Figure 3-1.

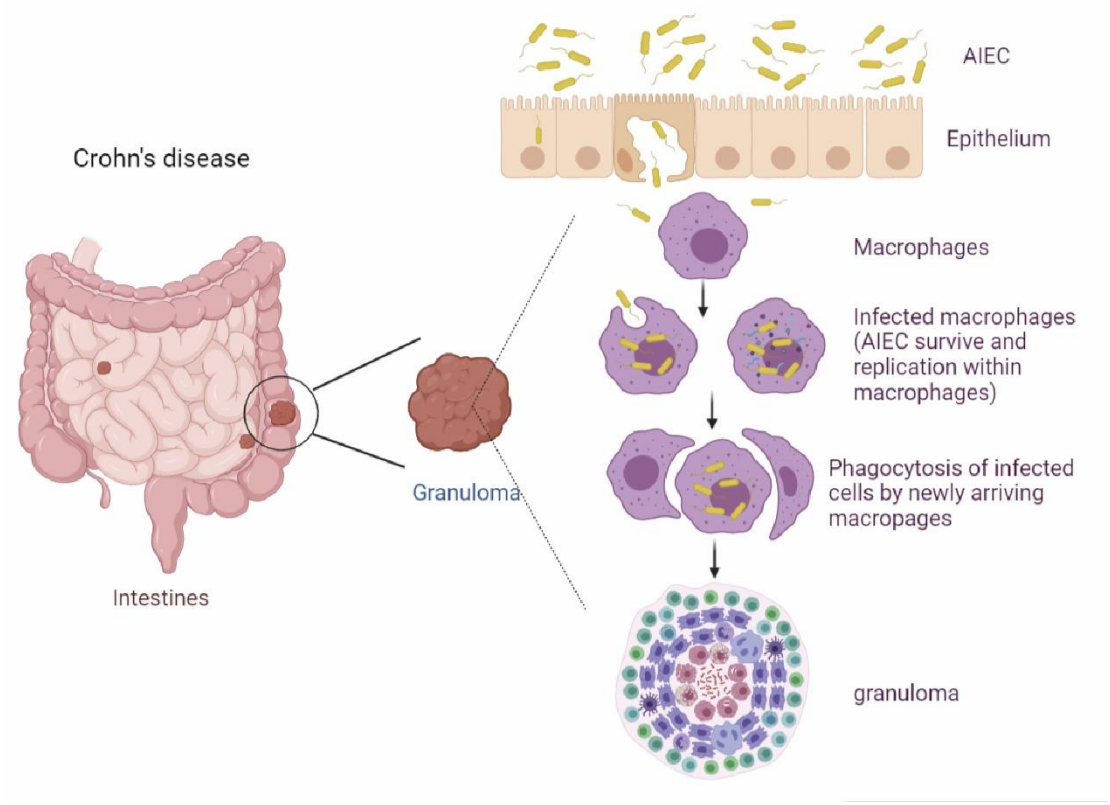

Figure 3-1 The putative role of macrophages during the formation and function of AIEC granulomas.

Once AIEC cross the epithelial barrier, they are phagocytosed by macrophages. Intracellular AIEC survive and replicate within macrophages without inducing cell death. Infected cells are phagocytosed by newly arrived macrophages. Continued phagocytosis causes macrophages to aggregate and leading to granulomas.

AIEC plays a key role in inducing cell aggregates, however, despite accumulating knowledge of the association of pathogenic bacteria with the formation of granulomas, few studies have investigated the interaction between AIEC and MGCs. Here during a preliminary immunofluorescent experiments, at 24 hours post-infection, the presence of multinucleated macrophages was confirmed during LF82 infection (Figure 3-2). To further understand how LF82 regulates cell-cell interaction during infection, we investigated LF82-host interactions using both fluorescent microscopy and IFC.

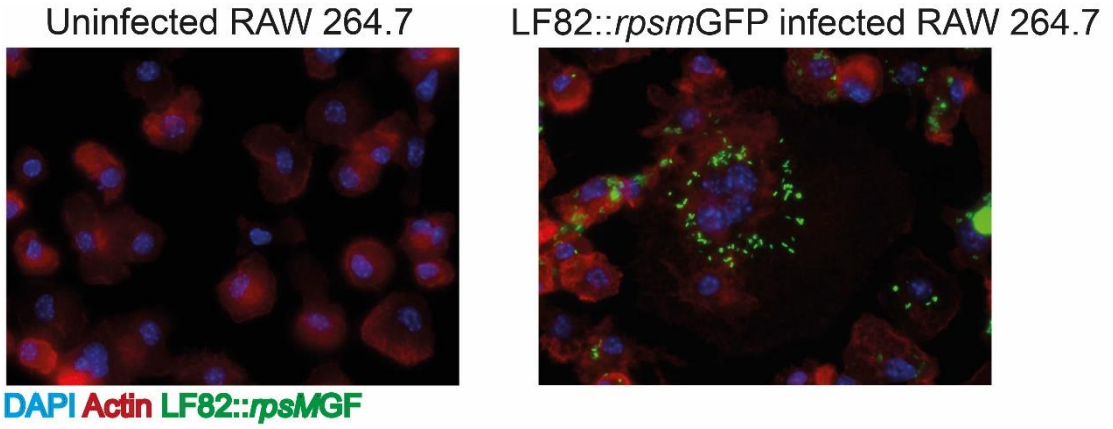

Figure 3-2 Observation of multinucleated cells at 24 hours post-infection (hpi).

RAW 264.7 cells were infected with LF82::*rpsM*GFP alongside with uninfected cells. Twenty four hpi, infected or uninfected cells were fixed and stained with phalloidin for visualising cytoplasmic actin and DAPI for nucleic acid in the nucleus. Samples were imaged using fluorescent microscopy. Single cells containing more than 2 nuclei were determined to be multinucleated cells.

The aim of this chapter was to establish IFC or fluorescent microscopy approaches to monitor LF82-macrophages interactions: (1) quantify intracellular bacteria in individual cells; (2) quantify the population of multinucleated cells during infection; and (3) explore specific aspects of cell-cell interactions and cell population dynamics during LF82 infection.

3.2 Methods and Materials

3.2.1 Electrotransformation of LF82 with a GFP plasmid

A fluorescent reporter plasmid pAJR70 a kind gift from Professor Andrew Roe's lab was previously constructed based on a promoter-less plasmid pACYC184 containing a chloramphenicol resistance gene, an origin of replication (p15A) of *E. coli*, and GFP was cloned in with *Ban*HI/*Bgl*II sites (Roe *et al.*, 2003). Competent LF82 was suspended in 50 μl of distilled water and gently mixed with 1 μg of plasmid pAJR70 in a cooled electroporation cuvette on ice for 1 minute. Electroporation was carried out with an electroporator device (Biorad gene Pulser) with a voltage of 1.8 kV. After transformation, the bacterial suspension was immediately topped up with 1 ml of super optimal broth with catabolite repression (SOC) medium (2% Bacto tryptone, 0.5% Bacto yeast extract, 10 mM NaCl, 2.5 mM KCl, 10 mM $MgCl_2$, 10 mM $MgSO_4$, 20 mM glucose) and incubated at 37°C for 1 hour with shaking at 180 rpm. Two hundreds μl of bacterial suspension

was plated onto an LB agar plate with 34 µg/ml chloramphenicol. Plates were incubated overnight at 37°C and candidate colonies were harvested.

3.2.2 LF82 infection assays using IFC

Data analysis—IDEAS software

Data for samples was collected using the ImageStream X MKII (ISX, Amnis), analysis was performed using IDEAS software. Using IDEAS software, masks (areas of interest) and features (calculations made from masks) were generated to give a quantitative measurement of the images collected.

Identification of in-focus single-cell events

To quantify variable numbers of intracellular bacteria in each single cell, firstly single cell events in focus were identified employing the scatter plot utilizing area versus aspect ratio as described in Figure 3-3a (representative images of single cell (Figure 3-3c) and duplet cells (Figure 3-3d). In focus cells were determined by a gradient RMS bright field channel of greater than 50 value (Figure 3-3b) with representative images [out of focus cells (Figure 3-3e) and in focus cells (Figure 3-3f)]. The first filter step was necessary to eliminate debris and cell aggregates.

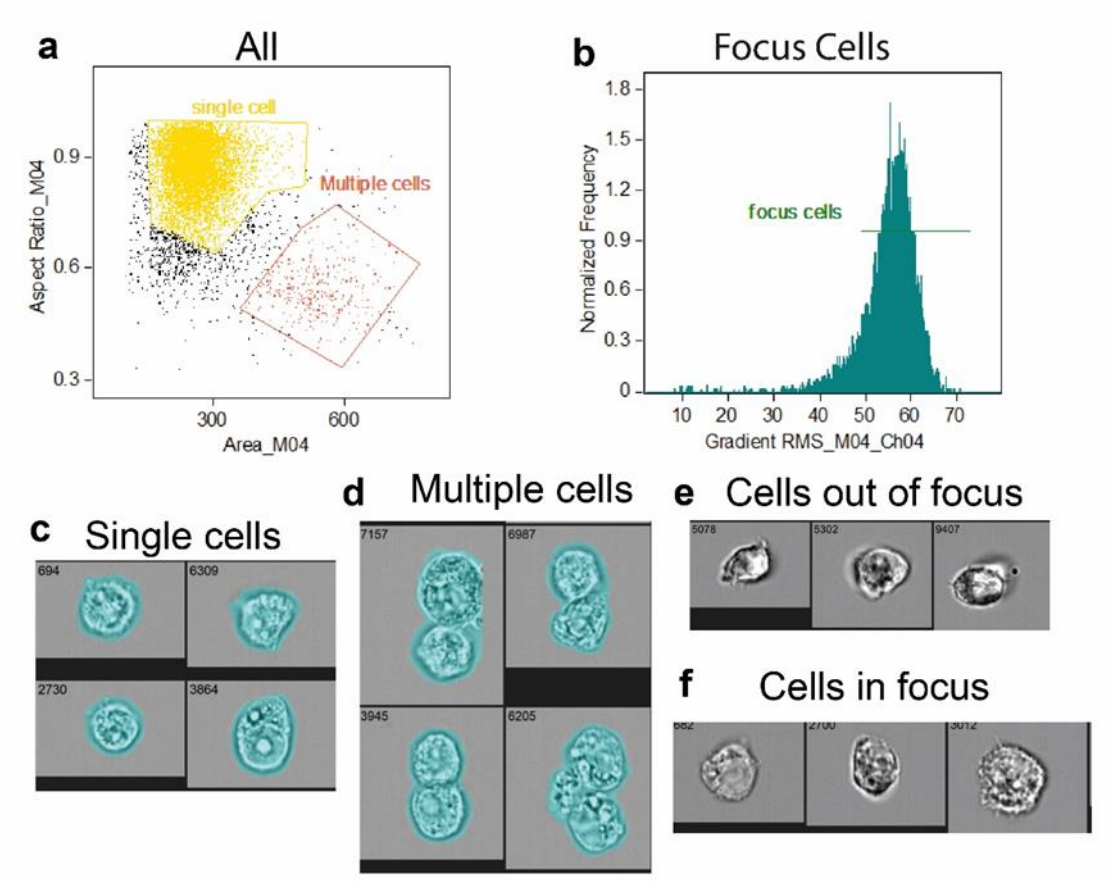

Figure 3-3 IDEAS analysis of LF82::*rpsM*GFP infected cells.

RAW 264.7 cells were infected with LF82::*rpsM*GFP (MOI 100) for 1 h and analysed by IFC at 6 and 12 hpi. (a) Single-cell population was defined by Area/Aspect ratio dot plot. (b) Objects in best focus were gated as those events with gradient RMS values greater than 50. Examples of cells that were included and excluded by the gating strategy; (c) single cells, (d) multiple cells, (e) cells out of focus; (f) RMS value less than 50 (as in [b]) and cells in focus RMS value greater than 50 (as in [b]).

Intracellular spot count mask creation

Bacterial fluorescence measurements were collected by a 488 nm laser of 5 mW. To quantify intercellular bacteria, a mask was created to select just the intracellular portion of the cell (Figure 3-4a) and a bacterial spot mask was created as in Figure 3-4b. Intracellular spot count masks (Figure 3-4c) were finally used to accurately count the bacterial spot only in present of "intracellular mask". The numbers on each image indicate the spot count feature value for the spot count mask applied to that cell and it can be seen that the mask for spot count analysis was accurate and successfully excluded extracellular bacteria (column 3, Figure 3-4c). The output of the spot count of all the in-focus single cells was presented as a histogram (Figure 3-4d).

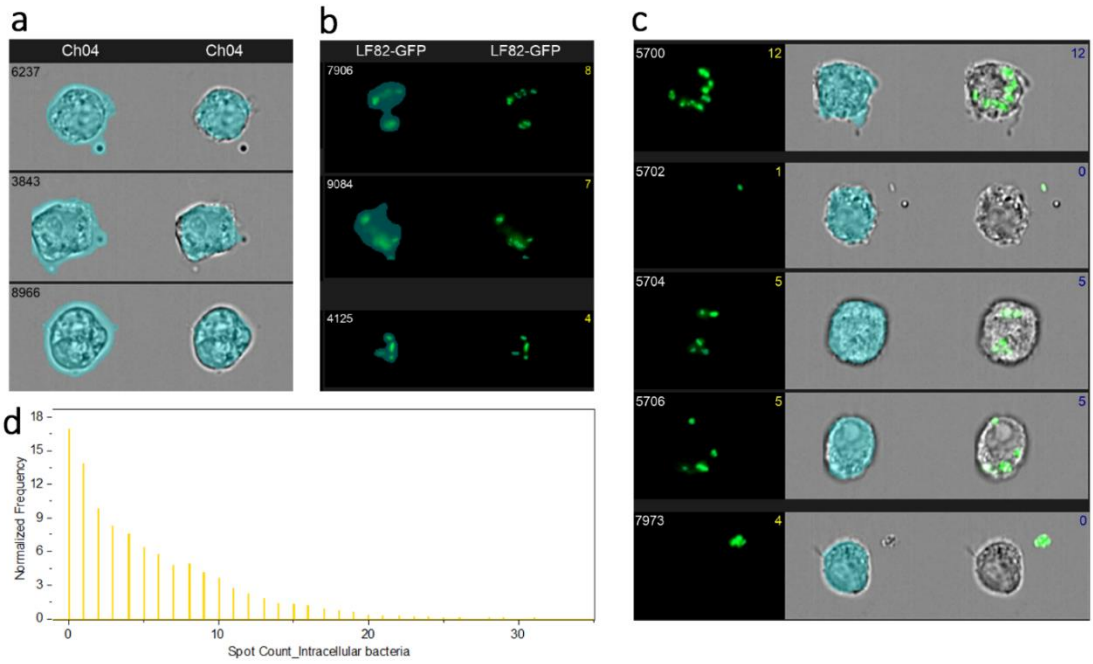

Figure 3-4 Creation of intracellular bacterial spot count mask.

(a) Intracellular bacterial localisation was measured by creating an intracellular mask. (b) The spot count feature was used to quantify fluorescent spots identified using spot mask (computer code: Intensity(Peak(Spot(M02, LF82-GFP, Bright, 3.5, 3, 1), LF82-GFP, Bright, 1)). (c) The spot mask in conjunction with the erode mask was used to create an intracellular fluorescence count (computer code: Spot count-Intensity(Peak(Spot(M02, LF82-GFP, Bright, 3.5, 3, 1), LF82-GFP, Bright, 1) And AdaptiveErode(M04, Bright Field, 87), LF82-GFP, 80-4095)). (d) Quantitative distribution of GFP positive inside LF82-infected cells.

Nuclei count mask creation

A threshold of up to 70% was applied to the nuclei to highlight the structures to count and a set range of sizes to remove any noise or background pixels. By using the Watershed function, the software then accurately differentiates the merged particles by cutting them apart by a line of 1 pixel thick where it automatically thinks there should be a division. In order to count the nuclei, a feature function (Spot_count) was used to compute the number of nuclei for each image after a precise nucleus mask was created. The computing code for a nucleus counting mask was Spot_count(range(watershed(threshold, 70)) 150-1500, 0.2-1).

3.2.3 Cell Fusion Experiment

RAW 264.7 cells were stained with 10 μM orange cell tracker (ThermoFisher) or 1 μM deep red cell tracker (ThermoFisher) for 30 minutes for 37°C separately, then the two different colour cells were mixed at ratio of 1:1. Cell mixtures

were seeded into 24 well plate at 2 X 10^5 cells/ml. Cells were activated by adding 1 µg/ml of LPS overnight. Activated cells were infected with LF82 *rpsM*::GFP at an MOI of 100. Twenty four hours post-infection, cells were fixed and nuclei stained with 1 µg/ml Hoechst stain. Samples were processed using ImageStream. The procedure is based on identifying two cell populations by staining using two different CellTracker dyes, where fluorescent dyes are retained in living cells through several generations. The dyes are transferred to daughter cells but not adjacent cells in the population.

Immunofluorescence for cell fusion experiments

Images for all experiments were captured using an inverted immunofluorescence microscope (CRG Axioimager, Leica DiMi 8 or Spinning Disk). RAW 264.7 cells were plated onto glass coverslips in 24-well-plates at 2 x 10^5 cells per well. Cells were infected with LF82::*rpsM*GFP for 1 h then extracellular bacteria were removed by gentamicin treatment or left untreated for indicated time points. At each time point, cells were fixed immediately with 4% paraformaldehyde (PFA) solution and permeabilized with 0.2% Triton X-100 after rinsing with Dulbecco's Phosphate-Buffered Saline (DPBS). Coverslips were treated with Phalloidin (ThermoFisher) and DAPI (VECTOR) for visualizing F-actin and the nucleus, respectively.

Imaging flow cytometry for cell fusion experiments

Imaging flow cytometry (IFC) data acquisition was performed using an ImageStream X MKII (ISX, Amnis) equipped with dual cameras and 405 nm, 488 nm, and 642 nm excitation lasers. All samples were acquired at x60 magnification giving an optimal 7 µM visual slide through the cell, and a minimum of 10,000 single cell events were collected for each sample. In focus cells were determined by a gradient root mean square (RMS) Brightfield of greater than 50 and single cells were identified by area versus aspect ratio. Only data from relevant channels were collected including Channel 01 (Ch01, DAPI; Nuclear florescence), Ch02 (GFP fluorescence), Ch03 (Orange CellTracker fluorescence), Ch04 (bright field)and Ch05 (Far red Cell Tracker fluorescence). Single colour compensation controls were also acquired, and a compensation file was generated via IDEAS.

3.2.4 Statistical analysis

Statistical analysis was performed using GraphPad Prism software. At least three biological replicates were carried out in this study; that is, experiments were repeated with fresh bacterial cultures or mammalian cell lines, according to the needs of the experiment. Values are represented as means ± SEM. As shown in the figure legends, significant differences were determined using t-tests (multiple and individual) and ANOVA (one-way or two-way) corrected for multiple comparisons using a Tukey's post hoc test. The statistical significance for the data was established by referring to $*P < 0.05$, $**P < 0.01$, $***P < 0.001$.

3.3 Results

3.3.1 LF82::*rpsM*GFP readily detectable in fluorescent-based experiments

Feasibility of using the GFP reporter vector in LF82 was confirmed by transforming strain LF82 with the vector and successfully observing green fluorescence in LF82 transformants via fluorescence microscopy. Transformation of LF82 with the fluorescent *rpsM*GFP marker did not alter the bacterial phenotype or growth rate of LF82::*rpsM*GFP. Comparisons of the growth rates indicated that there was no statistical difference in growth rate between GFP expressing LF82 and wild-type LF82 (Figure 3-5a). An intracellular infection model, where the output is viable bacterial counts, was then used to assess the bacterial replication and survival in RAW 264.7 macrophages (Figure 3-5b). Comparison of intracellular replication of LF82 and LF82::*rpsM*GFP at 6, 12 and 24 hpi demonstrated that there was no significant difference in intracellular survival or replication between the strains, making LF82::*rpsM*GFP a suitable fluorescent reporter strain.

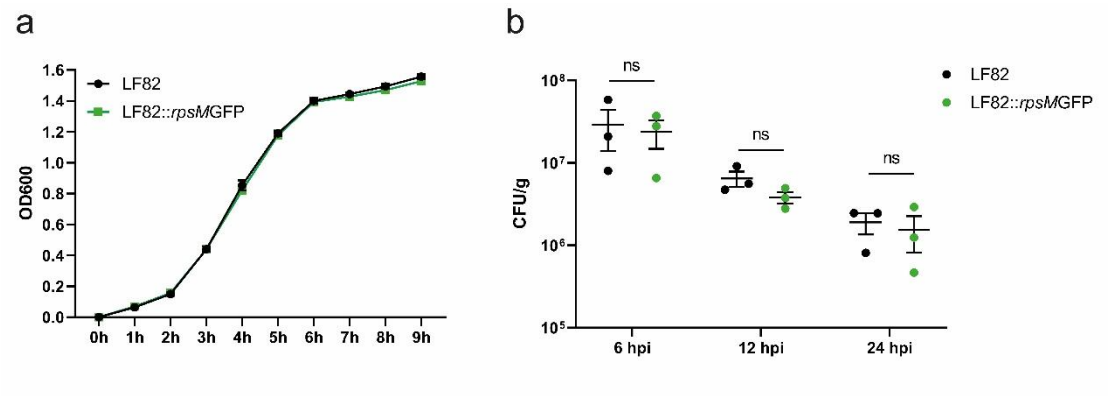

Figure 3-5 Growth curve analysis and intracellular infection of LF82 and LF82:: *rpsM*GFP.

(a) LF82 and LF82::*rpsM*GFP growth curves demonstrated there was no statistical difference in growth between the wild type and fluorescent strains. (b) RAW 264.7 murine macrophages were infected with LF82 and LF82::*rpsM*GFP at an MOI of 100. After an initial infection period of 1 hour, gentamicin was used to kill extracellular bacteria and then at 6, 12 and 24 hpi, cells were lysed and intracellular bacteria were enumerated using serial dilution onto LB-agar plates. All experiments represent the average of at least three biological replicates with three technical replicates per experiment. Error bars represent SEM. Statistical test: two-way ANOVA.

3.3.2 Evaluation of the internalization frequency of LF82 by IFC at different infection times.

With use of IFC, measurement samples can be separated into two major groups based on whether they contain bacteria or not. The population of cells positive for bacterial fluorescence was achieved using raw max pixel (brightest pixel in an image) versus intensity of bacterial fluorescence and these two plots were used to depict the character of uninfected and LF82-infected samples (Figure 3-6a). The percentage of bacteria positive cells was presented in Figure 3-6b. It has been shown that approximately 20% fewer cells are infected with LF82::*rpsM*GFP following 24 h infection, in comparison with 6 hpi or 12 hpi, indicating that some infected cells may undergo apoptosis, or that bacteria may be eliminated. Similarly, in infection experiments using traditional spot counts, the CFUs recovered also presented a trend of reduction along the course of time (Figure 3-5b). To be noted, IFC analysis had a similar trend to the CFU data set demonstrating that the IFC method was efficient and accurate for analysing and studying the *in vitro* bacterial infection model.

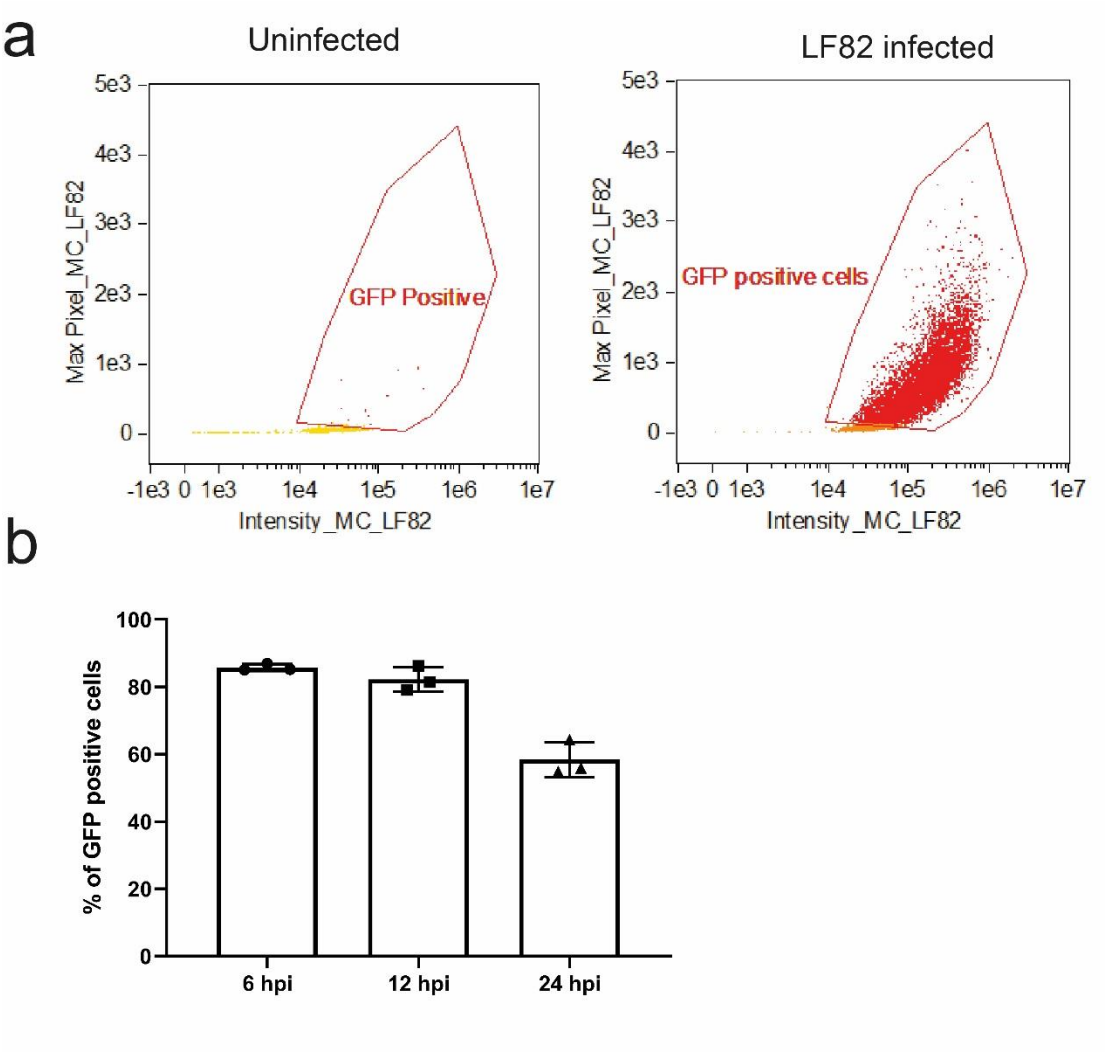

Figure 3-6 Evaluation of the internalization frequency of LF82 by IFC at different infection time.

RAW 264.7 cells were infected with LF82::*rpsM*GFP at an MOI of 100. Cells were harvested 6, 12 and 24 hpi and fixed before being analysed via IFC. (a) A gated selection of cells positive for bacterial fluorescence was made using Max Pixel (brightest pixel in the image) versus intensity of LF82::*rpsM*GFP. (b) The graph reports the percentage of GFP positive cells are the mean of three biological repeats. Error bar represents the ± SEM.

3.3.3 Quantification of Intracellular LF82::*rpsM*GFP by IFC

Quantifying the number of bacteria in a single cell is something that cannot be achieved by viable count assays and is time consuming using microscopy. IFC provides a very powerful tool for researching intracellular pathogens. The number pf fluorescent spots per cell was measured by IDEAS software spot count analysis. Spot count masks were created and used in conjunction with the spot count feature to produce spot count profiles for each time point (Figure 3-7). In this study, to facilitate analysis, cells were assigned to groups with those with

greater than 10 bacteria deemed to have a “high” bacterial burden, those with 6-10 bacteria assigned to an “intermediate” bacterial burden, and those with five or less as having a “low” bacterial burden (representative images are showed in Figure 3-7b-e). The cells that conform to each parameter were gated and the percentage population plotted over the time course (Figure 3-6a). On the basis of results from three different infection times (6, 12 and 24 hpi), it can be seen that cells infected with LF82::*rpsM*GFP have no significant difference in the population of "low" bacterial burden cells. It was however noted that at 24 hpi, there were significantly fewer cells with an "intermediate" or "high" bacterial burden relative to the corresponding populations at 6 and 12 hpi (Figure 3-6b). As compared to the percentage of infected cells at different infection time points, 80 % of cells contain bacteria at the first time point (6 hpi), but by 24 hpi, this percentage has decreased to 55 %. There is no clear explanation for the decrease of the populations of "intermediate" or "high" bacterial burden. Two possible mechanisms are: (1) high levels of bacterial replication place metabolic and physical stress on macrophages, resulting in cell death; (2) macrophages are capable of killing intracellular bacteria, even though 55 % of cells maintain intracellular bacteria at 24 hpi.

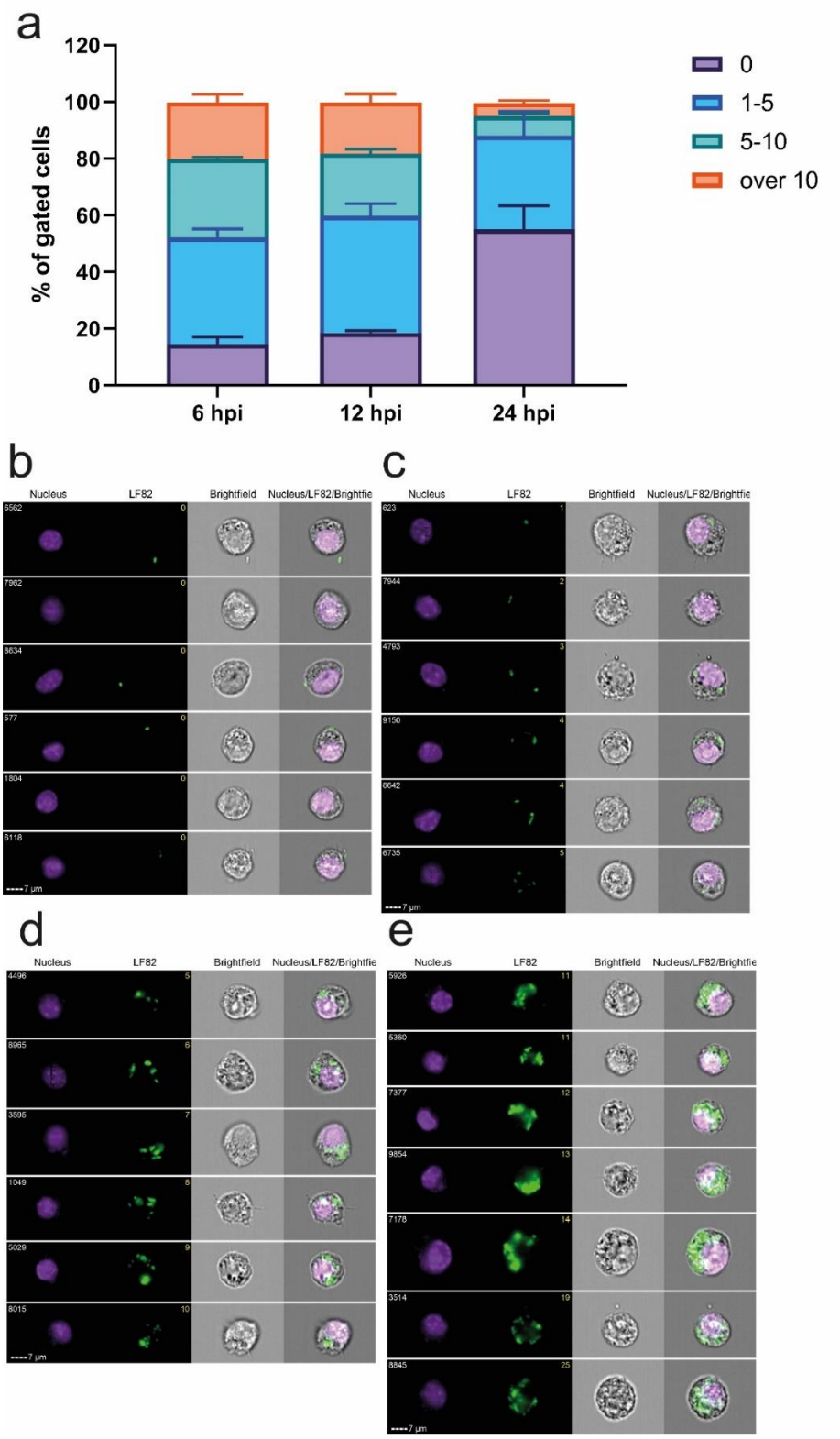

Figure 3-7 Evaluation of bacterial burden among LF82 infected cell populations.

The spot count feature was used to quantify fluorescent spots, which had previously been described in the section Methods and Materials 3.2.2. (a) The spot count profiles at 6, 12 and 24 hpi can be separated into 4 groups of cells with: 0, 1-5, 6-10 and over 10 intracellular bacteria. The graph represents the mean of three biological repeats. Error bars represent SEM. Images are representative of the groups with; 0 bacteria (b), 1-5 bacteria (c), 6-10 bacteria (d) and over 10 bacteria (e).

3.3.4 Macrophages present an elongated morphology post-AIEC infection

To determine whether LF82 had the ability to directly induce multinucleated macrophages, firstly it was important to understand the timing of multinucleated cell formation. Therefore, RAW 264.7 cells were infected with LF82 at infection periods (6, 24, 48 and 72 hours). As shown in Figure 3-8a, uninfected or LF82-infected cells were imaged by fluorescent microscopy. Infected macrophages present an enlarged and elongated morphology during LF82 infection in comparison to uninfected cells. Moreover, infected cells become larger and longer with longer infection time, which demonstrated that these characteristic morphological changes are time dependent. Meanwhile, multinucleated macrophages could be observed at 6, 24, 48 and 72 hpi, suggesting that multinucleated cells can be formed early in infection.

At 48 and 72 hpi , an increase in cell density was observed in cells that were uninfected. As a way to determine if LF82 infection has any impact upon cell proliferation, images captured from the microscopy system were analysed by software ImageJ to count the number of cells at various times. Figure 3-8b shows that the number of uninfected cells increased with incubation time, whereas cell proliferation was inhibited during LF82 infection. It is interesting to note that even at 72 hpi, the number of cells in the infected cultures remained similar to those at the earlier infection period of 6 hours. Coupled with the results of IFC analysis, macrophages may kill intracellular bacteria instead of causing cell death. A more detailed examination of cell morphology as well as the cellular activity may help to explain this phenomenon.

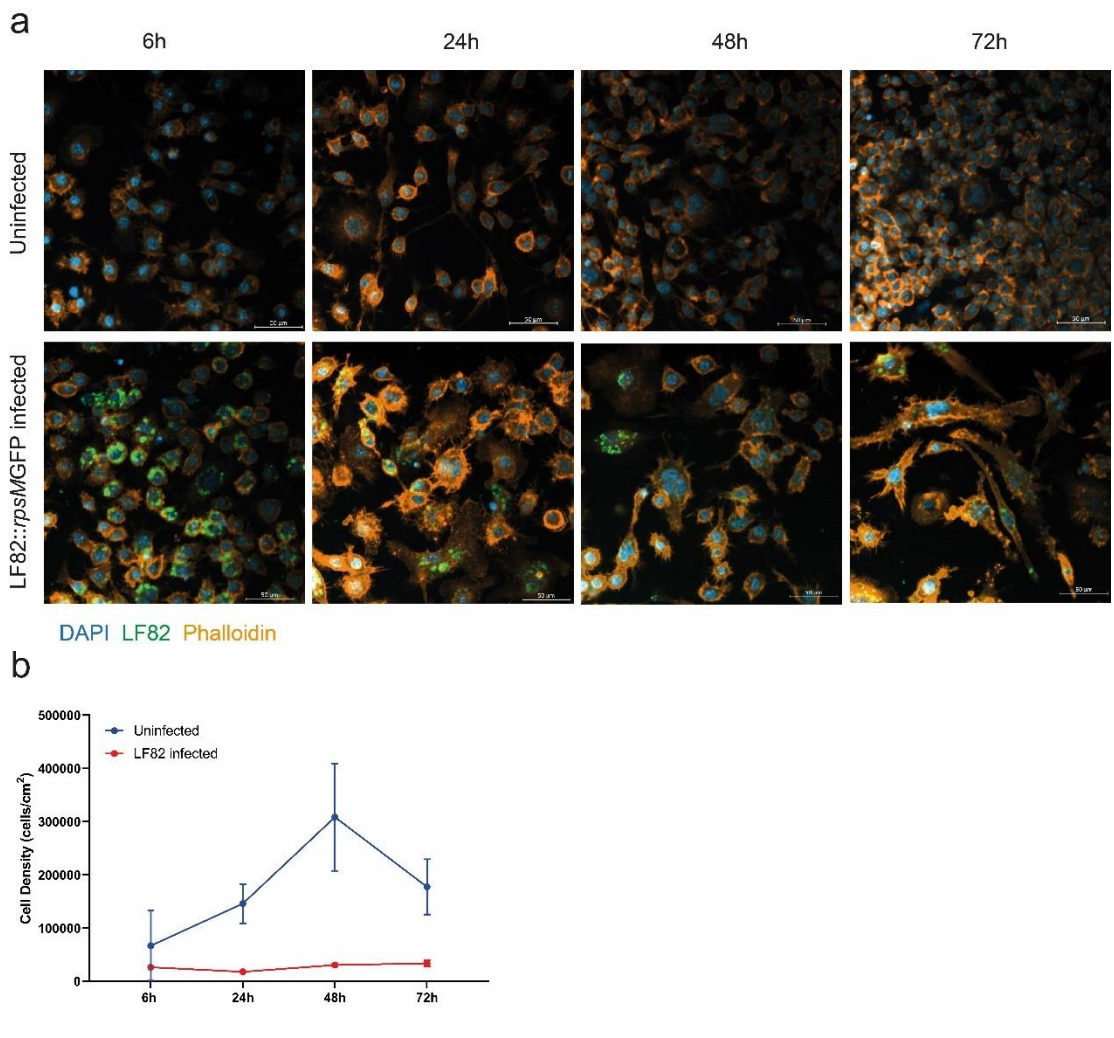

Figure 3-8 Quantitative macrophage cell number over time infection.

(a) Confocal microscopy images of uninfected and LF82::*rpsM*GFP infected RAW 264.7 cells at 1, 24, 48 and 72 hpi. The cells were then fixed and stained with DAPI (nuclei) and phalloidin (actin) and analysed by confocal microscopy. (b) Time-course changes cell number of uninfected macrophages but does not alter number in LF82 infected cells. Data represent the mean of three biological repeats. Error bars represent SEM.

3.3.5 LF82 infection increases multinucleated giant cells

In Figure 3-9a, the smaller picture depicts cells that have multinucleated structures. Viewed at a greater magnification, the image showed aggregates of multinucleated cells, tetranucleated cells, and trinucleated cells, from left to right. In order to quantify multinucleated cells from each individual image, the ImageJ software was used to perform statistical analysis, as shown in Figure 3-9b-e. The cells in the image can be classified into three categories: mononucleated (N = 1), binucleated (N= 2) and multinucleated cells (N > 2). In general, uninfected macrophages had a significantly larger number of

mononucleated cells than the LF82 infected group at the four different time points, indicating that infected cells have a tendency to form multinucleated cells. An analysis comparing the portion of binucleated cells between infected and non-infected groups revealed that the LF82 infected group resulted in a statistically significant increase population in binucleated at 24 (Figure 3-9c), 48 (Figure 3-9d) and 72 hpi (Figure 3-9e). While at 6 hpi, there is no significant difference in the portion of binucleated cells between uninfected (7.144 ± 0.722 %) and infected cells (8.955 ± 1.023 %, Figure 3-9b). For instance, compared to uninfected groups (7.177 ± 0.563 %) it was found that at 24 hpi, the percentage of binucleated cells increases to 16.483 ± 1.514 % (Figure 3-9c). The analysis of multinucleated cells (N > 2) revealed that cells at 6 hpi (uninfected versus infected with 1.201 ± 0.29 % versus 5.651 ± 1.263 %) and 24 hpi (uninfected versus infected with 0.594 ± 0.049 % versus 6.506 ± 1.669) exhibited more multinucleated cells when compared to uninfected cells, however, this phenomenon was not detected in the cells at 48 and 72 hours after being infected (Figure 3-9b-e). At 24 hpi, both multinucleated and binucleated macrophage cells significantly increase during infection, suggesting that the optimal duration for the study macrophage cell-cell connection induced by LF82 is at 24 hpi.

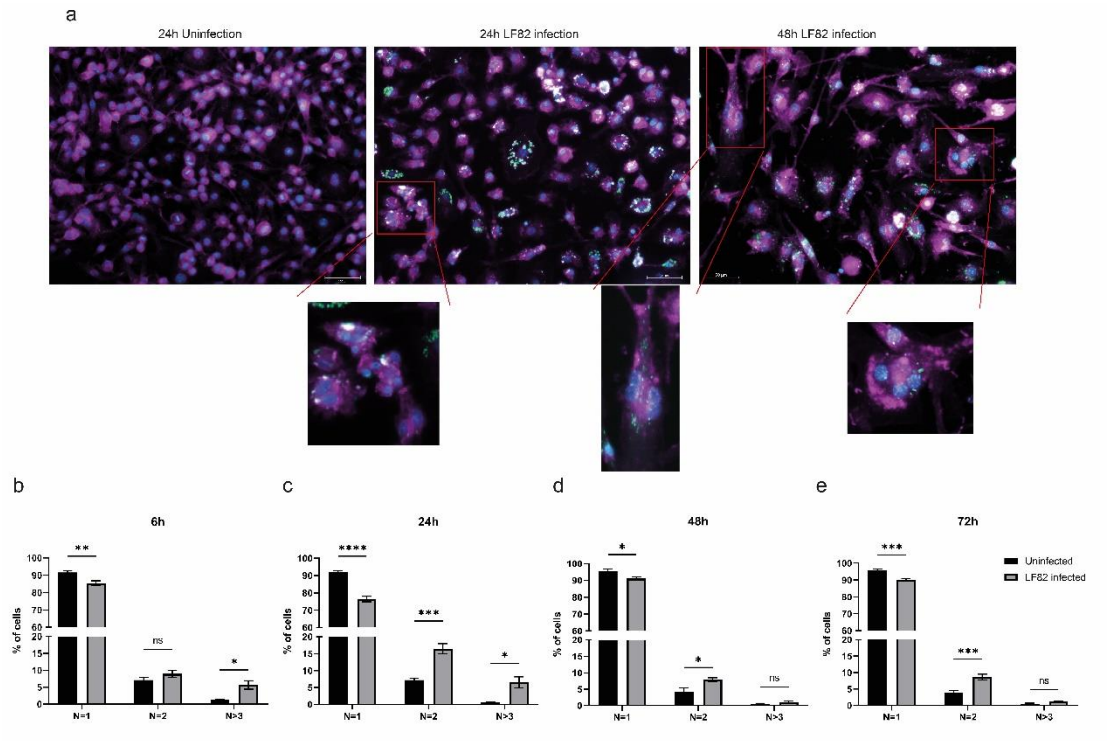

Figure 3-9 Quantitation of the portion of mononucleated, binucleated or polynucleated cells during LF82 infection at 6, 24, 48 and 72 hpi using fluorescent microscopy.

(a) Images are representative of uninfected or LF82 infected RAW 264.7 cells. The enlarged image shows examples of aggregate cells and multinucleated cells. Image cells were analysed by fluorescent microscopy (CRG Axioimager). Scale bars: 200 μM. (b) Uninfected and LF82 infected RAW 264.7 cells were harvested at 6, 24, 48 and 72 hpi. Cytoplasm was stained with phalloidin (violet), while nuclei were stained with DAPI (blue) and LF82::rpsMGFP were green. (b) Quantification of the number of nuclei was carried out with ImageJ. Results are shown as means ± SEM. Data represent the mean of three biological repeats. Statistical significance was determined by two-way ANOVA. *, *P* <0 0.05. **, *P* < 0.01. ***, *P* < 0.0001.

Here, we set out to investigate whether IFC is a viable platform for the detection of LF82 directly inducing multinucleated cells events *in vitro*. Figure 3-10clearly shows that with an IFC platform, images of mono-nucleated (Figure 3-10b), bi-nucleated (Figure 3-10c) and tri-nucleated cells (Figure 3-10d) can be captured accurately and the number of nuclei, can be matched to nuclei counting frequency histograms (Figure 3-10a). DNA content is typically doubled in proliferating cells going through cell cycle phases, which reflects an increase in cellular DNA content from the original amount of two copies (2N) in the G1 phase to twice the amount of four copies (4N) in the M/G2 phases. However, as shown in Figure 3-10b, LF82 inhibited cell proliferation suggesting that a higher population of binucleated cells in infected cells at 24 hpi occurred due to cell-cell interaction rather than a process of mitosis. Compared with the uninfected group, the population of mono-nucleated cells in infected cells decreased while

the proportion of bi-nucleated and multinucleated cells increased at 24 hpi according to IFC (Figure 3-10e). This finding is in agreement with what has been observed with fluorescence microscopy and provides further evidence for a phenomenon whereby LF82 induces cell-to-cell interaction directly.

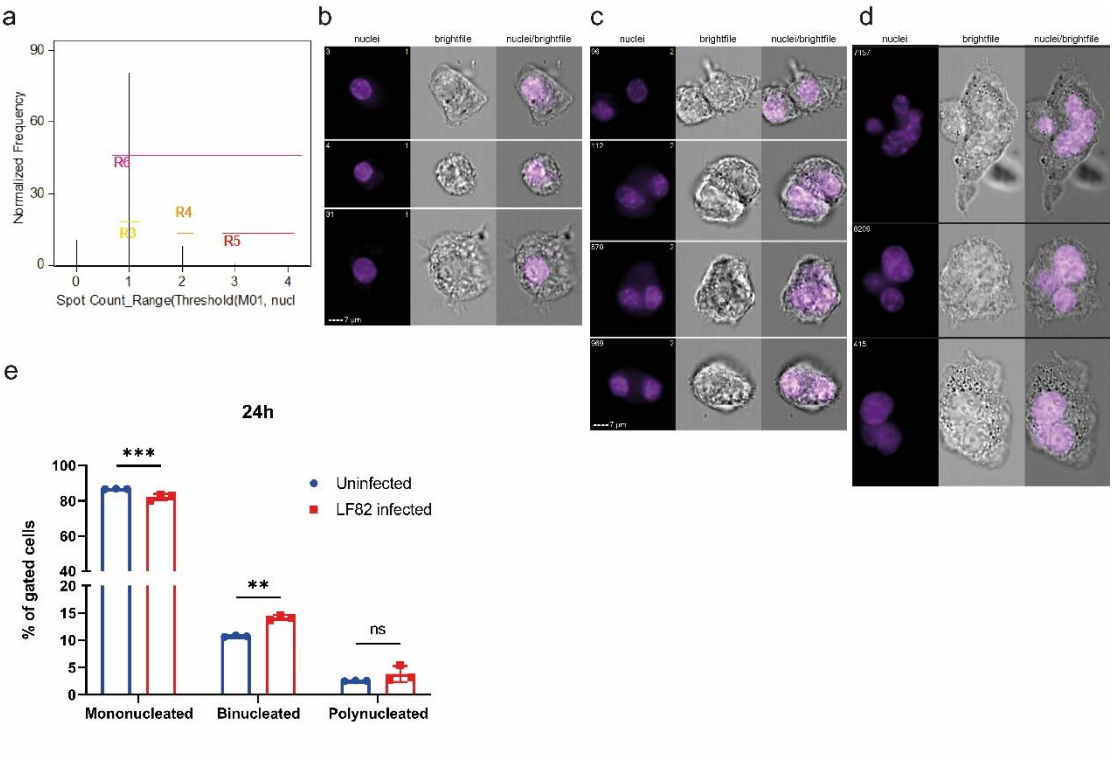

Figure 3-10 IFC to quantify the different populations of cells (mononucleated, binucleated or polynucleated cells) with or without LF82 infection at 24 hpi.

(a) IFC analysis of DNA content frequency histograms shows cells from uninfected and LF82 infected macrophages at 24 hpi. The number of nuclei from individual cells was quantified using a spot counting mask: Spot_count(range(watershed(threshold, 70)) 150-1500, 0.2-1). Representative IFC imagery of mononucleated cells (b), binucleated cells (c) and polynucleated cells (d) are consistent with their histograms. (e) Based on the histogram, mononucleated (N=1), binucleated (N=2) and polynucleated cells (N > 2) from uninfected or LF82-infected RAW 264.7 cells were quantified and graphed. Results are shown as means ± SEM. Data reported were obtained from three biological repeats. Statistical significance was determined by student t-test. *, *P* <0 0.05. **, *P* < 0.01. ***, *P* < 0.0001.

3.3.6 Exploring cell-to-cell connections through cell fusion experiments

Many studies have demonstrated that the formation of MGCs is supported by cell fusion. When performing cell fusion experiments, it is common to use two different dyes for the cell cytoplasm to enable visualisation of fusion of neighbouring cells. Therefore, it is important to test whether dyes have a crossing channel leakage prior to actual experiments. In a pilot study,

experiments were set up into 4 groups: (1) uninfected RAW 264.7 cells were stained orange only; (2) uninfected RAW 264.7 cells were stained red only; (3) uninfected cells stained two dyes separately but were cultured together; (4) RAW 264.7 cells were stained orange or red separately but co-culture and infected with LF82::*rpsM*GFP. All these samples were visualised using fluorescent microscopy and images from each of the four samples with each channels were shown in the Figure 3-11. During microscopy, unstained channels were set up using over exposure time to check if any signal leaked from the stained channel. As expected, orange or red fluorescent signal did not cross each other, in addition, LF82 expressing GFP could not be detected in either orange or red channels. Using fluorescent microscopy, in the two dyes mixed culture samples, it has been confirmed that dyes located in the cell cytoplasm do not move from one cell to another unless cell fusion occurs (Figure 3-11). Therefore the fluorescent-coloured dyes are ideal for observation by different channels without signal leakage or crossing into other channels. Given the results of this experiment, we decided to use it further to study cell-cell interaction by focusing on the two-colour positive cells. We found that there are two types of two-colour positive cells from fluorescent microscopy images: fusions of cells and aggregates of cells (Figure 3-12).

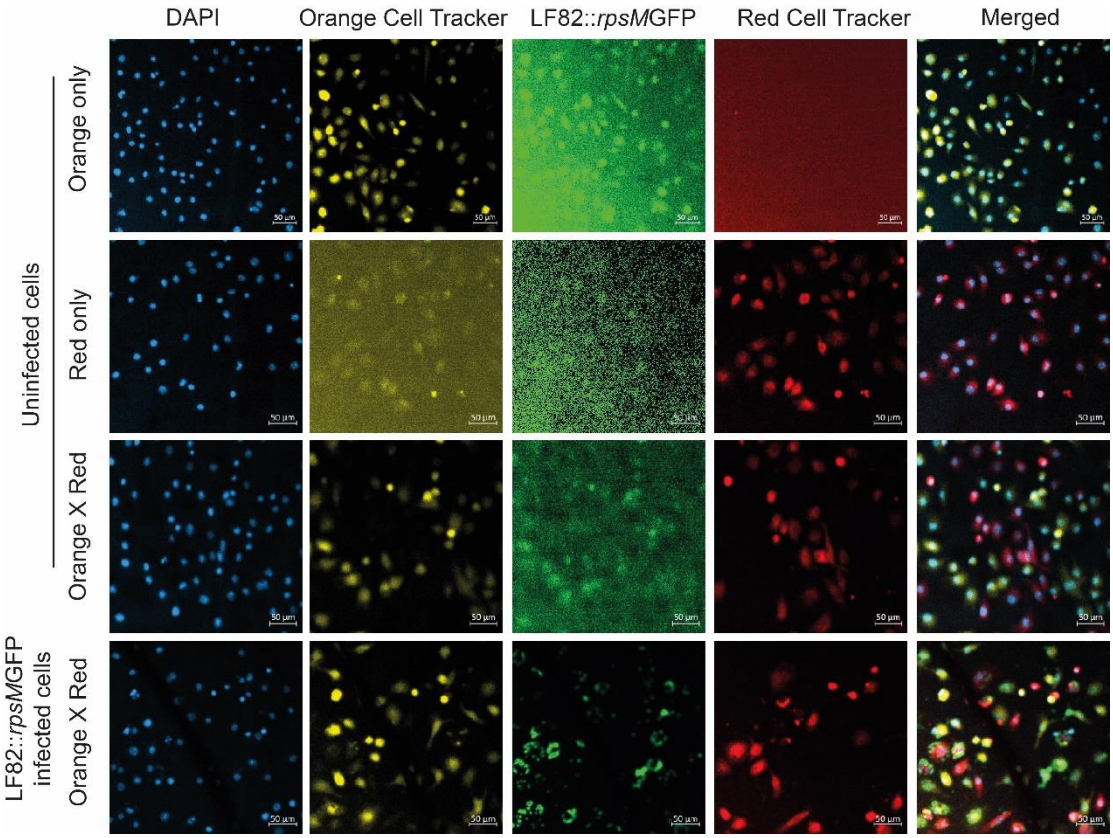

Figure 3-11 Evaluation of two cytoplasm dyes (OrangeCell Tracker and RedCell Tracker) in cell fusion experiments.

There are 4 groups: (1) uninfected RAW 264.7 cells stained with Orange Cell Tracker only; (2) uninfected cells stained with Red Cell Tracker only; (3) uninfected cells stained with the two dyes separately and cultures mixed together overnight; (4) RAW 264.7 cells were stained with Orange or Red Cell Tracker separately then co-cultured and infected with LF82::*rpsM*GFP at 1 hpi. All these samples were fixed and stained with DAPI for nuclei in blue. Cells stained with Orange Cell Tracker appear yellow in colour, while cells stained with Red Cell Tracker appear red in colour. LF82::*rpsM*GFP are green. Samples were visualised under fluorescent microscopy (Spinning Disk). Samples 1 to 4 are shown in order from top to bottom (single channels and merged pictures) with scale bar of 50 µm. The negative signal channels were set up with over exposure time to confirm whether dye signal leaks into neighbouring fluorescent channels.

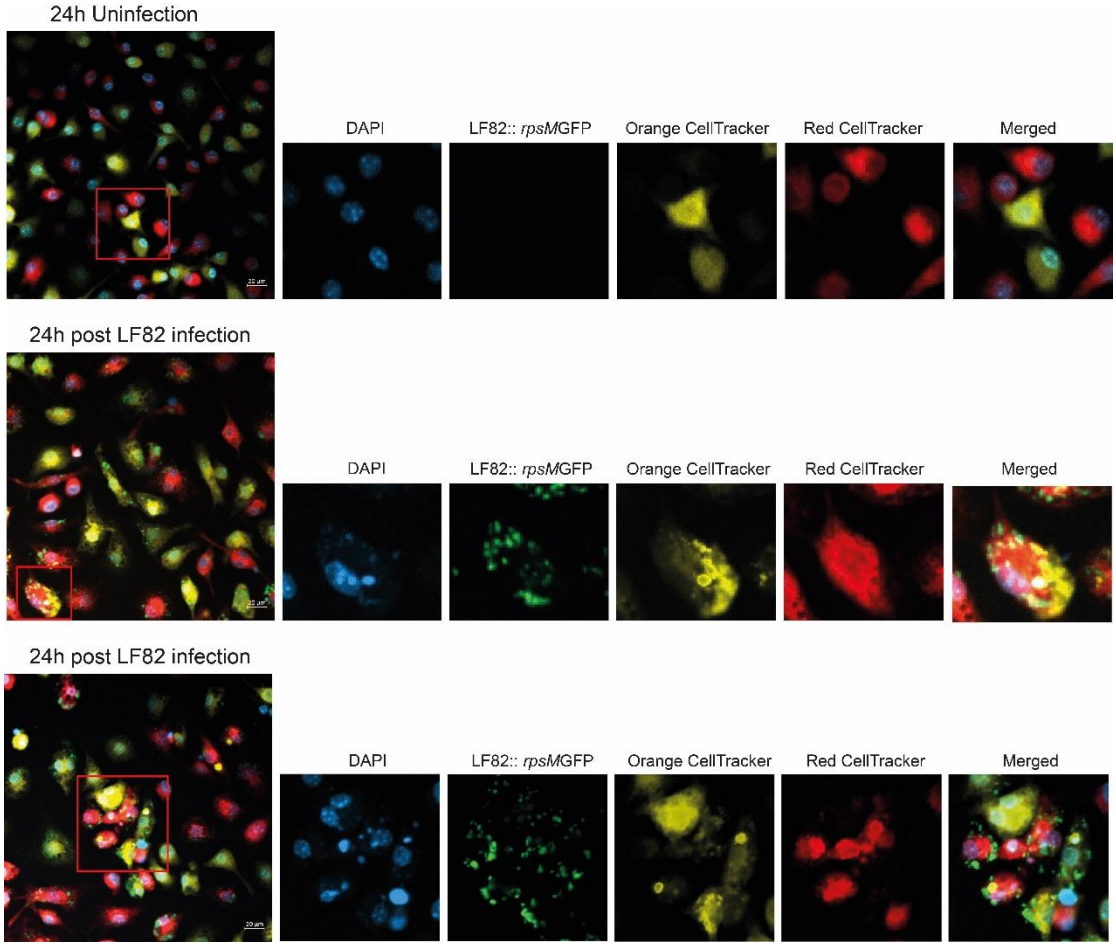

Figure 3-12 Cell fusion experiments were observed by fluorescent microscopy.

Orange-Cell Tracker stained and Red Cell Tracker-stained RAW 264.7 cells were mixed and co-incubated onto coverslips with a round 8 mm diameter. Cells were incubated overnight and then infected or with LF82::*rpsM*GFP at 24 hpi alongside control uninfected cells. After 24 hours, uninfected or LF82 infected RAW 264.7 cells were fixed and the nuclei were stained with DAPI. From top to bottom, enlarged images show examples of single cells without interaction, cell fusion, and cell aggregates. The nucleus is in blue, Orange Cell Tracker stained cells are yellow, Red Cell Tracker stained cells are red and LF82::*rpsM*GFP are *green*.

To further investigate the dynamics of cell-cell interaction during LF82 infection, we conducted a cell fusion experiment, as detailed inFigure 3-12a. Unstained murine macrophages RAW 264.7 cells were divided into two populations and were labelled with Red Cell Tracker (which exhibits red colour in the images) or Orange Cell Tracker (which exhibits yellow colour) respectively. This was confirmed by representative images of single colour populations: red stained cells or orange stained cells shown in Figure 3-12c and Figure 3-12d, respectively. The two populations of stained cells were then mixed and cultured until they become adherent. Uninfected or cells infected with LF82::*rpsM*GFP were harvested at 1, 24 and 48 hpi and imaged by IFC (Figure 3-13a). Fusion was assessed by detecting cells with both orange and red fluorescence and by

staining nuclei with Hoechst 33342. As expected, fewer macrophages carrying two colours were observed in the uninfected macrophage group. However, with LF82 infection, macrophages exhibited a prominent two-colour population (Figure 3-13b). Representative image of mixed cells are shown in Figure 3-13e. The population of mixed cells were gated and statistically presented in Figure 3-13f-h. More specificity, compared with uninfected cells there was an increased population of orange+/red+ cells in the infected group at 1, 24 and 48 hpi with p= 0.0132, p = 0.0016 and p = 0.0553, respectively. To be noted, the statistical difference (t-test p value) of orange+/red+ cells between uninfected and infected cells, decreased from 1 hpi to 24 hpi, but increased at 48 hpi. Meanwhile, there are more orange+/red+ cells during LF82 infection at 24 hpi with the percentage of the total population reaching 13.0 %, while the percentage of those cells was 10.5 % at 1 hpi and 9.3 % at 48 hpi. However, there was no clear indication of what would happen to orange+/red+ cells during longer term infection. Again, the increased two colour cell population of infected macrophages at 1, 24 and 48 hpi demonstrated that infected macrophages had a propensity to aggregate *in vitro*.

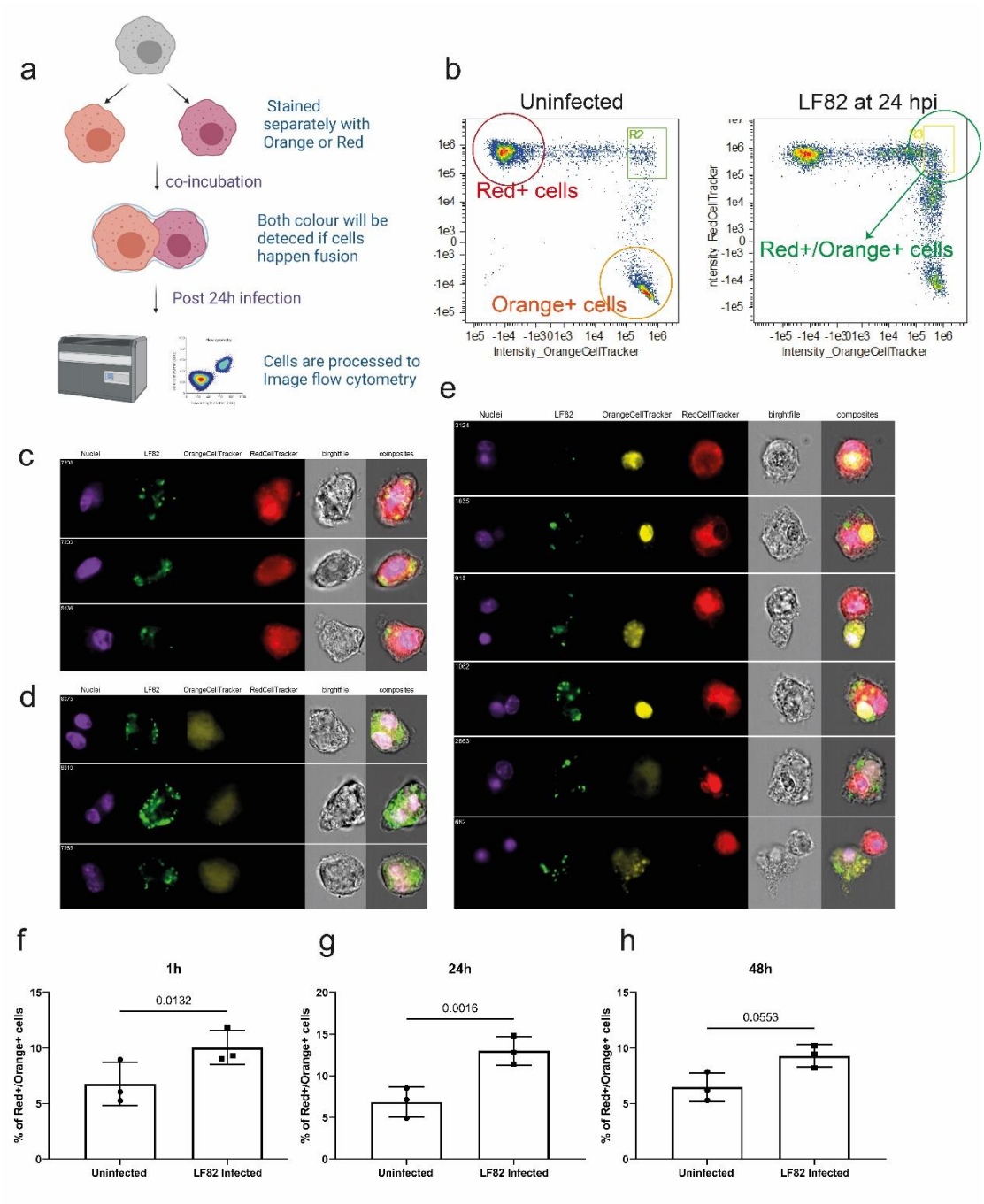

Figure 3-13 Cell fusion experiment showing LF82 modulating cell-cell interactions.

(a) Schematic representation of experimental outline: cell fusion experiments. (b) Flow cytometric analysis of individual cells in a mixed infected population (n=3) revealed a robust number of Orange+/Red+ double-labelled cells. Three populations: red positive cell; orange positive cell and both red positive and orange positive cells are defined in a red fluorescent intensity versus orange fluorescent intensity dot plot. Representative images of LF82 infected macrophages were captured through IFC: red positive cell populations (c), orange positive cell population (d) and dual colour stained cells (e). In the image gallery, the left panel shows nuclear fluorescence in purple (Hoescht), LF82::*rpsM*GFP in green, cell bodies with orange fluoresce or red fluorescence, brightfield images, and finally the composite overlay image. The portions of Orange+/Red+ double-labelled cells from LF82 infected or uninfected RAW 264.7 cells were showed at different time points: 1h (f), 24h (g) and 48h (h). Results are shown as means ± SEM. Data represent the mean of three biological repeats. Statistical significance was determined by Student's t test..

3.3.7 Analysis of cell colocalization using IFC

To understand how cells perform cell-cell fusion, the two colour-positive cell population was further monitored by IFC. We discovered that a single cell is engulfed and destroyed inside another cell, indicating that MGCs formation is supported by macrophage phagocytosis. To analyse the colocalization of two cells, we conducted IFC utilising cytoplasm similarity function to create a histogram for the population of cells that were dual colour positive (Figure 3-14a). Based on the similarity value, we divided cell-cell interactions into three categories: (1) cell-cell adherence (Figure 3-14b); (2) cell phagocytosis (Figure 3-14c) and (3) cell fusion (Figure 3-14d). It should be noted however that, even following phagocytosis of a cell, bacteria were noted not to be degraded and remained in the cell cytoplasm. This does not rule out the possibility that bacteria within an infected cell that is phagocytosed survive phagocytosis and transfer from an infected cell to an uninfected cell (Figure 3-14c). According to these three types of cell-cell interaction, we graphed the portion of these three subpopulations into Figure 3-14e. The graph showed that there are a higher population of cells with phagocytosis during LF82 infection (76.867 ± 1.090 %) versus uninfected cells (39.767 ± 6.308 %). In the IFC images of orange+/red+ cells, we did not identify MGCs. In this experiment, as adherent cells were harvested using cell scrapers and filtered before being run through IFC, to avoid blocking the machine, it is possible that cells with a larger size may have been inadvertently excluded. Given that aggregates of cells and MGCs were observed by microscopy, my hypothesis is that in the presence of LF82, the increased ability of macrophages to phagocytose may facilitate the formation of MGCs.

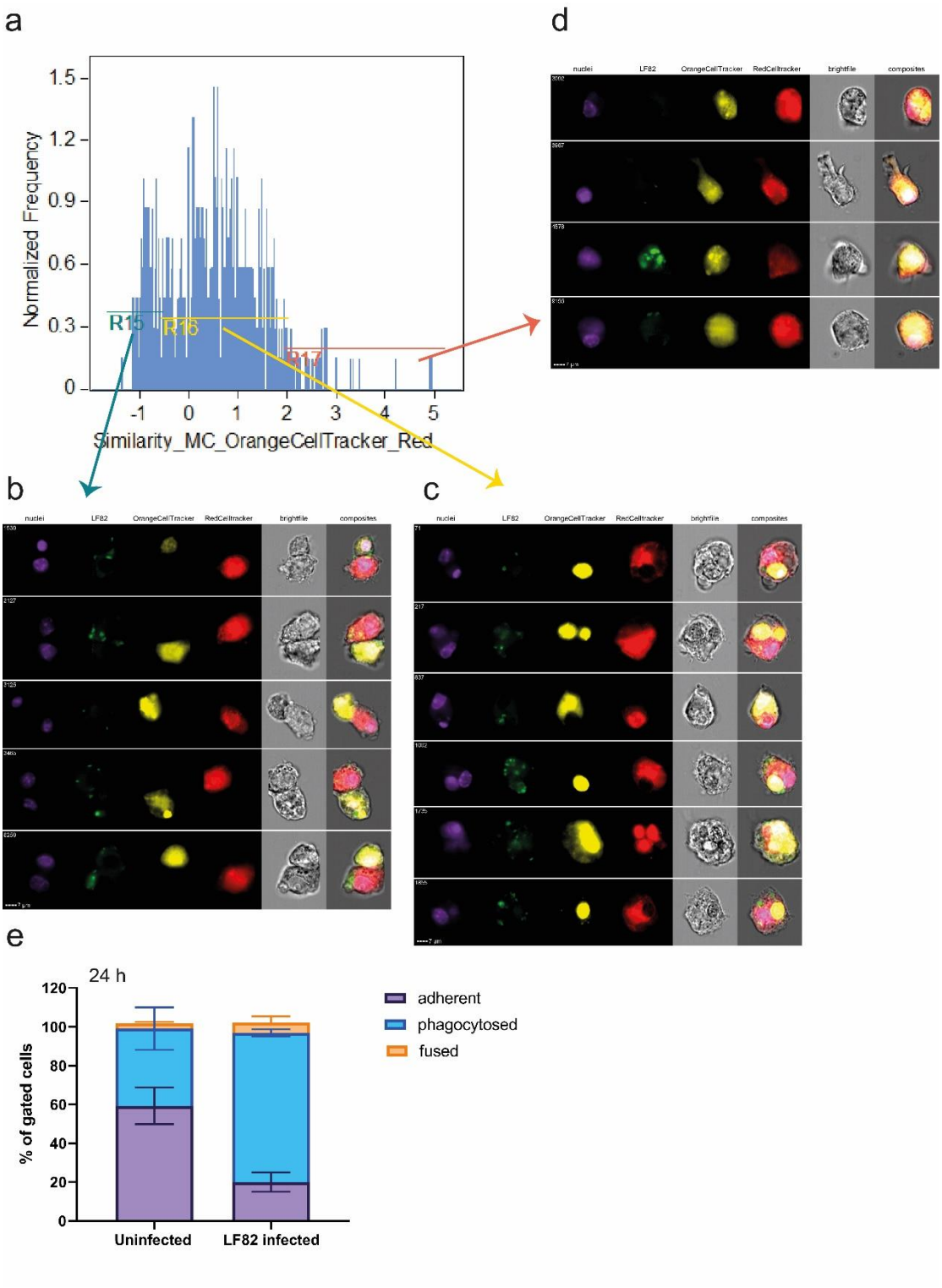

Figure 3-14 Analysis of co-localisation of orange stained cells with red stained cells.

RAW 264.7 cells were infected or uninfected at 24 hours. After 24 hours, cells were fixed and analysed by IFC. The two different colour masks (Orange and Red) in conjunction with the similarity feature were used to create a co-localisation histogram (a), where cells with a high score (over 2, Gate R17) they have an overlapping red and orange colour; while cells with a medium score (0.5-2, Gate R16) have a phagocytosis phenotype; when cells with a low score (< 0.5, Gated R16) they have the two colours separated indicating cell adhesion. Example images are representative adherent cells (b), phagocytosed cells (c) and fused cells (d). (e) When quantified at 24 hpi, a graph of the percentage of each cell-cell interaction type could be created.

3.4 Discussion

In order to fully comprehend bacterial infection, it is important to be able to visualise and quantify bacteria-host interactions and bacteria-inducing cell-cell communications. An effective investigation must take into account the stages of bacterial entry and replication, as well as cell-cell interaction. The use of fluorescent microscopy and IFC are highly practical and efficient techniques for the assessment of these processes. In this study, we show that; (1) IFC is an appropriate analysis technique to provide confidence for assessing intracellular bacterial counting in *in vitro* infection models; (2) IFC provides novel opportunities to examine in detail cell-cell interactions, demonstrating LF82 induced enhanced cell-cell interaction over the time course of infection; (3) increased cell to cell contact is driven by phagocytosis.

Application of Fluorescent Protein Expressing Plasmid

In image-based platforms, increasing development of fluorescent sensors has used fluorescent protein (FP) for analysis of intracellular bacteria *in vitro*. So far, there has been significant success. However, high-copy-number FP expression plasmids may lead to toxicity for bacterial cells when fusion proteins are expressed at a concentration that significantly exceeds expression of endogenous protein (Campbell *et al.*, 2002). Another concern is that the introduction of a plasmid expressing FP to a bacterial cell may lead to a reduced intracellular infection (Shemiakina *et al.*, 2012). Importantly, we analysed the growth and survival strategies and demonstrated the same pattern of infection as no obvious difference in phenotype between LF82::*rpsM*GFP and the wild-type strain were detectable in growth rate or viable counts post-infection (Figure 3-5).

Application of IFC for Analysis of Intracellular Bacteria

The use of IFC and other image-based technologies in the study of host-pathogen interactions enables us to gain a better understanding of these interactions and helps us identify novel potential therapeutic targets to fight off bacterial infection in humans. In spite of these positives, it should be taken into consideration that host-pathogen interactions are dynamic. To analyse bacterial

survival rates inside macrophages over different time courses, we were able to count specific intracellular bacterial by imaging high-resolution bacterial particles inside individual cells via IFC. The integration of IFC and statistical analysis, with different infection periods of internalisation (Figure 3-6) presented a similar trend to that detected via traditional bacterial enumeration (Figure 3-5b). However, it is not possible to distinguish between membrane-bound or intracellular bacteria using traditional viable bacteria counts. Intracellular bacteria can be identified using a microscope, but this approach lacks large-scale quantitation. IFC allowed rapid and easy quantitation of the population of cells with internalised bacteria in this *in vitro* infection model. However, IFC could not determine bacterial viability of a GFP labelled bacteria as a GFP spot could represent a dead bacterium, but still be counted. As a preliminary experiment, the traditional viable count method was necessary to get an understanding of the approximate number of intracellular bacteria. Here, neither a traditional viable bacteria count (Figure 3-5b) nor an initial general bacterial fluorescence intensity analysis (Figure 3-6b) gave confidence that either was an appropriate analysis technique for assessing intracellular bacterial infection. However, IFC enabled us to standardise the *in vitro* infection experiments. This method was more sensitive to allow high numbers of events (cells) to be tracked and was reproducible across all samples. The overall conclusions relating to the progression of infection were was consistent to the results using these two methods: traditional viable count, and IFC spot count, while IFC provides more information of morphological cellular features and heterogenous host-pathogen interaction. The IFC showed a similar pattern and confirmed previous data, that is, intracellular LF82 decrease over longer term infection but some bacteria still maintain within macrophages.

Application of Imaged-Based Techniques for Analysis of LF82-Induced Cell-Cell Interactions

To explore specific aspects of cell-cell interactions and cell population dynamics during LF82 infection, we used IFC and fluorescent microscopy. The effect of LF82 on cell proliferation was examined and compared by analysis of cell density using fluorescence microscopy which is not feasible by IFC. We have described here cell density measurements that show LF82 infection causes macrophage

proliferation to be inhibited without any cell number change (Figure 3-8). The underlying mechanism of LF82-induced inhibition of macrophage proliferation remains unknown. It has been shown that activation of the PI3K/Akt pathway inhibits macrophage proliferation (Linton, Moslehi and Babaev, 2019). A current study has demonstrated that in CD patients, elevated advanced oxidation protein products (AOPPs) impair autophagy in macrophages via activation of PI3K-AKT-mTOR pathways (Liao *et al.*, 2021). Together, AIEC may induce AOPPs accumulation in macrophages activating PI3K-AKT-mTOR pathways, leading to autophagy impairment and inhibition of macrophage proliferation. Since it was clear that the number of cells was not increased during LF82 infection over time, this indicated that mitosis is likely not occurring at a significant rate. A microscopy analysis has revealed that infection of macrophages with *C. albicans* can result in failure of macrophages to complete mitosis (Lewis *et al.*, 2012). Taken together, proliferation was inhibited during infection, increased bi-nucleated cells may be caused by cell fusion or phagocytosis instead of cell division.

Our work studied cell-cell interaction induced by LF82 using cell fusion assays and fluorescent microscopy coupled with IFC. Such studies reveal dynamic aspects of infection giving novel opportunities to analyse the cell cycle and cell-cell interactions. High-resolution images of mono- and bi-nucleated cells, as well as poly-nucleated cells, were captured. Although IFC can successfully sort and count the number of nuclear from individual events, a limitation of IFC is that it requires flowing cells and strict cell size restrictions , therefore adherent cells onto plastic wells must be harvested and filtered before IFC can be processed. Fixing and staining cells directly onto a coverslip and then examining under microscopy can address these problems without altering the morphology of cells. In the determination of the percentage of mono-, bi- and polynucleated cells in the samples of infected and non-infected control samples using IFC or fluorescent microscopy approach, it was found that there was a greater percentage of bi- and polynucleated cells in the infected samples than in the uninfected control.

Cell fusion experiments provide us with an insight into how cells interact with each other during infection. When compared with the portion of orange+/red+

cells in uninfected macrophages, increased dual fluorescing populations were detected during LF82 infection over 1, 24 and 48 h. To provide more details on how infected cells interact with neighbour cells. Dual fluorescing events were gated and then observed and cell colocalization was analysed by IFC. Three different types of cell-cell interaction were identified: adherent cells, phagocytosed cells and fused cells. From image observation of the categories of fused cells, an interesting phenomenon is shown that some fused cells exhibited two colour-dyes but only one nucleus. This raises a question as to whether one macrophage fused with another one after which it takes up the dye once it has been degraded. With respect to the population of phagocytosed cells, a higher population of those cells still carrying LF82 was observed within macrophages (Figure 3-13c). This finding leads to the hypothesis that LF82 transfers from one cell to another when macrophages continue to phagocytose infected cells. However, it appears that the process of the macrophage killing the phagocytosed cells has failed to complete. Taking this into consideration, LF82 likely contributes to the prevention of completion of the degradation of the phagocytosed cell.

A hypothesis is generated for the longer term infection, that macrophages may continue phagocytosing infected cells forming bi-nucleated or multinucleated cells which facilitate AIEC transfer from cell to cell, resulting in MGCs or granulomas (Figure 3-15). Our findings emphasize the role of AIEC in modulating the cell-cell interaction. The objective of future studies is to investigate whether inhibition of macrophage cell division, or phagocytosed cell degradation, is another virulence attribute of AIEC or is a mechanism that enables host macrophages to contain AIEC infection. Targeting host proteins involved these biological processes may provide a possibility for CD treatment in the future.

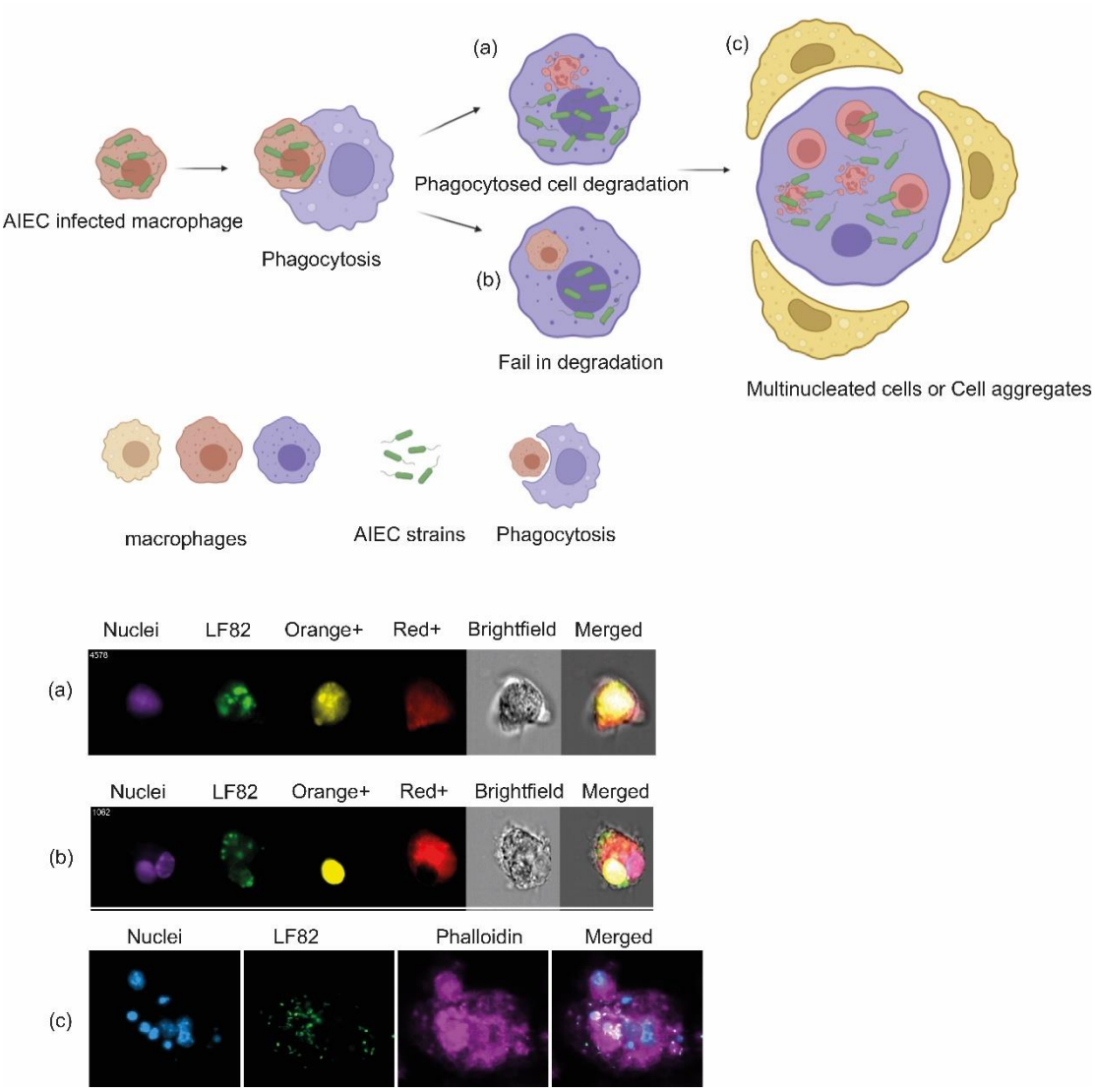

Figure 3-15 An overview of the hypothesized role of macrophages in longer-term AIEC infection.

AIEC infected macrophages can be phagocytosed by newly arrived macrophages which may lead to two possible outcomes: (a) phagocytosed cells undergo degradation and release intracellular AIEC to a new macrophage; (b) Infected macrophages resist being degraded within macrophages providing a niche for intracellular AIEC survival and replication. The constant recruitment of new macrophages by infected macrophages can eventually lead to aggregates and multinucleated cells. Images from IFC or fluorescence microscopy support the concepts described in (a), (b) and (c).

Formation of multinucleated cells possibly arises due to continuous phagocytosis by infected macrophages. Further studies are underway to elucidate the mechanisms behind this phenomenon. Hence, screening host proteins relating to cell proliferation and phagocytosis by transcriptomic analysis will enable an understanding of their expression and function during AIEC infection of macrophages. Future aims of this thesis include the investigation of macrophage-macrophage communication signals during bacterial infection that determine

cell fate, and bacterial regulation of virulence strategies to optimise pathogenicity in the host environment. These are fundamental points to understand more about infection biology and, by extension in the case of AIEC, to hopefully identify novel treatment options for CD. RNA sequencing profiling of either the host, the pathogen or both have been employed in recent years to uncover substantial molecular details about host and bacterial factors that underlie infection outcomes (Eriksson *et al.*, 2003). Macrophage and AIEC interaction is likely to result in a variety of subpopulations with diverse outcomes: some macrophages engulf the bacteria, while others remain uninfected; some macrophages lyse the ingested bacteria, while others are permissive to intracellular bacterial survival; some macrophages will restrict bacterial growth, while others survive and allow bacteria to multiply. However, we currently lack an understanding of the underlying molecular mechanisms in either the host or pathogen. There is little knowledge about the mechanism of macrophages that enables bacteria to survive. In Chapter 5 a combination of cell sorting, based on intracellular bacterial load, and RNA sequencing was conducted to better understand the intracellular bacterial number dependence of infection outcomes for host cells.

Chapter 4 Inhibition of Proline Tyrosine Kinase 2 (Pyk2) Phosphorylation During Adherent-Invasive *Escherichia coli* Infection Inhibits Intra-macrophage Replication and inflammatory Cytokine Release

4.1 Introduction

Intestinal macrophages enriched in the lamina propria, capture and eliminate any bacteria that cross the epithelial barrier. They are responsible for clearing apoptotic and senescent epithelial cells and are one of the most abundant leukocytes in the intestinal mucosa, particularly in the Peyer's patches, which underly the intestinal epithelium (Ohno, 2015). These sub-epithelial macrophages are essential for maintenance of mucosal homeostasis in the presence of the microbiota and play a pivotal role in protective immunity against pathogens (Bain and Mowat, 2014). Macrophages mount their response against microbial pathogens through binding of pattern recognition receptors (PRRs) to pathogen-associated molecular patterns (PAMPs) resulting in release of a variety of proinflammatory cytokines and chemoattractants, such as TNF-α. This cytokine is a key mediator of inflammation in CD, disrupting epithelial barrier function by altering the structure and function of tight junctions (Schmitz *et al.*, 1999; Lissner *et al.*, 2015). A milestone in treating CD was the introduction of anti-TNF-α agents, like infliximab and adalimumab (Hanauer SB *et al.*, 2002; Rutgeerts *et al.*, 2012).

Large-scale genome-wide association studies in cohorts of European patients resulted in the identification of candidate genes in the newly associated inflammatory bowel disease (IBD) susceptibility loci (Jimmy Z Liu *et al.*, 2015). These included proline-rich tyrosine kinase 2 (Pyk2), a non-receptor, Ca^{2+} dependent protein-tyrosine kinase that is expressed in numerous tissues and cell types and which is involved in innate immunity (Williams and Ridley, 2000). It is highly expressed in the central nervous system, epithelial cells, hematopoietic cells, and it is also over-expressed in various cancers (Kohno *et al.*, 2008; Zhu *et al.*, 2018). Activation of Pyk2 involves autophosphorylation at Tyr-402, which enables the binding of Src via the SH2 domain and phosphorylation of Pyk2 at Tyr-579 and Tyr-580, within the kinase domain activation loop, to generate

maximal kinase activity (Zhao *et al.*, 2016). Phosphorylated Pyk2 functions in the regulation of phagocytosis, migration, proliferation, invasion, oncogenesis and metastasis (Hudson, Bliska and Bouton, 2005; Schaller, 2010; Liu, Chen and Xu, 2018; Zhu *et al.*, 2018). In macrophages, Pyk2 has defined functions in regulating morphology, migration, and phagocytosis (Okigaki *et al.*, 2003; Paone *et al.*, 2016; Zhu *et al.*, 2018). It is therefore considered a valuable therapeutic target in various disease states, such as inflammation and cancer (Naser *et al.*, 2018).

In this study, the role of Pyk2 in facilitating intracellular replication of the AIEC type-strain LF82 in RAW 264.7 murine macrophage cells was determined. Through the use of high throughput imaging of individual cells via imaging flow cytometry, we have gained an increased understanding of the role of this kinase at the single cell level, demonstrating a key role for Pyk2 in controlling intramacrophage replication of this poorly understood pathogen.

4.2 Methods and Materials

4.2.1 AIEC phagocytosis assay

RAW 264.7 cells were plated in a 24-well plate at a density of 2 x 10^5 cells per-well. Cells were incubated (37°C, 5% CO2) for 6 h resulting in adherence to plates. Before infection, cells were activated by adding 1 µg/ml of LPS 12 h prior to infection. Activated cells were treated with the indicated concentrations of PF-431396 hydrate (Sigma-Aldrich) for 1 h. In the following content, PF-431396 hydrate is referred to as PF-431396 for short, and it suppresses the phosphorylation of Pyk2 (pPyk2) at its active tyrosine phosphorylation site, Y402, without decreasing total protein level of Pyk2, thus functionally blocking multiple cellular signalling pathways (Mills *et al.*, 2015). Supernatants were removed and cells were infected with an MOI of 100 in 200 µl of RPMI-1640 media containing 3% FCS and 1% L-glutamine. Cells were left for 1 h to allow bacterial phagocytosis to occur, before the supernatant was removed and 1 ml of fresh media containing gentamicin (50 µg/mL) was added for 1 h to kill any extracellular bacteria. Post-gentamicin treatment, supernatants were removed, cells were lysed with 200 µl PBS containing 2% Triton X-100 for 5 min and bacterial numbers calculated as described above.

4.2.2 Western Blotting Analysis

Bands on Western blots were quantified using ImageJ software (Schneider, Rasband and Eliceiri, 2012). To compare both Pyk2 and pPyk2 expression in infected or uninfected RAW 264.7 cells, with or without PF-431396 treatment, values from each blot were normalised by loading control (GAPDH) as Pyk2/GAPDH or pPyk2/GAPDH. The Pyk2/GAPDH and pPyk2/GAPDH values of control groups were set as 1 and the relatively densitometric change of test samples was calculated. All Western blots were performed in triplicate, with each performed on a biological replicate. All data are represented as the mean ± standard deviation for all performed repetitions.

4.2.3 Imaging flow cytometry

All samples were acquired at 60 times magnification giving an optimal 7 μM visual slide through the cell and a minimum of 10,000 single cell events were collected for each sample. In focus cells were determined by a gradient root mean square (RMS) for image sharpness. Brightfield of greater than 50 and single cells were identified by area versus aspect ratio. Only data from relevant channels were collected including Channel 02 (Ch02, GFP fluorescence), Ch04 (bright field), and Ch05 (pPyk2 conjugated AF647 fluorescence). Samples were run with a 488 nm laser with power of 5 mW and a 642 nm laser with power of 150 mW. Single colour compensation controls were also acquired, and a compensation file generated via IDEAS software (Luminex).

4.2.4 Calpain Assay

Calpain activity assays were performed using a calpain activity kit (ab65308, Abcam) according to manufacturer's protocols.

4.2.5 Cell counting kit 8 (CCK-8) assay

Cell survival rates were estimated by the CCK-8 assay (Abcam). Approximately 1 x 10^4 cells were seeded per well in 96-well plates with 100 μl medium in each well. After 24 h cultivation, different doses of PF-431396 were added for a further 6 h. Each well was incubated with 10 μl of CCK-8 solution for 2 h away from light before measuring the absorbance at 450 nm by FluoStar Optima

fluorescent plate reader (BMG Biotech). The relative viability was expressed by the formula: % of viability = ((Aexp – ABlank)/Acontrol - ABlank)) X 100%.

4.2.6 Real-Time PCR

Macrophages were harvested post-infection and RNA was isolated using a PureLink™ RNA Mini Kit (Life Technologies). RNA was reverse transcribed into cDNA using a high-capacity cDNA reverse transcription kit (Applied Biosystems). Levels of Pyk2 transcription were analysed by qRT-PCR using perfecta SYBR Green FastMix. Individual reactions were performed in triplicate within each of three biological replicates. The GAPDH gene was used to normalise the results (PYK2: forward: 5′ -GGACTATGTGGTGGTGGTGA-3; reverse: 5′ -TCTGCCAGGTCTTTGTTGAG-3; GAPDH: forward: 5′ -CAACTTTGGCATTGTGGAAGGGCTC-3; reverse: 5′ -GCAGGGATGATGTTCTGGGCAGC-3, obtained from DNA Oligos Sigma). qRT-PCR reactions were carried out using the CXF Connect Real-Time PCR Detection System (BIO-RAD Laboratories, Inc.) according to manufacturer's specifications and the data were analysed according to the $2^{-\Delta\Delta CT}$ method (Livak and Schmittgen, 2001).

4.2.7 Statistical analysis

Values are shown as means and standard deviation. All statistical tests were performed with GraphPad Prism software, version 8.3.0. All replicates in this study were biological; that is, repeat experiments were performed with freshly grown bacterial cultures and cells, as appropriate. Technical replicates of individual biological replicates were also conducted. Significance was determined as indicated in the figure legends. qRT-PCR data were log-transformed before statistical analysis. Values were considered statistically significant when p-values were ∗ = p<0.05; ∗∗ = p<0.01; ∗∗∗ = p<0.001; ∗∗∗∗ = p<0.0001.

4.3 Results

4.3.1 Survival and replication of AIEC within RAW 264.7 cells at different time points of infection

Initially, to examine the level of bacteria inside macrophages (CFU per gram of cellular protein) at different time points of infection, we carried out a traditional colony counting method to count the number of intracellular bacteria (Figure 4-1). As noted in the graph, in *in vitro* experiments the mean CFU value for the early period up to 6 h illustrates that the bacteria are replicating inside the cell, and then for the next period, 6 to 12 h, the bacteria maintain a stable level, before finally numbers of bacteria begin to decrease after 12 h. Our data confirmed that LF82 can replicate and survive within macrophages (Bringer *et al.*, 2006). It is therefore believed that different infection time points correspond to different survival states of bacteria within macrophages. When *in vitro* infection experiments were conducted, therefore, a window to monitor bacterial replication was identified up to 6 hpi, while studying bacteria at a non-growing stage could be carried out up to approximately 12 hpi, while finally it would be possible to investigate bacterial survival within macrophages for 24 hpi or longer. LF82 are able to remain in macrophages isolated from CD patients for a prolonged period evading the killing mechanism of macrophages, leading to disordered cytokine profiles (Vazeille *et al.*, 2015; Buisson *et al.*, 2016). As a result of the dynamic nature of infection, intracellular bacteria may replicate, be degraded, or remain within macrophages. During this pilot study, we found that intracellular LF82 still maintain within RAW 264.7 cells at a high level at 24 hpi. For this reason, we set up infection experiments for 24 hpi to evaluate the ability of intracellular LF82 to persist within macrophages.

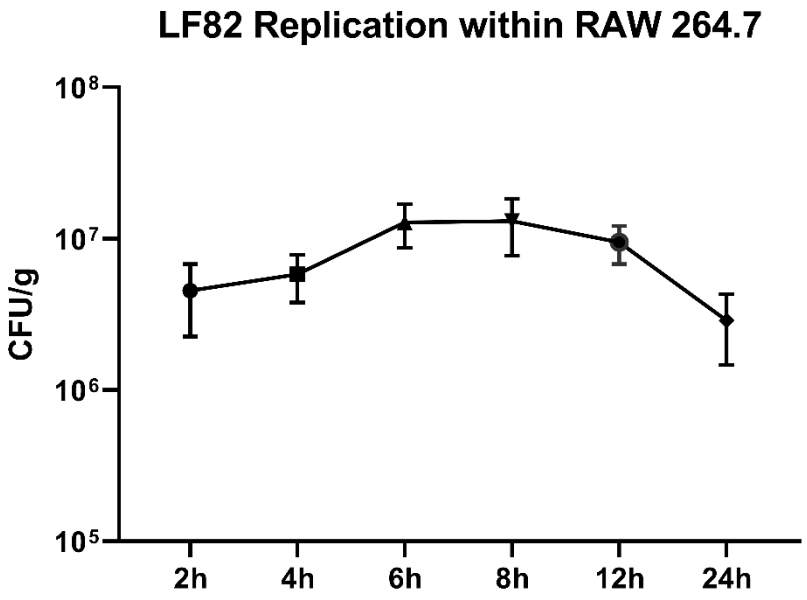

Figure 4-1 Murine RAW 264.7 macrophages infected with LF82 at different time points.

One hour post-infection, gentamicin was added to eliminate extracellular bacteria (designated as time zero (T0)). The viable colony counts of LF82 at 2, 4, 6, 8, 12 and 24 hpi were determined. The value represents the mean of three independent experiments and error bars are shown as ± SEM.

4.3.2 Screen host candidate proteins for inhibition of intracellular bacteria survival

Until now, little knowledge has been available regarding the interaction of specific macrophage proteins with AIEC. Previous work in our lab involved use of a protein array to screen for increased protein expression in infected macrophages, with several host proteins found to be upregulated during infection. Four host proteins (death associated protein kinase, P21 activated kinase 1, tryptophan hydroxylase and proline rich tyrosine kinase 2) were identified. Unfortunately, due to discontinuation of the protein arrays mid-project, this work could not be completed. Subsequently, inhibitors corresponding for each of these proteins were added during LF82 infection of macrophages in a preliminary experiment. *Salmonella enterica* serovar Typhimurium (*S.* Typhimurium) reference strain, SL1344, was added alongside LF82 as a control for these experiments. This strain of *S.* Typhimurium causes gastroenteritis, and it is capable of adapting and reproducing within macrophages, although it causes a more acute infection in comparison to LF82 (Knodler and Celli, 2011; Dunne *et al.*, 2013; Robinson, 2018).

RAW 264.7 cells were infected with SL1344 or LF82 for 1 hour at an MOI of 100. After 1 hour of infection, infected macrophages were washed and then exposed to a variety of inhibitors for a further 24 hours. Twenty four hours post-infection, cell lysates were collected for bacterial viable counts and caspase-3 assays. For comparison to different inhibitors treatment, the SL1344 or LF82 infected RAW 264.7 cells were treated with PBS as a control. Since all types of inhibitors were dissolved in DMSO, another control group was set up as infected cells were treated with DMSO only. In the results of the bacterial viable count, both SL1344 (Figure 4-2a) or LF82 (Figure 4-2b) were reduced significantly in macrophages when Pyk2 was inhibited. Notably, for SL1344 infected macrophages treated with 10 μM PF-414396, we observed a significant reduction in the number of intracellular bacteria (15.6-fold reduction) compared with cells treated with PBS. Meanwhile, the presence of intracellular LF82 within macrophages was also reduced by approximately 52-fold in the presence of 10 μM PF-414396, when compared with PBS treatment. These results suggest that PF-431396 affects phenotype of RAW 264 .7 cells reducing the abilities of pathogenic strains (both SL1344 and LF82) to survive intracellularly, a key trait of pathogenic strains thought to trigger the potent inflammatory response characteristic of CD.

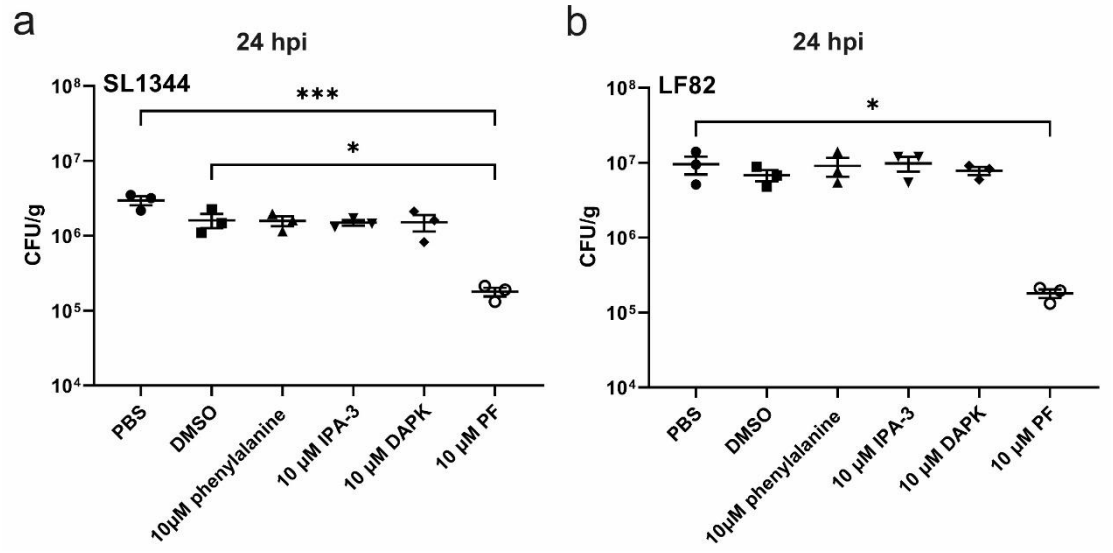

Figure 4-2 Intracellular SL1344 or LF82 were analysed by a gentamicin protection assay in the presence of a variety of inhibitors.

RAW 264.7 cells were infected with SL1344 (a) or LF82 (b) at an MOI of 100 for 1 h. Post-infection cells were washed and treated with phenylalanine (4-Chloro-DL-phenylalanine: tryptophan hydroxylase inhibitor), IPA-3 (allosteric inhibitor of Pak1), DAPK inhibitor (death-associated protein kinase inhibitor), or PF-431396 hydrate (Pyk2 inhibitor) for 24 h, in media containing 50 μg/ml gentamicin. Intracellular LF82 number was normalised to cell protein concentration and presented

as CFU per g of cell protein (CFU/g). Statistical analyses were preformed using GraphPad Prism, with data analysed by one-way ANOVA n= 3 (p<0.05 *; p<0.01 **; p<0.001 ***).

Previously, it was shown that during AIEC infection of macrophages, caspase-3 was trafficked to the proteasome for degradation (Dunne *et al.*, 2013). Caspase-3 was degraded by the proteasome in LF82 infected RAW 264.7 cells (14.3-fold decrease in caspase-3), but not those infected with SL1344 (1.8-fold decrease) (Dunne *et al.*, 2013). Here again the level of caspase-3 was measured during infection of RAW 264.7 cells treated with different chemical inhibitors. Interestingly, a significant increase in the level of capase-3 was observed in the LF82 infected RAW 264.7 cells in the presence of 10 μM PF-431396 (5.4-fold relative to PBS, 5.9-fold relative to DMSO; Figure 4-3b) but not be observed in SL1344 infected cells (Figure 4-3a). These results also confirmed that degradation of caspase-3 likely plays an important role in the persistence of LF82 within macrophages. Taken together, these results indicated that inhibition of Pyk2 during LF82 infected RAW 264.7 cells could reduce intracellular bacteria, likely via removing LF82 inhibition of caspase-3 activity. Although inhibition of pPyk2 increased the activity of caspase-3, the relationship between Pyk2 and the proteasome remains unclear. Therefore, to understand the potential use of PF-431396 as a candidate inhibitor of AIEC infection we focused on its effects during infection mediated through targeting Pyk2.

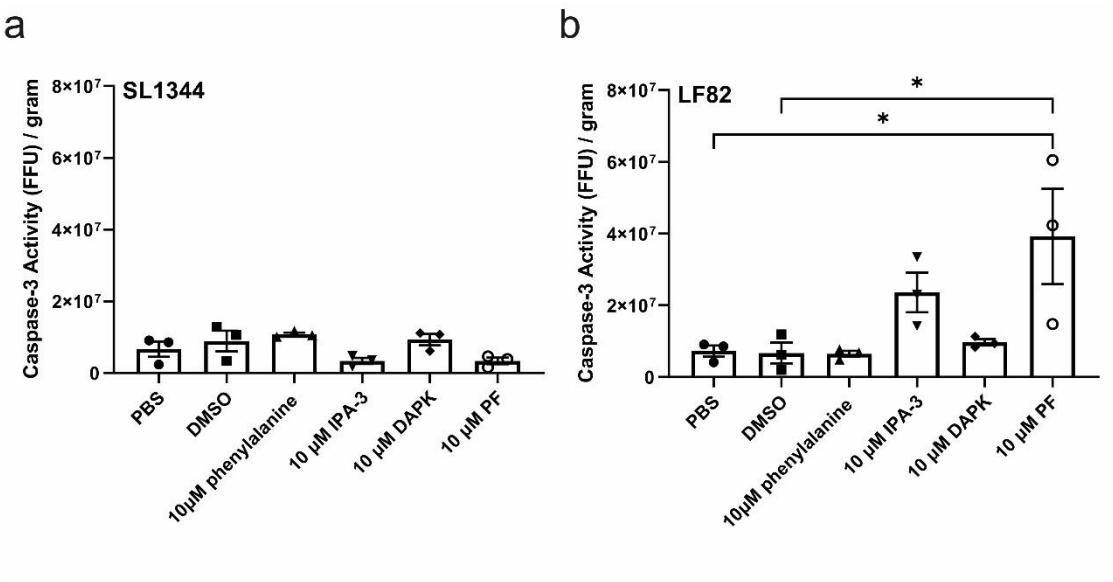

Figure 4-3 Caspase-3 levels were measured in SL1344 or LF82 infected RAW 264.7 cells.

RAW 264.7 cells were infected with SL1344 (a) or LF82 (b) and treated with different chemical inhibitors. At 24 hpi the supernatant of infected cells was collected and caspase-3 activity was measured using a fluorescence based enzyme assay (Apo One Caspase-3/7 activity kit). Statistical analyses were preformed using GraphPad Prism, with data analysed by one-way ANOVA n= 3 (p<0.05 *; p<0.01 **; p<0.001 ***)

4.3.3 Evaluation of macrophage Pyk2 protein levels in response to LF82 infection

To determine the change in Pyk2 expression in RAW 264.7 macrophages in response to LF82 infection, total Pyk2 and phosphorylated Pyk2 (pPyk2) levels were measured by immunoblotting (Figure 4-4) In Figure 4-4a, RAW 264.7 cells pre-stimulated with LPS significantly increased both Pyk2 and pPyk2, suggesting that Pyk2 is increased in response to bacterial infection. Quantification of Pyk2 or pPyk2 signalling by ImageJ showed increased Pyk2 protein level (1.8-fold change) at later times during LF82 infection compared to the initial infection time point with p = 0.0431 (1 hpi) (Figure 4-4b). However, this change was not observed in pPyk2 protein levels. RAW 264.7 cells pre-stimulated with LPS or not were infected by LF82 at 1, 6 and 24 hours. We next evaluated the ability of RAW 264.7 cells to phagocytose LF82 using viable colony counts when the cells had been stimulated, or not, with LPS overnight. LPS stimulation resulted in higher CFU count at 1 hpi (p = 0.0011) and 6 hpi (p = 0.0030) but not at 24 hpi (p = 0.3214), when compared to no LPS pre-treatment, indicating that LPS-induced Pyk2 expression may facilitate phagocytosis of LF82 by macrophages (Figure 4-4c).

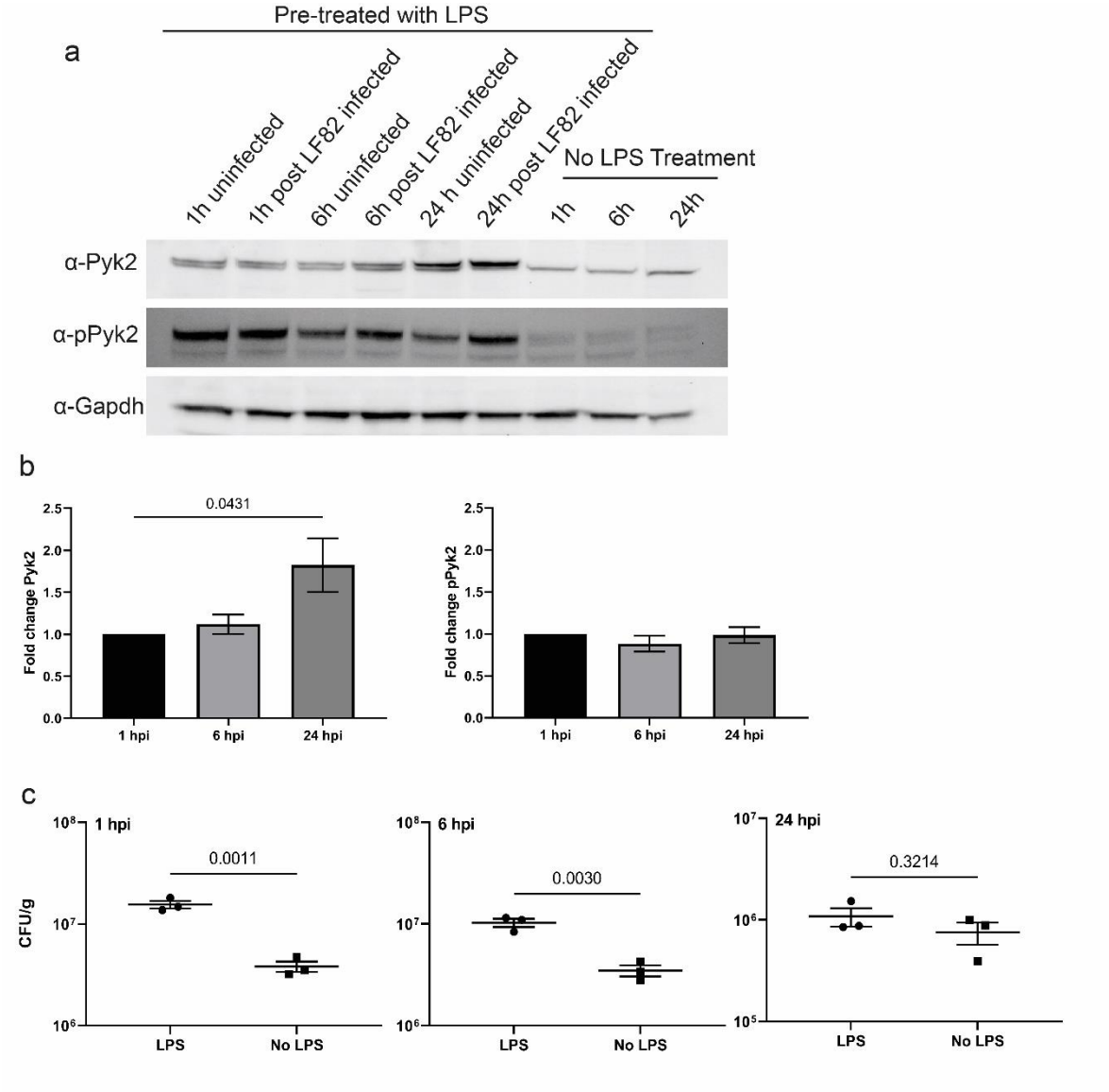

Figure 4-4 LPS-induced Pyk2 expression facilitates LF82 phagocytosis by RAW 264.7 cells.

(a) In an image, from left to right column 1 to 6 shown RAW 264.7 cells pre-treated with LPS overnight. Next day, after 1-hour infection with LF82, cells were washed and incubated further 1, 6 and 24 hour, along with uninfected cells. The last 3 column of the image represented that cells in absence of LPS treatment was incubated 1, 6 and 24 hours without LF82 infection. Cell lysates of all samples were extracted and immunoblotted using anti-Pyk2 (1:1000; abcam) or anti-pPyk2 (1:1000; abcam) and anti-Gapdh (1: 1000; abcam). Blots were visualised with HRP-conjugated goat anti-rabbit antibody (1:10,000) or HRP-conjugated goat anti-mouse (1:10,000) (both ThermoFisher) and developed using enhanced chemiluminescence (ECL). (b) Bar graphs represented LF82 infected RAW 264.7 cells at 1, 6 and 24 hpi, showing the Pyk2 and pPyk2 expression levels. Data with three biological repeats was analysed by software ImageJ and graphed by Prism 8; error bar represents as ± SEM. (c) RAW 264.7 cells were pre-treated with or without 100 ng/ml LPS overnight then were infected with LF82 at 1, 6 and 24 hpi. Intracellular LF82 were counted using viable colony counts. Data are representative of three independent biological experiments. Statistical analysis was using an unpaired Student's t-test. *P* value shown for comparison between LPS treatment and no LPS treatment,

When compared to uninfected cells, Western blot results showed that a significant increase (2.4-fold change, $p = 0.0063$) in total Pyk2 was observed at 6

hpi and pPyk2 levels were also slightly increased (1.3 fold change, p = 0.1163) versus uninfected cells (Figure 4-5a-b). To investigate this further in relation to infection, IFC was used to analyse pPyk2 levels simultaneously in thousands of individual uninfected and LF82-infected cells. IFC allows identification of all cells within a population that are infected with GFP-expressing bacteria. These cells can be counted and the individual bacterial load in each determined, allowing the separation of cells based on both their infection status and bacterial load in a way not possible with traditional colony-counts. Using this approach here it was determined that there was a significant increase in pPyk2 levels in response to LF82 infection infected cells compared to control uninfected cells (p = 0.0373; Figure 4-5 c-d).

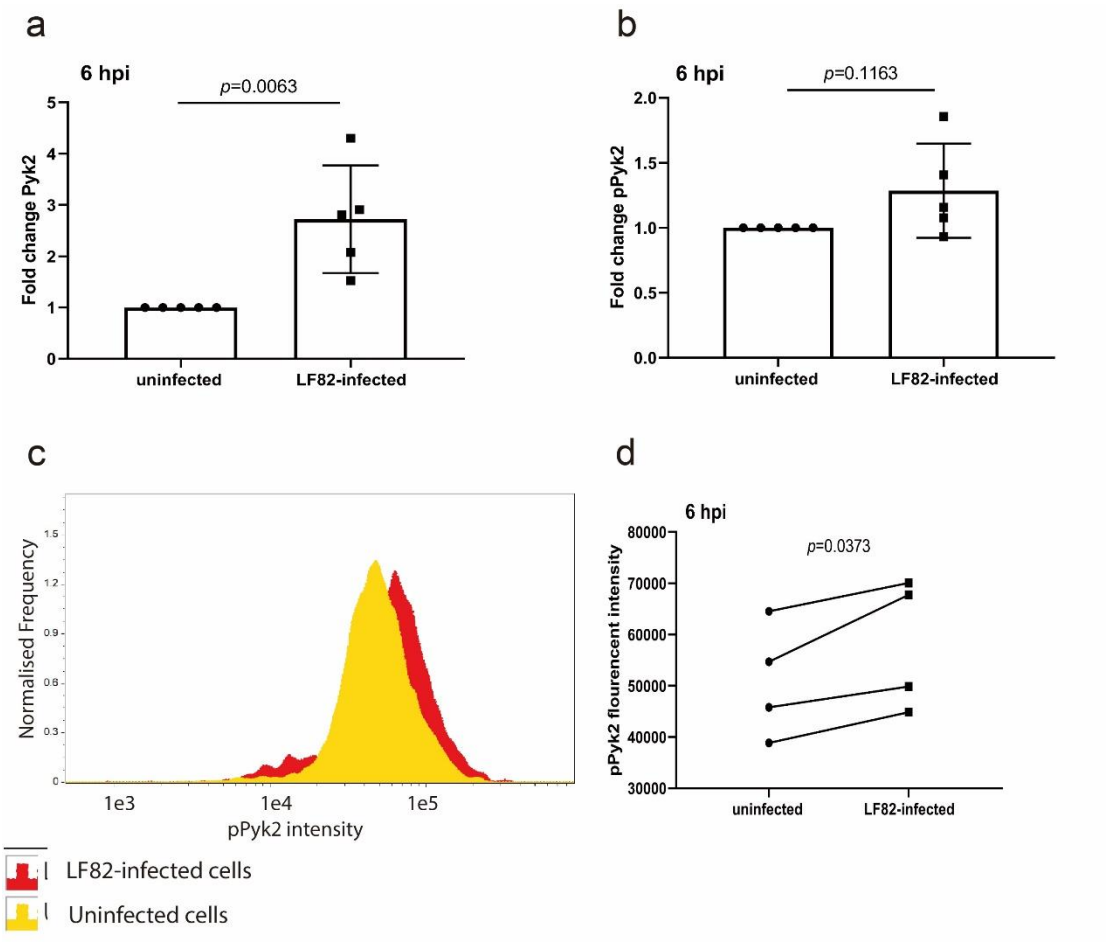

Figure 4-5 Pyk2 and phosphorylated Pyk2 (pPyk2 [Y402]) expression levels in RAW 264.7 macrophages.

Western blot of levels of Pyk2 (a) or pPyk2 (Y402) (b) at 6 hpi were compared between LF82-infected or uninfected RAW 264.7 cells using densitometric analysis of Western blots. Statistical analyses were conducted using a Student's t-test. Data are representative of five independent experiments. (c) A representative histogram showing imaging flow cytometry data displays the pPyk2 (Y402) intensity of control uninfected RAW 264.7 macrophages in yellow and LF82 infected cells at 6 hpi in red. (d) The level of pPyk2 (Y402) in infected RAW 264.7 cells at 6 hpi was

analysed by imaging flow cytometry and compared with that of uninfected cells, using a paired t-test statistical test. Results are representative of four biological independent experiments.

4.3.4 Pyk2 inhibitor PF-431396 hydrate successfully blocks phosphorylation of Pyk2 in uninfected and LF82 infected macrophages

PF-431396 hydrate inhibits phosphorylation of Pyk2 at its active site Y402, blocking multiple cellular signalling pathways (Mills *et al.*, 2015). Activated Pyk2 was measured by immunoblotting cell extracts with phospho-specific antibodies directed against the Pyk2 (Y402) autophosphorylation site. Six hpi levels of Pyk2 (Figure 4-6a and b) or pPyk2 (Y402; Figure 4-6a and c) were measured by Western blot in infected cells and controls, including those where PF-431396 had been added. PF-431396 significantly reduced levels of pPyk2 (Y402) were detected in LF82-infected and uninfected RAW 264.7 cells in response to the highest concentrations of PF-431396 tested post-treatment (5 and 10 μM; Figure 4-6 b-c). IFC analysis further confirmed that PF-431396 significantly reduced pPyk2 (Y402) levels in infected cells with the number of cells with detectable pPyk2 (Y402) significantly dropping at 6 hpi (Figure 4-6d) before reducing further at 12 hpi (Figure 4-6e).

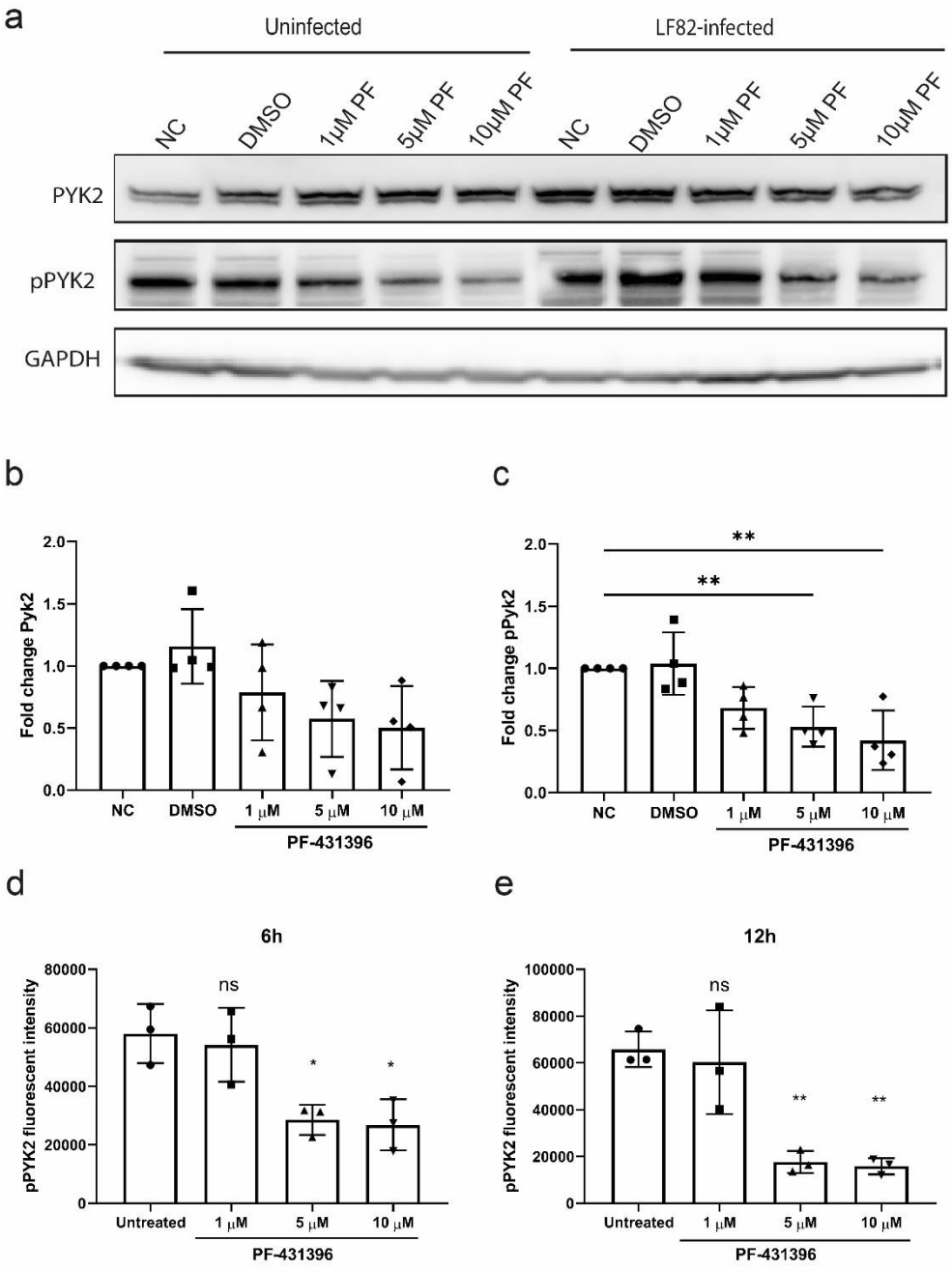

Figure 4-6 The inhibitor PF-431396 blocks phosphorylation of Pyk2 in both uninfected and LF82 infected cells in a dose dependent manner.

LF82 infected or control uninfected RAW 264.7 cells were treated with PF-414396 hydrate (0, 1, 5, 10 μM) for 6 h. Untreated cells were used as controls. (a) Immunoblotting was used to detect levels of pPyk2 (Y402) with Gapdh used as loading control. To determine relative pPyk2 (Y402) levels in inhibitor treated cells, imaging flow cytometric analysis was carried out on LF82 infected RAW 264.7 cells after treatment for 6 hpi (b) or 12 hpi (c) with PF-431396. Statistical analyses were conducted using an unpaired one-way ANOVA test. (ns, not significant, *$p < 0.05$, **$p < 0.01$, ***$p < 0.001$). Data are representative of three independent biological replicates.

To ensure that these decreases in pPyk2 (Y402) levels were not due to cytotoxicity of PF-431396 we demonstrated no increased release of lactate dehydrogenase (LDH), as a measure of cytotoxicity, or decreased viability in

uninfected or infected RAW 264.7 cells when PF-431396 was used at concentrations up to, and including, 10 μM (Figure 4-7). A measure of viability of uninfected or LF82 infected RAW 264.7 cells was used to examine the viability levels of RAW 264.7 cells (Figure 4-8). At 6 hours post-PF-431396 treatment, uninfected RAW 264.7 maintained over 80% viability within different concentrations of PF-431396 (DMSO only [88.95 ± 3.579%], 1 μM [83.17 ± 4.989%], 5 μM [99.56 ± 9.164%], 10 μM [92.51 ± 0.8929%]; Figure 4-8a). However, when RAW 264.7 cells were infected with LF82 at 6 hpi in the presence of 1, 5 and 10 μM of PF-431396, or with a DMSO control, the percentage of living cells was 86.52 ± 8.449 % or 87.97 ± 5.104 %, in DMSO or 1μM of PF-431396 treatment, respectively. However, the percentage of living cells decreased to 74.16 ± 1.390% or 66.65 ± 4.613% with 5 or 10 μM of PF-431396 treatment, respectively (Figure 4-8b). We hypothesized that this decreased viability, not seen in the corresponding PF-431396 treated uninfected cells, was as a result of cell death due to LF82 infection.

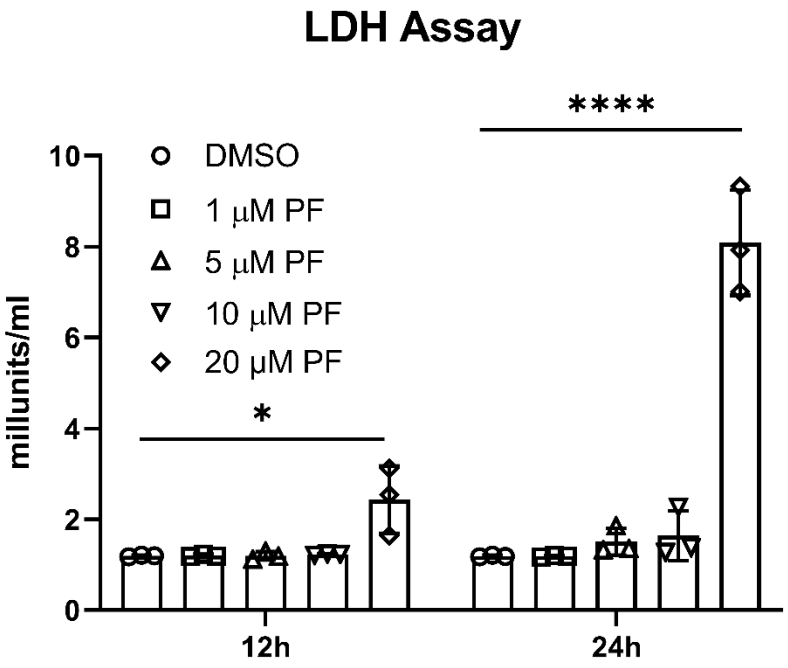

Figure 4-7 Low concentrations of Pyk2 inhibitor had no effect on cell toxicity.

LDH activity assays were conducted on supernatants collected from RAW 264.7 cells following infection and treatment with Pyk2 inhibitor PF-431396. LDH activity is reported as nmole/min/mL = milliunit/mL. Statistical analysis was conducted using a two-way ANOVA (ns, not significant, *p < 0.05, **p < 0.01, ***p < 0.001, ****p < 0.0001). Data are representative of three independent biological replicates.

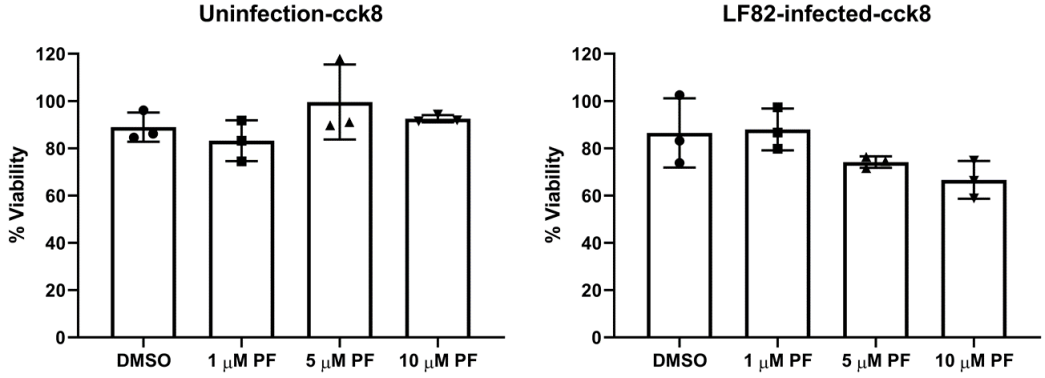

Figure 4-8 Measure of viability using a CCK8 assay for uninfected or LF82 infected RAW 264.7 cells in the presence of different concentrations of Pyk2 inhibitor.

After 6 hours of PF-431396 (0, 1, 5, 10 μM) treatment of LF82-infected or uninfected RAW 264.7 cells, cell viability was assayed by a cell counting 8 (CCK8) assay. Infected or uninfected cells without any treatment was set as a control. Viability values were presented as % of viability relative to control group. Plots represent three biological repeats. Values are means ± SEM. Statistical analyses were conducted using a unpaired one-way ANOVA test.

4.3.5 Pyk2 is important for phagocytosis of LF82 by macrophages

Given the previously reported role of Pyk2 in phagocytosis (Paone *et al.*, 2016), we analysed the role of Pyk2 in phagocytosis of LF82 by RAW 264.7 cells. RAW 264.7 cells were infected with LF82 following a 1 hour pre-treatment with the PF-431396 hydrate inhibitor and bacterial cfus were then counted. The highest concentration of inhibitor (10 μM), significantly impaired phagocytosis compared to cells that were untreated or treated with a lower concentration of inhibitor (Figure 4-9).

Having established that Pyk2 plays a role in phagocytosis of LF82, further treatments to inhibit Pyk2 were always carried out post-phagocytosis of LF82, that is the inhibitor was added after a defined period of LF82-macrophage interaction after which gentamicin was also added to remove extracellular bacteria. This was to ensure that any phenotypic effects on intracellular replication of LF82 were not masked by the initial inhibition of phagocytosis of the bacteria.

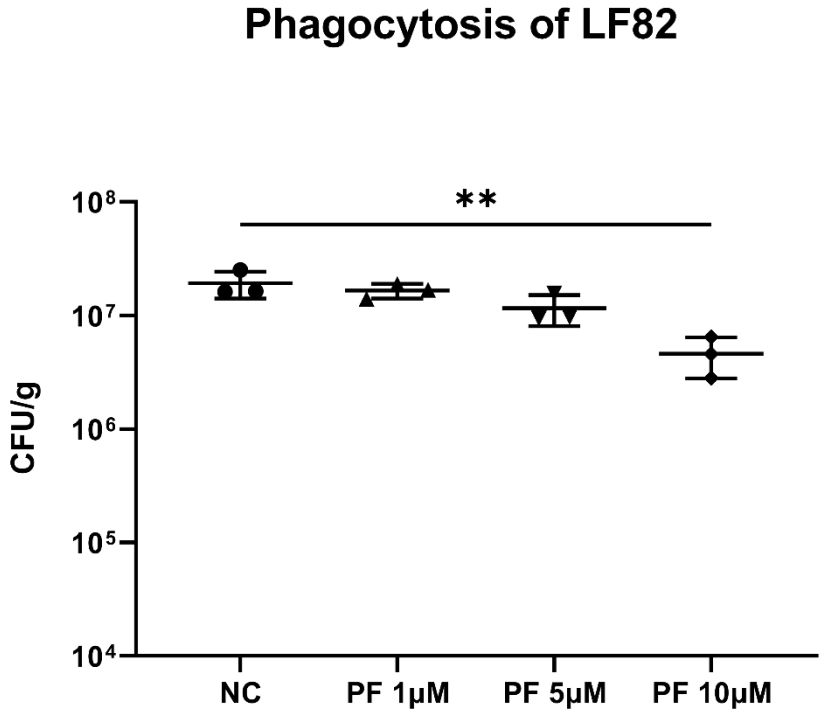

Figure 4-9 Pyk2 inhibition reduces the ability of macrophages to undertake phagocytosis.

To determine its effect on phagocytosis, RAW 264.7 cells were pre-treated with PF-431396 for 2 hours before infection with LF82 at an MOI of 100. PF-431396 was added to RAW 264.7 cells at concentrations of 0 µM (NC – negative control), 1 µM, 5 µM and 10 µM at 1 hpi. Plots represent three biological repeats. Values are means ± SEM. Statistical analyses were conducted using a unpaired one-way ANOVA test (ns, not significant, *$p < 0.05$, **$p < 0.01$, ***$p < 0.001$, ****$p < 0.0001$).

4.3.6 Inhibition of Pyk2 function significantly reduces intra-macrophage LF82 burden

Intracellular replication is a hallmark of the AIEC phenotype. To determine any role of Pyk2 in intracellular replication of LF82, the Pyk2 inhibitor PF-431396 was added at concentrations of 0, 1, 5 and or 10 µM at 1 hpi. Levels of intracellular bacteria were measured through colony counts at 6, 12 and 24 hpi. At 6 hpi, there was no significant difference in intracellular bacterial numbers relative to the control at any concentration of PF-431396 (Figure 4-10a). However, a significant reduction in intracellular LF82 number was seen at 12 hpi with 5 µM and 10 µM PF 431396 (Figure 4-10b) and at 24 hpi for all concentrations of PF-431396 (Figure 4-10c).

The interaction of intracellular pathogens with host cells is traditionally quantitated on a cellular population level. However, intracellular replication is heterogeneous and infection of host cells with a clonal population of any intracellular pathogen frequently results in variable numbers of bacteria in individual host cells. To confirm the results obtained by bacterial cell counting, immunofluorescence was conducted to permit direct visualisation of infected cells. In addition, IFC was conducted to allow quantification of morphological cellular features and spatial distribution of fluorescent markers at the single cell level in this heterogenous infected population. This made it possible to correlate acquired cellular images and accurately quantify intracellular bacteria.

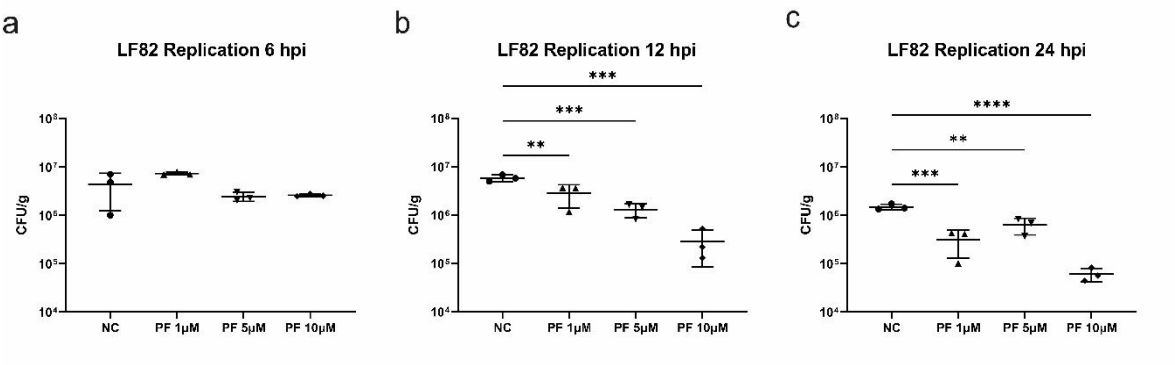

Figure 4-10 Pyk2 inhibition reduces intracellular LF82 in RAW 264.7 cells using viable colony counts.

Intracellular replication of LF82 in the presence of PF-431396 was measured by total viable counts at (b) 6 hpi, (c) 12 hpi and (d) 24 hpi. PF-431396 hydrate was added to RAW 264.7 cells at concentrations of 0 μM (NC – negative control), 1 μM, 5 μM or 10 μM. Statistical analyses were conducted using a one-way ANOVA. (ns, not significant, *$p < 0.05$, **$p < 0.01$, ***$p < 0.001$, ****$p < 0.0001$). Data are representative of three independent biological experiments.

The intracellular bacterial load of LF82::*rpsM*GFP in response to Pyk2 inhibition was examined by immunofluorescence microscopy (Figure 4-11). The presence of LF82::*rpsM*GFP and distribution of pPyk2 in RAW 264.7 cells was observed following PF-431396 treatment at 24 hpi (Figure 4-11). Immunofluorescence assays again demonstrated that LF82::*rpsM*GFP intramacrophage numbers were reduced upon inhibition of Pyk2 activation in agreement with quantitative assessment by cfu counting (Figure 4-11).

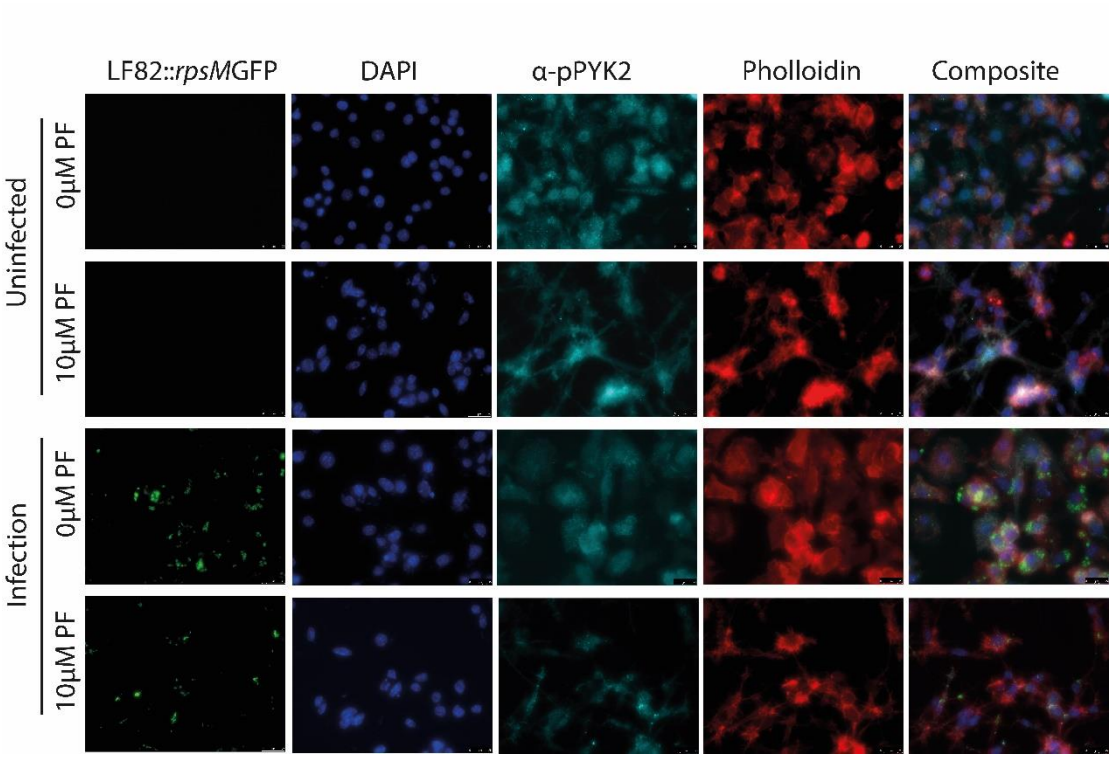

Figure 4-11 Pyk2 inhibition directly affects intracellular replication of LF82 using florescent microscopy.

Pyk2 inhibitor PF-431396 was added to RAW 264.7 cells at concentrations of 0 μM, 1 μM, 5 μM and 10 μM 1 hpi with LF82 transformed with LF82::*rpsM*GFP (MOI 100) where indicated. LF82::*rpsM*GFP-infected macrophages RAW 264.7 were examined at 12 hpi by immunofluorescence staining for the presence and localisation of LF82 (green staining), DAPI nuclei (blue staining), F-actin (red staining) and protein pPyk2 (cyan staining). Representative images of merged channels and individual colour staining are shown. All images were acquired at a X40 magnification and are representative of those from 3 biological repeats.

4.3.7 Pyk2 inhibition blocks LF82 replication intracellularly without affecting overall numbers of infected cells

Given that LF82 infection of RAW 264.7 cells is heterogenous with potentially large numbers of intracellular bacteria, IFC was employed to quantitatively correlate the number of intracellular bacteria with the level of Pyk2 phosphorylation and activation in single cells.

To facilitate analysis, cells were assigned to groups. Those with greater than 10 bacteria were deemed to have a “high” bacterial burden, those with 6-10 bacteria assigned to an “intermediate” bacterial burden, and those with five or less as having a “low” bacterial burden. While assigning cells to these groups was largely arbitrary, cells were assigned to groups based on the hypothesis that cells with greater than 10 bacteria were more likely to be representative of

those where intracellular replication of LF82 has taken place, whilst those with fewer than five 5 bacteria were more likely to be indicative of bacterial phagocytosis rather than replication. Separating the infected macrophage population into distinct populations based on bacterial load is a significant step forward in understanding the dynamics of LF82 infection, which was previously determined using a highly heterogenous populations of infected cells. For each of high, intermediate, and low bacterial burdens the percentage of the total population was plotted at 6 hpi (Figure 4-12a) and 12 hpi (Figure 4-12b), respectively. Since treatment with the Pyk2 inhibitor was initiated post-phagocytosis, and therefore did not influence bacterial uptake by the macrophages, there were as expected similar numbers of infected and uninfected cells across all treatment groups. Untreated cells or those treated with 1 μM of PF-431396, resulted in a significantly larger population of these cells having a high bacterial burden at both 6 hpi (18.57% and 16.96% of total cells respectively) and 12 hpi (17.56% and 17.26% respectively) when compared to 10 μM treatment. Correspondingly post-10 μM treatment, a significant decrease in cells with a high bacterial burden was noted (9.01% at 6 hpi and 6.87% at 12 hpi, Figure 4-12a and Figure 4-12b). In cells treated with 10 μM PF-431396, where less pPyk2 (Y402) protein was detectable, a significantly larger population of cells were observed to have a low bacterial burden at both 6 hpi (49.13%) and 12 hpi (53.43%), compared to untreated cells which had 39.65 % and 41.53 % of “low” bacterial burden cells.

This expansion of low bacterial burden cells in 10 μM PF-431396 treated cells was at the expense of those with a high bacterial burden, as there was a corresponding reduction in this subset. These data indicate that when phosphorylation of Pyk2 is inhibited it has a direct inhibitory effect on intracellular replication of LF82 in RAW 264.7 macrophages.

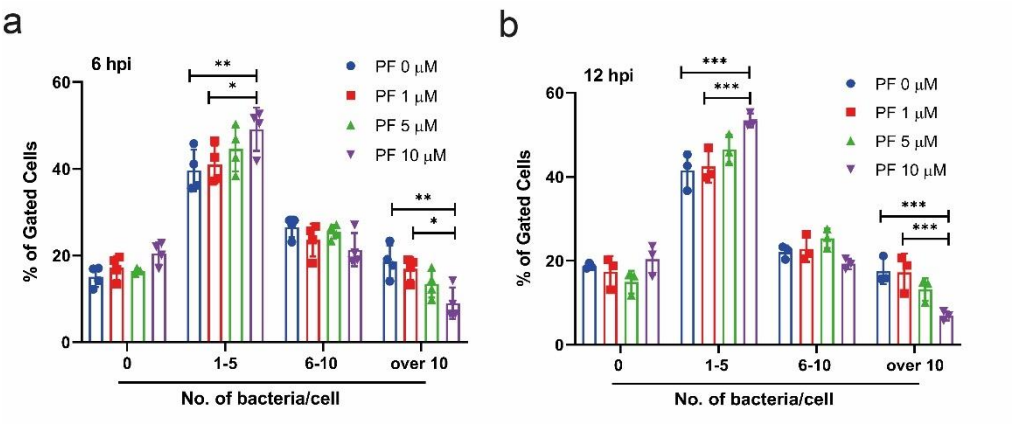

Figure 4-12 Treatment with PF-431396 inhibits Pyk2 phosphorylation and reduces intra-macrophage LF82 burden using IFC.

LF82::*rpsM*GFP burden in RAW 264.7 macrophages was analysed via IFC. The bacterial spot count profiles at 6 hpi (a) and 12 (b) hpi were separated into: groups representing uninfected cells (0 bacteria); cells with a low infection count (1-5 bacteria per cell); medium infection count (6-10 bacteria per cell); and highly infected cells (>10 bacteria per cell) where PF refers to concentration of PF-431396 hydrate added. Data are representative of three independent biological replicates. Statistical analyses were conducted using a two-way ANOVA (ns, not significant, *$p < 0.05$, **$p < 0.01$, ***$p < 0.001$, ****$p < 0.0001$).

4.3.8 PF-431396-mediated blocking of LF82 replication in macrophages significantly reduces TNF-α secretion

High levels of TNF-α are detected in CD patients and secretion of TNF-α occurs post-infection of macrophages by AIEC (Bringer *et al.*, 2012). High levels of TNF-α are released as consequence of mucosal injury and transmural inflammation in CD, primarily from lamina propria mononuclear cells (Adegbola *et al.*, 2018). Additionally previous studies have highlighted a role for Pyk2 activation in TNF-α secretion (Yang *et al.*, 2013; Murphy *et al.*, 2019). Given intracellular numbers of LF82 were directly affected by inhibition of Pyk2 using PF-431396 hydrate, we went on to determine if there was any downstream impact on TNF-α release. Treatment of macrophages with 5 μM and 10 μM PF-431396 induced a significant reduction in TNF-α release (between 15 to and 40 fold) (Figure 4-13). This reduction was not seen in untreated macrophages or those treated with 1 μM inhibitor (Figure 4-13). In addition, an assessment of cytotoxicity based on LDH release, showed that these decreases in TNF-α release could not be attributed to increased toxicity due to the inhibitor (Figure 4-7). While it is difficult to conclusively state conclude that this reduction in TNF-α secretion is a direct result of Pyk2 inhibition, rather than an indirect effect of the lower intracellular burden of LF82, the significant decrease in TNF-α release that was observed at 5

μM PF 431396 hydrate was not associated with a reduction in intracellular burden (Figure 4-10a).

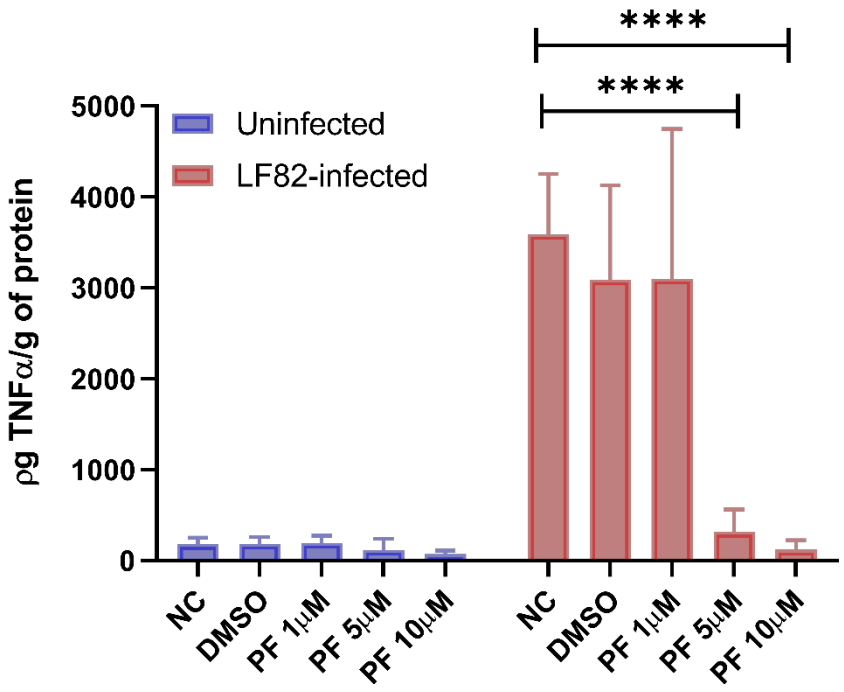

Figure 4-13 Inhibition of Pyk2 phosphorylation significantly reduces TNF-α secretion by RAW 264.7 cells post-LF82 infection.

Comparison of TNF-α secretion levels from supernatants of infected or uninfected RAW 264.7 cells. RAW264.7 cells were activated by LPS overnight then infected or uninfected with LF82 for 1 h followed by treatment with PF-431396 for 6 h. At 6 hpi, TNF-α levels in supernatants were examined by ELISA. Values are means ± SD (n = 3 per group). Statistical analysis was conducted using a two-way ANOVA test (ns, not significant, *$p < 0.05$, **$p < 0.01$, ***$p < 0.001$, ****$p < 0.0001$).

Finally, to understand if other types of cell death such as apoptosis may be induced, we determined caspase-3 activity post-infection and PF-431396 treatment. Previous work from the lab had shown that programmed cell death in LF82 infected macrophages was inhibited through caspase-3 degradation, a means to delay cell death and promote intracellular replication (Dunne *et al.*, 2013). Firstly, it was demonstrated again that caspase-3 activity was inhibited by LF82 infection compared to uninfected cells (Figure 4-14a). Upon blocking of Pyk2 phosphorylation with PF-431396 however, there was a significant increase in caspase-3 activity in LF82 infected cells (2.5-fold at 5 μM and 2.5 fold at 10 μM) but not in 1 μM of PF-431396 at 6 hpi (Figure 4-14b). Caspase-3 is recognized

as playing a fundamental role in ensuring cell survival and correct functioning, and not simply as a driver of apoptosis and cell death, something that is reflected in the viability data where increased activity does not necessarily lead to immediate reductions in viability (Figure 4-8). Here it can be observed that Pyk2 can influence caspase-3 activity, and therefore cell viability during infection, as well as directly influencing TNF-α secretion by infected cells. Given the importance of both these factors to AIEC infection and CD, this work has identified Pyk2 as a potentially important target for therapeutic intervention in AIEC infection.

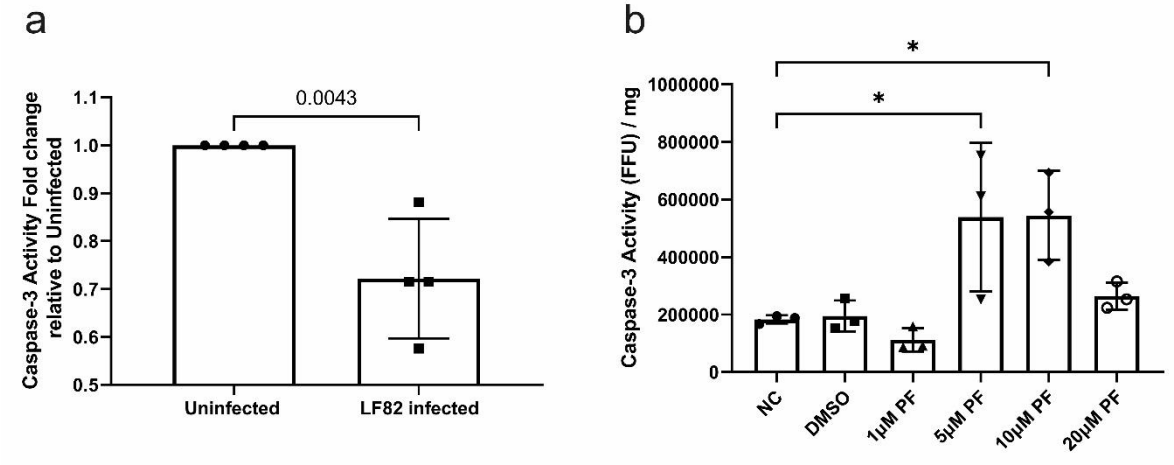

Figure 4-14 Caspase-3 activity in RAW 264.7 cells was measured at 6 hpi and expressed as caspase-3 activity in fluorescence focus units (FFU) per mg of protein.

(a) Compared to uninfected cells, LF82 infected cells had lower caspase-3 activity. Data are represented as fold change of infected groups relative to uninfected group which was set as 1-fold. Data were analysed by unpaired Student's t-test. (b) Cell lysates from RAW 264.7 cells at 6 hpi with different dose of PF-431396 or with DMSO or without any treatment (NC-negative control) were conducted to measure caspase-3 levels. Data were normalised by protein concentration as fluorescence value/ mg. Experiments were repeated three times in triplicate. Data represent the mean ± SD of three independent experiments and are analysed by one-way ANOVA (ns, not significant, *$p < 0.05$, **$p < 0.01$, ***$p < 0.001$, ****$p < 0.0001$).

4.3.9 Effect of Pyk2 inhibition during infection of RAW 264.7 cells with AIEC clinical isolates

The effects of Pyk2 inhibition were also observed in macrophages infected with *Salmonella enterica* serovar Typhimurium SL1344 and clinical isolates (B94, B115 and B125) from CD patients (Ormsby *et al.*, 2019, 2020). Pyk2 inhibition with PF-431396 resulted in reduced intracellular bacterial numbers at 24 hpi for all strains except commensal *E. coli* strain F18, and CD clinical isolate B122 (Figure 4-15 a-b). Again, Pyk2 inhibition significantly decreased TNF-α secretion from

macrophages infected with all CD clinical isolates at both 6 and 24 hpi (6 and 24 hpi; Figure 4-15 c-d). While SL1344 induced TNF-α release was reduced dramatically this was not statistically significant. However, it highlighted that Pyk2 activity may be relevant for other enteric pathogens also.

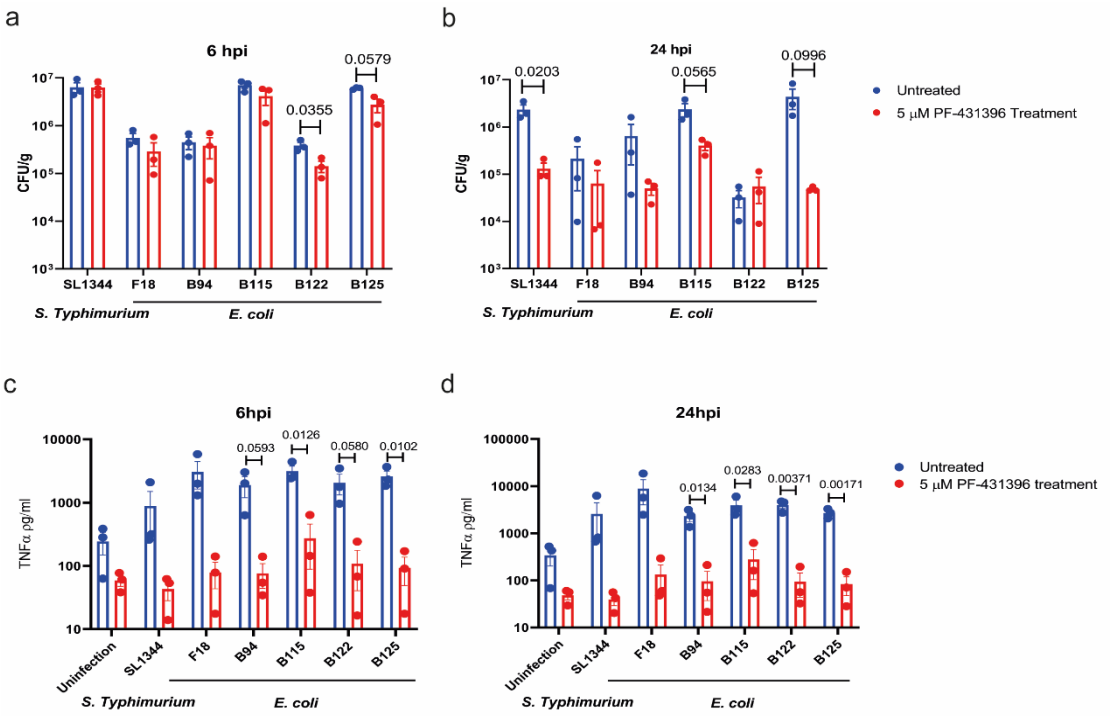

Figure 4-15 Pyk2 inhibition effects on intracellular survival of CD clinical isolates and TNF-α release during infection with macrophages.

RAW 264.7 macrophages were infected with *Salmonella* Typhimurium SL1344, commensal *E. coli* strain F18 and *E. coli* CD clinical isolates B94, B115, B122, and B125 for 1 h with an MOI of 100, with or without 5 μM of PF-431396 treatment for a further 6 and 24 hpi. (a and b) Intracellular bacterial count was determined by CFU count. (c and d) An ELISA was conducted to detect the secretion of TNF-α from the supernatant of uninfected or infected macrophages with or without 5 μM of PF-431396 treatment. Data displayed are of three independent experimental replicates, with each experiment including three independent biological replicates. Data are expressed as mean ± SEM; data were analysed using unpaired multiple t test. P-values less than 0.1 were labelled in the graph.

4.3.10 Evaluation of Pyk2 mRNA levels in response to LF82 infection *in vivo* and *in vitro* and PYK2 protein levels in CD patients

In order to evaluate expression of *Pyk2* during LF82 infection *in vitro* and *in vivo*. *Pyk2* mRNA levels (relative to *Gapdh* mRNA) were analysed by real-time RT-PCR, and the results of 3 biological experiments with 3 technical repeats at various infection times (2, 4, 6, 8 and 24 hpi) are depicted in Figure 4-16a. *Pyk2* showed no significant change in LF82 infected RAW 264.7 cells versus uninfected cells.

For *in vivo* measurements, 4 individual mice were culled and their colon and ileum were collected and RNA isolated to measure *Pyk2* mRNA levels. Animal tissue samples kept in RNAlater solution were kindly provided by Dr. Michael Ormsby using the protocol of Ormsby *et al.*, (2019). For *In vivo* infection experiments the LF82*lux* tagged strain was used as this strain contains the erythromycin cassette allows for selection of LF82 based on erythromycin resistance. Mice were treated with PBS as a control uninfected group. When compared with control groups, there was no significant change of *Pyk2* mRNA levels in LF82 or LF82 *lux* infected mice, in either colon (Figure 4-16b) or ileum (Figure 4-16c). However, while there was no change in *Pyk2* mRNA levels it does not discount that Pyk2 could be regulated by LF82 infection at the protein level.

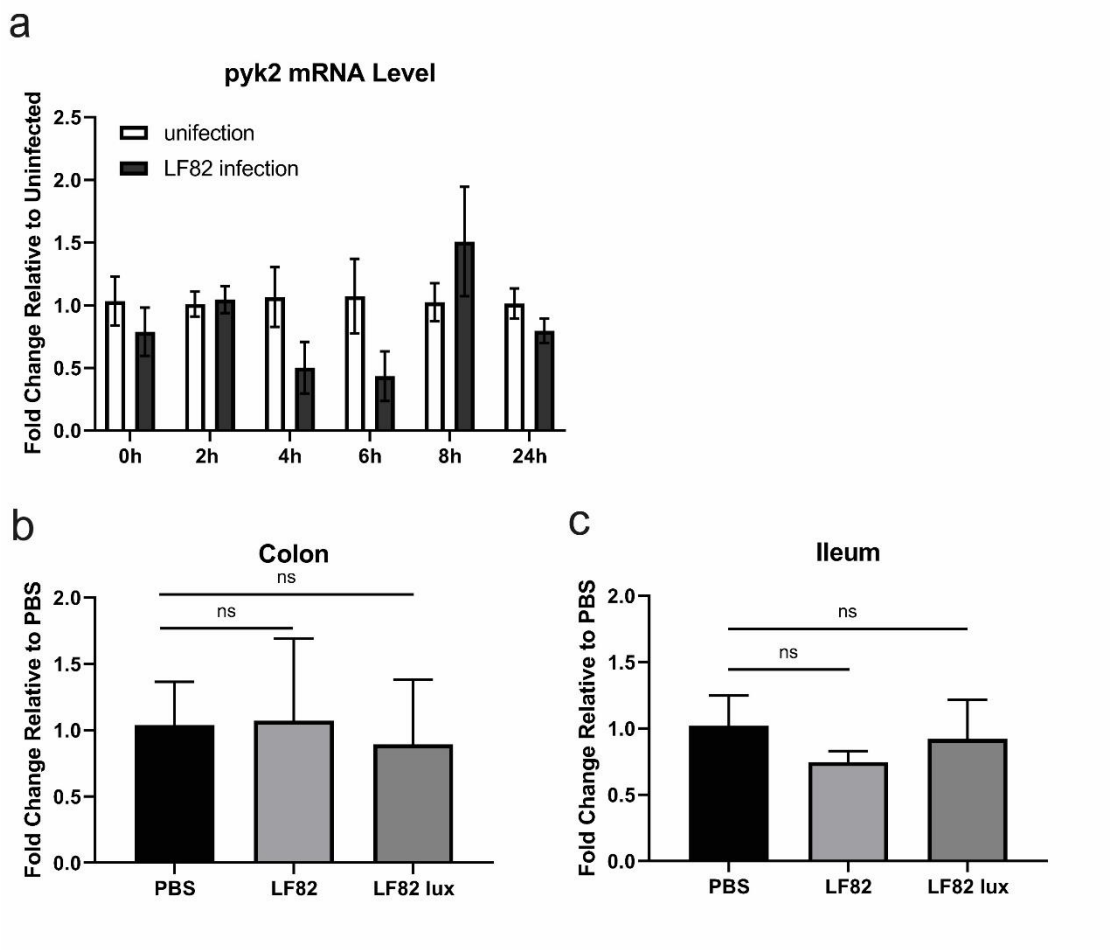

Figure 4-16 Pyk2 mRNA levels in response to LF82 infection *in vivo* and *in vitro*.

(a) Comparison of pyk2 mRNA expression in uninfected and LF82 infected macrophages. RNA extracts were analysed by RT-PCR for *Pyk2* mRNA levels and normalised to Gapdh mRNA. An n=3 was used in all experiments and each experiment was technically repeated three times. (b and c) The graph represents mean ± SD values of three experiments. Mice were infected with LF82 or LF82*lux* for 21 days or mice treated with PBS were included as controls. *Pyk2* mRNA was not significantly altered in either the colon (b) or ileum (c) compared to control mice. Data are

expressed as mean ± SD (n =4) and were analysed using one-way ANOVA test (ns, not significant).

Human intestinal biopsies embedded in paraffin blocks for histology were provided from Prof. Simon Milling's lab (Baer *et al.*, 2019). Immunochemistry (IHC) was performed on the colon of healthy individuals and CD patients, staining with an anti-Pyk2 antibody. Compared to healthy control tissue sections, higher levels of Pyk2 staining were visible in cells surrounding in Peyer's Patches. This is an area where immune cells accumulate during intestinal inflammation, suggesting that Pyk2 increases in immune cells in CD patients (Figure 4-17). However, an increased number of samples and further staining would be required to enable statistical analysis.

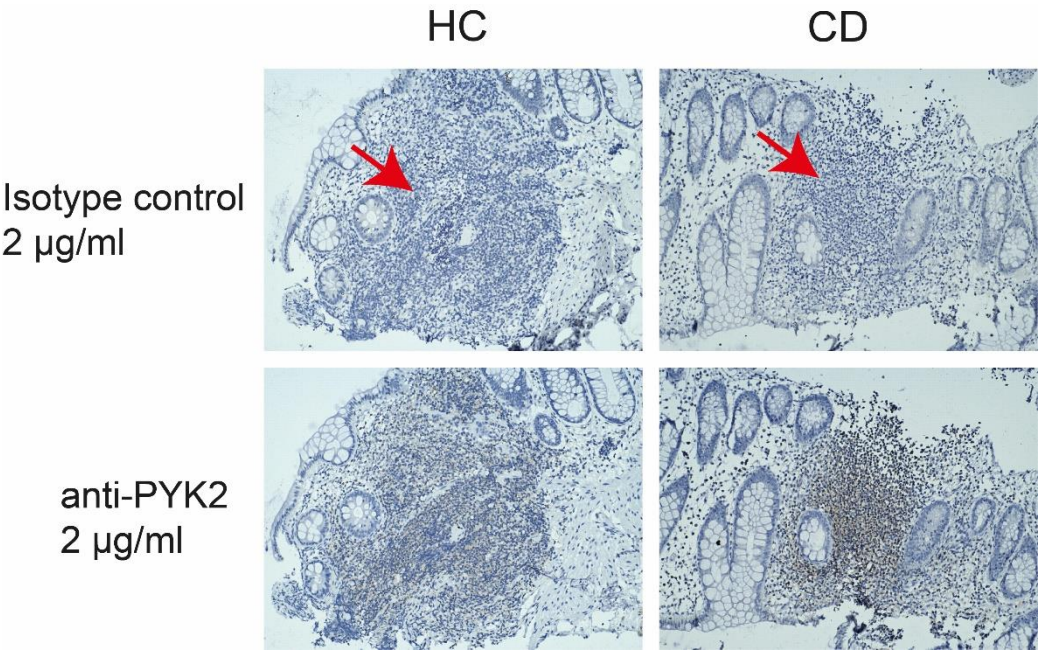

Figure 4-17 Immunohistochemistry of intestinal tissue sample from a CD patient.

Paraffin samples were provided by Prof. Simon Milling's Lab and the patients details were referred to in Baer, *et al*., (2019). Both CD and health samples were immunoreactive to anti-PYK2 antibody (2µg/ml; abcam), micrograph showing intestinal immune cells in Peyer's Patch (red arrows) Scale bars: 200 µm.

4.3.11 Measurement of Pyk2 cleaved enzyme calpain activity during AIEC infected macrophages

The result of the Western blot, with respect to Pyk2 protein levels, is intriguing, as this indicates that both Pyk2 and pPyk2 are increased in LF82-infected RAW

264.7 cells compared to uninfected macrophages (Figure 4-4 and Figure 4-5). However, there is no such difference seen in mRNA levels *in vitro* and *in vivo* experiments (Figure 4-16), which suggests there may possibly have been an inhibition of protein degradation occurring in LF82 infected RAW 264.7 cells. Currently, while there is no direct evidence that Pyk2 is cleaved by caspase, calpain, a calcium-dependent cysteine protease, has been reported to cleave Pyk2 by cleaving it into 80 kDa and 75 kDa fragments in human platelets (Raja, Avraham and Avraham, 1997). When a calpain inhibitor calpeptin was used, it successfully showed a complete blockage in Pyk2 cleavage (Raja, Avraham and Avraham, 1997). Therefore, we examined the calpain activity within LF82, SL1344 and *E. coli* F18 infected RAW 264.7 cells. Uninfected RAW 264.7 cells were examined as a control. Our results showed that calpain activity was decreased during LF82 infection and SL1344 infection in comparison to uninfected cells with adjusted *p* value of 0.0536, or 0.0077, respectively (Figure 4-18). Interestingly, the significant decrease appeared during LF82 and SL1344 infection but not during treatment with the commensal *E. coli* strain F18. This highlighted that pathogenic strains influenced regulation of calpain activity within macrophages. This could explain the increase in both Pyk2 and pPyk2 protein levels during LF82 infection. These findings raise considerable interest in enzyme activity during AIEC infection of macrophages.

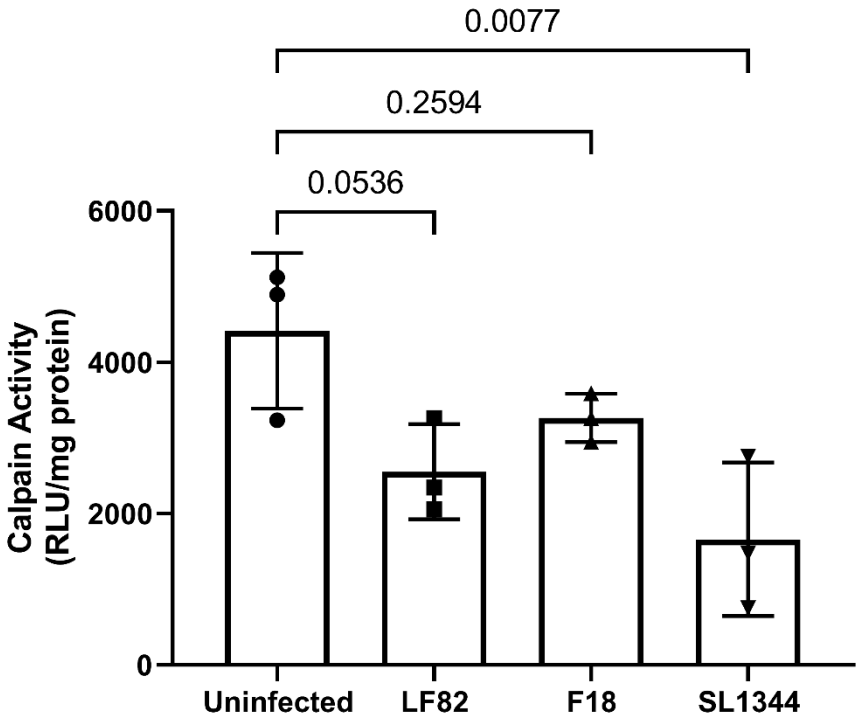

Figure 4-18 Calpain levels in RAW 264.7 cells at 24 hpi after infection with LF82, *E. coli* F18 and *Salmonella* Typhimurium SL1344.

Calpain activity was compared between infected and uninfected cells. Data were normalised by protein concentration and expressed as relative light units (RLU/mg protein in the cell lysate). Experiments were biologically repeated three times with three technical repeats. Data represent the mean ± SD of three independent experiments and were analysed by an unpaired one-way ANOVA.

4.4 Discussion

Macrophages are one of the most abundant leukocytes in the intestinal mucosa, where they play an essential role in maintaining homeostasis. However, they are also implicated in the pathogenesis of disorders such as CD, offering potential targets for novel therapies (Bain and Mowat, 2014). In this study PF-431396 treatment, blocking phosphorylation and activity of the host protein Pyk2, reduced the number of intracellular bacteria with an accompanying increase in macrophage caspase-3 activity and reduced TNF-α release. *Pyk2* has been identified as a susceptibility locus for IBD risk (Jimmy Z Liu *et al.*, 2015). In addition, it has been reported that spondin 2 (SPON2) stimulates the migration of monocytes across endothelial cells in colorectal tumour formation by activating the integrinβ1/PYK2 axis (Huang *et al.*, 2021). High levels of PYK2 were detected in the early stages of colon cancer, a condition often developed

in advanced CD patients (Gao *et al.*, 2015). However, an association between Pyk2 and AIEC, the *E. coli* pathotype consistently overrepresented in the CD intestinal microbiome, has never been investigated. For the first time, our work has demonstrated a direct link between AIEC intracellular replication and activation of Pyk2. Here we show that Pyk2 plays a dual-role in AIEC infection, by initially impacting bacterial phagocytosis before subsequently facilitating AIEC replication and survival within macrophages, as well as controlling TNF-α release from macrophages.

Phagocytosis and Pyk2

To date, only infection by *Y. pseudotuberculosis* has been shown to require Pyk2 for phagocytosis by macrophages (Hudson, Bliska and Bouton, 2005; Owen, Thomas and Bouton, 2007). Previous studies identified that the *Yersinia* outer surface protein, invasin, provides high-affinity interactions with host cell surface ß1 integrin receptors (Wiedemann *et al.*, 2001). Binding of integrins then induces integrin clustering and sustained activation of Pyk2, which has been implicated in numerous actin-based cellular processes including cell cycle progression, adhesion and migration (Avraham *et al.*, 2000). Consistent with this, Bruce-Staskal, et al. (2002) have shown that *Yersinia* uptake involved complex interplay between Crk-associated substrate (Cas), Focal adhesion kinase (Fak), Pyk2 and Rac1 cell signalling (Bruce-Staskal *et al.*, 2002). Through inhibition of Pyk2 phosphorylation, we first demonstrated that LF82 phagocytosis (Figure 4-9) was impeded, with phosphorylation of Pyk2 known to function in the regulation of phagocytosis (Paone *et al.*, 2016; Naser *et al.*, 2018). We then determined that in addition, LF82 is reduced intracellularly in a dose-dependent manner in response to inhibition of Pyk2 function. However, any role for Pyk2 in intracellular replication of *Yersinia* was previously not investigated (Hudson, Bliska and Bouton, 2005; Owen, Thomas and Bouton, 2007).

Phagocytosis is initiated by macrophage cell membrane TLR4 and TLR5, which recognise bacterial extracellular structures such as fimbriae, flagella, LPS and peptidoglycan (Smith, Thompson and Clarke, 2013). Upon phagocytosis of microbial pathogens, TLR4 recruits MyD88 initiating the NF-κB signalling cascade (Sanjuan, Milasta and Green, 2009). Xi et al. (2010) showed that Pyk2 interacts with MyD88 and regulates MyD88-mediated NF-κB activation in macrophages with

resulting TNF-α secretion (Xi *et al.*, 2010). Secretion of high levels of TNF-α are associated with AIEC replication and survival within macrophages without inducing cell death (Bringer *et al.*, 2012). To date, the most effective CD treatments include anti-TNF-α or anti-integrin treatments to lower the concentration of released TNF-α (reviewed in Larabi, Barnich and Nguyen, 2020). However, the cellular mechanisms underpinning the effect of TNF-α on AIEC replication have remained elusive. *In vivo* infection experiments have demonstrated that CD mucosa-associated *E. coli* killing by macrophages could be inhibited by microbial mannan in a TLR4 and MyD88-dependent manner (Mpofu *et al.*, 2007). Taken alongside our findings, this suggests a possible mechanism supporting AIEC replication and survival within macrophages via a TLR4-MyD88-Pyk2-NF-κB-TNF-α cascade.

Intracellular bacterial survival and Pyk2

Intracellular bacterial replication within macrophages is a characteristic trait of AIEC infection. To investigate this, we analysed intracellular replication using colony counts, immunofluorescence, and imaging flow cytometry. All three methods indicated that inhibition of Pyk2 function significantly decreases intracellular replication of LF82 at 12 hpi compared to untreated cells. A unique phenotype whereby increased proteasomal degradation of caspase-3 inhibits the ability of LF82 infected immune cells to induce apoptosis has been reported (Dunne *et al.*, 2013). Here when Pyk2 was inhibited this phenomenon was reversed, with increased caspase-3 activity seen in infected cells. The accumulation of active caspase-3 after Pyk2 inhibition suggests that Pyk2 plays an important role in controlling apoptosis in LF82 infected immune cells and this may underlie the ability of AIEC to prosper inside macrophages. However, to date we know very little about any direct relationship between Pyk2 and caspase-3.

In addition, our study also found that Pyk2 inhibition decreased TNF-α secretion during infection, not just for LF82, but other AIEC clinical isolates from CD patients as well as *S. Typhimurium* type strain SL1344. Previously it was shown that infected macrophages stimulated with exogenous TNF-α, increased the number of intracellular LF82, while neutralization of TNF-α secreted by AIEC-infected macrophages using anti-TNF-α antibodies decreased the number of

intracellular LF82 (Bringer *et al.*, 2012). Studies have directly linked pro-inflammatory gene expression to Pyk2 activity, including in cells which are secreting TNF-α or IL-1ß at high levels (Murphy *et al.*, 2019). Collectively these data, alongside the findings here, indicate a possible mechanism of Pyk2 control of intracellular LF82 numbers is through regulating the TNF-α pathway.

To date AIEC infection has been poorly understood relative to other pathogens, it's paucity of virulence factors rendering it difficult to study via traditional microbiological approaches of mutation and testing. Its virulence has been largely attributed to its unique ability to survive and rapidly replicate within macrophages, while inducing a strong inflammatory response in the form of TNF-α release. Here we focused on the AIEC-host interaction through high throughput imaging and phenotyping of infected cells populations and studying them in the context of Pyk2, a known susceptibility locus for development of IBD. Our approach enabled the removal of phenotypic noise introduced by the presence of many uninfected cells within infected cell populations, giving a clearer picture of the AIEC-macrophage relationship. Our results identified a crucial role for Pyk2 in facilitating AIEC uptake by macrophages, as previously reported for other pathogens, but remarkably also showed for the first time a critical role for Pyk2 in facilitating AIEC intra-macrophage replication and TNF-α release. We also demonstrated how pharmaceutical intervention to block Pyk2 function could block AIEC intracellular replication and subsequent TNF-α release, identifying a potential pathway towards an intervention strategy for CD patients where AIEC are dominant in the intestinal microbiome.

Chapter 5 Analysis of the Macrophage Response to Adherent-Invasive *E. coli* Infection Using RNA Sequencing

5.1 Introduction

Monocyte-derived macrophages (MDMs) from CD patients are impaired in their ability to control intracellular AIEC survival and replication and exhibit a disordered cytokine secretion profile (Vazeille *et al.*, 2015). A fundamental component of tackling infectious diseases and developing new treatment strategies is understanding host-pathogen interactions. Bacterial infection is a dynamic process with heterogeneous host-pathogen encounters (Bumann, 2015). AIEC infection of macrophages is likely to result in a variety of subpopulations with diverse outcomes; some macrophages engulf the bacteria, while others remain uninfected; some macrophages lyse the ingested bacteria, while others are permissive to intracellular bacterial survival; some macrophages will restrict bacterial growth, while other macrophages survive and allow bacteria to multiply. Previously in this thesis, IFC allowed me to identify three subpopulations during bacterial infection at 24 hpi: 55.0% of cells were bacteria free, 32.0% contained fewer than five bacteria, and 11.6% contained more than five bacteria. In our *in vitro* infection model, these IFC results suggest that even within the same well of a tissue culture plate, different intracellular bacterial burdens may determine the outcome of host-bacteria encounters. This variability in host–pathogen interactions might be responsible for therapeutic failures in CD as well as the emergence of chronic, recurring infections.

The complexities of host–pathogen interactions are popularly analysed through transcriptomics or RNA-sequencing (RNA-seq) due to its sensitivity, cost-efficiency, and generic nature (Colgan, Cameron and Kröger, 2017). A transcriptomics screen is a powerful approach to identify host genes that are differentially expressed between different populations with different bacterial burdens. To achieve this goal, subpopulations were isolated and purified by fluorescence-activated cell sorting (FACS) allowing for isolation and purification of macrophage subpopulations. Gene expression profiles within specific bacterial infection subpopulations are useful for understanding the AIEC of resisting killing

by mucosal macrophages and to what extent the expression of host protein affects AIEC intra-macrophage replication.

In this study, we used FACS combined with high-throughput RNA-seq to analyse the transcriptional response of murine macrophages when infected with AIEC type strain LF82. In order to quantitatively characterise outcomes of macrophages within different bacterial loads, cell sorting was conducted and based on a system of GFP-expressing bacteria. There were three possible outcomes during LF82 infection; (1) no infection, (2) low bacterial load and (3) high bacterial load. This is the first time that differential macrophage responses to LF82 infection have been examined with respect to intracellular bacterial number. Through this approach there are fundamental points of understanding to be gained about infection biology and potentially the elucidation of novel treatment options for Crohn's disease.

5.2 Methods and Materials

5.2.1 Sample preparation

RAW 264.7 cells were seeded at a density of 2 X 10^5 cells/ml into a T75 flask with 15 ml of RPMI media (3% FBS). Six hours post cell seeding, RAW 264.7 cells were treated with 100 ng/ml of LPS for overnight. The next day, RAW 264.7 cells in RPMI 1640 with 3% FBS without antibiotics, were infected with LF82::*rpsM*GFP at MOI of 100 for 1 hour. Then extracellular bacteria were removed by washing with fresh RPMI media (3% FBS) containing 50 µg/ml of gentamicin and the media was replaced with fresh RPMI media (3% FBS, 50 µg/ml gentamicin). After 24 hours, cells were harvested using cell scrapers. Suspended cells were washed and maintained in FACS solution (2% FBS in PBS). The viability of cell cultures was assessed using 7-aminoactinomycin D (7-AAD) viability staining solution (BioLegend, 420404) at a final concentration of 0.25 ug/million cells. Four independent biological experiments were set up and 4 technical replicates from each was prepared for FACS including uninfected cells (with or without 7-AAD staining) and LF82::*rpsM*GFP infected cells (with or without 7-AAD staining), as shown in a diagram in Figure 5-1a. The four samples were then subjected to FACS analysis and cell sorting.

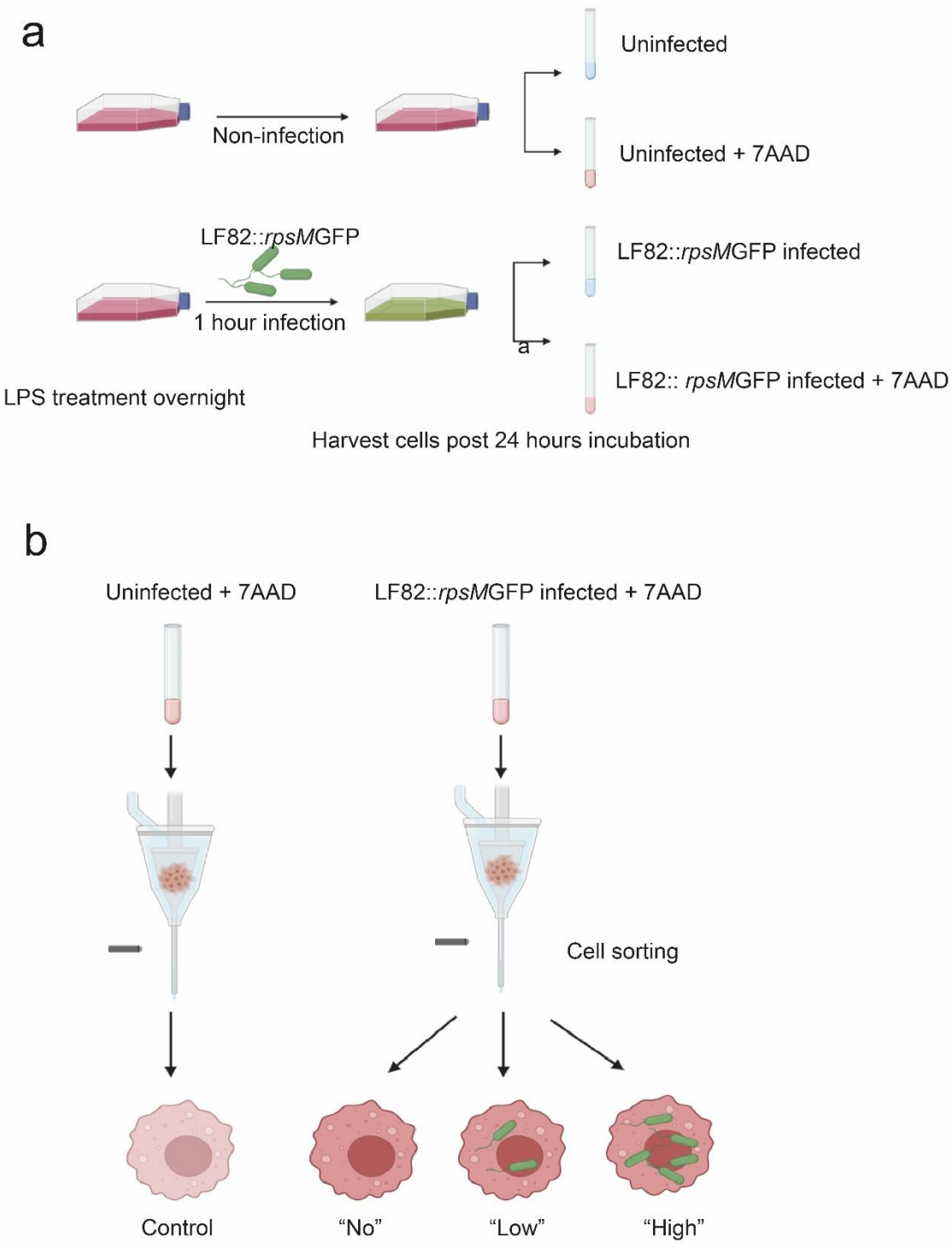

Figure 5-1 FACS experimental procedure.

(a) Sample preparation for FAC sorting. Post 24 hour infection, cells were harvest and stained with 7-AAD. Four biological replicates from each was prepared for FACS including uninfected cells with or without 7-AAD staining, and LF82::*rpsM*GFP with or without 7-AAD staining. (b) Schematic overview of FACS protocol for the isolation of three populations of cells from infected RAW 264.7 cells into three populations; (1) no infection, (2) low bacterial load and (3) high bacterial load. Living cells from the uninfected sample were sorted as a control group. Each population contained 80,000 cells.

5.2.2 Cell sorting by FACS

Flow cytometry was performed on a BD FACSAria with BD FACSDiva application software version 5.0.2 (BD Biosciences, Franklin Lakes, NJ) paired with FlowJo Version 6.3.2 analysis software (Tree Star Inc., Ashland, OR). Each sample was subjected to forward scatter (FSC) versus side scatter (SSC). GFP was detected with an excitation of 488 nm filter while 7-ADD was detected with excitation at 635 nm. Based on measurements obtained from the analysis of 10,000 events for each samples (4 prepared samples details as described in Figure 5-1a), gating strategies were established for the selection of cells of interest using FSC, SSC, and fluorescence emission properties. Actual cells were easily distinguished from debris by gating on forward (FSC) and side (SSC) scatter (Figure 5-2a). As 7AAD does not penetrate intact cell membranes, it only stained dead cells. In LF82::*rpsM*GFP infected RAW 264.7 cells, living cells were gated based on their lack of 7AAD staining (Figure 5-2b). A gating strategy was then established for the three populations of infected cells by determining their GFP fluorescence intensity. The identification of different intracellular bacterial burdens as *No, Low* and *High*, were used to sort the cells into three separate populations, representing cells with no bacteria (*No*), cells with less than 5 bacteria (*Low*) and cells with more than 5 bacteria (*High*) (Figure 5-2c). For a control group, cells from the uninfected sample were sorted in the same number as for the other three groups. Data from each population was acquired for 80,000 cells. In Figure 5-1b, a schematic representation of different groups of sorted cells is shown in a simplified manner. To simplify the description of the four groups of cells in the following text, the terms "*Control*", "*No*", "*Low*" and "*High*" will be used instead to indicate their infection status. Sorted cells were collected into 1.5 ml microfuge tubes containing 800 µl of RNAlater solution (Invitrogen AM7020) stopping cellular transcriptional changes. Four independent cell sorts as biological repeats were collected and kept at -80°C until RNA was extracted.

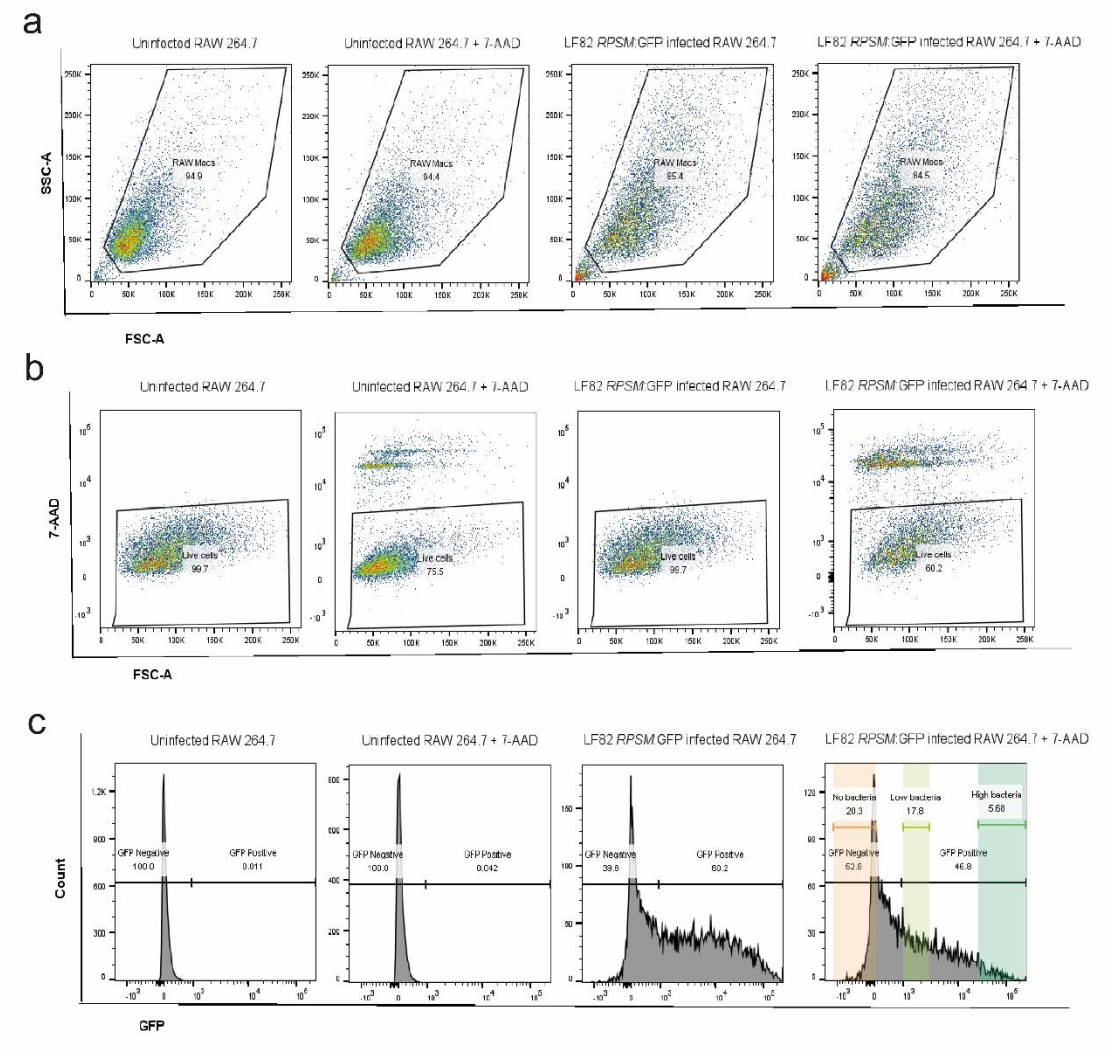

Figure 5-2 Gating strategy for isolation of LF82::*rpsM*GFP infected RAW 264.7 cells for three different populations (*No*, *Low* and *High*).

(a) For the isolation of a highly pure RAW 264.7 population, cells were gated on their forward scatter area (FSC-A) and side scatter area (SSC-A), excluding debris from the live gate. (b) Dead cells were further excluded based on FSC-A versus the intensity of 7AAD. (c) This was followed by gating out three sub-populations of living RAW 264.7 cells according to GFP intensity, resulting in sorting final three populations including cells with no bacterial burden, low bacterial burden and high bacterial burden.

5.2.3 RNA isolation

RNA was extracted using an RNeasy PowerMicrobiome Kit (QIAGEN, 26000-50) using the manufacturer's protocol. RNA extracts were kept at -80°C. Both quantity and quality of RNA were assessed by using an Agilent 2100 Bioanalyzer (Agilent Technologies). RNA yields ranged from 3.47 to 18.6 ng/µl. RNA integrity numbers (RIN) of a sample are generated by the 2100 Bioanalyzer to indicate the level of degradation and have been shown to predict gene expression suitability reliably (Schroeder *et al.*, 2006). RIN scores ranged from 8.7 to 10, indicating

high-quality RNA suitable for gene expression analysis by RNA-seq (Fleige and Pfaffl, 2006).

5.2.4 Library construction, RNA-seq, and bioinformatics

At least 10 ng of RNA was isolated per sample and provided to Glasgow Polyomics (University of Glasgow) for RNA sequencing, the generation of cDNA, sequencing, and bioinformatics. The cDNA libraries were created using the Quantseq (FWD) kit from Lexogen. The kit creates a library from the polyA end of transcripts, creating fragments terminating in the polyA sequence and sequencing towards this. The sequencing process was performed in paired ends, with a read length of 75 bp, the number of reads was 10 million. Galaxy is a powerful web-based platform for RNA-seq data analysis. It starts with quality control of reads using FastQC and Trimmomatic (Bolger, Lohse and Usadel, 2014) to remove the adaptor. The reads are then mapped to a reference genome using Hisat2 (Kim *et al.*, 2019). From the mapped sequences, the number of reads per annotated gene is counted using HTseq-count (Anders, Pyl and Huber, 2015). Counts were analysed and differentially expressed genes (DEGs) were identified with R (Team RC., 2014). Descriptive plots were generated, and Kyoto encyclopaedia of genes and genomes (KEGG), gene ontology (GO) analysis and hierarchical clustering were performed with R and Searchlight2 (Cole *et al.*, 2021).

5.3 Results

5.3.1 Isolation of RAW 264.7 cells with different LF82 burdens

A schematic representation of the workflow for quantifying bacterial content in single cells is shown in Figure 5-3a. Macrophages were sorted into groups according to fluorescence intensity (Figure 5-3b) and the number of intracellular bacteria enumerated by plating for colony-forming units (Figure 5-3c). From the FACS plot (Figure 5-3b), the gates set up for three different populations were sufficient to isolate differentially infected cell populations. As expected, no visible bacteria were recovered from *No* bacterial load RAW 264.7 cells, and an average of 1-2 bacteria per cell were recovered from *Low* bacterial load cells;

while *High* bacterial load macrophages contained around 7 bacteria per cell, which correlated with GFP intensity (Figure 5-3c).

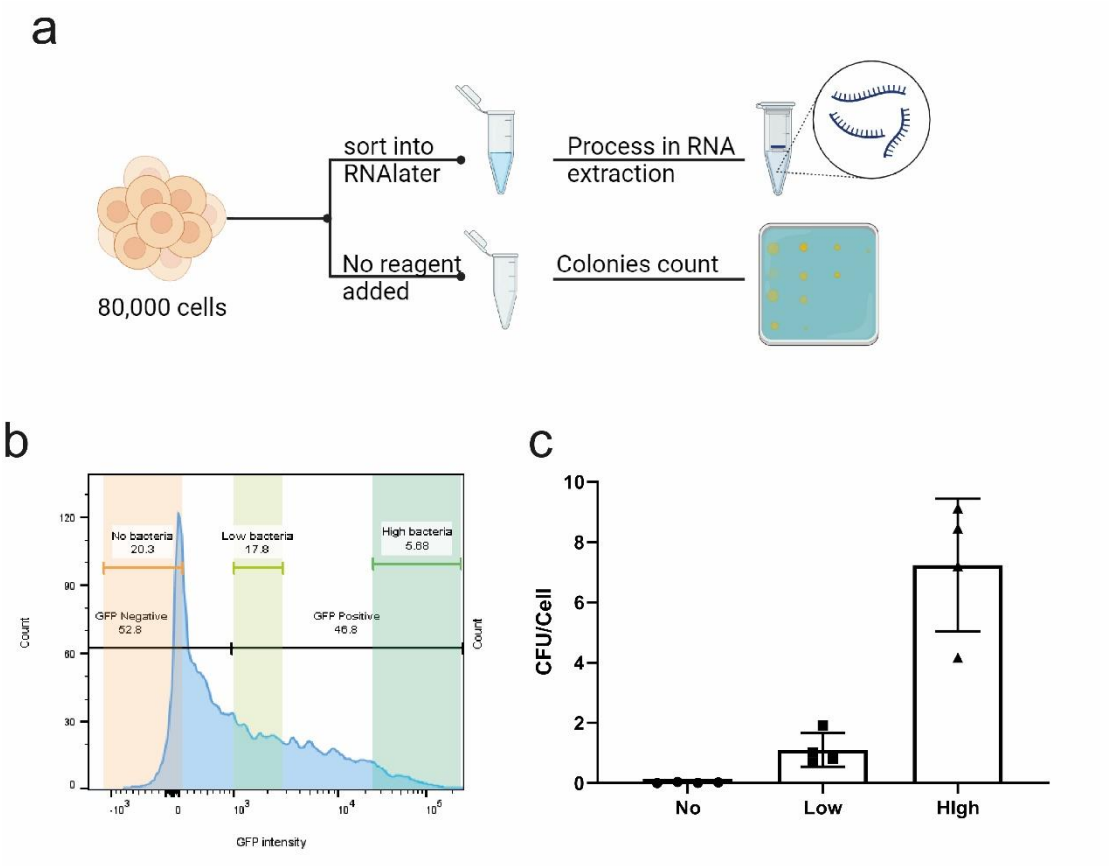

Figure 5-3 Macrophage sub-populations sorted by FACS and confirmation of intracellular bacteria number by traditional visible colony count.

(a) Schematic overview of the process of sorting RAW 264.7 cells for RNA-seq and viable count analysis. There were 4 independent biological repeats, each repeat includes two sorts: one was sorted into an RNAlater solution, enabling later RNA extraction; another sort was used for confirming the number of intracellular bacteria. (b) Three populations of cells were determined according to GFP intensity. (c) The number of intracellular bacteria from different populations was calculated after their recovery by plating it onto LB agar plate and CFU counting.

5.3.2 Functional genomics analysis reveals differential gene expression

Expression data were obtained from around 55,000 gene probes on each of 16 samples (4 biological replicate experiments, each comprising 4 sorted populations). As a result of the Principal Component Analysis (PCA) of gene expression across all populations, it was revealed that there is a certain degree of discrimination among them (Figure 5-4a). The populations (*No*, *Low* and *High*) from the same infected well were clustered closely indicating that these three groups have a very similar level of gene expression, but there was a relatively

wide distance between these populations and the *Control* group. DESeq and R software were used to identify differentially expressed genes (DEGs), which were then subjected to strict selection criteria based on expression level, fold-change, and statistical significance. After data normalisation and significant analysis filtering (log 2 fold change > 1.0 or <−1.0, adjusted $p < 0.05$), a total of 1011 genes were identified as significantly changed from either comparison (*Control* vs *No*, *Control* vs *Low*, *Control* vs *High*, *No* vs *Low*, *No* vs *High*, *Low* vs *High*) and computationally clustered as a heatmap (Figure 5-4b). It can be seen from the heatmap that there is a similar panel of gene expression among three groups: *No*, *Low* and *High*, but the *Control* group appears to have a different pattern of gene expression. The number of significant genes was computed based on three comparisons: *Control* vs *No*, *Control* vs *Low* and *Control* vs *High* resulting in 411, 542 and 752 significant genes, respectively (Figure 5-4c). In accordance with PCA plot and heatmap, a small number of significant genes were found when comparing *No* against *Low*, *Low* against *High*, and *No* against *High*, resulting in 24, 14 and 35 significant genes, respectively (Figure 5-4c).

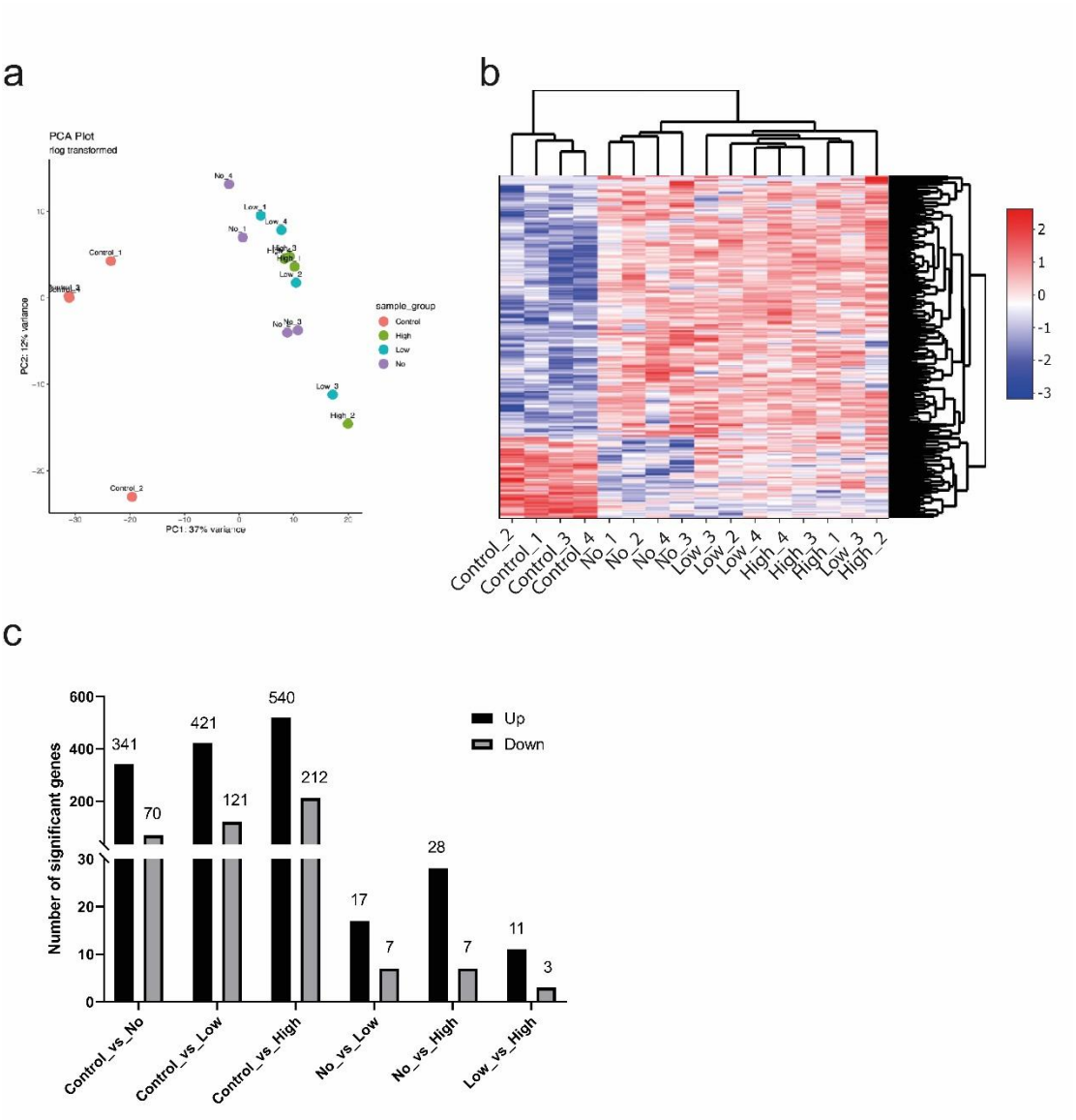

Figure 5-4 Sample clustering and differentially expressed genes (DEGs) between different macrophage populations with differing bacterial burdens.

(a) Principal component analysis (PCA) plot of samples. PC1: the first principal component; PC2: the second principal component. (b) Heatmap for any DEGs of 6 comparisons (*Control* vs *No*, *Control* vs *Low*, *Control* vs *High*, *No* vs *Low*, *No* vs *High*, *Low* vs *High*). (c) Histogram of the number of DEGs between two populations.

5.3.3 Differential expression of cytokines among four groups

Cytokines secreted by macrophages convey instructions and facilitate communication between immune and non-immune cells. Adaptive immunity is mediated by macrophages, which are sentries of the innate immune system with a portfolio of cytokines (Duque *et al.*, 2014). There has been an increased interest in the role of cytokines in the treatment of IBD in the past few decades. In addition, during the course of IBD, certain chemokines are secreted and these

are involved in mediating the recruitment of leucocyte effector populations to the site of inflammation (Laing and Secombes, 2004). To provide further insight into the changes in cytokine and chemokine production between the four different groups, any significant differences in cytokine or chemokine levels in any comparisons were analysed and graphed as a heatmap (Figure 5-5). A heatmap representation general revealed distinct differences in the factors secreted by sorted cells (*No*, *Low* and *High*) versus the *Control* group, with those from the former producing significantly higher levels of pro-inflammatory cytokines including IL-33, IL-1α, IL-1ß, TNF-α, IL-18, IL-6 and LIF, which suggests that the *No* behave very similarly to those that are infected *Low* and *High*. Similar higher levels of pro-inflammatory cytokines expressed among the three infected groups (*No*, *Low* and *High*) grouped the infected macrophages into a spectrum of inflammation-promoting "classically activated" macrophages.

Altered cytokine secretion is implicated in CD. A number of cytokines associated with CD are listed in Table 5-1, and all of these cytokines are expressed at a high level in the three populations sorted from the same well of infected RAW 264.7 cells. In transcription analysis, TNF-α gene expression is at high levels in the *No*, *Low* and *High* populations but TNF-α receptors Tnfrsf1b and Tnfrsf9 are expressed at lower levels in the *No* group when compared to the *High* group, indicating that TNF-α receptor expression levels are affected by intracellular bacterial burden, although the presence of infected cells induces TNF-α release by uninfected bystander cells.

Changes in the level of expression of chemokines was also observed. The genes CCL2, CCL3 and CCL7 were upregulated when RAW 264.7 cells were co-incubated with LF82::*rpsM*GFP. In particular CCL3, also named macrophage inflammatory protein-1α (MIP-1α), was of interest as it is actively expressed in inflamed colon tissue but barely expressed in uninfected sections of IBD patients (Grimm and Doe, 1996). Moreover, it is highly expressed by macrophage-like cells and T cells in loosely formed granulomas in intestinal mucosa affected by CD (Grimm and Doe, 1996). During *in vivo* experiments, CCL2 and CCL7 were increased in colonic resident macrophages promoting intestinal inflammation (He *et al.*, 2019).

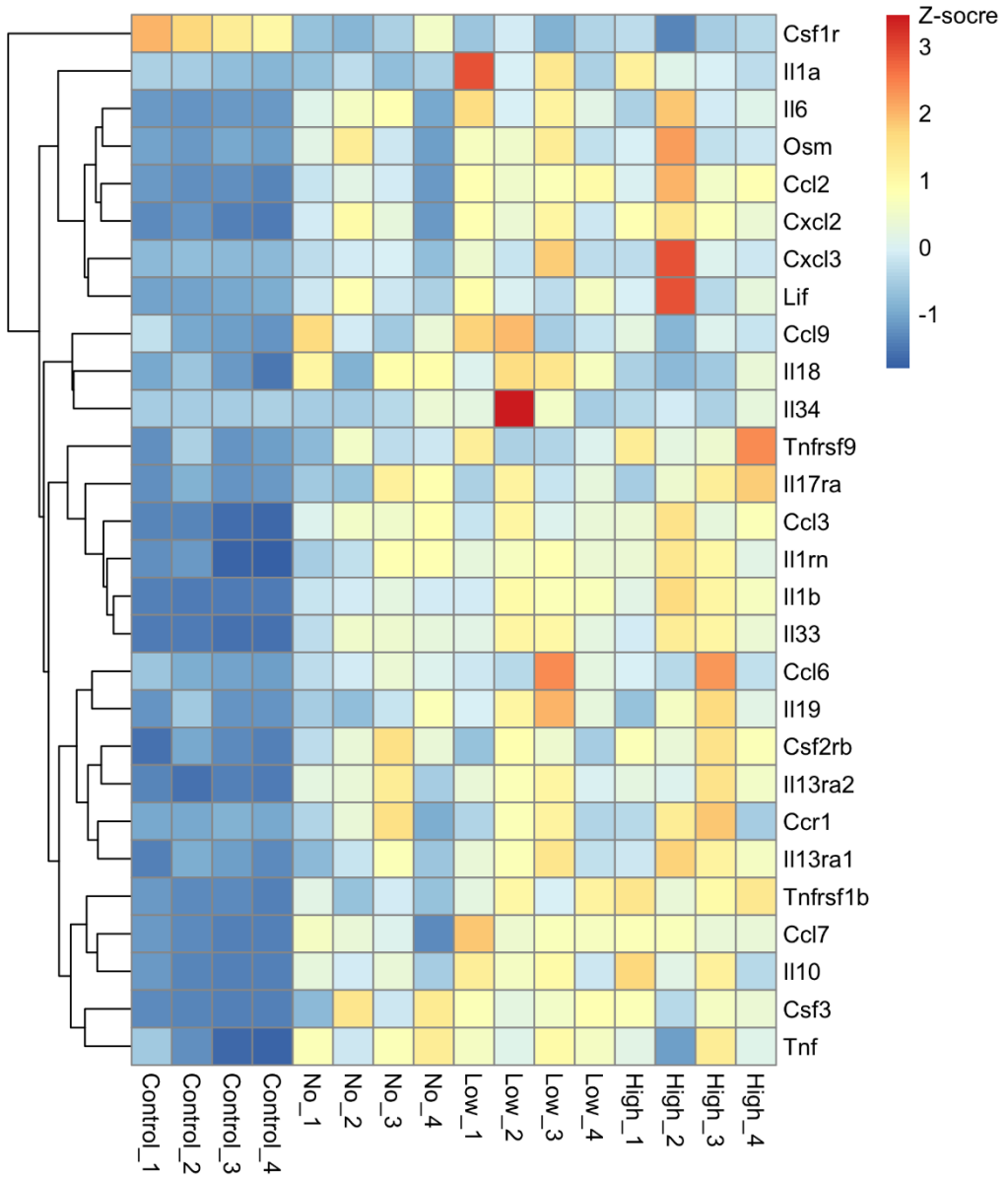

Figure 5-5 Heatmap of changes in gene expression levels of cytokine and chemokine genes in three groups infected with LF82 (*No*, *Low* and *High*) alongside the Control uninfected group.

Significantly changed cytokine/chemokine genes were sorted by the value of each population (*No*, *Low* and *High*) independently versus uninfected Control group with (log2 fold change > 1 or < -1 and adjusted p-value < 0.05). Values of four populations in the heatmap represent the z-score of normalised gene read counts. Colour codes in each panel refer to red for the highest expression and blue for low expression levels.

Table 5-1 Reference table of cytokines related to CD that are differentially regulated

Cytokine	Proposed Function	Reference
CSF3	Increase tissue neutrophil survival	K. Ina, 1999
IL1B	Co-stimulation in an inflammatory microenvironment	B. Hugle, 2017
IL1A	Co-stimulation in an inflammatory microenvironment	B. Hugle, 2017
IL6	Local and systemic inflammation, proliferation of epithelial cells, activation of T cells	R. Atreya, J, 2000
IL17A	Emergency granulopoiesis	M. Leppkes, 2009
TNF	Promotes acute-phase proteins	H.M. van Dullemen, 1995
IL33	Alarmin, tissue remodelling, goblet cell hyperplasia, Treg expansion	C. Schiering, 2014; M. Mahapatro, 2016
LIF	Stem cell maintenance and cell differentiation	R. Guimbaud, 1998
CSF1	Monocyte stimulation	J.C. Nieto, 2017
IL34	Growth and development of myeloid cells	S. Zwicker, 2015
OSM	Stromal cell-mediated chemoattraction and tissue retention of neutrophils, monocytes and T cells	N.R. West, 2017

5.3.4 Differential gene expression analysis among *No*, *Low* and *High* groups

Our study has four different groups and six potential comparisons between them. To better analyse the DEGs and pathway enrichment, we divided the analysis into two parts. It is clear from the heatmap display (Figure 5-4b) and cytokine expression (Figure 5-5) that the three groups (*No*, *Low*, and *High*) had similar gene expression levels, and exhibited similar cell phenotypes. However, as each of these groups had a different intracellular bacterial burden, analysis of the differences in gene expression between these three groups was carried out to gain a better understanding of which genes play a role in regulating intracellular bacteria number. In the first part of the analysis, the three populations (*No*, *Low* and *High*) were compared to each other without considering the *Control* group. The next section of the analysis focused on the analysis of these three populations individually but in comparison to the *control* group. The three

infected groups (*No*, *Low* and *High*) without a control group were the subject of initial analysis, and three differential comparisons were made with each group: *No* versus *Low*, *No* versus *High*, and *Low* versus *High*. As a way of generating an unbiased panel of genes that best represents the overlap of three different comparisons, a Venn diagram was drawn to identify genes that were common or unique in each comparison (Figure 5-6). In order to investigate whether high LF82 burden affects gene expression profiles, it was worthwhile to focus on the overlapped DEGs in two comparisons: *No* versus *High* and *Low* versus *High*. A total of 5 DEGs were identified, of which 2 were downregulated (*Zeb1* and *Selenop*) and 3 were upregulated genes (*Angptl7*, *Alas2* and *Kcnj11*) in the *High* group. These 5 DEGs are circled in the volcano plots (Figure 5-7). For a deeper understanding of the biological function of overlapped genes, two genes that may be of interest were *Angptl7* and *Alas2*. In particular, angiopoietin-like protein 7 (Angptl7) has been reported to promote an inflammatory phenotype in RAW264.7 macrophages via the P38 MAPK signalling pathway. Meanwhile, its overexpression enhances phagocytosis and inhibits proliferation of RAW 264.7 cells (Qian *et al.*, 2016). Little is known about the function of 5-aminolevulinate synthase 2 (*Alas2*) within macrophages, but its related pathways are haem biosynthesis and metabolism and this protein facilitates erythropoiesis (Burch *et al.*, 2018).

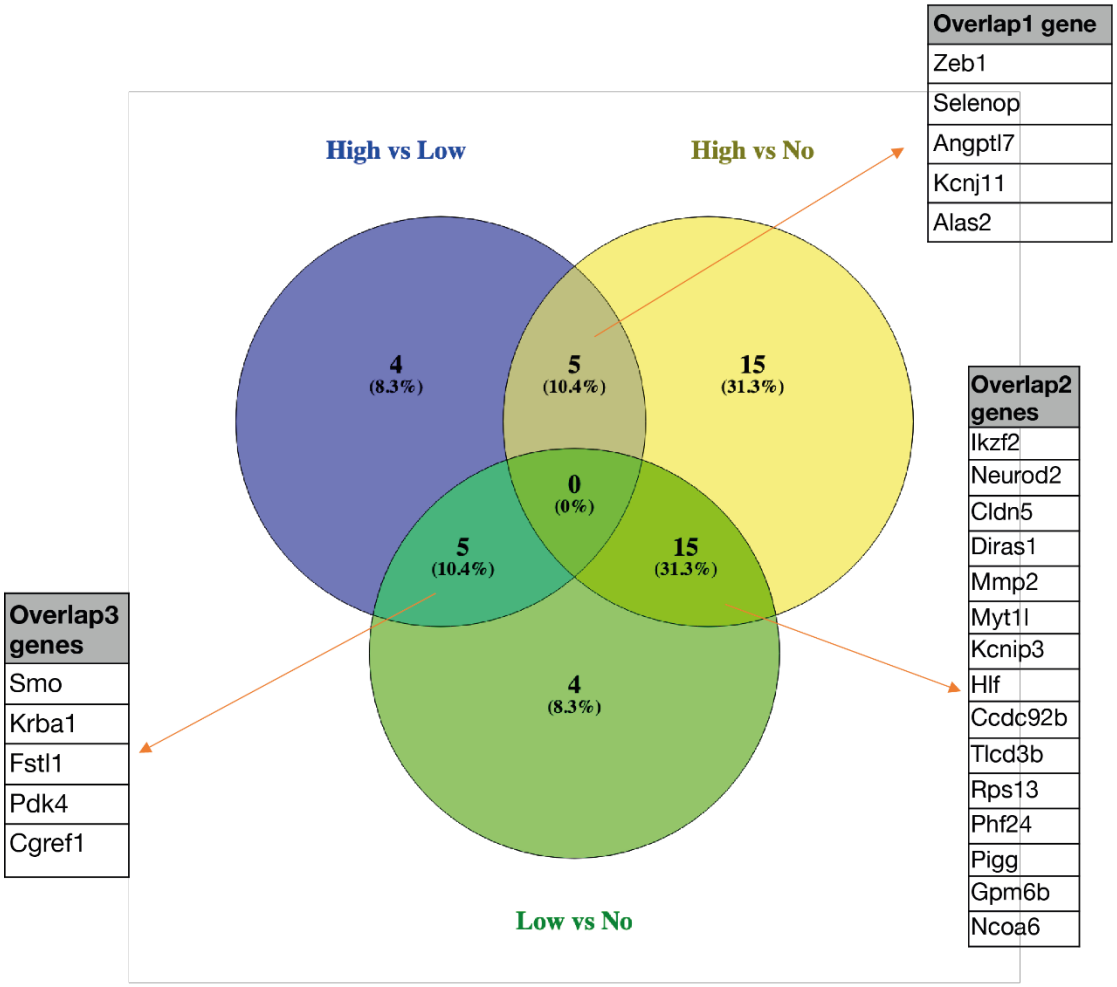

Figure 5-6 Venn diagram of three sets of DEGs between the three comparisons: *High* vs *Low*, *High* vs *No*, and *Low* vs *No*.

The common genes shared between each of the three comparisons of two conditions are highlighted; 5, 5 and 15 genes. Overlapping genes are listed. Overlap 1 genes represent common significant changed genes between two comparisons: *High* vs *Low* and *High* vs *No*. Overlap 2 genes represent common significant changed genes between two comparisons: *High* vs *No* and *Low* vs *No*. Overlap 3 genes represent common significant changed genes between two comparisons: *High* vs *Low* and *Low* vs *No*. Venn diagram was generated from the website: https://bioinfogp.cnb.csic.es/tools/venny/.

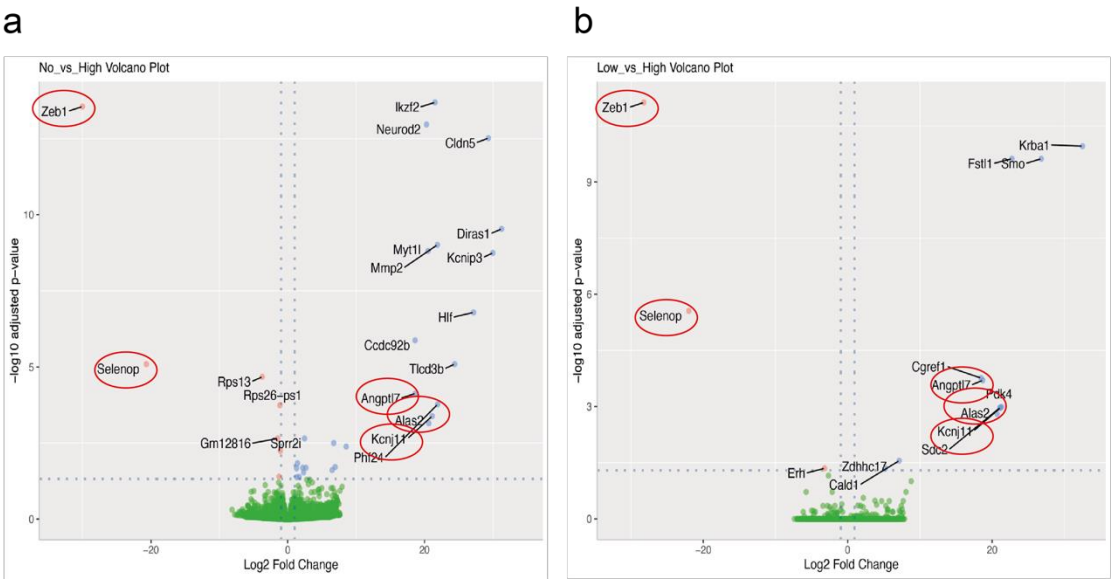

Figure 5-7 Volcano plot for the comparison of *No* versus *High* and *Low* versus *High*.

Volcano plot showing DEGs (log 2 fold changes > 1 or <-1, adjusted P-value < 0.05). Up- and down-regulated genes are represented by *blue* and *red* symbols. Genes with no significant expression change are represented by *green* symbols. Two comparisons: *No* vs *High* and *Low* vs *High* are shown in graphs a and b, respectively. The circled genes are the same significantly changed genes between these two comparisons.

5.3.5 Analysis of Gene Expression Differences and Pathway Enrichment Between Sorted Populations and Control Groups

Three comparison groups were established, *Control* vs *No*, *Control* vs *Low* and *Control* vs *High*. Using the Venn diagram analysis, it was found that 77, 111, and 310 significant unique genes were specifically expressed in *No*, *Low*, and *High* with respect to the Control group, respectively (Figure 5-8). Since expression levels of only a few genes were changed when comparison of the three subpopulations of bacterial infection was undertaken, it was not possible to utilize pathway enrichment analysis between the infected populations. In order to better screen the genes of interest, pathway enrichment was undertaken. DEGs involved in some interesting enriched pathways will be verified their role in the host-pathogen interaction via wet lab. To visualise the enriched KEGG pathways based on DEGs, an R package called PathFindeR (Partl *et al.*, 2016) was used to generate a pathway heatmap (Figure 5-8). Through KEGG analysis, significantly upregulated pathways in the *High* group were identified as being related to MAPK, phagocytosis, focal adhesion, calcium ion transport, and cell adhesion; and the significant downregulated KEGG pathways in the *High* group

were involved in the cell cycle, oxidative phosphorylation and apoptosis (Figure 5-8).

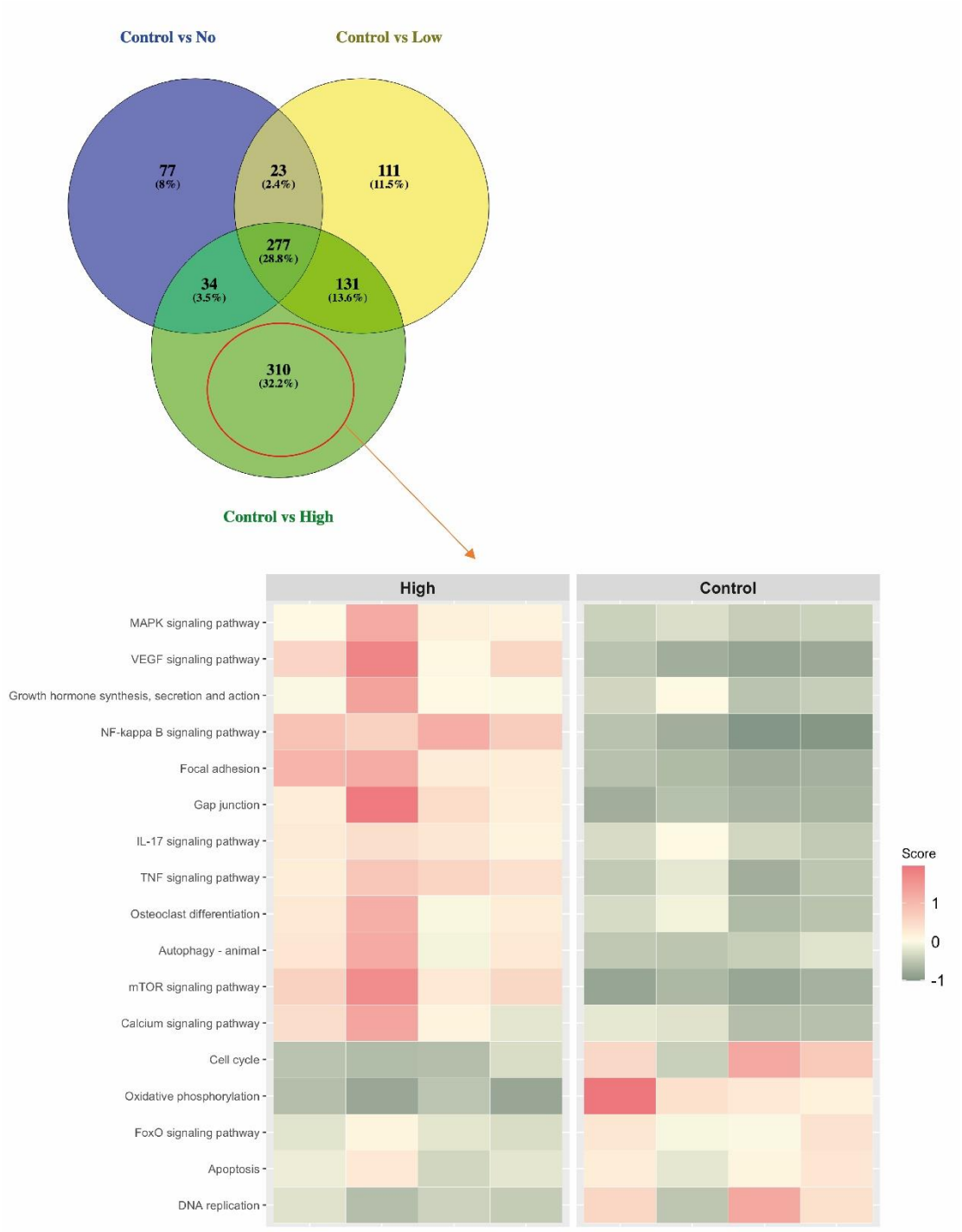

Figure 5-8 Characteristics of unique DEGs in the comparison of *Control* vs *High*.

Venn diagram showing the number of overlapped or unique DEGs in the three comparisons: *Control* vs *No*, *Control* vs *Low* and *Control* vs *High*. There are 310 unique DEGs during the comparison of Control and High. 310 DEGs were used for KEGG pathway analysis and the outcome of enriched pathways were clustered in the heatmap. In the heatmap, the value represents the average z-score of the expression levels from each of the total genes involved in a specific pathway. Each column of a group in the heatmap represents one biological repeat. *Red* colour represents the relative activated pathway and *green* represents the relative suppressed pathway.

Next, we sought to identify transcripts selectively reduced or enriched in the *Control* group by grouping these selected genes into specific signatures, which might serve as markers of host cell that are related to intracellular bacterial number. For this purpose, we focused on the transcripts that showed significant changes in at least one of the pairwise comparisons performed between the *Control*, *No*, *Low* and *High* groups. The term "gene signature" describes a particular gene or a group of genes in a way that is governed by either a changed biological process or altered pathogenic condition (Mallik and Zhao, 2018). There were two differential expression signatures of genes generated using a tool called Searchlight2 (Cole *et al.*, 2021). In signature 1, 516 genes were downregulated in *Control* groups and showed a step-up increase trend followed by *No*, *Low*, and *High*, as shown on the meta-gene violin plot (Figure 5-9a) and heatmap (Figure 5-9b). As for signature 2, it presented 222 enriched genes in *Control* and an inverse relationship between bacterial burden and gene expression levels where gene expression was seen to step-wise decrease in the presence of higher bacterial burdens (Figure 5-10a-c). Pathway analysis of these two gene lists of DEGs using Gene Ontology-Biological Processes (GO-BP) highlighted several pathways (Figure 5-9c and Figure 5-10c). According to signature 1, the top 10 most significantly upregulated pathways are those related to bacteria, biotic stimuli, inflammatory response regulation, and TNF-α production (Figure 5-9c), whereas terms associated with metabolic processes, ribosome assembly, and DNA conformation changes were enriched in the signature 2 GO-BP list (Figure 5-10c). The GO pathway analysis for different signatures demonstrated that over-represented pathways in signature 1 were more activated in the *High* group, while the pathways related to signature 2 were suppressed in the *High* group. There was significant overrepresentation and selection of specific GO categories shown in both tables (signature 1 in Table 5-2 and signature 2 in Table 5-3).

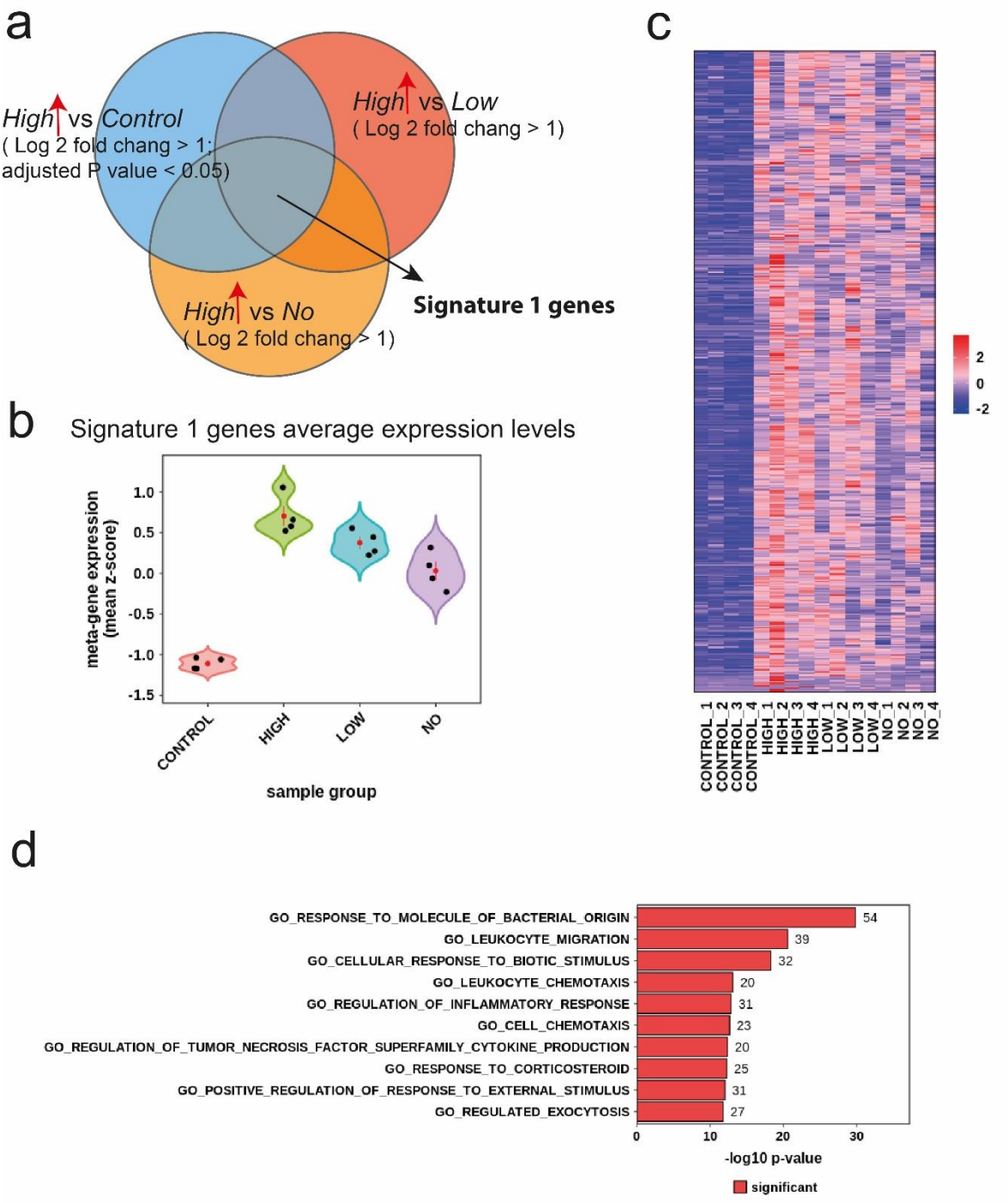

Figure 5-9 Signature 1 gene expression among 4 populations and their relevant enriched GO-BP pathways.

(a) Venn diagram showing the shared genes (up-regulated in *High* group) among three comparisons (*High* vs *Control*, *High* vs *Low* and *High* vs *No*). These common genes were described as Signature 1. Signature 1 genes overlap in the *High* against *Control* group (log 2 fold change >1, adjust p-valued < 0.05), *High* versus *Low* (log 2 fold change >1) and *High* versus *Low* (log 2 fold change >1) groups. Signature genes were sorted using R. (b) Differential expression signature meta-gene violin plot with jitter values for Signature 1. Values represents mean expression (Z-score) across all genes in this signature. Black dots denote individual samples. (b) Gene expression heatmap for Signature 1 genes. (c) Bar chart of the 10 most enriched gene-sets (GO-BP) for the genes in Signature 1.

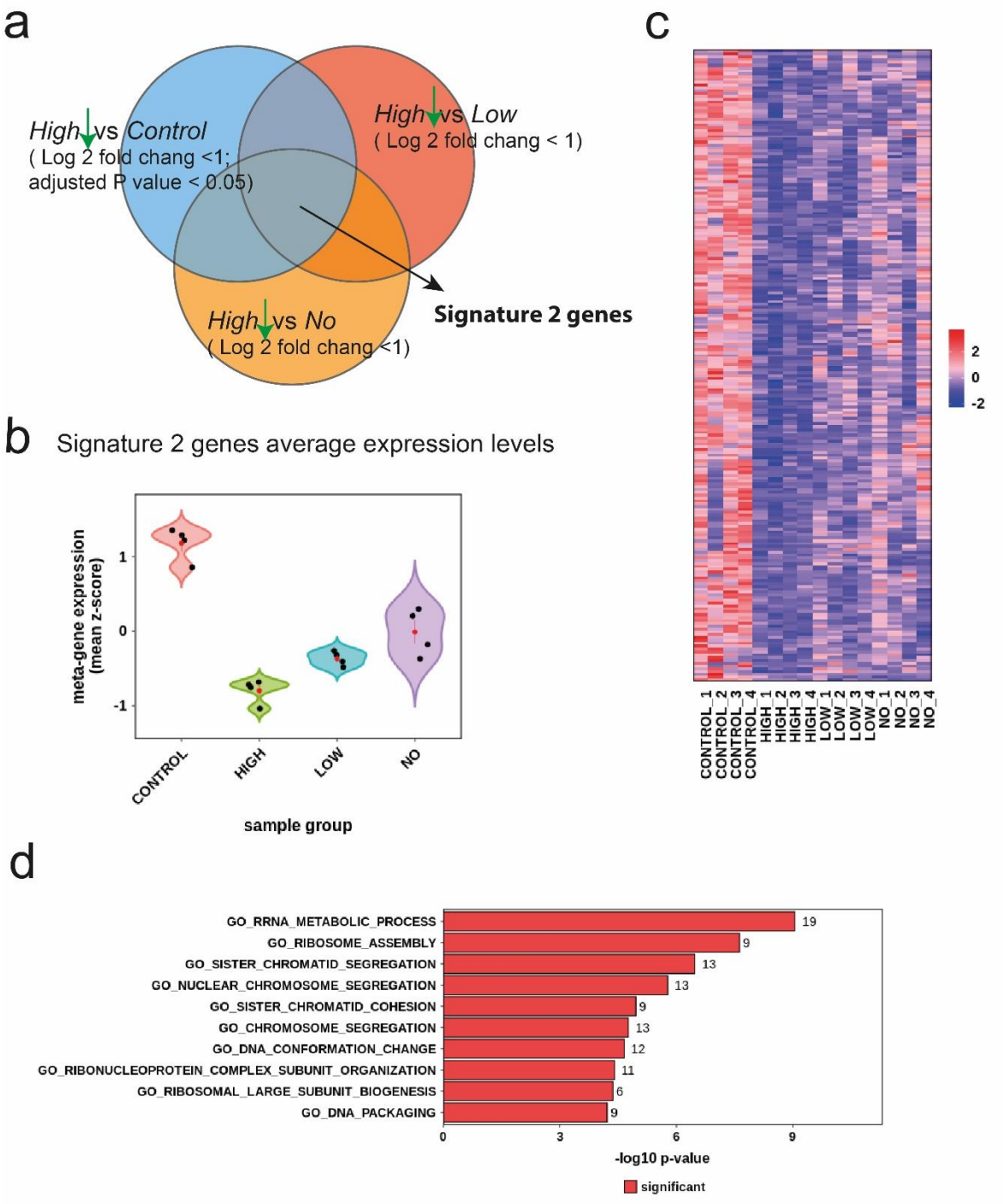

Figure 5-10 Signature 2 gene expression among the 4 populations and their relevant enriched GO-BP pathways.

(a) Venn diagram showing the shared genes (down-regulated in *High* group) among three comparisons (*High* vs *Control*, *High* vs *Low* and *High* vs *No*). These common genes were described as Signature 2. Signature 2 genes overlap in *High* against *Control* group (log 2 fold change <1, adjust p-valued < 0.05), *High* versus *Low* (log 2 fold change <1) and *High* versus *Low* (log 2 fold change <1) groups. Signature genes were sorted using R. (b) Differential expression signature meta-gene violin plot with jitter values for signature 2. Values represents mean expression (Z-score) across all genes in this signature. Black dots denote individual samples. (b) Gene expression heatmaps for Signature 2 genes. (c) Bar chart of the 10 most enriched gene-sets (GO-BP) for the genes in Signature 2.

Table 5-2 Go enrichment analysis for signature 1 genes (516 genes) in bp terms

Term	P value	p.BH value
GO_REGULATION_OF_NITRIC_OXIDE_BIOSYNTHETIC_PROCESS	1.065E-08	1.345E-06
GO_POSITIVE_REGULATION_OF_CELL_ADHESION	5.889E-08	5.409E-06
GO_REGULATION_OF_CALCIUM_ION_TRANSPORT	3.65E-05	8.343E-04
GO_PHAGOCYTOSIS	3.390E-06	1.305E-04
GO_REGULATION_OF_FATTY_ACID_TRANSPORT	1.846E-04	2.903E-03
GO_POSITIVE_REGULATION_OF_PHAGOCYTOSIS	1.278E-05	3.587E-04
GO_REGULATION_OF_TUMOR_NECROSIS_FACTOR_BIOSYNTHETIC_PROCESS	2.716E-05	6.457E-04
GO_NEGATIVE_REGULATION_OF_MEIOTIC_CELL_CYCLE	5.066E-03	3.630E-02
GO_APOPTOTIC_SIGNALING_PATHWAY	7.770E-06	2.483E-04
GO_PROTEIN_AUTOPHOSPHORYLATION	1.042E-04	1.854E-03
GO_REGULATION_OF_NF_KAPPAB_IMPORT_INTO_NUCLEUS	7.076E-07	3.762E-05

Table 5-3 GO enrichment analysis for signature 2 genes (222 genes) in BP terms

Term	P value	p.BH value
GO_CELLULAR_AMINO_ACID_METABOLIC_PROCESS	6.866E-05	2.522E-02
GO_DNA_CONFORMATION_CHANGE	2.176E-05	1.256E-02
GO_RIBOSOME_ASSEMBLY	2.381E-08	4.811E-05
GO_DNA_PACKAGING	6.047E-05	2.443E-02
GO_RRNA_METABOLIC_PROCESS	8.963E-10	3.622E-06
GO_ALPHA_AMINO_ACID_METABOLIC_PROCESS	1.359E-04	4.303E-02

The characteristic of signature 1 genes is that they have the highest expression levels in *High* populations compared to the other three populations and show decreasing expression relative to intracellular bacteria number. In contrast to signature 1, the signature 2 genes display the lowest expression levels in the *High* group. We were interested in further studying signature 1 genes and their relevant GO pathway analysis. Combining the previous KEGG analysis with signature 1 GO-BP pathway analysis, we have identified some common significant enrichment pathways. The KEGG pathway analysis presented

consistent pathways with GO-BP analysis: activated pathways in the *High* group include cell-cell adhesion, phagocytosis, TNF-α signalling pathway, autophagy and calcium signalling; suppressed pathways in the *High* group included cell cycle and apoptosis. In the following sections, relevant genes of interest were selected from these pathways for further analysis. A summary of the genes of interest and their associated pathways can be found in Table 5-4.

Table 5-4 Gene of interests from signature 1

Gene Symbol	Protein name	Prosed Functions	Involved both GObp and KEGG Pathways
Adcy1	Adenylate Cyclase 1	Catalyses the formation of the signalling molecule cAMP in response to G-protein signalling	Calcium signalling pathway
BCL3	B-Cell Lymphoma 3-Encoded Protein	the regulation of transcriptional activation of NFκB target genes	TNF signalling pathways
CCL2	C-C Motif Chemokine Ligand 2	mobilization of intracellular calcium ions	Phagocytosis; Calcium signalling pathway
CD44	CD44 Molecule	Cell-surface receptor that plays a role in cell-cell interactions, cell adhesion and migration	Cell adhesion
HIF1A	Hypoxia Inducible Factor 1 Subunit Alpha	transcriptional regulator of the adaptive response to hypoxia	Autophagy
ITCH	Itchy E3 Ubiquitin Protein Ligase	targeting specific proteins for lysosomal degradation	TNF signalling pathways, Apoptosis
LYN	Src Family Tyrosine Kinase	the regulation of innate and adaptive immune responses	Calcium signalling pathway
Map2k1	Mitogen-Activated Protein Kinase Kinase 1	Involvement in the ERK pathway by activation of ERK1 and ERK2	Cell adhesion; TNF signalling pathways
MLKL	mixed lineage kinase domain-like	key role in TNF-induced necroptosis, a programmed cell death process	Apoptosis; TNF signalling pathways
Myl2	Myosin Light Chain 2	plays a role in heart development and function	Cell adhesion
Pik3cb	Phosphatidylinositol-4,5-Bisphosphate 3-Kinase Catalytic Subunit Beta	activation pathway in neutrophils	Cell adhesion; TNF signalling pathways; Autophagy
PTPN2	Protein Tyrosine Phosphatase Non-Receptor Type 2	Regulate cell growth, differentiation, mitotic cycle, and oncogenic transformation	Cell adhesion
Vegfa	Vascular Endothelial Growth Factor A	proliferation and migration of vascular endothelial cells	Cell adhesion; Calcium signalling pathway

5.3.6 Candidate genes for understanding host response to different levels of bacterial number

From significantly regulated pathways common to both GO and KEGG analysis, five candidate genes were selected on the basis that their respective proteins could be targeted with inexpensive chemical inhibitors, widely used in published research, that could be applied in simple *in vitro* tests (Table 5.5). Target genes are involved in pathways including cell adhesion, phagocytosis, TNF signalling pathways, MAPK signalling pathway and apoptosis. Candidates and their relevant chemical inhibitors are listed in Table 5-5. The level of gene expression for the five genes is shown in Figure 5-11.

Table 5-5 Selective Genes and relevant chemical inhibitors

Targeting gene	Chemical inhibitor	Reference
Adcy1	ST034307	Watts, V.J., 2018
MLKL	Necrosulfonamide	Rübbelke, M., 2020
Map2k1	Trametinib (GSK1120212)	Khan, Z.M., 2020
Pik3cb	GSK2636771	Vanhaesebroeck, B., 2021
Itch	Clomipramine	Rossi, M., 2014

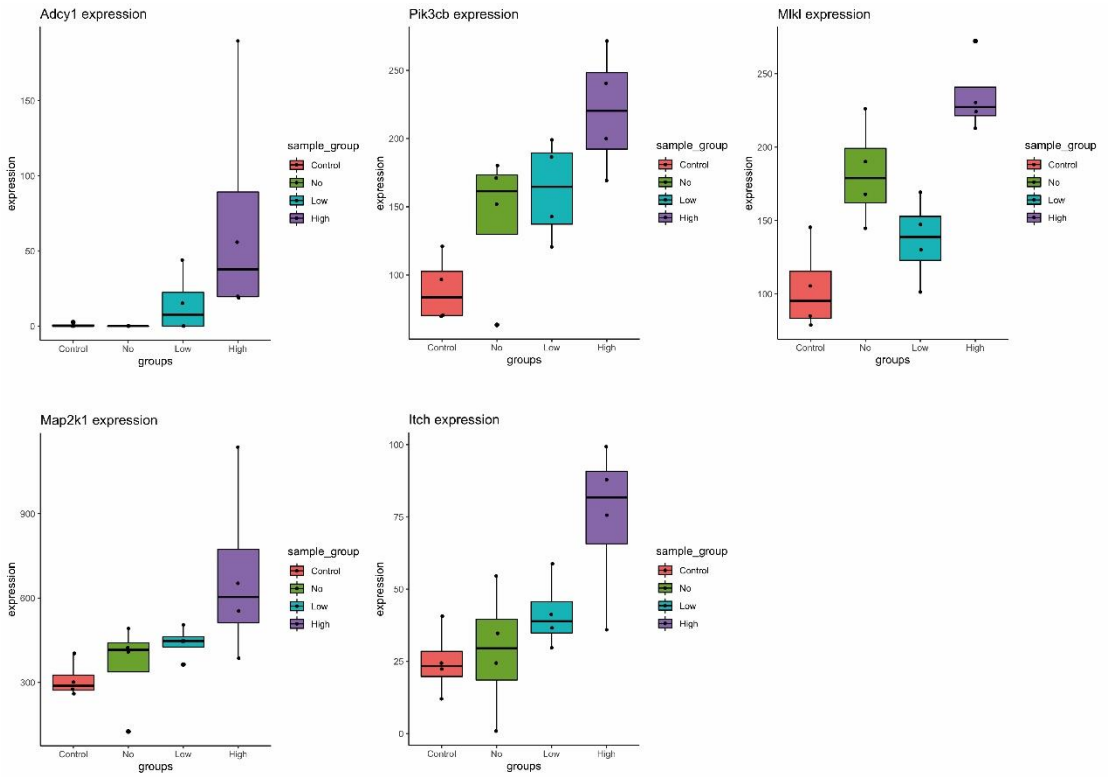

Figure 5-11 Genes expression levels of five candidate host DEGs selected for further testing.

Genes *Adcy1*, *Pik3cb*, *Mlkl*, *Map2k1* and *Itch* were selected from the signature 1 gene list involved in pathways; cell-cell adhesion, TNF signalling, necrotic cell death, MAPK pathways and NF-κB. Boxplots show expression of genes of interest in four groups: *Control* in red, *No* in green, *Low* in blue and *High* in purple. Black dots denote individual samples. Error bars represent SEM.

5.3.7 Effect of selective chemical inhibitors on LF82 infected RAW 264.7 cells

The efficacy of 5 chemical inhibitors against the proteins encoded by the candidate genes was evaluated in a well-established *in vitro* infection model. *In vitro* infection experiments combined with visible colonies counts were conducted to identify which of the target host proteins may promote bacterial survival and replication within macrophages. RAW 264.7 cells were infected with LF82 at an MOI of 100 for 1 hour, after which the cells were washed and treated with low or high concentrations of inhibitors for a further 6 or 24 hours. The five chemical inhibitors were evaluated through colony counts (CFU per gram of cell protein), as shown in Figure 5-12; including ST034307 (Figure 5-12a), Clomipramine (Figure 5-12b), Trametinib (Figure 5-12c), Necrosulfonamide (Figure 5-12d) and GSK2636771 (Figure 5-12e). Inhibitors were all dissolved in dimethyl sulfoxide (DMSO) solution. Each inhibitor treatment experiment was

designed with four groups (n= 3), consisting of; (1) treatment with DMSO as a control, (2) treatment with a low concentration of inhibitor, (3) treatment with a high concentration of inhibitor, or (4) no treatment as a control. Within different chemical inhibitor treatments, significant differences ($p < 0.05$) in intracellular bacteria burden at 6 or 24 hpi were observed between three of the treatment groups (ST034307, Clomipramine and GSK2636771) and the untreated control group. Infected cells treated with 1 μM ST034307 (4.156 X 10^6 CFU/g), 10 μM ST034307 (1.311 X 10^6 CFU/g) and 1 μM GSK2636771 (8.35 X 10^5 CFU/g) had slightly lower intracellular bacterial numbers than the control (1.064 X 10^7 CFU/g) at 24 hpi (Figure 5-12a and e). A significant reduction in intracellular bacteria was observed when using 10 μM of Clomipramine when compared to the untreated control group at both 6 and 24 hpi. After 6 hours of treatment, the mean bacterial counts of Clomipramine treatment and untreated control were 6.146 X 10^5 CFU/g and 1.003 X 10^7 CFU/g, respectively, a 16-fold reduction in intracellular bacterial load. The reductions in bacterial burden in Clomipramine treatment compared to that in the control were higher at 24 hpi at 1,924-fold reduction (Control, 1.064 X 10^7 CFU/g, Clomipramine 5.53 X 10^3 CFU/g; Figure 5-12b). The Trametinib or Necrosulforamide treatment groups did not differ statistically significantly from the untreated control group either at 6 or 24 hpi (Figure 5-12c and d).

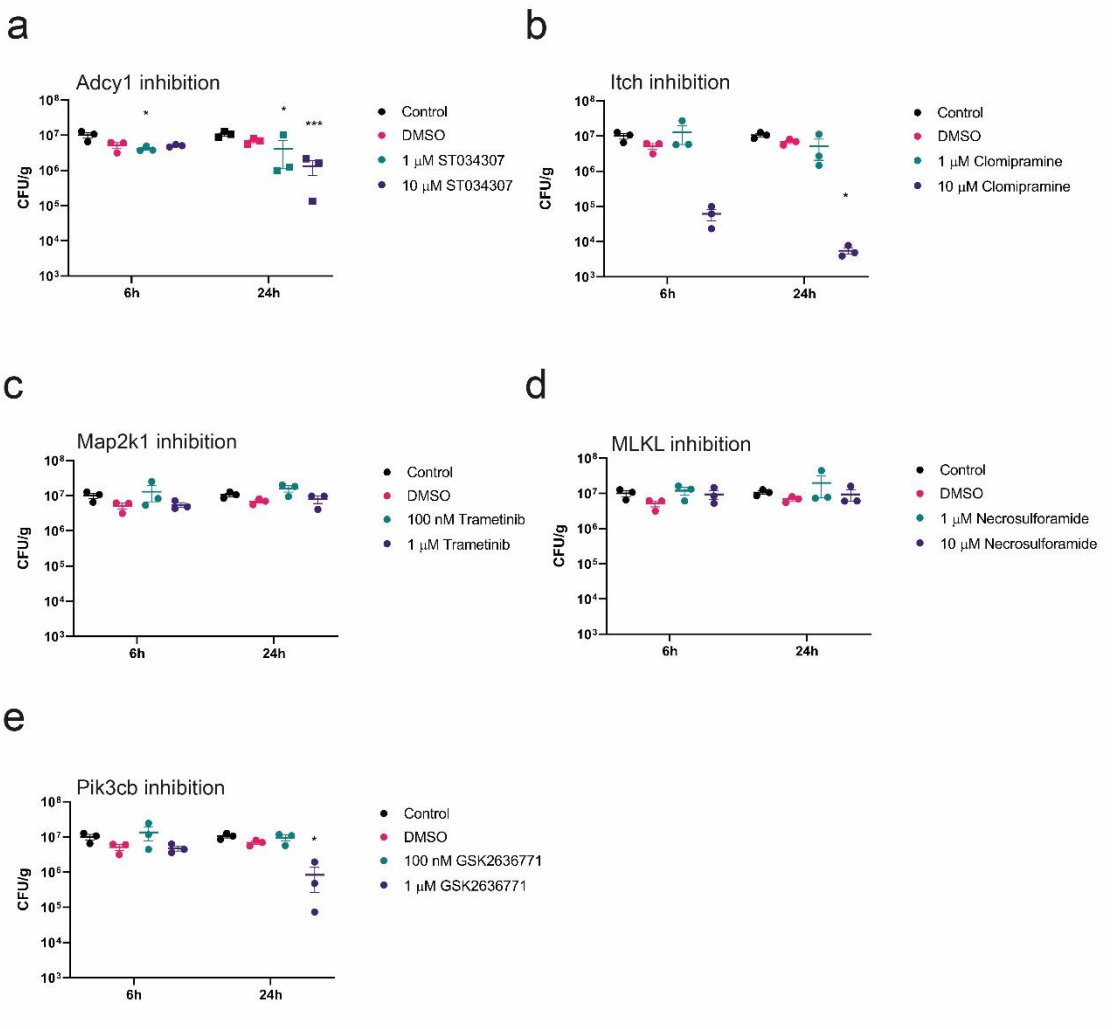

Figure 5-12 Evaluation of the effects of different chemical inhibitors on intracellular bacterial load in RAW 264.7 cells.

RAW 264.7 cells were infected with LF82 for 1 hour followed by treatment with different chemical inhibitors for a further 6 or 24 hpi; ST034307 (a), Clomipramine (b), Trametinib (c), Necrosulforamide (d), GSK2636771 (e). Bacterial recovery is displayed as CFU/g of protein. Data points represent the mean of three technical repeats plus the standard deviation at a timepoint of 6 or 24 hpi. Each treatment was compared to the untreated control group. Statistical significance was determined by two-way ANOVA. *, P <0 0.05. **, P < 0.01. ***, P < 0.0001.

For confirmation of these results and to understand the effect of inhibitor treatment over longer incubation periods, we carried out intracellular bacterial counts on single cells at 24 (Figure 5-13a), 48 (Figure 5-13b), and 72 hpi (Figure 5-13c) using IFC. Fluorescently labelled LF82::*rpsM*GFP was used during 1 hour of infection before cells were treated with the 5 different inhibitors. Within traditional visible colony count experiments, there are two concentrations for each inhibitor were used. In order to minimise the toxicity of the inhibitors during prolonged infection, we used the lower of the two concentrations here. DMSO treatment again served as a control. All treatments reduced the

population containing intracellular bacteria over time, but Clomipramine treatment caused a large decrease, resulting in a smaller population of cells containing over 5 intracellular bacteria. Clomipramine treatment results in 48.2 % of cells without any bacteria at 24 hpi, an 8.2% increase over DMSO treatment (40.0 %); at 48 hpi this population increases to 63.2% and at 72 hpi this population increases to 76.5%. DMSO treatment was maintained at 42.3% at 48 hpi, and increased slightly to 52.8% at 72 hpi, indicating that Clomipramine significantly reduced intracellular LF82 burden (Figure 5-13). The inhibitors were also examined through bacterial growth curves to ensure no negative growth effects were occurring through effects on LF82 (Figure 5-14a) and LDH assays to ensure no significant toxicity effects were associated with RAW 264.7 cell treatment (Figure 5-14b and c). The results indicated that these chemical compounds did not inhibit bacterial growth (Figure 5-14a). Using the highest concentrations of inhibitors, such as 100 µM of ST034307, 100 µM of Necrosulfonamide and 50 µM of Clomipramine, cytotoxicity was observed in both infected and uninfected cells, yet this was not observed at lower concentrations demonstrating that the concentration of inhibitors used in the *in vitro* infection experiments was not toxic for cells (Figure 5-14b and c).

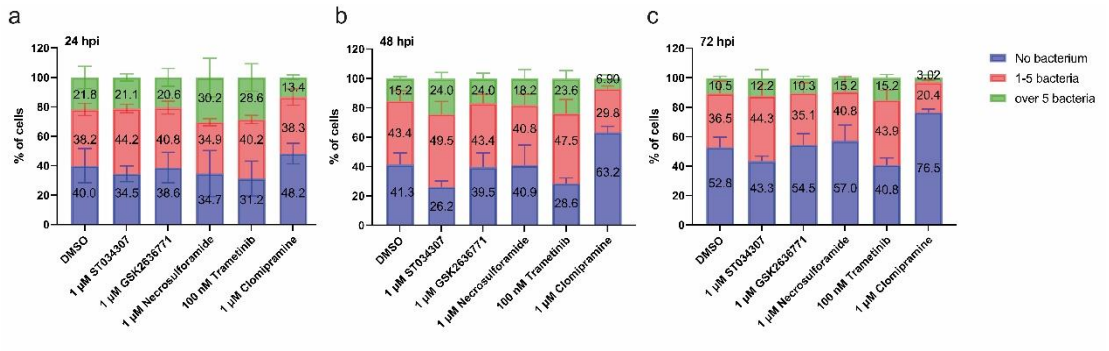

Figure 5-13 Quantification of intracellular LF82 burden post-inhibitor treatment using IFC.

RAW 264.7 cells infected with LF82::*rpsM*GFP were treated with 1 µM ST034307, 1 uM GSK2636771, 1 uM Necrosulforamide, 100 nM Trametinib or 1 uM Clomipramine for 24 hpi (a), 48 hpi (b) and 72 hpi (c). Infected cells treated with DMSO were used as a control. Intracellular LF82::*rpsM*GFP was counted via IFC. The spot count profile separated cells into those with no bacteria, cells containing 1-5 bacteria, or cells containing over 5 bacteria. The sub-populations of a graph represent the mean of three biological repeats. Error bars represent SEM. The number of portion of sub-populations represents the mean of three biological repeats.

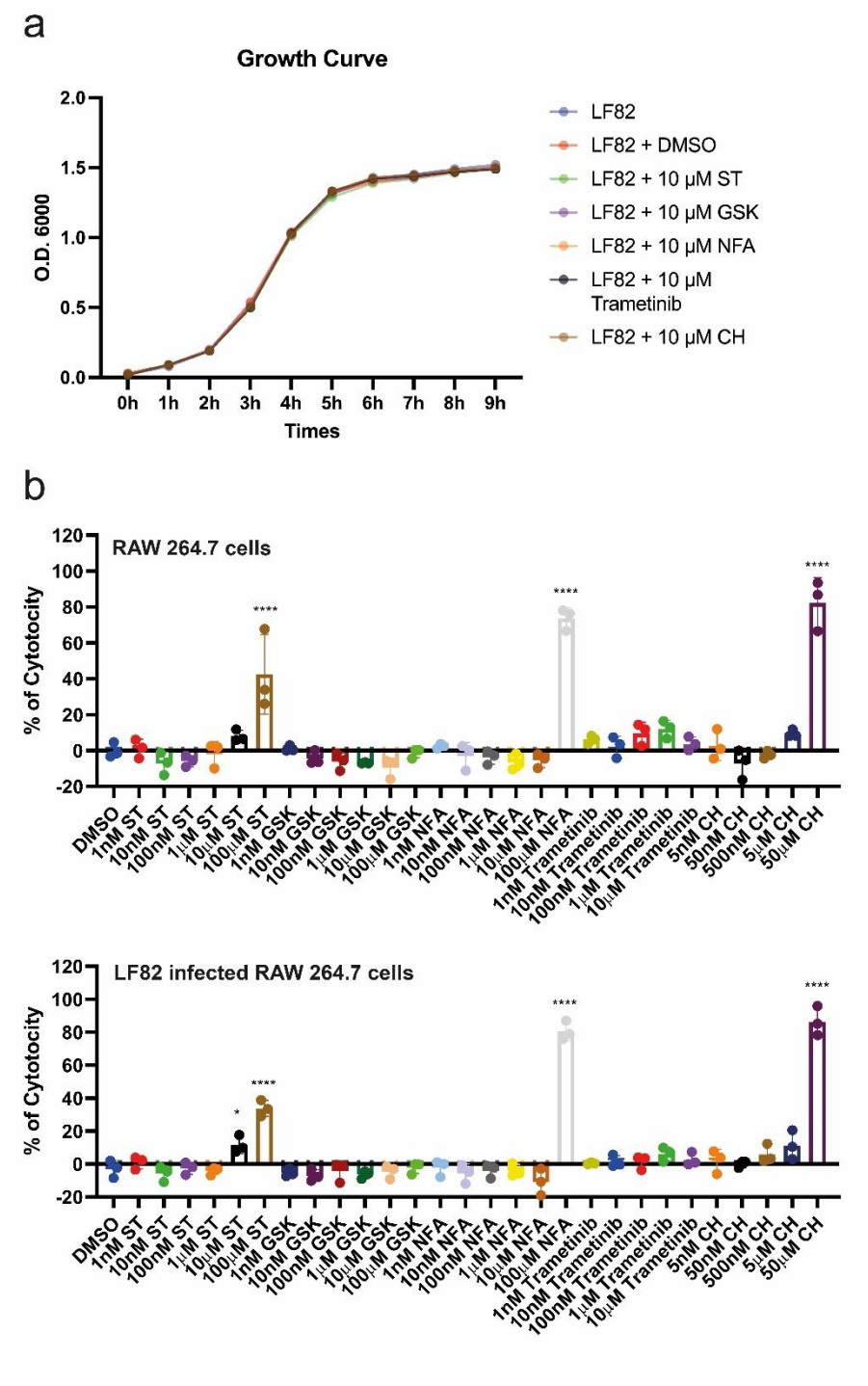

Figure 5-14 Effects of the different chemical inhibitors on LF82 growth and cytotoxicity to RAW 264.7 cells.
(a) Growth curve of LF82 after treatment with DMSO or the five chemical inhibitors (10 μM ST034307, 10 μM GSK2636771, 10 μM Necrosulforamide, 10 μM Trametinib or 10 μM Clomipramine). (b) LDH cytotoxicity assay was undertaken for uninfected or LF82 infected RAW 264.7 cells treated with different concentrations of chemical inhibitors. DMSO, a diluent for the inhibitors, was used as a control. Experimental groups were compared to the control. Statistical significance was determined by one-way ANOVA. Statistical significance was determined by one-way ANOVA. *, P <0 0.05. **, P < 0.01. ***, P < 0.0001.

Lastly, we analysed TNF-α secretion from infected and uninfected cells when they were treated with a low and a high concentration of the same chemical inhibitors. It was found that uninfected cells secreted significantly increased amounts of TNF-α after 6 or 24 hours of Necrosulfonamide treatment compared to the untreated control group (Figure 5-15a and c), but this was not observed in infected cells (Figure 5-15b and d). The secretion of TNF-α was significantly decreased in 10 μM ST034307, 100 nM Trametinib and 1 μM Trametinib treated infected cells compared with the untreated infected control group at 24 hpi (Figure 5-15d). Clomipramine treatment, associated with a decrease in intracellular bacteria, surprisingly did not elicit a change in TNF-α levels, compared to the control group. In contrast to clomipramine, Trametinib inhibits TNF-α secretion but does not affect intracellular bacterial numbers. While AIEC replication and TNF-α secretion have long been thought to interplay during infection, these findings indicate that inhibitors can disconnect the two, suggesting that in macrophages TNF-α may not play a critical role in regulating intracellular AIEC survival and replication as previously thought. However, there is little known of the mechanism of Clomipramine reducing intracellular bacteria.

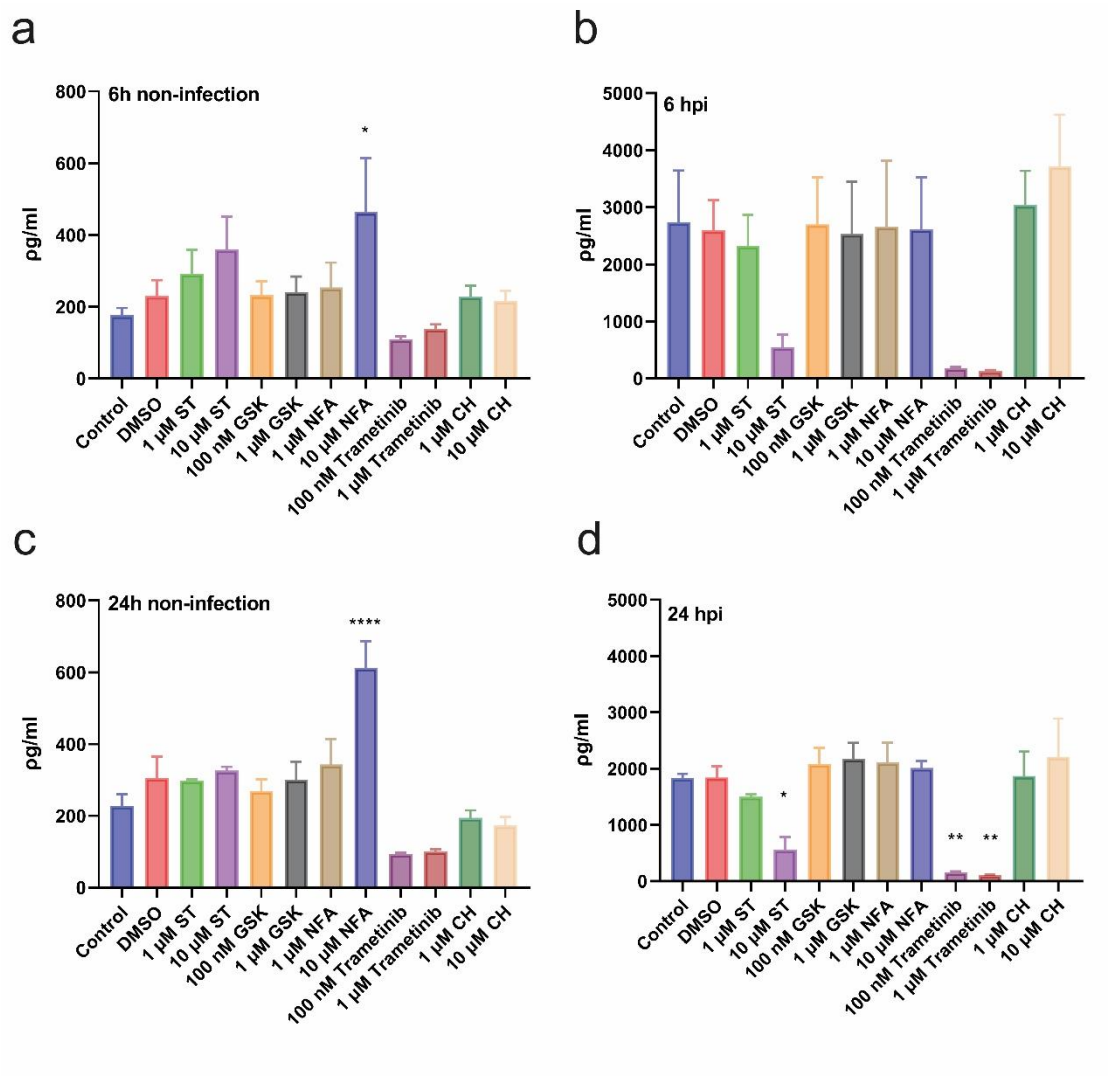

Figure 5-15 ELISA for TNFα measurement post-inhibitor treatment.

RAW 264.7 cells were stimulated overnight by 100 ng/ml LPS. Activated RAW 264,7 cells were then infected with LF82 at MOI of 100 or treated with bacteria-free medium (as uninfected RAW 264.7 cells) for 1 hour. Post 1 hour, infected or uninfected RAW 264.7 cells were washed and treated with different chemical inhibitors at two different concentrations for further indicated times. Infected or uninfected cells in absence of chemical treatment was regarded as a control. Graph (a) represents uninfected RAW 264.7 cells that were treated with or without chemical treatments for 6 hpi. (b) As described for (a) but for infected RAW 264.7 cells. (c) Uninfected RAW 264.7 cells were treated with chemical inhibitors for 24 hpi. (d) As for (c) but for infected RAW 264.7 cells. Statistical significance was determined by one-way ANOVA. *, P <0 0.05. **, P < 0.01. ***, P < 0.0001.

5.4 Discussion

An approach of combining FACS and RNA-seq

In this study, we described for the first time a protocol for sorting RAW 264.7 cells containing GFP-expressing LF82 for RNA-sequencing. It has long been recognised that the key characteristic of AIEC isolated from CD patients is their

ability to survive and replicate in activated phagosomes within macrophages, along with the release of large amounts of TNF-α (Barnich and Darfeuille-Michaud, 2007; Rolhion and Darfeuille-Michaud, 2007). Nevertheless, the analysis of the macrophage response to AIEC has been limited by the heterogeneity of outcomes within the infected cell population. The number of AIEC taken up by individual cells was variable. To overcome this limitation of previous analysis, we exploited this variability using FACS to successfully separate cells that were burdened with different intracellular bacterial loads (*No*, *Low* and *High*) within infected populations. A transcriptomic analysis on these three populations, plus control uninfected cells, identified differentially expressed genes between all populations. There were a total of 1011 differentially expressed genes determined within six comparisons of the four sample groups. To better understand the interaction of LF82 with RAW 264.7 cells, we were particularly interested in using enrichment pathway analysis. The significantly enriched overlap terms of GO and KEGG pathway analysis included cell-cell adhesion, phagocytosis, TNF signalling, autophagy, calcium signalling, cell cycle and apoptosis. As expected, the pathways of cell adhesion, phagocytosis, TNF signalling, NFκB pathways, and MAPK pathways were activated in the *High* group against the *Control* group, on the contrary, suppressed pathways such as cell cycle were enriched in the *High* group. Understanding the importance of these pathways may explain some of the phenomena we discovered in previous chapters.

Identifying relevant pathways during AIEC infection

In summary of cytokine transcriptomic analysis, LF82-infected macrophages demonstrated a pro-inflammatory phenotype with elevated expression levels of various cytokines including TNF-α, IL-6 and IL-1. In the context of CD, one of the key mechanisms involved in the impaired inflammatory response that characterizes CD is the dysregulation of the transcription factor NF-κB (Hayden and Ghosh, 2012). It was found that macrophages isolated from inflamed intestinal biopsies expressed higher levels of NF-κB, a key transcription factor promoting the transcription of genes encoding pro-inflammatory cytokines (Rogler *et al.*, 1998). Upon activation, inhibitory κB proteins (IκBs) are degraded via ubiquitin-proteasome process before the NF-κB translocates into the nucleus

where it regulates transcription (Chen, 2005). In this pathway, when the signalling cascade is activated, a variety of inflammation-related mediators are produced, including IL-1β, TNF, and IL-6 (McDaniel *et al.*, 2016). In macrophages, releasing TNF-α could further induce the activation of NF-κB when it binds to the TNF receptor TNFRII, which then triggers the RIP1-MEKK3-TAK1 cascade in the process (Parameswaran and Patial, 2010). Given that the NF-κB pathway and TNF signalling has extensively investigated for therapeutic interventions in the field of CD, we screened genes of interest relating to these pathways including the genes *Itch*, *Pik3cb* and *Map2k1*. There are several current drugs used to treat CD, including corticosteroids, anti-TNF agents, and 5-aminosalicylates, that either directly or indirectly affect the NF-κB pathway. However, these treatments are ineffective for a proportion of patients (Peyrin-Biroulet and Lémann, 2011; Martínez-Montiel *et al.*, 2015; Roda *et al.*, 2016).

In addition to accumulated phosphorylated Pyk2, inhibited cell proliferation, and enhanced cell-cell connections during AIEC infection, our attention has also been drawn to enriched pathways such as cell-cell adhesion, calcium signalling, and necrotic cell death. Genes of interest were also selected based on these pathways. For example, *Mlkl* is involved in necrotic cell death and *Adcy1* is involved in regulating calcium signalling.

Among all pathways, we therefore identified five potential genes (*Adcy1*, *Mlkl*, *Pik3cb*, *Map2k1* and *Itch*) for further infection experiments with specific targeting of their protein products by chemical inhibition. Considering the results from both CFU and IFC experiments, there are two drugs of great interest: Trametinib and Clomipramine, targeting Map2k1 and Itch, respectively. As a result of treatment with Clomipramine, which inhibits the host protein Itch, we found that LF82 intracellular levels dramatically decreased over drug treatment time. Clomipramine, an anti-obsessional drug has an anticholinergic effect *in vitro* and *in vivo* and clinically is effectively used for obsessive-compulsive disorder and panic disorder (Montgomery, 1996). To be noted, pharmacological inhibition utilises various chemical compounds which may directly bind with the protein and only blocks the function of a protein but the protein is still present. This has important implications: they can also have many off-target effects and drug-inhibited protein may lack a certain activity but may

still interact with some binding partners or assemble into macromolecular complexes. In addition, chemical compound may potentially contribute to interplay with similar structure protein.

Clomipramine, Itch and AIEC infection

Clomipramine (Anafranil) was the first drug to be approved by FDA for patients with obsessive-compulsive disorders in 1989 (Hollander *et al.*, 2000). In drug screening studies, Clomipramine was reported to inhibit the ubiquitin E3 ligase Itch (Rossi *et al.*, 2014). In the past few years, there have been many publications on the role that Itch plays as a negative regulator of macrophage cytokine production by suppressing innate immune pathways, particularly NF-κB signalling by regulating Cyld and Nod2 within the NF-κB pathway (Shembade *et al.*, 2008; Ahmed *et al.*, 2011; Kathania *et al.*, 2015; Theivanthiran *et al.*, 2015). *CYLD* and *NOD2*, have also been linked to CD (Lapaquette, M.-A. Bringer and Darfeuille-Michaud, 2012; Cleynen *et al.*, 2014). In bone marrow-derived macrophages (BMDMs), Itch forms a complex with the deubiquitinase Cyld, recruiting A20 to the substrate Tak1 which is downstream of TNF-α signalling, resulting in the restricted transcription of IL-6, TNF-α, and IL-1ß (Ahmed *et al.*, 2011; Kathania *et al.*, 2015). Tao *et al.*, found that ITCH polyubiquitinates RIP2 to allow RIP2 binding to NOD2 then signalling though p38 and JNK pathways (Tao *et al.*, 2009). In Itch-deficient BMDMs, it has been found that increased phosphorylated p38α could stimulate the secretion of TNF-α (Tao *et al.*, 2009; T., Xiaodong and W., 2013; Theivanthiran *et al.*, 2015). Our infection experiments using the drug Clomipramine for blocking Itch resulted in lower levels of intracellular bacteria in the cells, but could not modulate TNF-α secretion during LF82 infection. Future studies would conduct longer-term studies on LF82-infected macrophages under the influence of Clomipramine in order to determine whether reduction of bacteria results in a reduction of TNF-α release. Clomipramine may provide a potential treatment for CD patients by regulating intracellular bacterial numbers within macrophages. However, since Clomipramine was introduced as an anti-depressant treatment, it was noted to induce suicidal tendencies meaning that while informative in identifying Itch as a drug target, it is unlikely to be used for CD treatment.

TNF-a expression inhibition related to CD

Our transcriptomics analysis revealed that the TNF receptor gene was expressed at low levels in the *No* group compared to the *High* group, while TNF expression at high levels in all three groups (*No*, *Low* and *High*) relative to the uninfected control group. As shown in the infection experiments, Trametinib was not effective in reducing intracellular bacteria, but it reduced TNF-α secretion. Based on these results, it may be the case that soluble TNF-α is not the main factor promoting intracellular bacteria survival and replication.

Map2k1 also named Mek-1, is involved in MAPK pathway. Trametinib, is a highly selective and potent kinase inhibitor of MEK1/2. Trametinib blocks MAPK/MEK-ERK cascade activation leading to a defect in TNF-α response (Shi-lin *et al.*, 2015). In light of this information, MEK-ERK signalling represents an important therapeutic target for the development of drugs against severe and acute inflammation. In our study, we show that Trametinib resulted in a defective TNF-α response induced by LF82 in macrophages but it failed to decrease intracellular LF82.

Anti-TNF-α agents for CD treatment are able to block overexpression of TNF-α via binding soluble or transmembrane TNF-α and inhibiting binding to its receptors, resulting in blockage of proinflammatory signals or molecules that are upregulated by TNF-α (Eissner, Kolch and Scheurich, 2004). However, these treatments are ineffective for a proportion of patients (Roda *et al.*, 2016). The reasons for treatment failure are not completely understood. The possibility exists that anti-TNF-α agents may reduce inflammation symptoms, but the inability to remove intracellular pathogens may contribute to recurrences. Therefore combinations of drugs, as identified here, that block both TNF-α release and intracellular bacterial replication may be a way forward.

Chapter 6 Final Conclusions and Future Perspectives

Flow cytometry coupled with fluorescent microscopy makes IFC a powerful tool alongside advances in data-processing algorithms. With this methodology, thousands of individual cellular events can be analysed multiparametrically and morphologically. A flow cytometric analysis of host-pathogen interaction can therefore provide quantitative answers to a variety of biological questions including intracellular pathogens counting, DNA content analysis, cell-cell connection and subcellular patterns of co-localisation. In this thesis, I have described achievements in the use of fluorescently labelled AIEC strain LF82 in macrophage cellular infections to analyse host-pathogen interactions.

Our aim in this thesis was to study cell-cell interaction and the host-pathogen dynamic during AIEC infection. Based on the images of cell-cell interaction obtained during AIEC infection, we identified three different forms of cell-cell interaction including; cell adhesion, phagocytosis and cell fusion. AIEC-induced cell-cell connection could be a means for bacterial spread. Currently, little is known about AIEC-induced cell-cell connection, nor is it known what host protein facilitates the process. There is a possibility that macrophages are infectious hubs that remain infected with AIEC for extended periods and seed bacteria to other macrophages through cell-cell interactions. It is unclear how AIEC invades macrophages and then transmits to other cells *in vivo*, but it could be related to phagocytosis and cell fusion. The AIEC enhanced RAW 264.7 cell-cell connections, as evidenced by cell fusion experiments after 24 hour infection. Additionally, a much higher population of bi-nucleated cells were observed in AIEC infected RAW 264.7 cells at 24 hpi. Among the images of bi-nucleated and polynucleated infected macrophages, a phenomenon was shown whereby macrophages carrying AIEC continue to phagocytose uninfected cells. It is possible that infected cells may continue to phagocytose, resulting in the formation of MNGCs.

According to the evidence obtained by observing characteristics of RAW 264.7 cells infected with LF82, the enhancement of cell-cell connection and phagocytosis may be the first steps of granuloma formation. The presence of granulomas is one of the hallmarks used to histologically diagnose CD and

significantly alters clinical features in CD patients, suggesting a more aggressive form of the CD (Soh *et al.*, 2020). Since host-pathogen interaction lasts for a long period of time, longer experiments are preferred (Fonseca *et al.*, 2017). However, the longest infection time in this thesis was 72 hpi, and at this time point, MNGCs and cell aggregates were observed. An *in vitro* granuloma formation experiment by Delcroix and colleagues found that *Mycobacterium tuberculosis* (Mtb) infection resulted in an increase in the number of granulomas produced after 21 days (Delcroix *et al.*, 2018). Therefore, in future studies, a longer infection time is necessary to follow granuloma formation. Furthermore, during AIEC infection, macrophage proliferation was inhibited, so an ideal system should allow continued addition of immune cells, since granulomas are dynamic environments where new cells are recruited (Schreiber *et al.*, 2011). A workflow of a future granuloma formation experiment for AIEC-macrophage interaction is shown in Figure 6-1.

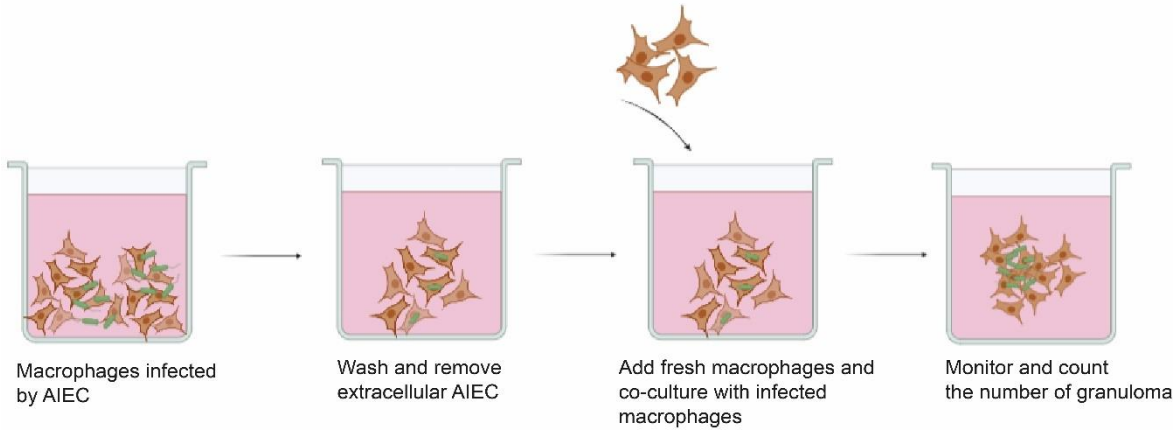

Figure 6-1 Schematic of *in vitro* granuloma formation.

Following infection with AIEC, RAW 264.7 cells are washed with PBS and fresh medium is added containing gentamicin to remove extracellular AIEC. Fresh suspensions of uninfected macrophages are co-cultured with infected cells. Plates are incubated at 37°C (5% CO2) and granuloma formation is monitored on indicated days post-infection by imaging using microscopy or fixed and stained for fluorescent microscopy imaging. Then images can be used to count the number, and measure the size, of aggregates.

In light of the successful construction of a method using IFC for studying host-AIEC interactions, we set out to use this method for identifying the role of specific host proteins involved in bacterial infection. To identify the function of a novel CD risk locus, *PYK2*, we used an *in vitro* infection model with Pyk2 inhibition (Jimmy Z. Liu *et al.*, 2015). pPyk2 protein levels were identified as

being significantly altered during AIEC infection. The Pyk2 inhibitor PF-431396 significantly decreased intramacrophage replication of LF82 as determined by viable colony count, fluorescence immunostaining and IFC. Meanwhile, the inhibition of Pyk2 also significantly reduced the abundance of AIEC clinical isolates within macrophages. Based on the histological results of a few samples, we found higher PYK2 expression levels in CD patients compared to healthy control. Therefore, for the next step, more human histological samples are needed in order to investigate the differences in PYK2 protein levels between CD patients and healthy individuals. Besides, It is expected that more studies involving macrophages isolated from CD patients for AIEC infection in the presentence of PYK2 inhibition will shed light on the role played by PYK2 in CD promoting AIEC survival and replication. Besides, the PF-431396 inhibitors should also be tested on the macrophages from CD patients, where macrophages might be NOD2 or other mutations.

Modelling of bacterial infection *in vitro* and *in vivo* is increasingly used for drug development and pathophysiological studies. Even though *in vivo* models are the most effective way to evaluate safety and efficacy, drug susceptibility testing and mechanism studies utilise *in vitro* models due to their cost-effectiveness, ease of setup, and ability to perform high-throughput experiments. Further, *in vitro* systems have also been useful for studying the complex interaction between host and pathogen in disease pathogenesis. In the case of AIEC infection, where macrophages are known to play such an important role, studies involving monocyte-derived macrophages (MDMs) isolated from CD patients are highly informative. While AIEC has been investigated in CD, various other pathogens have also been implicated, including *Mycobacterium avium* (Sartor, 2005), *Salmonella typhimurium* (Gulan *et al.*, 2010), *Yersinia enterocolitica* and *Listeria monocytogenes* (Liu *et al.*, 1995). In order to gain a better understanding of the role of PYK2 in CD, future studies should not be restricted to AIEC. It would be beneficial to utilize different CD-associated pathogens or clinical isolates of these bacteria from CD patients. Taken together, future studies of PYK2 in clinical samples will address three research questions: (1) Is there an increase in PYK2 protein levels in the intestines of CD patients? (2) Does inhibiting PYK2 reduce AIEC in MDMs isolated from CD patients? (3) Can PYK2 inhibition prevent other CD-associated pathogenic strains from surviving and

replicating within MDMs, including those from CD patients? PYK2 future studies are summarized in the Figure 6-2 below to answer these questions.

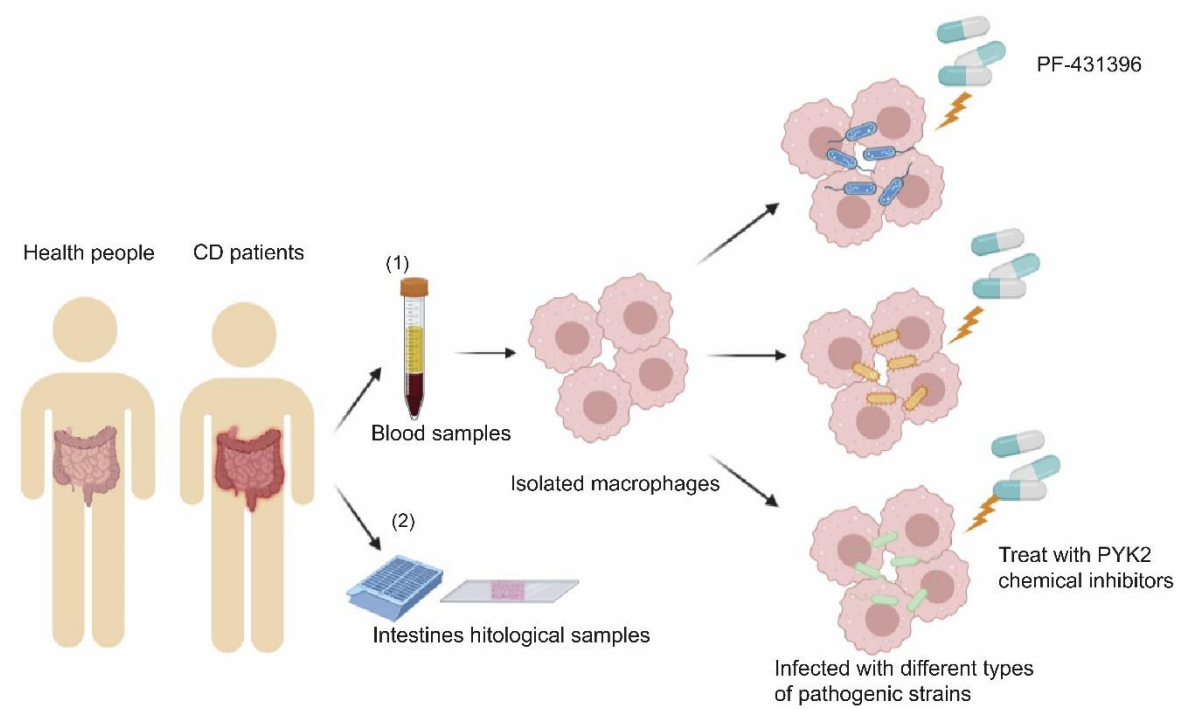

Figure 6-2 Schematic of Pyk2 future studies using clinical samples.

(1) To identify the role of PYK2 in human macrophages infected with different pathogens, blood samples are collected from healthy individuals or CD patients. Monocytes purified from blood are differentiated to macrophages prior to infection with pathogenic strains at MOI of 100 for 1 hour. Post-infection, infected cells are washed and further incubated at indicated times in presence of PF-431396 or not. Intracellular bacteria can be measured using viable colonies count, IFC or fluorescent microscopy. (2) To evaluate the PYK2 protein expression levels between healthy and CD patients, colon or ileum biopsies from healthy individuals or CD patients are embedded in paraffin. Samples sections are then probed with anti-Pyk2 antibody.

Bacterial infection leads to heterogeneous cell populations with respect to the amount of intracellular bacteria present within cells. In the *in vitro* infection model, IFC identified that less than 50% of cells were actually infected by AIEC strain LF82 at 24 hpi. To quantitatively characterise macrophage outcomes within different bacterial loads, FACS was carried out using GFP-expressing bacteria, which resulted in three outcomes: uninfected cells or infected cells with either low or high bacterial burden. Through a combination of FACS with RNA sequencing, we were able to gain a better understanding of host-pathogen and cell-cell interactions during infection, including cell-cell fusion triggered by intracellular bacteria. The transcriptomic responses of host cells could be analysed based on the intracellular pathogen burden of cells, suggesting why

some cells may be more permissive to intracellular pathogen replication. There can be a great deal of value in this approach in sorting truly infected cells from the uninfected cells.

During the analysis of transcription profiles, genes were sorted based on the extent to which their expression increases when intracellular bacteria burdens increase. GO pathway analysis of these sorted genes has demonstrated that the significantly enriched terms of GO-bp include cell-cell adhesion, positive regulation of phagocytosis, TNF-α signalling pathway, autophagy and calcium signalling pathway, negative regulation of cell cycle and apoptosis. Bacterial-induced cell fusion and bacterial-derived inhibition of cell proliferation may be explained by the enrichment of pathways for cell-cell adhesion and negative regulation of the cell cycle. The significantly increased genes, *Itch* and *Map2k1*, involved in TNF signalling pathways, apoptosis, and calcium signalling pathways was selected for study in the context of AIEC infection of macrophages in presence of chemical inhibitors treatments. In comparison to the LF82-infected RAW 264.7 cells without inhibitors treatment, Clomipramine targeting Itch, was highly effective at reducing intracellular bacteria inside macrophages but not alter TNF-α secretion. Whereas, another tested inhibitor that targets Map2k1, Trametinib, does not reduce bacteria but does decrease TNF-α level. These findings showing that intracellular bacterial content does not directly correlate with TNF-α secretion, which means anti-TNF-α agents reduce inflammation symptoms but may fail in removing intracellular pathogens. To some extent, it may explain that anti-TNF-α agents treatments are ineffective for some CD patients. Therefore, pharmaceutical combination therapy for CD patients would be more effective with blockage of TNF-α release and intracellular pathogens.

Currently, the mechanism by which Itch regulates intracellular bacteria within macrophages is unknown. As discussed in Chapter 5, Itch may interact with Cyld or Nod2 in downregulation of NF-κB pathway (Tao *et al.*, 2009; Zhang *et al.*, 2013). Both *CYLD* and *NOD2* genes have been directly linked to CD (Hugot *et al.*, 2001; Huang *et al.*, 2017). In this case, a direction for future study of the interplay between Itch and Cyld or Nod2 in AIEC-infected macrophages can be drawn. Hypothetical roles of Itch during AIEC infection are shown in the Figure 6-3.

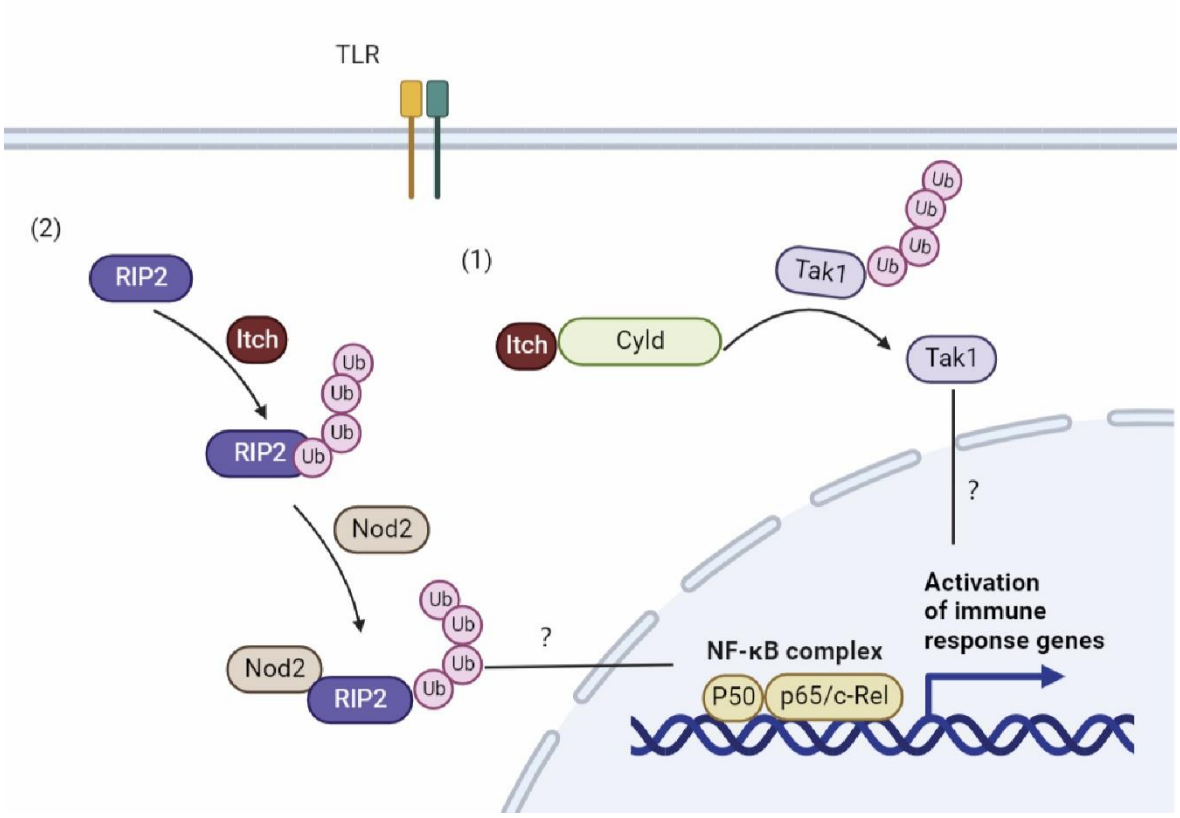

Figure 6-3 Proposed roles of Itch during AIEC infection of macrophages.

(1) In macrophages Itch forms complexes with de-ubiquitination enzyme (DUB) Cyld, regulating inflammation by removing the Lys-63–ub on Tak1 (Neesar Ahmed, 2011). A study by Cleynen et al. found that LF82 decreased Cyld protein levels, increasing the ability of LF82 to invade and replicate (Cleynen et al., 2014). (2) Adaptor protein RIP2 is ubiquitinated directly by Itch in response to bacterial infection and CD-associated protein Nod2 can bind polyubiquitinated RIP2 leading to p38 and JNK activation, as well as NFκB (Tao et al., 2009). Two proposed mechanisms that Itch may interact with Cyld or Nod2 to regulate inflammatory response pathways.

Herein, we have demonstrated that IFC is a powerful tool for studying the heterogenous interaction between host and pathogens. There are two main characteristics of LF82 infected RAW 264.7 cells identified by imaged-based experiments, one of which is that they increase the amount of cell-to-cell contact by continuing phagocytosis post-infection, and the other is that AIEC infection inhibits host cell proliferation. Despite the short duration of our *in vitro* infection experiments, cell aggregates and MGCs can be observed under fluorescent microscopy. Using our *in vitro* model of LF82 infection of RAW 264.7 cells, we also identified two chemical inhibitors that are effective at reducing intracellular bacteria inside macrophages. PF-431396 hydrate targets phosphorylation of Pyk2 while Clomipramine directly inhibits Itch. Although the signalling pathways involved in inhibition by Pyk2 or Itch defence against AIEC

remain largely unknown, they have identified novel targets in the treatment of CD.

List of References

Abraham, C. and Cho, J. (2009) 'Interleukin-23/Th17 pathways and inflammatory bowel disease', *Inflammatory bowel diseases*. Oxford University Press Oxford, UK, 15(7), pp. 1090–1100.

Adams, D. (1976) 'The granulomatous inflammatory response. A review.', *The American journal of pathology*. American Society for Investigative Pathology, 84(1), p. 164.

Adegbola, S. O. *et al.* (2018) 'Anti-TNF therapy in Crohn's disease', *International Journal of Molecular Sciences*, 19(8), pp. 1–21. doi: 10.3390/ijms19082244.

Aguilar, C. *et al.* (2014) 'Characterization of Crohn disease in X-linked inhibitor of apoptosis–deficient male patients and female symptomatic carriers', *Journal of allergy and clinical immunology*. Elsevier, 134(5), pp. 1131–1141.

Ahern, P. P. *et al.* (2010) 'Interleukin-23 drives intestinal inflammation through direct activity on T cells', *Immunity*. Elsevier, 33(2), pp. 279–288.

Ahmed, N. *et al.* (2011) 'The E3 ligase Itch and deubiquitinase Cyld act together to regulate Tak1 and inflammation', *Nature Immunology*, 12(12), pp. 1176–1183. doi: 10.1038/ni.2157.

Alexander, K. L., Targan, S. R. and Elson III, C. O. (2014) 'Microbiota activation and regulation of innate and adaptive immunity', *Immunological Reviews*. John Wiley & Sons, Ltd, 260(1), pp. 206–220. doi: https://doi.org/10.1111/imr.12180.

Allison, M. C. and Poulter, L. W. (1991) 'Changes in phenotypically distinct mucosal macrophage populations may be a prerequisite for the development of inflammatory bowel disease', *Clinical & Experimental Immunology*. Wiley Online Library, 85(3), pp. 504–509.

Alpuche-Aranda, C. M. *et al.* (1994) 'Salmonella stimulate macrophage macropinocytosis and persist within spacious phagosomes.', *The Journal of experimental medicine*, 179(2), pp. 601–608.

Amre, D. K. *et al.* (2007) 'Imbalances in dietary consumption of fatty acids, vegetables, and fruits are associated with risk for crohn's disease in children', *American Journal of Gastroenterology*, 102(9), pp. 2016–2025. doi: 10.1111/j.1572-0241.2007.01411.x.

Ananthakrishnan, A. N., Khalili, H., *et al.* (2013) 'A prospective study of long-term intake of dietary fiber and risk of Crohn's disease and ulcerative colitis', *Gastroenterology*. Elsevier, Inc, 145(5), pp. 970–977. doi: 10.1053/j.gastro.2013.07.050.

Ananthakrishnan, A. N., Cagan, A., *et al.* (2013) 'Normalization of plasma 25-hydroxy vitamin D is associated with reduced risk of surgery in Crohn's disease', *Inflammatory Bowel Diseases*, 19(9), pp. 1921–1927. doi: 10.1097/MIB.0b013e3182902ad9.

Anders, S., Pyl, P. T. and Huber, W. (2015) 'HTSeq—a Python framework to work with high-throughput sequencing data', *Bioinformatics*, 31(2), pp. 166–169. doi: 10.1093/bioinformatics/btu638.

Anderson, G. G. *et al.* (2010) 'Polysaccharide capsule and sialic acid-mediated regulation promote biofilm-like intracellular bacterial communities during cystitis', *Infection and immunity*. Am Soc Microbiol, 78(3), pp. 963–975.

Ansel, K. M. *et al.* (2006) 'Regulation of Th2 differentiation and Il4 locus accessibility', *Annu. Rev. Immunol.* Annual Reviews, 24, pp. 607–656.

Asakura, H. *et al.* (2008) 'Is there a link between food and intestinal microbes and the occurrence of Crohn's disease and ulcerative colitis?', *Journal of Gastroenterology and Hepatology (Australia)*, 23(12), pp. 1794–1801. doi: 10.1111/j.1440-1746.2008.05681.x.

Atreya, I., Atreya, R. and Neurath, M. F. (2008) 'NF-κB in inflammatory bowel disease', *Journal of Internal Medicine*. John Wiley & Sons, Ltd, 263(6), pp. 591–596. doi: https://doi.org/10.1111/j.1365-2796.2008.01953.x.

Atreya, R. *et al.* (2011) 'Antibodies against tumor necrosis factor (TNF) induce T-cell apoptosis in patients with inflammatory bowel diseases via TNF receptor 2 and intestinal CD14+ macrophages', *Gastroenterology*. Elsevier, 141(6), pp. 2026–2038.

Atreya, R. and Neurath, M. F. (2005) 'Involvement of IL-6 in the pathogenesis of inflammatory bowel disease and colon cancer', *Clinical reviews in allergy & immunology*. Springer, 28(3), pp. 187–195.

Avraham, H. *et al.* (2000) 'RAFTK/Pyk2-mediated cellular signalling', *Cellular Signalling*, 12(3), pp. 123–133. doi: 10.1016/S0898-6568(99)00076-5.

Baer, H. M. *et al.* (2019) 'PTH-075 Identification of IBD immunopathotypes', *Gut*, 68(Suppl 2), p. A69 LP-A70. doi: 10.1136/gutjnl-2019-BSGAbstracts.134.

de Baey, A. *et al.* (2003) 'A subset of human dendritic cells in the T cell area of mucosa-associated lymphoid tissue with a high potential to produce TNF-α', *The Journal of Immunology*. Am Assoc Immnol, 170(10), pp. 5089–5094.

Bain, C. C. and Mowat, A. M. (2014) 'Macrophages in intestinal homeostasis and inflammation', *Immunological Reviews*, 260(1), pp. 102–117. doi: 10.1111/imr.12192.

Balfour Sartor, R. (2006) 'Microbial and dietary factors in the pathogenesis of chronic, immune-mediated intestinal inflammation', *Immune mechanisms in inflammatory bowel disease*. Springer, pp. 35–54.

Barnich, N. *et al.* (2007) 'CEACAM6 acts as a receptor for adherent-invasive E. coli, supporting ileal mucosa colonization in Crohn disease', *The Journal of clinical investigation*. Am Soc Clin Investig, 117(6), pp. 1566–1574.

Barnich, N. and Darfeuille-Michaud, A. (2007) 'Role of bacteria in the etiopathogenesis of inflammatory bowel disease.', *World journal of gastroenterology*, 13(42), pp. 5571–5576. doi: 10.3748/wjg.v13.i42.5571.

Barnich, N. and Darfeuille-Michaud, A. (2010) ‘Abnormal CEACAM6 expression in Crohn disease patients favors gut colonization and inflammation by adherent-invasive E. coli’, *Virulence*. Taylor & Francis, 1(4), pp. 281–282.

Barollo, M. *et al.* (2011) ‘Antioxidative potential of a combined therapy of anti TNFα and Zn acetate in experimental colitis.’, *World journal of gastroenterology*, 17(36), pp. 4099–4103. doi: 10.3748/wjg.v17.i36.4099.

Baumgart, D. C. *et al.* (2009) ‘Exaggerated inflammatory response of primary human myeloid dendritic cells to lipopolysaccharide in patients with inflammatory bowel disease’, *Clinical & Experimental Immunology*. Oxford University Press, 157(3), pp. 423–436.

Baumgart, D. C. and Sandborn, W. J. (2012) ‘Crohn’s disease’, *The Lancet*. Elsevier, 380(9853), pp. 1590–1605.

Bäumler, A. J. *et al.* (1994) ‘Salmonella typhimurium loci involved in survival within macrophages’, *Infection and Immunity*. Am Soc Microbiol, 62(5), pp. 1623–1630.

Becker, C. *et al.* (2006) ‘Cutting edge: IL-23 cross-regulates IL-12 production in T cell-dependent experimental colitis’, *The Journal of Immunology*. Am Assoc Immnol, 177(5), pp. 2760–2764.

Bel, S. *et al.* (2017) ‘Paneth cells secrete lysozyme via secretory autophagy during bacterial infection of the intestine’, *Science*. American Association for the Advancement of Science, 357(6355), pp. 1047–1052. doi: 10.1126/science.aal4677.

Bell, S. J. and Kamm, M. A. (2000) ‘Review article: the clinical role of anti-TNFalpha antibody treatment in Crohn’s disease’, *Alimentary pharmacology & therapeutics*. St. Mark’s Hospital, London, UK., 14(5), pp. 501–514. doi: 10.1046/j.1365-2036.2000.00777.x.

Beltrán, C. J. *et al.* (2010) 'Characterization of the novel ST2/IL-33 system in patients with inflammatory bowel disease', *Inflammatory bowel diseases*. Oxford University Press Oxford, UK, 16(7), pp. 1097–1107.

Benchimol, E. I. *et al.* (2015) 'Inflammatory bowel disease in immigrants to Canada and their children: A population-based cohort study', *American Journal of Gastroenterology*. Nature Publishing Group, 110(4), pp. 553–563. doi: 10.1038/ajg.2015.52.

Berg, D. J. *et al.* (1996) 'Enterocolitis and colon cancer in interleukin-10-deficient mice are associated with aberrant cytokine production and CD4 (+) TH1-like responses.', *The Journal of clinical investigation*. Am Soc Clin Investig, 98(4), pp. 1010–1020.

Berns, M. and Hommes, D. W. (2016) 'Anti-TNF-α therapies for the treatment of Crohn's disease: the past, present and future', *Expert opinion on investigational drugs*. Taylor & Francis, 25(2), pp. 129–143.

Bernstein, C. N. *et al.* (2001) 'The prevalence of extraintestinal diseases in inflammatory bowel disease: A population-based study', *American Journal of Gastroenterology*, 96(4), pp. 1116–1122. doi: 10.1016/S0002-9270(01)02319-X.

Bernstein, C. N. *et al.* (2006) 'The epidemiology of inflammatory bowel disease in Canada: A population-based study', *American Journal of Gastroenterology*, 101(7), pp. 1559–1568. doi: 10.1111/j.1572-0241.2006.00603.x.

Berrebi, D. *et al.* (2003) 'Cytokines, chemokine receptors, and homing molecule distribution in the rectum and stomach of pediatric patients with ulcerative colitis', *Journal of pediatric gastroenterology and nutrition*. LWW, 37(3), pp. 300–308.

Bhatnagar, S. *et al.* (2007) 'Exosomes released from macrophages infected with intracellular pathogens stimulate a proinflammatory response in vitro and in vivo', *Blood, The Journal of the American Society of Hematology*. American Society of Hematology Washington, DC, 110(9), pp. 3234–3244.

Boada-Romero, E. *et al*. (2016) 'The T300A Crohn's disease risk polymorphism impairs function of the WD40 domain of ATG16L1', *Nature Communications*, 7(1), p. 11821. doi: 10.1038/ncomms11821.

Bolger, A. M., Lohse, M. and Usadel, B. (2014) 'Trimmomatic: a flexible trimmer for Illumina sequence data', *Bioinformatics*, 30(15), pp. 2114–2120. doi: 10.1093/bioinformatics/btu170.

Boudeau, J. *et al*. (1999) 'Invasive ability of an Escherichia coli strain isolated from the ileal mucosa of a patient with Crohn's disease', *Infection and immunity*. Am Soc Microbiol, 67(9), pp. 4499–4509.

Van den Brande, J. M. H. *et al*. (2003) 'Infliximab but not etanercept induces apoptosis in lamina propria T-lymphocytes from patients with Crohn's disease', *Gastroenterology*, 124(7), pp. 1774–1785. doi: https://doi.org/10.1016/S0016-5085(03)00382-2.

Van den Brande, J. M. H. *et al*. (2007) 'Prediction of antitumour necrosis factor clinical efficacy by real-time visualisation of apoptosis in patients with Crohn's disease', *Gut*, 56(4), pp. 509 LP – 517. doi: 10.1136/gut.2006.105379.

Brandtzaeg, P. (2007) 'Why We Develop Food Allergies: Coached by breast milk and good bacteria, the immune system strives to learn the difference between food and pathogens before the first morsel crosses out lips', *American scientist*. JSTOR, 95(1), pp. 28–35.

Brandtzaeg, P. (2009) 'Mucosal immunity: Induction, dissemination, and effector functions', *Scandinavian Journal of Immunology*, 70(6), pp. 505–515. doi: 10.1111/j.1365-3083.2009.02319.x.

Brazil, J. C., Louis, N. A. and Parkos, C. A. (2013) 'The role of polymorphonuclear leukocyte trafficking in the perpetuation of inflammation during inflammatory bowel disease', *Inflammatory bowel diseases*. Oxford University Press Oxford, UK, 19(7), pp. 1556–1565.

Bringer, M.-A. *et al.* (2007) 'The oxidoreductase DsbA plays a key role in the ability of the Crohn's disease-associated adherent-invasive Escherichia coli strain LF82 to resist macrophage killing.', *Journal of bacteriology*, 189(13), pp. 4860–4871. doi: 10.1128/JB.00233-07.

Bringer, M. A. *et al.* (2005) 'HtrA stress protein is involved in intramacrophagic replication of adherent and invasive Escherichia coli strain LF82 isolated from a patient with Crohn's disease', *Infection and Immunity*, 73(2), pp. 712–721. doi: 10.1128/IAI.73.2.712-721.2005.

Bringer, M. A. *et al.* (2006) 'The Crohn's disease-associated adherent-invasive Escherichia coli strain LF82 replicates in mature phagolysosomes within J774 macrophages', *Cellular Microbiology*, 8(3), pp. 471–484. doi: 10.1111/j.1462-5822.2005.00639.x.

Bringer, M. A. *et al.* (2012) 'Replication of Crohn's disease-associated AIEC within macrophages is dependent on TNF-α secretion', *Laboratory Investigation*, 92(3), pp. 411–419. doi: 10.1038/labinvest.2011.156.

Bruce-Staskal, P. J. *et al.* (2002) 'Cas, Fak and Pyk2 function in diverse signaling cascades to promote Yersinia uptake', *Journal of Cell Science*, 115(13), pp. 2689–2700.

Brument, S. *et al.* (2013) 'Thiazolylaminomannosides as potent antiadhesives of type 1 piliated Escherichia coli isolated from Crohn's disease patients', *Journal of medicinal chemistry*. ACS Publications, 56(13), pp. 5395–5406.

Brun, P. (2019) 'The profiles of dysbiotic microbial communities.', *AIMS microbiology*, 5(1), pp. 87–101. doi: 10.3934/microbiol.2019.1.87.

Brunner, M. *et al.* (2019) 'Permacol™ collagen paste for cryptoglandular and Crohn's anal fistula', *Techniques in Coloproctology*. Springer, 23(2), pp. 135–141.

Buisson, A. *et al.* (2016) 'Macrophages versus Escherichia coli: A decisive fight in Crohn's disease', *Inflammatory Bowel Diseases*, 22(12), pp. 2943–2955. doi: 10.1097/MIB.0000000000000946.

Bumann, D. (2015) 'Heterogeneous Host-Pathogen Encounters: Act Locally, Think Globally', *Cell Host & Microbe*, 17(1), pp. 13–19. doi: https://doi.org/10.1016/j.chom.2014.12.006.

Burch, J. S. *et al.* (2018) 'Glutamine via α-ketoglutarate dehydrogenase provides succinyl-CoA for heme synthesis during erythropoiesis.', *Blood*, 132(10), pp. 987–998. doi: 10.1182/blood-2018-01-829036.

Buttó, L. F. and Haller, D. (2016) 'Dysbiosis in intestinal inflammation: Cause or consequence', *International Journal of Medical Microbiology*, 306(5), pp. 302–309. doi: https://doi.org/10.1016/j.ijmm.2016.02.010.

Cadwell, K. *et al.* (2008) 'A key role for autophagy and the autophagy gene Atg16l1 in mouse and human intestinal Paneth cells', *Nature*, 456(7219), pp. 259–263. doi: 10.1038/nature07416.

Campbell, R. E. *et al.* (2002) 'A monomeric red fluorescent protein', *Proceedings of the National Academy of Sciences*. Proceedings of the National Academy of Sciences, 99(12), pp. 7877–7882. doi: 10.1073/pnas.082243699.

Carrière, J. *et al.* (2016) 'Exosomes Released from Cells Infected with Crohn's Disease–associated Adherent-Invasive Escherichia coli Activate Host Innate Immune Responses and Enhance Bacterial Intracellular Replication', *Inflammatory bowel diseases*. Oxford University Press Oxford, UK, 22(3), pp. 516–528.

Carvalho, F. A. *et al.* (2008) 'Crohn's disease-associated Escherichia coli LF82 aggravates colitis in injured mouse colon via signaling by flagellin', *Inflammatory bowel diseases*. Oxford University Press Oxford, UK, 14(8), pp. 1051–1060.

Carvalho, F. A. *et al.* (2009) 'Crohn's disease adherent-invasive Escherichia coli colonize and induce strong gut inflammation in transgenic mice expressing human CEACAM', *Journal of Experimental Medicine*. The Rockefeller University Press, 206(10), pp. 2179–2189.

Casén, C. *et al.* (2015) 'Deviations in human gut microbiota: a novel diagnostic test for determining dysbiosis in patients with IBS or IBD', *Alimentary Pharmacology & Therapeutics*. John Wiley & Sons, Ltd, 42(1), pp. 71–83. doi: https://doi.org/10.1111/apt.13236.

Casini-Raggi, V. *et al.* (1995) 'Mucosal imbalance of IL-1 and IL-1 receptor antagonist in inflammatory bowel disease. A novel mechanism of chronic intestinal inflammation.', *The Journal of Immunology*. Am Assoc Immnol, 154(5), pp. 2434–2440.

Cerf-Bensussan, N. and Gaboriau-Routhiau, V. (2010) 'The immune system and the gut microbiota: friends or foes?', *Nature Reviews Immunology*, 10(10), pp. 735–744. doi: 10.1038/nri2850.

Céspedes, S. *et al.* (2017) 'Genetic diversity and virulence determinants of Escherichia coli strains isolated from patients with Crohn's disease in Spain and Chile', *Frontiers in microbiology*. Frontiers Media Sa, 8, p. 639.

Chalopin, T. *et al.* (2016) 'Second generation of thiazolylmannosides, FimH antagonists for E. coli-induced Crohn's disease', *Organic & Biomolecular Chemistry*. Royal Society of Chemistry, 14(16), pp. 3913–3925.

Chen, Z. J. (2005) 'Ubiquitin signalling in the NF-κB pathway', *Nature Cell Biology*, 7(8), pp. 758–765. doi: 10.1038/ncb0805-758.

Cheng, Y. *et al.* (2019) 'Effect of pH, temperature and freezing-thawing on quantity changes and cellular uptake of exosomes', *Protein & Cell*, 10(4), pp. 295–299. doi: 10.1007/s13238-018-0529-4.

Chervy, M., Barnich, N. and Denizot, J. (2020) 'Adherent-invasive E. coli: Update on the lifestyle of a troublemaker in Crohn's disease', *International Journal of Molecular Sciences*, 21(10), pp. 1–34. doi: 10.3390/ijms21103734.

Chevalier, G. *et al.* (2021) 'Blockage of bacterial FimH prevents mucosal inflammation associated with Crohn's disease', *Microbiome*. BioMed Central, 9(1), pp. 1–16.

Chu, H. *et al.* (2016) 'Gene-microbiota interactions contribute to the pathogenesis of inflammatory bowel disease', *Science*. American Association for the Advancement of Science, 352(6289), pp. 1116–1120. doi: 10.1126/science.aad9948.

Cieza, J. R. *et al.* (2015) 'The IbeA Invasin of Adherent-Invasive Escherichia coli Mediates Interaction with Intestinal Epithelia and Macrophages', *Infection and Immunity*. American Society for Microbiology, 83(5), pp. 1904–1918. doi: 10.1128/IAI.03003-14.

Cipolla, G. *et al.* (2002) 'Nonsteroidal anti-inflammatory drugs and inflammatory bowel disease: Current perspectives', *Pharmacological Research*, 46(1), pp. 1–6. doi: 10.1016/S1043-6618(02)00033-6.

Cleynen, I. *et al.* (2014) 'Genetic and microbial factors modulating the ubiquitin proteasome system in inflammatory bowel disease.', *Gut*. England, 63(8), pp. 1265–1274. doi: 10.1136/gutjnl-2012-303205.

Cohen, L. J. *et al.* (2019) 'Genetic Factors and the Intestinal Microbiome Guide Development of Microbe-Based Therapies for Inflammatory Bowel Diseases', *Gastroenterology*, 156(8), pp. 2174–2189. doi: https://doi.org/10.1053/j.gastro.2019.03.017.

Cole, J. J. *et al.* (2021) 'Searchlight: automated bulk RNA-seq exploration and visualisation using dynamically generated R scripts', *BMC Bioinformatics*, 22(1), p. 411. doi: 10.1186/s12859-021-04321-2.

Colgan, A. M., Cameron, A. D. S. and Kröger, C. (2017) 'If it transcribes, we can sequence it: mining the complexities of host–pathogen–environment interactions using RNA-seq', *Current opinion in microbiology*. Elsevier, 36, pp. 37–46.

Colombel, J. F. *et al.* (2010) 'Infliximab, azathioprine, or combination therapy for Crohn's disease', *New England journal of medicine*. Mass Medical Soc, 362(15), pp. 1383–1395.

Conte, M. P. *et al.* (2014) 'Adherent-invasive Escherichia coli (AIEC) in pediatric Crohn's disease patients: phenotypic and genetic pathogenic features', *BMC research notes*. Springer, 7(1), pp. 1–12.

Cooney, R. *et al.* (2010) 'NOD2 stimulation induces autophagy in dendritic cells influencing bacterial handling and antigen presentation', *Nature Medicine*, 16(1), pp. 90–97. doi: 10.1038/nm.2069.

Corthésy, B. (2010) 'Role of secretory immunoglobulin A and secretory component in the protection of mucosal surfaces', *Future microbiology*. Future Medicine, 5(5), pp. 817–829.

Cosnes, J. *et al.* (2011) 'Epidemiology and natural history of inflammatory bowel diseases', *Gastroenterology*. Elsevier Inc., 140(6), pp. 1785-1794.e4. doi: 10.1053/j.gastro.2011.01.055.

Couturier-Maillard, A. *et al.* (2013) 'NOD2-mediated dysbiosis predisposes mice to transmissible colitis and colorectal cancer', *The Journal of Clinical Investigation*. The American Society for Clinical Investigation, 123(2), pp. 700–711. doi: 10.1172/JCI62236.

Crohn, B. B., Ginzburg, L. and Oppenheimer, G. D. (1932) 'Regional ileitis: A pathologic and clinical entity', *Journal of the American Medical Association*, 99(16), pp. 1323–1329. doi: 10.1001/jama.1932.02740680019005.

Cronan, M. R. *et al.* (2016) 'Macrophage epithelial reprogramming underlies mycobacterial granuloma formation and promotes infection', *Immunity*. Elsevier, 45(4), pp. 861–876.

Cui, D. *et al.* (2013) 'Efficacy and safety of interferon-gamma-targeted therapy in Crohn's disease: a systematic review and meta-analysis of randomized controlled trials', *Clinics and research in hepatology and gastroenterology*. Elsevier, 37(5), pp. 507–513.

Cuthbert, A. P. *et al.* (2002) 'The contribution of NOD2 gene mutations to the risk and site of disease in inflammatory bowel disease', *Gastroenterology*, 122(4), pp. 867–874. doi: https://doi.org/10.1053/gast.2002.32415.

D'Haens, G. *et al.* (2018) 'Effect of PF-00547659 on central nervous system immune surveillance and circulating ß7+ T cells in Crohn's disease: report of the TOSCA study', *Journal of Crohn's and Colitis*. Oxford University Press UK, 12(2), pp. 188–196.

Dale, A. P. and Woodford, N. (2015) 'Extra-intestinal pathogenic Escherichia coli (ExPEC): disease, carriage and clones', *Journal of Infection*. Elsevier, 71(6), pp. 615–626.

Danese, S. *et al.* (2019) 'Randomised trial and open-label extension study of an anti-interleukin-6 antibody in Crohn's disease (ANDANTE I and II)', *Gut*. BMJ Publishing Group, 68(1), pp. 40–48.

Darfeuille-Michaud, A. *et al.* (1998) 'Presence of adherent Escherichia coli strains in ileal mucosa of patients with Crohn's disease', *Gastroenterology*, 115(6), pp. 1405–1413. doi: 10.1016/S0016-5085(98)70019-8.

Darfeuille-Michaud, A., Boudeau, J., Bulois, P., Neut, C., Glasser, A. L., *et al.* (2004) 'High prevalence of adherent-invasive Escherichia coli associated with ileal mucosa in Crohn's disease', *Gastroenterology*, 127(2), pp. 412–421. doi: 10.1053/j.gastro.2004.04.061.

Darfeuille-Michaud, A., Boudeau, J., Bulois, P., Neut, C., Glasser, A.-L., *et al.* (2004) 'High prevalence of adherent-invasive Escherichia coli associated with ileal mucosa in Crohn's disease', *Gastroenterology*, 127(2), pp. 412–421. doi: https://doi.org/10.1053/j.gastro.2004.04.061.

Davis, K. G. (2015) ‘Crohn’s disease of the foregut’, *Surgical Clinics*. Elsevier, 95(6), pp. 1183–1193.

DeFife, K. M. *et al*. (1997) ‘Interleukin-13 induces human monocyte/macrophage fusion and macrophage mannose receptor expression.’, *The Journal of Immunology*. Am Assoc Immnol, 158(7), pp. 3385–3390.

Delcroix, M. *et al*. (2018) ‘Flow-cytometric analysis of human monocyte subsets targeted by Mycobacterium bovis BCG before granuloma formation.’, *Pathogens and disease*, 76(8). doi: 10.1093/femspd/fty080.

Demarre, G. *et al*. (2019) ‘The Crohn’s disease-associated Escherichia coli strain LF82 relies on SOS and stringent responses to survive, multiply and tolerate antibiotics within macrophages’, *PLoS pathogens*. Public Library of Science San Francisco, CA USA, 15(11), p. e1008123.

Dickson, I. (2016) ‘Impaired bacterial clearance in IBD’, *Nature Reviews Gastroenterology & Hepatology*, 13(5), p. 251. doi: 10.1038/nrgastro.2016.55.

Dige, A. *et al*. (2014) ‘Soluble CD163, a Specific Macrophage Activation Marker, is Decreased by Anti-TNF-α Antibody Treatment in Active Inflammatory Bowel Disease’, *Scandinavian Journal of Immunology*. John Wiley & Sons, Ltd, 80(6), pp. 417–423. doi: https://doi.org/10.1111/sji.12222.

Dreux, N. *et al*. (2013) ‘Point mutations in FimH adhesin of Crohn’s disease-associated adherent-invasive Escherichia coli enhance intestinal inflammatory response’, *PLoS pathogens*. Public Library of Science San Francisco, USA, 9(1), p. e1003141.

Dunne, K. A. *et al*. (2013) ‘Increased S-Nitrosylation and Proteasomal Degradation of Caspase-3 during Infection Contribute to the Persistence of Adherent Invasive Escherichia coli (AIEC) in Immune Cells’, *PLoS ONE*, 8(7). doi: 10.1371/journal.pone.0068386.

Duque, A. G. *et al.* (2014) 'Leishmania Promastigotes Induce Cytokine Secretion in Macrophages through the Degradation of Synaptotagmin XI', *The Journal of Immunology*, 193(5), pp. 2363 LP – 2372. doi: 10.4049/jimmunol.1303043.

Eaves-Pyles, T. *et al.* (2008) 'Escherichia coli isolated from a Crohn's disease patient adheres, invades, and induces inflammatory responses in polarized intestinal epithelial cells', *International Journal of Medical Microbiology*, 298(5–6), pp. 397–409. doi: 10.1016/j.ijmm.2007.05.011.

Ebert, E. C. *et al.* (1984) 'T-cell abnormalities in inflammatory bowel disease are mediated by interleukin 2', *Clinical immunology and immunopathology*. Elsevier, 33(2), pp. 232–244.

Eissner, G. *et al.* (2000) 'Reverse signaling through transmembrane TNF confers resistance to lipopolysaccharide in human monocytes and macrophages', *The Journal of Immunology*. Am Assoc Immnol, 164(12), pp. 6193–6198.

Eissner, G., Kolch, W. and Scheurich, P. (2004) 'Ligands working as receptors: reverse signaling by members of the TNF superfamily enhance the plasticity of the immune system', *Cytokine & growth factor reviews*. Elsevier, 15(5), pp. 353–366.

Elenkov, I. J. *et al.* (2005) 'Cytokine dysregulation, inflammation and well-being', *Neuroimmunomodulation*. Karger Publishers, 12(5), pp. 255–269.

Elliott, T. R. *et al.* (2015) 'Defective macrophage handling of Escherichia coli in Crohn's disease', *Journal of Gastroenterology and Hepatology*. John Wiley & Sons, Ltd, 30(8), pp. 1265–1274. doi: https://doi.org/10.1111/jgh.12955.

Elson, C. O. *et al.* (2005) 'Experimental models of inflammatory bowel disease reveal innate, adaptive, and regulatory mechanisms of host dialogue with the microbiota', *Immunological reviews*. Wiley Online Library, 206(1), pp. 260–276.

Elson, C. O. *et al.* (2007) 'Monoclonal anti–interleukin 23 reverses active colitis in a T cell–mediated model in mice', *Gastroenterology*. Elsevier, 132(7), pp. 2359–2370.

Elzer, P. H. *et al.* (1996) 'The HtrA stress response protease contributes to resistance of Brucella abortus to killing by murine phagocytes', *Infection and Immunity*. American Society for Microbiology, 64(11), pp. 4838–4841. doi: 10.1128/iai.64.11.4838-4841.1996.

Eriksson, S. *et al.* (2003) 'Unravelling the biology of macrophage infection by gene expression profiling of intracellular Salmonella enterica', *Molecular Microbiology*. John Wiley & Sons, Ltd, 47(1), pp. 103–118. doi: https://doi.org/10.1046/j.1365-2958.2003.03313.x.

Fava, F. and Danese, S. (2011) 'Intestinal microbiota in inflammatory bowel disease: friend of foe?', *World journal of gastroenterology*, 17(5), pp. 557–566. doi: 10.3748/wjg.v17.i5.557.

Feagan, B. G. *et al.* (2014) 'Methotrexate in combination with infliximab is no more effective than infliximab alone in patients with Crohn's disease', *Gastroenterology*. Elsevier, 146(3), pp. 681–688.

Ferrante, M. *et al.* (2007) 'New serological markers in inflammatory bowel disease are associated with complicated disease behaviour', *Gut*. BMJ Publishing Group, 56(10), pp. 1394–1403.

Fleige, S. and Pfaffl, M. W. (2006) 'RNA integrity and the effect on the real-time qRT-PCR performance', *Molecular Aspects of Medicine*, 27(2), pp. 126–139. doi: https://doi.org/10.1016/j.mam.2005.12.003.

Fonseca, K. L. *et al.* (2017) 'Experimental study of tuberculosis: From animal models to complex cell systems and organoids', *PLoS Pathogens*. Public Library of Science San Francisco, CA USA, 13(8), p. e1006421.

Fournier, B. M. and Parkos, C. A. (2012) 'The role of neutrophils during intestinal inflammation', *Mucosal immunology*. Nature Publishing Group, 5(4), pp. 354–366.

Franze, E. *et al.* (2013) 'Lesional accumulation of CD163-expressing cells in the gut of patients with inflammatory bowel disease', *PloS one*. Public Library of Science San Francisco, USA, 8(7), p. e69839.

Fuchs, T. M. *et al.* (2012) 'Metabolic adaptation of human pathogenic and related nonpathogenic bacteria to extra-and intracellular habitats', *FEMS microbiology reviews*. Blackwell Publishing Ltd Oxford, UK, 36(2), pp. 435–462.

Fujimoto, T. *et al.* (2013) 'Decreased abundance of Faecalibacterium prausnitzii in the gut microbiota of Crohn's disease', *Journal of Gastroenterology and Hepatology*. John Wiley & Sons, Ltd, 28(4), pp. 613–619. doi: https://doi.org/10.1111/jgh.12073.

Fujimura, Y., Kamoi, R. and Iida, M. (1996) 'Pathogenesis of aphthoid ulcers in Crohn's disease: correlative findings by magnifying colonoscopy, electron microscopy, and immunohistochemistry.', *Gut*. BMJ Publishing Group, 38(5), pp. 724–732.

Fujino, S. *et al.* (2003) 'Increased expression of interleukin 17 in inflammatory bowel disease', *Gut*. BMJ Publishing Group, 52(1), pp. 65–70.

Fujita, N. *et al.* (2008) 'The Atg16L Complex Specifies the Site of LC3 Lipidation for Membrane Biogenesis in Autophagy', *Molecular Biology of the Cell*. American Society for Cell Biology (mboc), 19(5), pp. 2092–2100. doi: 10.1091/mbc.e07-12-1257.

Fuss, I. J. *et al.* (1996) 'Disparate CD4+ lamina propria (LP) lymphokine secretion profiles in inflammatory bowel disease. Crohn's disease LP cells manifest increased secretion of IFN-gamma, whereas ulcerative colitis LP cells manifest increased secretion of IL-5.', *The Journal of Immunology*. Am Assoc Immnol, 157(3), pp. 1261–1270.

Fuss, I. J. *et al.* (2004) 'Nonclassical CD1d-restricted NK T cells that produce IL-13 characterize an atypical Th2 response in ulcerative colitis', *The Journal of clinical investigation*. Am Soc Clin Investig, 113(10), pp. 1490–1497.

Gallo, R. L. and Hooper, L. V (2012) ‘Epithelial antimicrobial defence of the skin and intestine’, *Nature Reviews Immunology*, 12(7), pp. 503–516. doi: 10.1038/nri3228.

Gao, C. *et al.* (2015) ‘FAK/PYK2 promotes the Wnt/β-catenin pathway and intestinal tumorigenesis by phosphorylating GSK3β’, *eLife*. Edited by J. A. Cooper. eLife Sciences Publications, Ltd, 4, p. e10072. doi: 10.7554/eLife.10072.

Gayathri, R. *et al.* (2020) ‘Efficacy of Saccharomyces cerevisiae CNCM I-3856 as an add-on therapy for irritable bowel syndrome’, *International Journal of Colorectal Disease*, 35(1), pp. 139–145. doi: 10.1007/s00384-019-03462-4.

Gearry, R. B. *et al.* (2006) ‘High incidence of Crohn’s disease in Canterbury, New Zealand: Results of an epidemiologic study’, *Inflammatory Bowel Diseases*, 12(10), pp. 936–943. doi: 10.1097/01.mib.0000231572.88806.b9.

Gibold, L. *et al.* (2016) ‘The Vat-AIEC protease promotes crossing of the intestinal mucus layer by Crohn’s disease-associated Escherichia coli’, *Cellular Microbiology*. Wiley Online Library, 18(5), pp. 617–631.

Giri, P. K. *et al.* (2010) ‘Proteomic analysis identifies highly antigenic proteins in exosomes from M. tuberculosis-infected and culture filtrate protein-treated macrophages’, *Proteomics*. Wiley Online Library, 10(17), pp. 3190–3202.

Giri, P. K. and Schorey, J. S. (2008) ‘Exosomes derived from M. Bovis BCG infected macrophages activate antigen-specific CD4+ and CD8+ T cells in vitro and in vivo’, *PloS one*. Public Library of Science San Francisco, USA, 3(6), p. e2461.

Glass, C. K. *et al.* (2010) ‘Mechanisms underlying inflammation in neurodegeneration’, *Cell*. Elsevier, 140(6), pp. 918–934.

Glasser, A. L. *et al.* (2001) ‘Adherent invasive Escherichia coli strains from patients with Crohn’s disease survive and replicate within macrophages without

inducing host cell death', *Infection and Immunity*, 69(9), pp. 5529–5537. doi: 10.1128/IAI.69.9.5529-5537.2001.

Glick, D., Barth, S. and Macleod, K. F. (2010) 'Autophagy: cellular and molecular mechanisms', *The Journal of Pathology*. John Wiley & Sons, Ltd, 221(1), pp. 3–12. doi: https://doi.org/10.1002/path.2697.

Greening, D. W. *et al.* (2015) 'Exosomes and their roles in immune regulation and cancer', in *Seminars in cell & developmental biology*. Elsevier, pp. 72–81.

Greuter, T. *et al.* (2021) 'Emerging treatment options for extraintestinal manifestations in IBD', *Gut*, 70(4), pp. 796 LP – 802. doi: 10.1136/gutjnl-2020-322129.

Griffith, J. W., Sokol, C. L. and Luster, A. D. (2014) 'Chemokines and chemokine receptors: positioning cells for host defense and immunity', *Annu rev immunol*, 32(1), pp. 659–702.

Grimm, M. C. and Doe, W. F. (1996) 'Chemokines in Inflammatory Bowel Disease Mucosa: Expression of RANTES, Macrophage Inflammatory Protein (MIP)-1α, MIP-1ß, and γ-Interferon-Inducible Protein-10 by Macrophages, Lymphocytes, Endothelial Cells, and Granulomas', *Inflammatory Bowel Diseases*, 2(2), pp. 88–96. doi: 10.1097/00054725-199606000-00004.

Grip, O., Janciauskiene, S. and Lindgren, S. (2004) 'Circulating monocytes and plasma inflammatory biomarkers in active Crohn's disease: elevated oxidized low-density lipoprotein and the anti-inflammatory effect of atorvastatin', *Inflammatory Bowel Diseases*. Oxford University Press Oxford, UK, 10(3), pp. 193–200.

Gulan, G. *et al.* (2010) 'Salmonella typhimurium osteomyelitis of the femur in patient with Crohn's disease', *Wiener klinische Wochenschrift*. Springer, 122(13), pp. 437–440.

Gullberg, E. and Söderholm, J. D. (2006) 'Peyer's patches and M cells as potential sites of the inflammatory onset in Crohn's disease', *Annals of the New York Academy of Sciences*. Wiley Online Library, 1072(1), pp. 218–232.

Günther, C. *et al.* (2011) 'Caspase-8 regulates TNF-α-induced epithelial necroptosis and terminal ileitis', *Nature*. Nature Publishing Group, 477(7364), pp. 335–339.

Hanauer SB *et al.* (2002) 'Manteniance infliximab in Crohn's disease: The ACCENT I randomised trial', *The Lancet*, 359, pp. 1541–1549.

Hansen, R. *et al.* (2013) 'The Microaerophilic Microbiota of De-Novo Paediatric Inflammatory Bowel Disease: The BISCUIT Study', *PLOS ONE*. Public Library of Science, 8(3), p. e58825. Available at: https://doi.org/10.1371/journal.pone.0058825.

Haridas, V. *et al.* (2017) 'Imaging flow cytometry analysis of intracellular pathogens', *Methods*, 112, pp. 91–104. doi: 10.1016/j.ymeth.2016.09.007.

Hart, A. L. *et al.* (2005) 'Characteristics of intestinal dendritic cells in inflammatory bowel diseases', *Gastroenterology*. Elsevier, 129(1), pp. 50–65.

Hase, K. *et al.* (2009) 'Uptake through glycoprotein 2 of FimH+ bacteria by M cells initiates mucosal immune response', *Nature*. Nature Publishing Group, 462(7270), pp. 226–230.

Hausmann, M. *et al.* (2002) 'Toll-like receptors 2 and 4 are up-regulated during intestinal inflammation', *Gastroenterology*. Elsevier, 122(7), pp. 1987–2000.

Hayden, M. S. and Ghosh, S. (2012) 'NF-κB, the first quarter-century: remarkable progress and outstanding questions.', *Genes & development*, 26(3), pp. 203–234. doi: 10.1101/gad.183434.111.

He, J. *et al.* (2019) 'Fbxw7 increases CCL2/7 in CX3CR1hi macrophages to promote intestinal inflammation', *The Journal of Clinical Investigation*. The

American Society for Clinical Investigation, 129(9), pp. 3877–3893. doi: 10.1172/JCI123374.

He, Y. *et al.* (2021) 'Milk Exosomes Transfer Oligosaccharides into Macrophages to Modulate Immunity and Attenuate Adherent-Invasive E. coli (AIEC) Infection', *Nutrients*. MDPI, 13(9), p. 3198.

Heddle, R. J., La Brooy, J. T. and Shearman, D. J. (1982) 'Escherichia coli antibody-secreting cells in the human intestine.', *Clinical and Experimental Immunology*. Oxford University Press, 48(2), p. 469.

Helaine, S. *et al.* (2010) 'Dynamics of intracellular bacterial replication at the single cell level', *Proceedings of the National Academy of Sciences of the United States of America*, 107(8), pp. 3746–3751. doi: 10.1073/pnas.1000041107.

Helming, L. and Gordon, S. (2009) 'Molecular mediators of macrophage fusion', *Trends in cell biology*. Elsevier, 19(10), pp. 514–522.

Henderson, I. R. *et al.* (2004) 'Type V protein secretion pathway: the autotransporter story', *Microbiology and molecular biology reviews*. Am Soc Microbiol, 68(4), pp. 692–744.

Heras, B. *et al.* (2009) 'DSB proteins and bacterial pathogenicity', *Nature Reviews Microbiology*. Nature Publishing Group, 7(3), pp. 215–225.

Hibi, T. *et al.* (1990) 'In vitro anticolon antibody production by mucosal or peripheral blood lymphocytes from patients with ulcerative colitis.', *Gut*. BMJ Publishing Group, 31(12), pp. 1371–1376.

Higuchi, L. M. *et al.* (2012) 'A prospective study of cigarette smoking and the risk of inflammatory bowel disease in women', *American Journal of Gastroenterology*, 107(9), pp. 1399–1406. doi: 10.1038/ajg.2012.196.

Hollander, E. *et al.* (2000) 'PHARMACOTHERAPY FOR OBSESSIVE-COMPULSIVE DISORDER', *Psychiatric Clinics of North America*, 23(3), pp. 643–656. doi: https://doi.org/10.1016/S0193-953X(05)70186-6.

Holtmann, M. H. *et al.* (2002) 'Tumor necrosis factor-receptor 2 is up-regulated on lamina propria T cells in Crohn's disease and promotes experimental colitis in vivo', *European journal of immunology*. Wiley Online Library, 32(11), pp. 3142–3151.

Homer, C. R. *et al.* (2010) 'ATG16L1 and NOD2 Interact in an Autophagy-Dependent Antibacterial Pathway Implicated in Crohn's Disease Pathogenesis', *Gastroenterology*, 139(5), pp. 1630-1641.e2. doi: https://doi.org/10.1053/j.gastro.2010.07.006.

Hooper, K. M. *et al.* (2019) 'Interactions Between Autophagy and the Unfolded Protein Response: Implications for Inflammatory Bowel Disease', *Inflammatory Bowel Diseases*, 25(4), pp. 661–671. doi: 10.1093/ibd/izy380.

Hooper, L. V, Littman, D. R. and Macpherson, A. J. (2012) 'Interactions Between the Microbiota and the Immune System', *Science*. American Association for the Advancement of Science, 336(6086), pp. 1268–1273. doi: 10.1126/science.1223490.

Huang, C. *et al.* (2021) 'Tumor cell-derived SPON2 promotes M2-polarized tumor-associated macrophage infiltration and cancer progression by activating PYK2 in CRC', *Journal of Experimental & Clinical Cancer Research*, 40(1), p. 304. doi: 10.1186/s13046-021-02108-0.

Huang, H. *et al.* (2017) 'Fine-mapping inflammatory bowel disease loci to single-variant resolution', *Nature*. Nature Publishing Group, 547(7662), pp. 173–178. doi: 10.1038/nature22969.

Hudson, K. J., Bliska, J. B. and Bouton, A. H. (2005) 'Distinct mechanisms of integrin binding by Yersinia pseudotuberculosis adhesins detssermine the phagocytic response of host macrophages', *Cellular Microbiology*, 7(10), pp. 1474–1489. doi: 10.1111/j.1462-5822.2005.00571.x.

Hugot, J.-P. *et al.* (2001) 'Association of NOD2 leucine-rich repeat variants with susceptibility to Crohn's disease', *Nature*, 411(6837), pp. 599–603. doi: 10.1038/35079107.

Hyams, J. *et al.* (2006) 'The Natural History of Corticosteroid Therapy for Ulcerative Colitis in Children', *Clinical Gastroenterology and Hepatology*, 4(9), pp. 1118–1123. doi: https://doi.org/10.1016/j.cgh.2006.04.008.

Italiani, P. and Boraschi, D. (2014) 'From monocytes to M1/M2 macrophages: phenotypical vs. functional differentiation', *Frontiers in immunology*. Frontiers Media SA, 5, p. 514.

Ito, H. *et al.* (2004) 'A pilot randomized trial of a human anti-interleukin-6 receptor monoclonal antibody in active Crohn's disease', *Gastroenterology*. Elsevier, 126(4), pp. 989–996.

Izcue, A. *et al.* (2008) 'Interleukin-23 restrains regulatory T cell activity to drive T cell-dependent colitis', *Immunity*. Elsevier, 28(4), pp. 559–570.

Jandhyala, S. M. *et al.* (2015) 'Role of the normal gut microbiota.', *World journal of gastroenterology*, 21(29), pp. 8787–8803. doi: 10.3748/wjg.v21.i29.8787.

Jann, K. and Jann, B. (1992) 'Capsules of Escherichia coli, expression and biological significance', *Canadian journal of microbiology*. NRC Research Press Ottawa, Canada, 38(7), pp. 705–710.

Jarry, A. *et al.* (2015) 'Subversion of human intestinal mucosa innate immunity by a Crohn's disease-associated E. coli', *Mucosal immunology*. Nature Publishing Group, 8(3), pp. 572–581.

Joossens, M. *et al.* (2011) 'Dysbiosis of the faecal microbiota in patients with Crohn's disease and their unaffected relatives', *Gut*, 60(5), pp. 631 LP – 637. doi: 10.1136/gut.2010.223263.

Jostins, L. *et al.* (2012) 'Host–microbe interactions have shaped the genetic architecture of inflammatory bowel disease', *Nature*. Nature Publishing Group, 491(7422), pp. 119–124.

Kagnoff, M. F. (2014) ‘The intestinal epithelium is an integral component of a communications network’, *The Journal of clinical investigation*. Am Soc Clin Investig, 124(7), pp. 2841–2843.

Kai, Y. *et al.* (2005) ‘Colitis in mice lacking the common cytokine receptor γ chain is mediated by IL-6-producing CD4+ T cells’, *Gastroenterology*. Elsevier, 128(4), pp. 922–934.

Kamada, N. *et al.* (2005) ‘Abnormally differentiated subsets of intestinal macrophage play a key role in Th1-dominant chronic colitis through excess production of IL-12 and IL-23 in response to bacteria’, *The Journal of Immunology*. Am Assoc Immnol, 175(10), pp. 6900–6908.

Kamada, N. *et al.* (2010) ‘TL1A produced by lamina propria macrophages induces Th1 and Th17 immune responses in cooperation with IL-23 in patients with Crohn’s disease’, *Inflammatory bowel diseases*. Oxford University Press Oxford, UK, 16(4), pp. 568–575.

Kanai, T. *et al.* (2001) ‘Macrophage-derived IL-18–mediated intestinal inflammation in the murine model of Crohn’s disease’, *Gastroenterology*. Elsevier, 121(4), pp. 875–888.

Katakura, K. *et al.* (2005) ‘Toll-like receptor 9–induced type I IFN protects mice from experimental colitis’, *The Journal of clinical investigation*. Am Soc Clin Investig, 115(3), pp. 695–702.

Kathania, M. *et al.* (2015) ‘Ndfip1 Regulates Itch Ligase Activity and Airway Inflammation via UbcH7’, *The Journal of Immunology*, 194(5), pp. 2160 LP – 2167. doi: 10.4049/jimmunol.1402742.

Kayama, H. and Takeda, K. (2016) ‘Functions of innate immune cells and commensal bacteria in gut homeostasis’, *The Journal of Biochemistry*. Oxford University Press, 159(2), pp. 141–149.

Khalili, H. *et al.* (2013) 'Oral contraceptives, reproductive factors and risk of inflammatory bowel disease', *Gut*, 62(8), pp. 1153–1159. doi: 10.1136/gutjnl-2012-302362.

Khalili, H. (2016) 'Risk of Inflammatory Bowel Disease with Oral Contraceptives and Menopausal Hormone Therapy: Current Evidence and Future Directions', *Drug Safety*, 39(3), pp. 193–197. doi: 10.1007/s40264-015-0372-y.

Khalili, H., Talasaz, A. H. and Salarifar, M. (2012) 'Serum vitamin D concentration status and its correlation with early biomarkers of remodeling following acute myocardial infarction', *Clinical Research in Cardiology*, 101(5), pp. 321–327. doi: 10.1007/s00392-011-0394-0.

Khan, N. *et al.* (2018) 'Overall and Comparative Risk of Herpes Zoster With Pharmacotherapy for Inflammatory Bowel Diseases: A Nationwide Cohort Study', *Clinical Gastroenterology and Hepatology*, 16(12), pp. 1919-1927.e3. doi: https://doi.org/10.1016/j.cgh.2017.12.052.

Khor, B., Gardet, A. and Xavier, R. J. (2011) 'Genetics and pathogenesis of inflammatory bowel disease', *Nature*, 474(7351), pp. 307–317. doi: 10.1038/nature10209.

Kim, D. *et al.* (2019) 'Graph-based genome alignment and genotyping with HISAT2 and HISAT-genotype', *Nature Biotechnology*, 37(8), pp. 907–915. doi: 10.1038/s41587-019-0201-4.

King, D. *et al.* (2020) 'Changing patterns in the epidemiology and outcomes of inflammatory bowel disease in the United Kingdom: 2000-2018', *Alimentary Pharmacology and Therapeutics*, 51(10), pp. 922–934. doi: 10.1111/apt.15701.

Kiss, E. A. *et al.* (2011) 'Natural aryl hydrocarbon receptor ligands control organogenesis of intestinal lymphoid follicles', *Science*, 334(6062), pp. 1561–1565. doi: 10.1126/science.1214914.

Knodler, L. A. and Celli, J. (2011) 'Eating the strangers within: host control of intracellular bacteria via xenophagy', *Cellular Microbiology*. John Wiley & Sons,

Ltd, 13(9), pp. 1319–1327. doi: https://doi.org/10.1111/j.1462-5822.2011.01632.x.

Kobayashi, K. S. *et al.* (2005) 'Nod2-Dependent Regulation of Innate and Adaptive Immunity in the Intestinal Tract', *Science*. American Association for the Advancement of Science, 307(5710), pp. 731–734. doi: 10.1126/science.1104911.

Kodama, M. *et al.* (2020) 'Epithelioid Cell Granulomas in Crohn's Disease Are Differentially Associated With Blood Vessels and Lymphatic Vessels: A Sequential Double Immunostaining Study', *Journal of Histochemistry and Cytochemistry*, 68(8), pp. 553–560. doi: 10.1369/0022155420939535.

Kohno, T. *et al.* (2008) 'Protein-tyrosine kinase CAKß/PYK2 is activated by binding Ca 2+/calmodulin to FERM F2 α2 helix and thus forming its dimer', *Biochemical Journal*, 410(3), pp. 513–523. doi: 10.1042/BJ20070665.

Kole, A. *et al.* (2013) 'Type I IFNs regulate effector and regulatory T cell accumulation and anti-inflammatory cytokine production during T cell–mediated colitis', *The Journal of Immunology*. Am Assoc Immnol, 191(5), pp. 2771–2779.

Kostic, A. D., Xavier, R. J. and Gevers, D. (2014) 'The Microbiome in Inflammatory Bowel Disease: Current Status and the Future Ahead', *Gastroenterology*, 146(6), pp. 1489–1499. doi: https://doi.org/10.1053/j.gastro.2014.02.009.

Kronman, M. P. *et al.* (2012) 'Antibiotic Exposure and IBD Development Among Children: A Population-Based Cohort Study', *Pediatrics*, 130(4), pp. e794–e803. doi: 10.1542/peds.2011-3886.

Kullberg, M. C. *et al.* (2006) 'IL-23 plays a key role in Helicobacter hepaticus–induced T cell–dependent colitis', *The Journal of experimental medicine*. Rockefeller University Press, 203(11), pp. 2485–2494.

Kumar, S. *et al.* (2020) 'Mammalian Atg8 proteins and the autophagy factor IRGM control mTOR and TFEB at a regulatory node critical for responses to pathogens',

Nature Cell Biology. Springer US, 22(8), pp. 973–985. doi: 10.1038/s41556-020-0549-1.

L., P. L. *et al.* (2001) 'HtrA Homologue of Legionella pneumophila: an Indispensable Element for Intracellular Infection of Mammalian but Not Protozoan Cells', *Infection and Immunity*. American Society for Microbiology, 69(4), pp. 2569–2579. doi: 10.1128/IAI.69.4.2569-2579.2001.

Lahiri, A. and Abraham, C. (2014) 'Activation of Pattern Recognition Receptors Up-Regulates Metallothioneins, Thereby Increasing Intracellular Accumulation of Zinc, Autophagy, and Bacterial Clearance by Macrophages', *Gastroenterology*, 147(4), pp. 835–846. doi: https://doi.org/10.1053/j.gastro.2014.06.024.

Laing, K. J. and Secombes, C. J. (2004) 'Chemokines', *Developmental & Comparative Immunology*, 28(5), pp. 443–460. doi: https://doi.org/10.1016/j.dci.2003.09.006.

Lapaquette, P. *et al.* (2010) 'Crohn's disease-associated adherent-invasive E. coli are selectively favoured by impaired autophagy to replicate intracellularly', *Cellular Microbiology*. John Wiley & Sons, Ltd, 12(1), pp. 99–113. doi: https://doi.org/10.1111/j.1462-5822.2009.01381.x.

Lapaquette, P., Bringer, M.-A. and Darfeuille-Michaud, A. (2012) 'Defects in autophagy favour adherent-invasive Escherichia coli persistence within macrophages leading to increased pro-inflammatory response', *Cellular Microbiology*. John Wiley & Sons, Ltd, 14(6), pp. 791–807. doi: https://doi.org/10.1111/j.1462-5822.2012.01768.x.

Lapaquette, P., Bringer, M. A. and Darfeuille-Michaud, A. (2012) 'Defects in autophagy favour adherent-invasive Escherichia coli persistence within macrophages leading to increased pro-inflammatory response', *Cellular Microbiology*, 14(6), pp. 791–807. doi: 10.1111/j.1462-5822.2012.01768.x.

Lapaquette, P., Nguyen, H. T. T. and Faure, M. (2017) '[Regulation of immunity and inflammation by autophagy: « All is well, all is fine, all goes as well as possible»]', *Medecine sciences : M/S*. Univ. Bourgogne Franche-Comté, AgroSup

Dijon, PAM UMR A 02.102, F-21000 Dijon, France., 33(3), pp. 305–311. doi: 10.1051/medsci/20173303018.

Larabi, A., Barnich, N. and Nguyen, H. T. T. (2020a) ‘Emerging role of exosomes in diagnosis and treatment of infectious and inflammatory bowel diseases’, *Cells*. MDPI, 9(5), p. 1111.

Larabi, A., Barnich, N. and Nguyen, H. T. T. (2020b) ‘New insights into the interplay between autophagy, gut microbiota and inflammatory responses in IBD’, *Autophagy*. Taylor & Francis, 16(1), pp. 38–51. doi: 10.1080/15548627.2019.1635384.

Lee, J. M. and Lee, K.-M. (2016) ‘Endoscopic Diagnosis and Differentiation of Inflammatory Bowel Disease.’, *Clinical endoscopy*, 49(4), pp. 370–375. doi: 10.5946/ce.2016.090.

Lei, H. *et al.* (2022) ‘Loss of PTPN2 Activity Alters Iron Handling Protein Expression in IBD Patients and Causes Iron Deficiency in Mice’, *The FASEB Journal*. John Wiley & Sons, Ltd, 36(S1). doi: https://doi.org/10.1096/fasebj.2022.36.S1.R3208.

Levin, A. D. *et al.* (2016) ‘Autophagy contributes to the induction of anti-TNF induced macrophages’, *Journal of Crohn’s and Colitis*, 10(3), pp. 323–329. doi: 10.1093/ecco-jcc/jjv174.

Levine, A. *et al.* (2011) ‘Pediatric modification of the Montreal classification for inflammatory bowel disease: The Paris classification’, *Inflammatory Bowel Diseases*, 17(6), pp. 1314–1321. doi: 10.1002/ibd.21493.

Lewis, L. E. *et al.* (2012) ‘Candida albicans infection inhibits macrophage cell division and proliferation’, *Fungal Genetics and Biology*, 49(9), pp. 679–680. doi: https://doi.org/10.1016/j.fgb.2012.05.007.

Li, J. *et al.* (2004) ‘Regulation of IL-8 and IL-1ß expression in Crohn’s disease associated NOD2/CARD15 mutations’, *Human Molecular Genetics*, 13(16), pp. 1715–1725. doi: 10.1093/hmg/ddh182.

Liao, Y. *et al.* (2021) 'Advanced oxidation protein products impair autophagic flux in macrophage by inducing lysosomal dysfunction via activation of PI3K-Akt-mTOR pathway in Crohn's disease', *Free Radical Biology and Medicine*, 172, pp. 33–47. doi: https://doi.org/10.1016/j.freeradbiomed.2021.05.018.

Lindsay, J. O. *et al.* (2006) 'Clinical, microbiological, and immunological effects of fructo-oligosaccharide in patients with Crohn's disease', *Gut*. BMJ Publishing Group, 55(3), pp. 348–355.

Linton, M. F., Moslehi, J. J. and Babaev, V. R. (2019) 'Akt Signaling in Macrophage Polarization, Survival, and Atherosclerosis', *International Journal of Molecular Sciences*. doi: 10.3390/ijms20112703.

Lissner, D. *et al.* (2015) 'Monocyte and M1 macrophage-induced barrier defect contributes to chronic intestinal inflammation in IBD', *Inflammatory Bowel Diseases*, 21(6), pp. 1297–1305. doi: 10.1097/MIB.0000000000000384.

Liu, Jimmy Z. *et al.* (2015) 'Association analyses identify 38 susceptibility loci for inflammatory bowel disease and highlight shared genetic risk across populations', *Nature Genetics*, 47(9), pp. 979–986. doi: 10.1038/ng.3359.

Liu, Jimmy Z *et al.* (2015) 'Association analyses identify 38 susceptibility loci for inflammatory bowel disease and highlight shared genetic risk across populations', *Nature Genetics*, 47(9), pp. 979–986. doi: 10.1038/ng.3359.

Liu, S., Chen, L. and Xu, Y. (2018) 'Significance of PYK2 level as a prognosis predictor in patients with colon adenocarcinoma after surgical resection', *OncoTargets and Therapy*, 11, pp. 7625–7634. doi: 10.2147/OTT.S169531.

Liu, Y. *et al.* (1995) 'Immunocytochemical evidence of Listeria, Escherichia coil, and Streptococcus antigens in Crohn's disease', *Gastroenterology*, 108(5), pp. 1396–1404. doi: https://doi.org/10.1016/0016-5085(95)90687-8.

Liu, Z.-J. *et al.* (2009) 'Potential role of Th17 cells in the pathogenesis of inflammatory bowel disease', *World journal of gastroenterology: WJG*. Baishideng Publishing Group Inc, 15(46), p. 5784.

Livak, K. J. and Schmittgen, T. D. (2001) 'Analysis of relative gene expression data using real-time quantitative PCR and the 2− ΔΔCT method', *methods*. Elsevier, 25(4), pp. 402–408.

Lo, S. Z. Y., Steer, J. H. and Joyce, D. A. (2011) 'TNF-α renders macrophages resistant to a range of cancer chemotherapeutic agents through NF-κB-mediated antagonism of apoptosis signalling', *Cancer letters*. Elsevier, 307(1), pp. 80–92.

Loh, G. and Blaut, M. (2012) 'Role of commensal gut bacteria in inflammatory bowel diseases', *Gut Microbes*. Taylor & Francis, 3(6), pp. 544–555. doi: 10.4161/gmic.22156.

Looijer-van Langen, M. *et al*. (2011) 'Estrogen receptor-β signaling modulates epithelial barrier function', *American Journal of Physiology-Gastrointestinal and Liver Physiology*. American Physiological Society, 300(4), pp. G621–G626. doi: 10.1152/ajpgi.00274.2010.

Lügering, A. *et al*. (2001) 'Infliximab induces apoptosis in monocytes from patients with chronic active Crohn's disease by using a caspase-dependent pathway', *Gastroenterology*, 121(5), pp. 1145–1157. doi: https://doi.org/10.1053/gast.2001.28702.

Luk, H. H. *et al*. (2002) 'Delineation of the protective action of zinc sulfate on ulcerative colitis in rats', *European Journal of Pharmacology*, 443(1), pp. 197–204. doi: https://doi.org/10.1016/S0014-2999(02)01592-3.

MacDonald, T. T. *et al*. (1990) 'Tumour necrosis factor-alpha and interferon-gamma production measured at the single cell level in normal and inflamed human intestine', *Clinical & Experimental Immunology*. Oxford University Press, 81(2), pp. 301–305.

Mahida, Y. R. (2000) 'The key role of macrophages in the immunopathogenesis of inflammatory bowel disease', *Inflammatory bowel diseases*. Oxford University Press Oxford, UK, 6(1), pp. 21–33.

Mallik, S. and Zhao, Z. (2018) 'Identification of gene signatures from RNA-seq data using Pareto-optimal cluster algorithm', *BMC Systems Biology*, 12(8), p. 126. doi: 10.1186/s12918-018-0650-2.

Mannon, P. J. *et al.* (2004) 'Anti–interleukin-12 antibody for active Crohn's disease', *New England Journal of Medicine*. Mass Medical Soc, 351(20), pp. 2069–2079.

Marinković, G. *et al.* (2014) 'Inhibition of GTPase Rac1 in endothelium by 6-mercaptopurine results in immunosuppression in nonimmune cells: new target for an old drug', *The Journal of Immunology*. Am Assoc Immnol, 192(9), pp. 4370–4378.

Markowitz, J. *et al.* (2006) 'Corticosteroid Therapy in the Age of Infliximab: Acute and 1-Year Outcomes in Newly Diagnosed Children With Crohn's Disease', *Clinical Gastroenterology and Hepatology*, 4(9), pp. 1124–1129. doi: https://doi.org/10.1016/j.cgh.2006.05.011.

Marshall, J. D. (1995) *The language of interpretation: Patterns of discourse in discussions of literature*. ERIC.

Martinez-Medina, M. *et al.* (2009) 'Biofilm formation as a novel phenotypic feature of adherent-invasive Escherichia coli (AIEC)', *BMC microbiology*. BioMed Central, 9(1), pp. 1–16.

Martínez-Montiel, M. P. *et al.* (2015) 'Pharmacologic therapy for inflammatory bowel disease refractory to steroids.', *Clinical and experimental gastroenterology*, 8, pp. 257–269. doi: 10.2147/CEG.S58152.

Maurice, M. M. *et al.* (1999) 'Treatment with monoclonal anti–tumor necrosis factor α antibody results in an accumulation of Th1 CD4+ T cells in the peripheral blood of patients with rheumatoid arthritis', *Arthritis & Rheumatism*. John Wiley & Sons, Ltd, 42(10), pp. 2166–2173. doi: https://doi.org/10.1002/1529-0131(199910)42:10<2166::AID-ANR18>3.0.CO;2-K.

Maynard, C. L. and Weaver, C. T. (2009) 'Intestinal effector T cells in health and disease', *Immunity*. Elsevier, 31(3), pp. 389–400.

Mazzarella, G. *et al*. (2017) 'Pathogenic role of associated adherent-invasive Escherichia coli in Crohn's disease', *Journal of cellular physiology*. Wiley Online Library, 232(10), pp. 2860–2868.

McCarroll, S. A. *et al*. (2008) 'Deletion polymorphism upstream of IRGM associated with altered IRGM expression and Crohn's disease', *Nature Genetics*, 40(9), pp. 1107–1112. doi: 10.1038/ng.215.

McDaniel, D. K. *et al*. (2016) 'Emerging Roles for Noncanonical NF-κB Signaling in the Modulation of Inflammatory Bowel Disease Pathobiology', *Inflammatory Bowel Diseases*, 22(9), pp. 2265–2279. doi: 10.1097/MIB.0000000000000858.

McDonnell, M. *et al*. (2011) 'Systemic Toll-like receptor ligands modify B-cell responses in human inflammatory bowel disease', *Inflammatory bowel diseases*. Oxford University Press Oxford, UK, 17(1), pp. 298–307.

McGovern, D. P. B. *et al*. (2010) 'Genome-wide association identifies multiple ulcerative colitis susceptibility loci', *Nature Genetics*, 42(4), pp. 332–337. doi: 10.1038/ng.549.

McKay, L. I. and Cidlowski, J. A. (1998) 'Cross-Talk between Nuclear Factor-κB and the Steroid Hormone Receptors: Mechanisms of Mutual Antagonism', *Molecular Endocrinology*, 12(1), pp. 45–56. doi: 10.1210/mend.12.1.0044.

McNally, A. K. and Anderson, J. M. (2015) 'Phenotypic expression in human monocyte-derived interleukin-4-induced foreign body giant cells and macrophages in vitro: Dependence on material surface properties', *Journal of Biomedical Materials Research Part A*. Wiley Online Library, 103(4), pp. 1380–1390.

Meconi, S. *et al*. (2007) 'Adherent-invasive Escherichia coli isolated from Crohn's disease patients induce granulomas in vitro', *Cellular Microbiology*, 9(5), pp. 1252–1261. doi: 10.1111/j.1462-5822.2006.00868.x.

Meijer, M. J. *et al.* (2007) 'Effect of the anti-tumor necrosis factor-α antibody infliximab on the ex vivo mucosal matrix metalloproteinase–proteolytic phenotype in inflammatory bowel disease', *Inflammatory bowel diseases*. Oxford University Press Oxford, UK, 13(2), pp. 200–210.

Michaudel, C. and Sokol, H. (2020) 'The Gut Microbiota at the Service of Immunometabolism', *Cell Metabolism*, 32(4), pp. 514–523. doi: 10.1016/j.cmet.2020.09.004.

Milajerdi, A. *et al.* (2021) 'Association of Dietary Fiber, Fruit, and Vegetable Consumption with Risk of Inflammatory Bowel Disease: A Systematic Review and Meta-Analysis', *Advances in Nutrition*. Oxford University Press, 12(3), pp. 735–743. doi: 10.1093/advances/nmaa145.

Mills, R. D. *et al.* (2015) 'A role for the tyrosine kinase Pyk2 in depolarization-induced contraction of vascular smooth muscle', *Journal of Biological Chemistry*, 290(14), pp. 8677–8692. doi: 10.1074/jbc.M114.633107.

Mimouna, S. *et al.* (2011) 'Crohn disease-associated Escherichia coli promote gastrointestinal inflammatory disorders by activation of HIF-dependent responses', *Gut microbes*. Taylor & Francis, 2(6), pp. 335–346.

Mitoma, H. *et al.* (2018) 'Molecular mechanisms of action of anti-TNF-α agents-Comparison among therapeutic TNF-α antagonists', *Cytokine*. Elsevier, 101, pp. 56–63.

Mitsuyama, K. *et al.* (1991) 'Colonic mucosal interleukin-6 in inflammatory bowel disease', *Digestion*. Karger Publishers, 50(2), pp. 104–111.

Miyamoto, T. (2013) 'STATs and macrophage fusion', *Jak-Stat*. Taylor & Francis, 2(3), p. e24777.

Mizoguchi, A. *et al.* (2007) 'Dependence of intestinal granuloma formation on unique myeloid DC-like cells', *The Journal of clinical investigation*. Am Soc Clin Investig, 117(3), pp. 605–615.

Moeslinger, T., Friedl, R. and Spieckermann, P. G. (2006) 'Inhibition of inducible nitric oxide synthesis by azathioprine in a macrophage cell line', *Life sciences*. Elsevier, 79(4), pp. 374–381.

Molodecky, N. A. *et al.* (2012) 'Increasing incidence and prevalence of the inflammatory bowel diseases with time, based on systematic review', *Gastroenterology*. Elsevier Inc., 142(1), pp. 46-54.e42. doi: 10.1053/j.gastro.2011.10.001.

Monteleone, G. *et al.* (1997) 'Interleukin 12 is expressed and actively released by Crohn's disease intestinal lamina propria mononuclear cells', *Gastroenterology*. Elsevier, 112(4), pp. 1169–1178.

Monteleone, I. *et al.* (2012) 'The aryl hydrocarbon receptor in inflammatory bowel disease: Linking the environment to disease pathogenesis', *Current Opinion in Gastroenterology*, 28(4), pp. 310–313. doi: 10.1097/MOG.0b013e328352ad69.

Montgomery, S. A. (1996) 'Long-term management of obsessive-compulsive disorder', *International clinical psychopharmacology*. Imperial College School of Medicine at St Mary's, London, UK., 11 Suppl 5, pp. 23–29. doi: 10.1097/00004850-199612005-00004.

Morgan, X. C. *et al.* (2012) 'Dysfunction of the intestinal microbiome in inflammatory bowel disease and treatment', *Genome Biology*, 13(9), p. R79. doi: 10.1186/gb-2012-13-9-r79.

Morise, K. *et al.* (1994) 'Expression of adhesion molecules and HLA-DR by macrophages and dendritic cells in aphthoid lesions of Crohn's disease: an immunocytochemical study', *Journal of Gastroenterology*. Springer, 29(3), pp. 257–264.

Motwani, M. P. and Gilroy, D. W. (2015) 'Macrophage development and polarization in chronic inflammation', *Semin Immunol*, 27(4), pp. 257–266.

Mpofu, C. M. *et al.* (2007) 'Microbial Mannan Inhibits Bacterial Killing by Macrophages: A Possible Pathogenic Mechanism for Crohn's Disease', *Gastroenterology*, 133(5), pp. 1487–1498. doi: 10.1053/j.gastro.2007.08.004.

Murphy, J. M. *et al.* (2019) 'FAK and Pyk2 activity promote TNF-α and IL-1ß-mediated pro-inflammatory gene expression and vascular inflammation', *Scientific Reports*. Springer US, 9(1), pp. 1–14. doi: 10.1038/s41598-019-44098-2.

Murphy, K. M. and Reiner, S. L. (2002) 'The lineage decisions of helper T cells', *Nature Reviews Immunology*. Nature Publishing Group, 2(12), pp. 933–944.

Murthy, A. *et al.* (2014) 'A Crohn's disease variant in Atg16l1 enhances its degradation by caspase 3', *Nature*. Nature Publishing Group, 506(7489), pp. 456–462. doi: 10.1038/nature13044.

Na, Y. R. *et al.* (2019) 'Macrophages in intestinal inflammation and resolution: a potential therapeutic target in IBD', *Nature Reviews Gastroenterology & Hepatology*, 16(9), pp. 531–543. doi: 10.1038/s41575-019-0172-4.

Al Nabhani, Z. *et al.* (2016) 'Nod2 Deficiency Leads to a Specific and Transmissible Mucosa-associated Microbial Dysbiosis Which Is Independent of the Mucosal Barrier Defect', *Journal of Crohn's and Colitis*, 10(12), pp. 1428–1436. doi: 10.1093/ecco-jcc/jjw095.

Al Nabhani, Z. *et al.* (2017) 'Complementary Roles of Nod2 in Hematopoietic and Nonhematopoietic Cells in Preventing Gut Barrier Dysfunction Dependent on MLCK Activity', *Inflammatory Bowel Diseases*, 23(7), pp. 1109–1119. doi: 10.1097/MIB.0000000000001135.

Naser, R. *et al.* (2018) 'Endogenous control mechanisms of FAK and PYK2 and their relevance to cancer development', *Cancers*, 10(6). doi: 10.3390/cancers10060196.

Nazareth, N. *et al.* (2014) 'Infliximab therapy increases the frequency of circulating CD16+ monocytes and modifies macrophage cytokine response to

bacterial infection', *Clinical and Experimental Immunology*, 177(3), pp. 703–711. doi: 10.1111/cei.12375.

Nazareth, N. *et al.* (2015) 'Prevalence of Mycobacterium avium subsp. paratuberculosis and Escherichia coli in blood samples from patients with inflammatory bowel disease', *Medical Microbiology and Immunology*, 204(6), pp. 681–692. doi: 10.1007/s00430-015-0420-3.

Neurath, M. F. (2014) 'Cytokines in inflammatory bowel disease', *Nature Reviews Immunology*. Nature Publishing Group, 14(5), pp. 329–342.

Ng, S. C. *et al.* (2011) 'Relationship between human intestinal dendritic cells, gut microbiota, and disease activity in Crohn's disease', *Inflammatory Bowel Diseases*. Oxford University Press Oxford, UK, 17(10), pp. 2027–2037.

Ng, S. C. *et al.* (2013) 'Incidence and phenotype of inflammatory bowel disease based on results from the Asia-Pacific Crohn's and colitis epidemiology study', *Gastroenterology*. Elsevier, Inc, 145(1), pp. 158-165.e2. doi: 10.1053/j.gastro.2013.04.007.

Nguyen, H. T. T. *et al.* (2013) 'Autophagy and Crohn's Disease', *Journal of Innate Immunity*, 5(5), pp. 434–443. doi: 10.1159/000345129.

Niess, J. H. and Reinecker, H.-C. (2005) 'Lamina propria dendritic cells in the physiology and pathology of the gastrointestinal tract', *Current opinion in gastroenterology*. LWW, 21(6), pp. 687–691.

Nishida, A. *et al.* (2018) 'Gut microbiota in the pathogenesis of inflammatory bowel disease', *Clinical Journal of Gastroenterology*, 11(1), pp. 1–10. doi: 10.1007/s12328-017-0813-5.

Nold-Petry, C. A. *et al.* (2017) 'Gp96 peptide antagonist gp96-II confers therapeutic effects in murine intestinal inflammation', *Frontiers in immunology*. Frontiers Media SA, 8, p. 1531.

Noronha, A. M. *et al.* (2009) 'Hyperactivated B cells in human inflammatory bowel disease', *Journal of leukocyte biology*. Wiley Online Library, 86(4), pp. 1007–1016.

O'Brien, C. L. *et al.* (2017) 'Comparative genomics of Crohn's disease-associated adherent-invasive Escherichia coli', *Gut*. BMJ Publishing Group, 66(8), pp. 1382–1389.

O'Leary, J. G. *et al.* (2006) 'T cell– and B cell–independent adaptive immunity mediated by natural killer cells', *Nature Immunology*, 7(5), pp. 507–516. doi: 10.1038/ni1332.

Ogura, Y. *et al.* (2001) 'A frameshift mutation in NOD2 associated with susceptibility to Crohn's disease', *Nature*, 411(6837), pp. 603–606. doi: 10.1038/35079114.

Ohno, H. (2015) 'Intestinal M cells', *Journal of Biochemistry*, 159(2), pp. 151–160. doi: 10.1093/jb/mvv121.

Okazawa, A. *et al.* (2002) 'Th1-mediated intestinal inflammation in Crohn's disease may be induced by activation of lamina propria lymphocytes through synergistic stimulation of interleukin-12 and interleukin-18 without T cell receptor engagement', *The American journal of gastroenterology*. Elsevier, 97(12), pp. 3108–3117.

Okigaki, M. *et al.* (2003) 'Pyk2 regulates multiple signaling events crucial for macrophage morphology and migration', *Proceedings of the National Academy of Sciences of the United States of America*, 100(19), pp. 10740–10745. doi: 10.1073/pnas.1834348100.

Oliva, G., Sahr, T. and Buchrieser, C. (2015) 'Small RNAs, 5′ UTR elements and RNA-binding proteins in intracellular bacteria: impact on metabolism and virulence', *FEMS microbiology reviews*. Oxford University Press, 39(3), pp. 331–349.

Olsen, N. J., Spurlock, C. F. and Aune, T. M. (2014) 'Methotrexate induces production of IL-1 and IL-6 in the monocytic cell line U937', *Arthritis research & therapy*. Springer, 16(1), pp. 1–8.

Ormsby, M. J. *et al.* (2019) 'Inflammation associated ethanolamine facilitates infection by Crohn's disease-linked adherent-invasive Escherichia coli', *EBioMedicine*, 43, pp. 325–332. doi: https://doi.org/10.1016/j.ebiom.2019.03.071.

Ormsby, M. J. *et al.* (2020) 'Propionic Acid Promotes the Virulent Phenotype of Crohn's Disease-Associated Adherent-Invasive Escherichia coli', *Cell Reports*, 30(7), pp. 2297-2305.e5. doi: https://doi.org/10.1016/j.celrep.2020.01.078.

Ouellette, A. J. (2010) 'Paneth cells and innate mucosal immunity', *Current opinion in gastroenterology*. LWW, 26(6), pp. 547–553.

Owen, K. A., Thomas, K. S. and Bouton, A. H. (2007) 'The differential expression of Yersinia pseudotuberculosis adhesins determines the requirement for FAK and/or Pyk2 during bacterial phagocytosis by macrophages', *Cellular Microbiology*, 9(3), pp. 596–609. doi: 10.1111/j.1462-5822.2006.00811.x.

Pagán, A. J. and Ramakrishnan, L. (2018) 'The formation and function of granulomas', *Annual review of immunology*. Annual Reviews, 36, pp. 639–665.

Palmela, C. *et al.* (2018) 'Adherent-invasive Escherichia coli in inflammatory bowel disease', *Gut*, 67(3), pp. 574–587. doi: 10.1136/gutjnl-2017-314903.

Palomino-Morales, R. J. *et al.* (2009) 'Association of ATG16L1 and IRGM genes polymorphisms with inflammatory bowel disease: a meta-analysis approach', *Genes & Immunity*, 10(4), pp. 356–364. doi: 10.1038/gene.2009.25.

Paone, C. *et al.* (2016) 'The tyrosine kinase Pyk2 contributes to complement-mediated phagocytosis in murine macrophages', *Journal of Innate Immunity*, 8(5), pp. 437–451. doi: 10.1159/000442944.

Parameswaran, N. and Patial, S. (2010) *Tumor necrosis factor-a signaling in macrophages*, *Critical Reviews in Eukaryotic Gene Expression*. doi: 10.1615/CritRevEukarGeneExpr.v20.i2.10.

Parkes, M. *et al*. (2007) 'Sequence variants in the autophagy gene IRGM and multiple other replicating loci contribute to Crohn's disease susceptibility', *Nature Genetics*, 39(7), pp. 830–832. doi: 10.1038/ng2061.

Parreira, V. R. and Gyles, C. L. (2003) 'A novel pathogenicity island integrated adjacent to the thrW tRNA gene of avian pathogenic Escherichia coli encodes a vacuolating autotransporter toxin', *Infection and immunity*. Am Soc Microbiol, 71(9), pp. 5087–5096.

Partl, C. *et al*. (2016) 'Pathfinder: Visual Analysis of Paths in Graphs', *Computer Graphics Forum*. John Wiley & Sons, Ltd, 35(3), pp. 71–80. doi: https://doi.org/10.1111/cgf.12883.

Perrier, C. *et al*. (2013) 'Neutralization of membrane TNF, but not soluble TNF, is crucial for the treatment of experimental colitis', *Inflammatory bowel diseases*. Oxford University Press Oxford, UK, 19(2), pp. 246–253.

Petersen, A. M. *et al*. (2009) 'A phylogenetic group of Escherichia coli associated with active left-sided inflammatory bowel disease', *BMC microbiology*. Springer, 9(1), pp. 1–7.

Peterson, L. W. and Artis, D. (2014) 'Intestinal epithelial cells: regulators of barrier function and immune homeostasis', *Nature Reviews Immunology*. Nature Publishing Group, 14(3), pp. 141–153.

Petnicki-Ocwieja, T. *et al*. (2009) 'Nod2 is required for the regulation of commensal microbiota in the intestine', *Proceedings of the National Academy of Sciences*. Proceedings of the National Academy of Sciences, 106(37), pp. 15813–15818. doi: 10.1073/pnas.0907722106.

Peyrin-Biroulet, L. *et al.* (2007) 'IBD serological panels: facts and perspectives', *Inflammatory bowel diseases*. Oxford University Press Oxford, UK, 13(12), pp. 1561–1566.

Peyrin-Biroulet, L. and Lémann, M. (2011) 'Review article: remission rates achievable by current therapies for inflammatory bowel disease', *Alimentary Pharmacology & Therapeutics*. John Wiley & Sons, Ltd, 33(8), pp. 870–879. doi: https://doi.org/10.1111/j.1365-2036.2011.04599.x.

Piovani, D. *et al.* (2019) 'Environmental Risk Factors for Inflammatory Bowel Diseases: An Umbrella Review of Meta-analyses', *Gastroenterology*. Elsevier, Inc, 157(3), pp. 647-659.e4. doi: 10.1053/j.gastro.2019.04.016.

Pizarro, T. T. *et al.* (1999) 'IL-18, a novel immunoregulatory cytokine, is up-regulated in Crohn's disease: expression and localization in intestinal mucosal cells', *The Journal of Immunology*. Am Assoc Immnol, 162(11), pp. 6829–6835.

Pols, T. W. H. *et al.* (2010) '6-mercaptopurine inhibits atherosclerosis in apolipoprotein e* 3-leiden transgenic mice through atheroprotective actions on monocytes and macrophages', *Arteriosclerosis, thrombosis, and vascular biology*. Am Heart Assoc, 30(8), pp. 1591–1597.

Ponder, A. and Long, M. D. (2013) 'A clinical review of recent findings in the epidemiology of inflammatory bowel disease', *Clinical Epidemiology*, 5(1), pp. 237–247. doi: 10.2147/CLEP.S33961.

Powrie, F. *et al.* (1994) 'Inhibition of Thl responses prevents inflammatory bowel disease in scid mice reconstituted with CD45RBhi CD4+ T cells', *Immunity*. Elsevier, 1(7), pp. 553–562.

Prudent, V. *et al.* (2021) 'The Crohn's disease-related bacterial strain LF82 assembles biofilm-like communities to protect itself from phagolysosomal attack', *Communications Biology*. Springer US, 4(1). doi: 10.1038/s42003-021-02161-7.

Puissegur, M. *et al.* (2004) ‘An in vitro dual model of mycobacterial granulomas to investigate the molecular interactions between mycobacteria and human host cells’, *Cellular microbiology*. Wiley Online Library, 6(5), pp. 423–433.

Qian, T. *et al.* (2016) ‘Angiopoietin-Like Protein 7 Promotes an Inflammatory Phenotype in RAW264.7 Macrophages Through the P38 MAPK Signaling Pathway’, *Inflammation*, 39(3), pp. 974–985. doi: 10.1007/s10753-016-0324-4.

Quévrain, E. *et al.* (2016) ‘Identification of an anti-inflammatory protein from Faecalibacterium prausnitzii, a commensal bacterium deficient in Crohn’s disease’, *Gut*, 65(3), pp. 415 LP – 425. doi: 10.1136/gutjnl-2014-307649.

Raja, S., Avraham, S. and Avraham, H. (1997) ‘Tyrosine Phosphorylation of the Novel Protein-tyrosine Kinase RAFTK during an Early Phase of Platelet Activation by an Integrin Glycoprotein IIb-IIIa-independent Mechanism *’, *Journal of Biological Chemistry*. Elsevier, 272(16), pp. 10941–10947. doi: 10.1074/jbc.272.16.10941.

Ramanan, D. *et al.* (2014) ‘Bacterial Sensor Nod2 Prevents Inflammation of the Small Intestine by Restricting the Expansion of the Commensal Bacteroides vulgatus’, *Immunity*, 41(2), pp. 311–324. doi: https://doi.org/10.1016/j.immuni.2014.06.015.

Reaves, T. A., Chin, A. C. and Parkos, C. A. (2005) ‘Neutrophil transepithelial migration: role of toll-like receptors in mucosal inflammation’, *Memórias do Instituto Oswaldo Cruz*. SciELO Brasil, 100, pp. 191–198.

Rehman, M. Q. *et al.* (2013) ‘B cells secrete eotaxin-1 in human inflammatory bowel disease’, *Inflammatory Bowel Diseases*. Oxford University Press Oxford, UK, 19(5), pp. 922–933.

Reinisch, W. *et al.* (2006) ‘A dose escalating, placebo controlled, double blind, single dose and multidose, safety and tolerability study of fontolizumab, a humanised anti-interferon γ antibody, in patients with moderate to severe Crohn’s disease’, *Gut*. BMJ Publishing Group, 55(8), pp. 1138–1144.

Roberts, C. L. *et al.* (2010) 'Translocation of Crohn's disease Escherichia coli across M-cells: Contrasting effects of soluble plant fibres and emulsifiers', *Gut*, 59(10), pp. 1331–1339. doi: 10.1136/gut.2009.195370.

Robinson, N. (2018) 'Salmonella Typhimurium infection: Type I Interferons integrate cellular networks to disintegrate macrophages.', *Cell stress*, 2(2), pp. 37–39. doi: 10.15698/cst2018.02.125.

Roda, G. *et al.* (2016) 'Loss of Response to Anti-TNFs: Definition, Epidemiology, and Management.', *Clinical and translational gastroenterology*, 7(1), p. e135. doi: 10.1038/ctg.2015.63.

Roda, G. *et al.* (2020) 'Crohn's disease', *Nature Reviews Disease Primers*. Springer US, 6(1). doi: 10.1038/s41572-020-0156-2.

Roe, A. J. *et al.* (2003) 'Heterogeneous Surface Expression of EspA Translocon Filaments by', *Society*, 71(10), pp. 5900–5909. doi: 10.1128/IAI.71.10.5900.

Rogler, G. *et al.* (1998) 'Nuclear factor κB is activated in macrophages and epithelial cells of inflamed intestinal mucosa', *Gastroenterology*, 115(2), pp. 357–369. doi: https://doi.org/10.1016/S0016-5085(98)70202-1.

Rogler, G. *et al.* (1999) 'T-cell co-stimulatory molecules are upregulated on intestinal macrophages from inflammatory bowel disease mucosa.', *European journal of gastroenterology & hepatology*, 11(10), pp. 1105–1111.

Rolhion, N. *et al.* (2010) 'Abnormally expressed ER stress response chaperone Gp96 in CD favours adherent-invasive Escherichia coli invasion', *Gut*. BMJ Publishing Group, 59(10), pp. 1355–1362.

Rolhion, N. and Darfeuille-Michaud, A. (2007) 'Adherent-invasive Escherichia coli in inflammatory bowel disease', *Inflammatory bowel diseases*. Oxford University Press Oxford, UK, 13(10), pp. 1277–1283.

Rolhion, N., Hofman, P. and Darfeuille-Michaud, A. (2011) 'The endoplasmic reticulum stress response chaperone Gp96, a host receptor for Crohn disease-

associated adherent-invasive Escherichia coli', *Gut Microbes*. Taylor & Francis, 2(2), pp. 115–119.

Rooks, M. G. *et al.* (2017) 'QseC inhibition as an antivirulence approach for colitis-associated bacteria', *Proceedings of the National Academy of Sciences*. National Acad Sciences, 114(1), pp. 142–147.

Rosen, D. J. and Dubinsky, M. C. (2016) 'The evolving role of thiopurines for inflammatory bowel disease', *Inflammatory Bowel Diseases*. Oxford University Press Oxford, UK, 22(1), pp. 234–240.

Rossi, M. *et al.* (2014) 'High throughput screening for inhibitors of the HECT ubiquitin E3 ligase ITCH identifies antidepressant drugs as regulators of autophagy', *Cell Death & Disease*, 5(5), pp. e1203–e1203. doi: 10.1038/cddis.2014.113.

Rutgeerts, P. *et al.* (2012) 'Adalimumab induces and maintains mucosal healing in patients with Crohn's Disease: Data from the EXTEND trial', *Gastroenterology*. Elsevier Inc., 142(5), pp. 1102-1111.e2. doi: 10.1053/j.gastro.2012.01.035.

S. Mahid, S. *et al.* (2006) 'Smoking and Inflammatory Bowel Disease: A Meta-analysis', *Mayo Clinic Proceedings*, 81(11), pp. 1462–1471. Available at: https://www.sciencedirect.com/science/article/abs/pii/S0025619611612536.

Di Sabatino, A. *et al.* (2007) 'Functional modulation of Crohn's disease myofibroblasts by anti-tumor necrosis factor antibodies', *Gastroenterology*. Elsevier, 133(1), pp. 137–149.

Salim, S. Y. *et al.* (2009) 'CD83+ CCR7-dendritic cells accumulate in the subepithelial dome and internalize translocated Escherichia coli HB101 in the Peyer's patches of ileal Crohn's disease.', *The American journal of pathology*. American Society for Investigative Pathology, 174(1), pp. 82–90.

Sandborn, W. J. *et al.* (2012) 'Adalimumab induces and maintains clinical remission in patients with moderate-to-severe ulcerative colitis', *Gastroenterology*. Elsevier, 142(2), pp. 257–265.

Sands, B. E. (2004) ‘From symptom to diagnosis: Clinical distinctions among various forms of intestinal inflammation’, *Gastroenterology*, 126(6), pp. 1518–1532. doi: 10.1053/j.gastro.2004.02.072.

Sands, B. E. *et al.* (2017) ‘Efficacy and safety of MEDI2070, an antibody against interleukin 23, in patients with moderate to severe Crohn’s disease: a phase 2a study’, *Gastroenterology*. Elsevier, 153(1), pp. 77–86.

Sanjuan, M. A., Milasta, S. and Green, D. R. (2009) ‘Toll-like receptor signaling in the lysosomal pathways’, *Immunological Reviews*, 227(1), pp. 203–220. doi: 10.1111/j.1600-065X.2008.00732.x.

Sartor, R. B. (2005) ‘Does Mycobacterium avium subspecies paratuberculosis cause Crohn’s disease?’, *Gut*. BMJ Publishing Group, 54(7), pp. 896–898.

Sasaki, M. *et al.* (2007) ‘Invasive Escherichia coli are a feature of Crohn’s disease’, *Laboratory Investigation*, 87(10), pp. 1042–1054. doi: 10.1038/labinvest.3700661.

Sauer, E., Schmidt, S. and Weichenrieder, O. (2012) ‘Small RNA binding to the lateral surface of Hfq hexamers and structural rearrangements upon mRNA target recognition’, *Proceedings of the National Academy of Sciences*. Proceedings of the National Academy of Sciences, 109(24), pp. 9396–9401. doi: 10.1073/pnas.1202521109.

Scallon, B. J. *et al.* (1995) ‘Chimeric anti-TNF-α monoclonal antibody cA2 binds recombinant transmembrane TNF-α and activates immune effector functions’, *Cytokine*, 7(3), pp. 251–259. doi: https://doi.org/10.1006/cyto.1995.0029.

Schaller, M. D. (2010) ‘Cellular functions of FAK kinases: Insight into molecular mechanisms and novel functions’, *Journal of Cell Science*, 123(7), pp. 1007–1013. doi: 10.1242/jcs.045112.

Schmitz, H. *et al.* (1999) ‘Tumor necrosis factor-alpha (TNFα) regulates the epithelial barrier in the human intestinal cell line HT-29/B6’, *Journal of Cell Science*, 112(1), pp. 137–146. doi: 10.1242/jcs.112.1.137.

Schneider, C. A., Rasband, W. S. and Eliceiri, K. W. (2012) 'NIH Image to ImageJ: 25 years of image analysis', *Nature Methods*. Nature Publishing Group, 9(7), pp. 671–675. doi: 10.1038/nmeth.2089.

Schreiber, H. A. *et al.* (2011) 'Inflammatory dendritic cells migrate in and out of transplanted chronic mycobacterial granulomas in mice', *The Journal of clinical investigation*. Am Soc Clin Investig, 121(10), pp. 3902–3913.

Schroeder, A. *et al.* (2006) 'The RIN: an RNA integrity number for assigning integrity values to RNA measurements', *BMC Molecular Biology*, 7(1), p. 3. doi: 10.1186/1471-2199-7-3.

Schwenger, P. (1998) *Actions of sodium salicylate on MAP kinase-mediated cytokine signaling pathways*. New York University.

Seldenrijk, C. A. *et al.* (1989) 'Dendritic cells and scavenger macrophages in chronic inflammatory bowel disease.', *Gut*. BMJ Publishing Group, 30(4), pp. 486–491.

Sellin, J. H. and Shah, R. R. (2012) 'The promise and pitfalls of serologic testing in inflammatory bowel disease', *Gastroenterology Clinics*. Elsevier, 41(2), pp. 463–482.

Shale, M., Schiering, C. and Powrie, F. (2013) 'CD 4+ T-cell subsets in intestinal inflammation', *Immunological reviews*. Wiley Online Library, 252(1), pp. 164–182.

Shawki, A. *et al.* (2020) 'The autoimmune susceptibility gene, PTPN2, restricts expansion of a novel mouse adherent-invasive E. coli', *Gut Microbes*. Taylor & Francis, 11(6), pp. 1547–1566. doi: 10.1080/19490976.2020.1775538.

Shembade, N. *et al.* (2008) 'The E3 ligase Itch negatively regulates inflammatory signaling pathways by controlling the function of the ubiquitin-editing enzyme A20', *Nature Immunology*, 9(3), pp. 254–262. doi: 10.1038/ni1563.

Shemiakina, I. I. *et al.* (2012) 'A monomeric red fluorescent protein with low cytotoxicity', *Nature Communications*, 3(1), p. 1204. doi: 10.1038/ncomms2208.

Shen, C. *et al.* (2005) 'Adalimumab induces apoptosis of human monocytes: a comparative study with infliximab and etanercept', *Alimentary Pharmacology & Therapeutics*. John Wiley & Sons, Ltd, 21(3), pp. 251–258. doi: https://doi.org/10.1111/j.1365-2036.2005.02309.x.

Shi-lin, D. *et al.* (2015) 'Trametinib, a novel MEK kinase inhibitor, suppresses lipopolysaccharide-induced tumor necrosis factor (TNF)-α production and endotoxin shock', *Biochemical and Biophysical Research Communications*, 458(3), pp. 667–673. doi: https://doi.org/10.1016/j.bbrc.2015.01.160.

Shoenfeld, Y. *et al.* (2008) 'The mosaic of autoimmunity: Hormonal and environmental factors involved in autoimmune diseases - 2008', *Israel Medical Association Journal*, 10(1), pp. 8–12.

Siegmund, B. *et al.* (2001) 'Neutralization of interleukin-18 reduces severity in murine colitis and intestinal IFN-γ and TNF-α production', *American Journal of Physiology-Regulatory, Integrative and Comparative Physiology*. American Physiological Society Bethesda, MD, 281(4), pp. R1264–R1273.

De Silva, H. J. *et al.* (1991) 'Lymphocyte and macrophage subpopulations in pelvic ileal pouches.', *Gut*. BMJ Publishing Group, 32(10), pp. 1160–1165.

Silva, M. A. (2009) 'Intestinal dendritic cells and epithelial barrier dysfunction in Crohn's disease', *Inflammatory bowel diseases*. Oxford University Press Oxford, UK, 15(3), pp. 436–453.

De Silva, P. and Ananthakrishnan, A. N. (2012) 'Vitamin D and IBD: More Pieces to the Puzzle, Still No Complete Picture', *Inflammatory Bowel Diseases*, 18(7), pp. 1391–1393. doi: 10.1002/ibd.22854.

Simonsen, K. T. *et al.* (2011) 'A role for the RNA chaperone Hfq in controlling adherent-invasive Escherichia coli colonization and virulence', *PloS one*. Public Library of Science San Francisco, USA, 6(1), p. e16387.

Singh, P. P. *et al.* (2012) ‘Exosomes Isolated from Mycobacteria-Infected Mice or Cultured Macrophages Can Recruit and Activate Immune Cells In Vitro and In Vivo’, *The Journal of Immunology*, 189(2), pp. 777 LP – 785. doi: 10.4049/jimmunol.1103638.

Singh, S. B. *et al.* (2006) ‘Human IRGM Induces Autophagy to Eliminate Intracellular Mycobacteria’, *Science*. American Association for the Advancement of Science, 313(5792), pp. 1438–1441. doi: 10.1126/science.1129577.

Sivignon, A. *et al.* (2015) ‘Saccharomyces cerevisiae CNCM I-3856 prevents colitis induced by AIEC bacteria in the transgenic mouse model mimicking Crohn’s disease’, *Inflammatory bowel diseases*. Oxford University Press Oxford, UK, 21(2), pp. 276–286.

Sivignon, A. *et al.* (2021) ‘Heteropolysaccharides from S. cerevisiae show anti-adhesive properties against E. coli associated with Crohn’s disease’, *Carbohydrate Polymers*. Elsevier, 271, p. 118415.

Smith, E. J., Thompson, A. P. and Clarke, D. J. (2013) ‘Pathogenesis of adherent–invasive’, 8, pp. 1289–1300.

Smith, M. S. H. and Wakefield, A. J. (1993) ‘Viral association with Crohn’s disease’, *Annals of medicine*. Taylor & Francis, 25(6), pp. 557–561.

Soh, H. *et al.* (2020) ‘Crohn’s disease and ulcerative colitis are associated with different lipid profile disorders: a nationwide population-based study’, *Alimentary Pharmacology & Therapeutics*. John Wiley & Sons, Ltd, 51(4), pp. 446–456. doi: https://doi.org/10.1111/apt.15562.

Sokol, H. *et al.* (2008) ‘Faecalibacterium prausnitzii is an anti-inflammatory commensal bacterium identified by gut microbiota analysis of Crohn disease patients’, *Proceedings of the National Academy of Sciences*. Proceedings of the National Academy of Sciences, 105(43), pp. 16731–16736. doi: 10.1073/pnas.0804812105.

Sokurenko, E. V *et al.* (1997) 'Diversity of the Escherichia coli type 1 fimbrial lectin: differential binding to mannosides and uroepithelial cells', *Journal of Biological Chemistry*. ASBMB, 272(28), pp. 17880–17886.

Sood, A. *et al.* (2006) 'Long term results of use of azathioprine in patients with ulcerative colitis in India', *World Journal of Gastroenterology*, 12(45), pp. 7332–7336. doi: 10.3748/wjg.v12.i45.7332.

De Souza, H. S. P. and Fiocchi, C. (2016) 'Immunopathogenesis of IBD: current state of the art', *Nature reviews Gastroenterology & hepatology*. Nature Publishing Group, 13(1), pp. 13–27.

Steinbach, E. C. and Plevy, S. E. (2014) 'The role of macrophages and dendritic cells in the initiation of inflammation in IBD', *Inflammatory bowel diseases*. Oxford University Press Oxford, UK, 20(1), pp. 166–175.

Stevenson, M., Baillie, A. J. and Richards, R. M. E. (1984) 'An in-vitro model of intracellular bacterial infection using the murine macrophage cell line J774·2', *Journal of Pharmacy and Pharmacology*. John Wiley & Sons, Ltd, 36(2), pp. 90–94. doi: https://doi.org/10.1111/j.2042-7158.1984.tb03000.x.

Strober, W., Fuss, I. J. and Blumberg, R. S. (2002) 'The immunology of mucosal models of inflammation', *Annual review of immunology*. Annual Reviews, Inc., 20, p. 495.

Strober, W., Fuss, I. and Mannon, P. (2007) 'The fundamental basis of inflammatory bowel disease', *The Journal of clinical investigation*. Am Soc Clin Investig, 117(3), pp. 514–521.

Strober, W. and Watanabe, T. (2011) 'NOD2, an intracellular innate immune sensor involved in host defense and Crohn's disease', *Mucosal Immunology*, 4(5), pp. 484–495. doi: 10.1038/mi.2011.29.

Su, L. *et al.* (2013) 'TNFR2 activates MLCK-dependent tight junction dysregulation to cause apoptosis-mediated barrier loss and experimental colitis', *Gastroenterology*. Elsevier, 145(2), pp. 407–415.

Subramanian, S. *et al.* (2008) 'Characterization of epithelial IL-8 response to inflammatory bowel disease mucosal E. coli and its inhibition by mesalamine', *Inflammatory bowel diseases*. Oxford University Press Oxford, UK, 14(2), pp. 162–175.

Swidsinski, A. *et al.* (2002) 'Mucosal flora in inflammatory bowel disease', *Gastroenterology*, 122(1), pp. 44–54. doi: https://doi.org/10.1053/gast.2002.30294.

T., T.-A. J., Xiaodong, B. and W., A. D. (2013) 'A Discrete Ubiquitin-Mediated Network Regulates the Strength of NOD2 Signaling', *Molecular and Cellular Biology*. American Society for Microbiology, 33(1), pp. 146–158. doi: 10.1128/MCB.01049-12.

Tao, M. *et al.* (2009) 'ITCH K63-Ubiquitinates the NOD2 Binding Protein, RIP2, to Influence Inflammatory Signaling Pathways', *Current Biology*, 19(15), pp. 1255–1263. doi: https://doi.org/10.1016/j.cub.2009.06.038.

Tawfik, A., Flanagan, P. K. and Campbell, B. J. (2014) 'Escherichia coli-host macrophage interactions in the pathogenesis of inflammatory bowel disease.', *World journal of gastroenterology*, 20(27), pp. 8751–8763. doi: 10.3748/wjg.v20.i27.8751.

Tesija Kuna, A. (2013) 'Serological markers of inflammatory bowel disease', *Biochemia Medica*. Medicinska naklada, 23(1), pp. 28–42.

Theivanthiran, B. *et al.* (2015) 'The E3 ubiquitin ligase Itch inhibits p38α signaling and skin inflammation through the ubiquitylation of Tab1', *Science Signaling*. American Association for the Advancement of Science, 8(365), pp. ra22–ra22. doi: 10.1126/scisignal.2005903.

Thia, K. T. *et al.* (2008) 'An update on the epidemiology of inflammatory bowel disease in Asia', *American Journal of Gastroenterology*, 103(12), pp. 3167–3182. doi: 10.1111/j.1572-0241.2008.02158.x.

Thia, K. T. *et al.* (2010) 'Risk factors associated with progression to intestinal complications of Crohn's disease in a population-based cohort', *Gastroenterology*, 139(4), pp. 1147–1155. doi: 10.1053/j.gastro.2010.06.070.

Thomas, S. and Baumgart, D. C. (2012) 'Targeting leukocyte migration and adhesion in Crohn's disease and ulcerative colitis', *Inflammopharmacology*. Springer, 20(1), pp. 1–18.

Torres, J. *et al.* (2017) 'Crohn's disease', *The Lancet*, 389(10080), pp. 1741–1755. doi: 10.1016/S0140-6736(16)31711-1.

Tran, C. D. *et al.* (2007) 'The Role of Zinc and Metallothionein in the Dextran Sulfate Sodium-Induced Colitis Mouse Model', *Digestive Diseases and Sciences*, 52(9), pp. 2113–2121. doi: 10.1007/s10620-007-9765-9.

Troy, F. A. (1995) 'Sialobiology and the Polysialic Acid Glycotope Occurrence, Structure, Function, Synthesis, and Glycopathology', in *Biology of the Sialic Acids*. Springer, pp. 95–144.

Uhlig, H. H. *et al.* (2006) 'Differential activity of IL-12 and IL-23 in mucosal and systemic innate immune pathology', *Immunity*. Elsevier, 25(2), pp. 309–318.

Uhlig, H. H. and Powrie, F. (2018) 'Translating immunology into therapeutic concepts for inflammatory bowel disease', *Annual review of immunology*. Annual Reviews, 36, pp. 755–781.

Underhill, D. M. and Goodridge, H. S. (2012) 'Information processing during phagocytosis', *Nature Reviews Immunology*, 12(7), pp. 492–502. doi: 10.1038/nri3244.

Ungaro, R. *et al.* (2014) 'Antibiotics associated with increased risk of New-Onset Crohn's disease but not ulcerative colitis: A meta-analysis', *American Journal of Gastroenterology*, 109(11), pp. 1728–1738. doi: 10.1038/ajg.2014.246.

Vazeille, E. *et al.* (2011) 'Role of Meprins to Protect Ileal Mucosa of Crohn's Disease Patients from Colonization by Adherent-Invasive E. coli', *PLOS ONE*.

Public Library of Science, 6(6), p. e21199. Available at: https://doi.org/10.1371/journal.pone.0021199.

Vazeille, E. *et al*. (2015) 'Monocyte-derived macrophages from Crohn's disease patients are impaired in the ability to control intracellular adherent-invasive Escherichia coli and exhibit disordered cytokine secretion profile', *Journal of Crohn's & colitis*, 9(5), pp. 410–420. doi: 10.1093/ecco-jcc/jjv053.

Vazeille, E. *et al*. (2016) 'GipA factor supports colonization of Peyer's patches by Crohn's disease-associated Escherichia coli', *Inflammatory bowel diseases*. Oxford University Press Oxford, UK, 22(1), pp. 68–81.

Velde, A. A. te *et al*. (2003) 'Increased expression of DC-SIGN+ IL-12+ IL-18+ and CD83+ IL-12–IL-18–dendritic cell populations in the colonic mucosa of patients with Crohn's disease', *European journal of immunology*. Wiley Online Library, 33(1), pp. 143–151.

Vogel, J. and Luisi, B. F. (2011) 'Hfq and its constellation of RNA', *Nature Reviews Microbiology*. Nature Publishing Group, 9(8), pp. 578–589.

Wallace, J. L. (2008) 'Prostaglandins, NSAIDs, and gastric mucosal protection: Why doesn't the stomach digest itself?', *Physiological Reviews*, 88(4), pp. 1547–1565. doi: 10.1152/physrev.00004.2008.

Weaver, C. T. *et al*. (2007) 'IL-17 family cytokines and the expanding diversity of effector T cell lineages', *Annual review of immunology*, 25(1), pp. 821–852.

Wiedemann, A. *et al*. (2001) 'Yersinia enterocolitica invasin triggers phagocytosis via ß1 integrins, CDC42Hs and WASp in macrophages', *Cellular Microbiology*, 3(10), pp. 693–702. doi: 10.1046/j.1462-5822.2001.00149.x.

Williams, L. M. and Ridley, A. J. (2000) 'Lipopolysaccharide Induces Actin Reorganization and Tyrosine Phosphorylation of Pyk2 and Paxillin in Monocytes and Macrophages', *The Journal of Immunology*, 164(4), pp. 2028–2036. doi: 10.4049/jimmunol.164.4.2028.

Wine, E. *et al.* (2009) 'Adherent-invasive Escherichia coli, strain LF82 disrupts apical junctional complexes in polarized epithelia', *BMC microbiology*. Springer, 9(1), pp. 1–11.

Wolfe, M. M., Lichtenstein, D. R. and Singh, G. (1999) 'Gastrointestinal Toxicity of Nonsteroidal Antiinflammatory Drugs', *the new england journal of medicine*, (340), pp. 1888–1899. doi: 10.1056/NEJM199906173402407.

Xi, C.-X. *et al.* (2010) 'PYK2 interacts with MyD88 and regulates MyD88-mediated NF- B activation in macrophages', *Journal of Leukocyte Biology*, 87(3), pp. 415–423. doi: 10.1189/jlb.0309125.

Yagi, M. *et al.* (2005) 'DC-STAMP is essential for cell–cell fusion in osteoclasts and foreign body giant cells', *The Journal of experimental medicine*. Rockefeller University Press, 202(3), pp. 345–351.

Yamamoto, M. *et al.* (2000) 'IL-6 is required for the development of Th1 cell-mediated murine colitis', *The Journal of Immunology*. Am Assoc Immnol, 164(9), pp. 4878–4882.

Yan, X. *et al.* (2015) 'Glycopolymers as antiadhesives of E. coli strains inducing inflammatory bowel diseases', *Biomacromolecules*. ACS Publications, 16(6), pp. 1827–1836.

Yang, C. M. *et al.* (2013) 'NADPH oxidase/ROS-dependent PYK2 activation is involved in TNF-α-induced matrix metalloproteinase-9 expression in rat heart-derived H9c2 cells', *Toxicology and Applied Pharmacology*. Elsevier Inc., 272(2), pp. 431–442. doi: 10.1016/j.taap.2013.05.036.

Yang, S. K. *et al.* (2000) 'Incidence and prevalence of ulcerative colitis in the Songpa-Kangdong district, Seoul, Korea, 1986-1997', *Journal of Gastroenterology and Hepatology (Australia)*, 15(9), pp. 1037–1042. doi: 10.1046/j.1440-1746.2000.02252.x.

Yen, D. *et al.* (2006) 'IL-23 is essential for T cell–mediated colitis and promotes inflammation via IL-17 and IL-6', *The Journal of clinical investigation*. Am Soc Clin Investig, 116(5), pp. 1310–1316.

Zamani, S. *et al.* (2017) 'Detection of enterotoxigenic Bacteroides fragilis in patients with ulcerative colitis', *Gut pathogens*. BioMed Central, 9(1), pp. 1–7.

Zareie, M. *et al.* (2006) 'Probiotics prevent bacterial translocation and improve intestinal barrier function in rats following chronic psychological stress', *Gut*, 55(11), pp. 1553 LP – 1560. doi: 10.1136/gut.2005.080739.

Zeng, M. Y., Inohara, N. and Nuñez, G. (2017) 'Mechanisms of inflammation-driven bacterial dysbiosis in the gut', *Mucosal immunology*. Nature Publishing Group, 10(1), pp. 18–26.

Zhang, H. *et al.* (2013) 'Ubiquitin E3 ligase Itch negatively regulates osteoclast formation by promoting deubiquitination of tumor necrosis factor (TNF) receptor-associated factor 6', *Journal of Biological Chemistry*. ASBMB, 288(31), pp. 22359–22368.

Zhang, Z.-T. *et al.* (2015) 'Is the CARD8 rs2043211 polymorphism associated with susceptibility to Crohn's disease? A meta-analysis', *Autoimmunity*. Taylor & Francis, 48(8), pp. 524–531.

Zhao, M. *et al.* (2016) 'Novel role of Src in priming Pyk2 phosphorylation', *PLoS ONE*, 11(2), pp. 1–14. doi: 10.1371/journal.pone.0149231.

Zhu, X. *et al.* (2018) 'Proline-rich protein tyrosine Kinase 2 in inflammation and cancer', *Cancers*, 10(5), pp. 1–14. doi: 10.3390/cancers10050139.

Zoeten, E. F. de and Fuss, I. J. (2013) 'Cytokines and inflammatory bowel disease', in *Pediatric Inflammatory Bowel Disease*. Springer, pp. 25–33.

Zumla, A. and James, D. G. (1996) 'Granulomatous infections: etiology and classification', *Clinical infectious diseases*. The University of Chicago Press, 23(1), pp. 146–158.

Appendices

Appendix 1 Signature 1 genes list

ID	Symbol
ENSMUSG00000097134	1110002J07RIK
ENSMUSG00000000682	CD52
ENSMUSG00000027782	KPNA4
ENSMUSG00000027087	ITGAV
ENSMUSG00000003316	GLG1
ENSMUSG00000002332	DHRS1
ENSMUSG00000004936	MAP2K1
ENSMUSG00000027368	DUSP2
ENSMUSG00000031647	MFAP3L
ENSMUSG00000058407	TXNDC9
ENSMUSG00000078816	PRKCG
ENSMUSG00000020674	PXDN
ENSMUSG00000078566	BNIP3
ENSMUSG00000046318	CCBE1
ENSMUSG00000000290	ITGB2
ENSMUSG00000024190	DUSP1
ENSMUSG00000025959	KLF7
ENSMUSG00000040711	SH3PXD2B
ENSMUSG00000086804	GM43154
ENSMUSG00000026984	IL1F6
ENSMUSG00000045098	KMT5B
ENSMUSG00000047945	MARCKSL1
ENSMUSG00000058755	OSM
ENSMUSG00000020108	DDIT4
ENSMUSG00000032479	MAP4
ENSMUSG00000027309	4930402H24RIK
ENSMUSG00000074743	THBD
ENSMUSG00000066152	SLC31A2
ENSMUSG00000032845	ALPK2
ENSMUSG00000024743	SYT7
ENSMUSG00000040528	MILR1
ENSMUSG00000018965	YWHAH
ENSMUSG00000063406	TMED5
ENSMUSG00000020120	PLEK
ENSMUSG00000003617	CP
ENSMUSG00000034850	TMEM127
ENSMUSG00000020611	GNA13
ENSMUSG00000040370	ETFRF1
ENSMUSG00000069237	FAM8A1
ENSMUSG00000053113	SOCS3
ENSMUSG00000013921	CLIP3
ENSMUSG00000072844	G530011O06RIK
ENSMUSG00000002897	IL17RA
ENSMUSG00000059182	SKAP2
ENSMUSG00000097418	MIR155HG

ENSMUSG00000028369	SVEP1
ENSMUSG00000025791	PGM2
ENSMUSG00000018882	MRPL45
ENSMUSG00000037012	HK1
ENSMUSG00000015944	GATSL2
ENSMUSG00000025044	MSR1
ENSMUSG00000049719	PRSS46
ENSMUSG00000026977	Mar-07
ENSMUSG00000024236	SVIL
ENSMUSG00000042228	LYN
ENSMUSG00000056671	PRELID2
ENSMUSG00000104340	GM10522
ENSMUSG00000059146	NTRK3
ENSMUSG00000058966	FAM57B
ENSMUSG00000032487	PTGS2
ENSMUSG00000005125	NDRG1
ENSMUSG00000032688	MALT1
ENSMUSG00000039196	ORM1
ENSMUSG00000001542	ELL2
ENSMUSG00000033684	QSOX1
ENSMUSG00000026222	SP100
ENSMUSG00000026271	GPR35
ENSMUSG00000033730	EGR3
ENSMUSG00000017639	RAB11FIP4
ENSMUSG00000063229	LDHA
ENSMUSG00000026896	IFIH1
ENSMUSG00000055435	MAF
ENSMUSG00000024737	SLC15A3
ENSMUSG00000039236	ISG20
ENSMUSG00000054404	SLFN5
ENSMUSG00000009093	GSTT4
ENSMUSG00000021025	NFKBIA
ENSMUSG00000029309	SPARCL1
ENSMUSG00000024754	TMEM2
ENSMUSG00000024789	JAK2
ENSMUSG00000058927	GM10053
ENSMUSG00000026981	IL1RN
ENSMUSG00000050212	EVA1B
ENSMUSG00000022973	SYNJ1
ENSMUSG00000049686	ORAI1
ENSMUSG00000000628	HK2
ENSMUSG00000002602	AXL
ENSMUSG00000007655	CAV1
ENSMUSG00000030659	NUCB2
ENSMUSG00000038151	PRDM1
ENSMUSG00000000805	CAR4
ENSMUSG00000079523	TMSB10
ENSMUSG00000003865	GYS1
ENSMUSG00000019987	ARG1
ENSMUSG00000026740	DNAJC1
ENSMUSG00000027611	PROCR
ENSMUSG00000047557	LXN

ENSMUSG00000035778	GGTA1
ENSMUSG00000018500	ADORA2B
ENSMUSG00000016528	MAPKAPK2
ENSMUSG00000072235	TUBA1A
ENSMUSG00000030830	ITGAL
ENSMUSG00000027555	CAR13
ENSMUSG00000012519	MLKL
ENSMUSG00000033352	MAP2K4
ENSMUSG00000061451	TMEM151A
ENSMUSG00000046203	SPRR2G
ENSMUSG00000026576	ATP1B1
ENSMUSG00000042312	S100A13
ENSMUSG00000033933	VHL
ENSMUSG00000031762	MT2
ENSMUSG00000026509	CAPN2
ENSMUSG00000035692	ISG15
ENSMUSG00000038612	MCL1
ENSMUSG00000039753	FBXL5
ENSMUSG00000032860	P2RY2
ENSMUSG00000079056	KCNIP3
ENSMUSG00000000078	KLF6
ENSMUSG00000046259	SPRR2H
ENSMUSG00000024810	IL33
ENSMUSG00000025161	SLC16A3
ENSMUSG00000026664	PHYH
ENSMUSG00000042608	STK40
ENSMUSG00000029082	BST1
ENSMUSG00000029135	FOSL2
ENSMUSG00000044162	TNIP3
ENSMUSG00000031586	RBPMS
ENSMUSG00000032899	STYK1
ENSMUSG00000038150	ORMDL3
ENSMUSG00000085949	GM14275
ENSMUSG00000041378	CLDN5
ENSMUSG00000022148	FYB
ENSMUSG00000015850	ADAMTSL4
ENSMUSG00000030208	EMP1
ENSMUSG00000038518	JARID2
ENSMUSG00000044330	GM9790
ENSMUSG00000017057	IL13RA1
ENSMUSG00000075302	ERICH2
ENSMUSG00000015243	ABCA1
ENSMUSG00000029254	STAP1
ENSMUSG00000034591	SLC41A2
ENSMUSG00000095115	ITPRIPL2
ENSMUSG00000028300	3110043O21RIK
ENSMUSG00000024053	EMILIN2
ENSMUSG00000028439	FAM219A
ENSMUSG00000029373	PF4
ENSMUSG00000073131	VMA21
ENSMUSG00000016534	LAMP2
ENSMUSG00000043421	HILPDA

ENSMUSG00000030530	FURIN
ENSMUSG00000028434	EPB41L4B
ENSMUSG00000034394	LIF
ENSMUSG00000028602	TNFRSF8
ENSMUSG00000017002	SLPI
ENSMUSG00000025130	P4HB
ENSMUSG00000023349	CLEC4N
ENSMUSG00000026177	SLC11A1
ENSMUSG00000040105	PLPP6
ENSMUSG00000033355	RTP4
ENSMUSG00000070056	MFHAS1
ENSMUSG00000038179	SLAMF7
ENSMUSG00000031207	MSN
ENSMUSG00000004730	ADGRE1
ENSMUSG00000004961	SYT5
ENSMUSG00000032691	NLRP3
ENSMUSG00000022126	ACOD1
ENSMUSG00000003541	IER3
ENSMUSG00000049214	SKINT7
ENSMUSG00000052270	FPR2
ENSMUSG00000029314	GPAT3
ENSMUSG00000097558	GM26902
ENSMUSG00000043388	TMEM130
ENSMUSG00000066406	AKAP13
ENSMUSG00000042677	ZC3H12A
ENSMUSG00000025059	GK
ENSMUSG00000040274	CDK6
ENSMUSG00000026656	FCGR2B
ENSMUSG00000015396	CD83
ENSMUSG00000002847	PLA1A
ENSMUSG00000079293	CLEC7A
ENSMUSG00000063531	SEMA3E
ENSMUSG00000027925	SPRR2J-PS
ENSMUSG00000026883	DAB2IP
ENSMUSG00000001666	DDT
ENSMUSG00000047786	LIX1
ENSMUSG00000001348	ACP5
ENSMUSG00000085628	APPBP2OS
ENSMUSG00000025272	TRO
ENSMUSG00000049775	TMSB4X
ENSMUSG00000008859	RALA
ENSMUSG00000036181	HIST1H1C
ENSMUSG00000097048	1600020E01RIK
ENSMUSG00000041488	STX3
ENSMUSG00000028851	NUDC
ENSMUSG00000034640	TIPARP
ENSMUSG00000049037	CLEC4A1
ENSMUSG00000068874	SELENBP1
ENSMUSG00000026749	NEK6
ENSMUSG00000021990	SPATA13
ENSMUSG00000030447	CYFIP1
ENSMUSG00000003283	HCK

ENSMUSG00000050440	HAMP
ENSMUSG00000024644	CNDP2
ENSMUSG00000069792	WFDC17
ENSMUSG00000027422	RRBP1
ENSMUSG00000033581	IGF2BP2
ENSMUSG00000034459	IFIT1
ENSMUSG00000018930	CCL4
ENSMUSG00000050635	SPRR2F
ENSMUSG00000020077	SRGN
ENSMUSG00000021024	PSMA6
ENSMUSG00000049940	PGRMC2
ENSMUSG00000004085	MAP3K20
ENSMUSG00000026480	NCF2
ENSMUSG00000058427	CXCL2
ENSMUSG00000042157	SPRR2I
ENSMUSG00000041992	RAPGEF5
ENSMUSG00000016496	CD274
ENSMUSG00000017737	MMP9
ENSMUSG00000028465	TLN1
ENSMUSG00000022500	LITAF
ENSMUSG00000029683	LMOD2
ENSMUSG00000019564	ARID3A
ENSMUSG00000070702	CSN1S1
ENSMUSG00000026822	LCN2
ENSMUSG00000020227	IRAK3
ENSMUSG00000078616	TRIM30C
ENSMUSG00000040253	GBP7
ENSMUSG00000051159	CITED1
ENSMUSG00000034480	DIAPH2
ENSMUSG00000054905	STFA3
ENSMUSG00000030142	CLEC4E
ENSMUSG00000027506	TPD52
ENSMUSG00000055447	CD47
ENSMUSG00000041598	CDC42EP4
ENSMUSG00000032561	ACPP
ENSMUSG00000048895	CDK5R1
ENSMUSG00000026728	VIM
ENSMUSG00000020592	SDC1
ENSMUSG00000022018	RGCC
ENSMUSG00000026121	SEMA4C
ENSMUSG00000020841	CPD
ENSMUSG00000030067	FOXP1
ENSMUSG00000052928	CTIF
ENSMUSG00000022037	CLU
ENSMUSG00000022475	HDAC7
ENSMUSG00000035107	DCBLD2
ENSMUSG00000030287	ITPR2
ENSMUSG00000066150	SLC31A1
ENSMUSG00000030790	ADM
ENSMUSG00000044447	DOCK5
ENSMUSG00000034765	DUSP5
ENSMUSG00000029648	FLT1

ENSMUSG00000027997	CASP6
ENSMUSG00000021109	HIF1A
ENSMUSG00000000982	CCL3
ENSMUSG00000032017	GRIK4
ENSMUSG00000023087	NOCT
ENSMUSG00000025757	HSPA4L
ENSMUSG00000024401	TNF
ENSMUSG00000042207	KDM5B
ENSMUSG00000094733	GM5416
ENSMUSG00000015340	CYBB
ENSMUSG00000042485	MUSTN1
ENSMUSG00000030342	CD9
ENSMUSG00000032324	TSPAN3
ENSMUSG00000037503	FAM168B
ENSMUSG00000071713	CSF2RB
ENSMUSG00000083899	GM12346
ENSMUSG00000052397	EZR
ENSMUSG00000032849	ABCC4
ENSMUSG00000027546	ATP9A
ENSMUSG00000017009	SDC4
ENSMUSG00000028649	MACF1
ENSMUSG00000001025	S100A6
ENSMUSG00000032020	UBASH3B
ENSMUSG00000020610	AMZ2
ENSMUSG00000028793	RNF19B
ENSMUSG00000038067	CSF3
ENSMUSG00000007097	ATP1A2
ENSMUSG00000031825	CRISPLD2
ENSMUSG00000096917	2500002B13RIK
ENSMUSG00000032462	PIK3CB
ENSMUSG00000042129	RASSF4
ENSMUSG00000016349	EEF1A2
ENSMUSG00000033565	RBFOX2
ENSMUSG00000013936	MYL2
ENSMUSG00000028527	AK4
ENSMUSG00000095042	GM12537
ENSMUSG00000044786	ZFP36
ENSMUSG00000032515	CSRNP1
ENSMUSG00000067889	SPTBN2
ENSMUSG00000073411	H2-D1
ENSMUSG00000025025	MXI1
ENSMUSG00000008496	POU2F2
ENSMUSG00000044103	IL1F9
ENSMUSG00000052310	SLC39A1
ENSMUSG00000047798	CD300LF
ENSMUSG00000022831	HCLS1
ENSMUSG00000085498	GM14023
ENSMUSG00000026525	OPN3
ENSMUSG00000031765	MT1
ENSMUSG00000035640	CBARP
ENSMUSG00000029334	PRKG2
ENSMUSG00000031289	IL13RA2

ENSMUSG00000101625	GM29371
ENSMUSG00000051832	E230016K23RIK
ENSMUSG00000037172	E330009J07RIK
ENSMUSG00000036499	EEA1
ENSMUSG00000001175	CALM1
ENSMUSG00000028480	GLIPR2
ENSMUSG00000028412	SLC44A1
ENSMUSG00000029385	CCNG2
ENSMUSG00000022892	APP
ENSMUSG00000024679	MS4A6D
ENSMUSG00000062345	SERPINB2
ENSMUSG00000030214	PLBD1
ENSMUSG00000015312	GADD45B
ENSMUSG00000072572	SLC39A2
ENSMUSG00000039735	FNBP1L
ENSMUSG00000050957	INSL6
ENSMUSG00000055030	SPRR2E
ENSMUSG00000020826	NOS2
ENSMUSG00000021892	SH3BP5
ENSMUSG00000038936	SCCPDH
ENSMUSG00000033306	LPP
ENSMUSG00000009376	MET
ENSMUSG00000028599	TNFRSF1B
ENSMUSG00000019370	CALM3
ENSMUSG00000035373	CCL7
ENSMUSG00000027333	SMOX
ENSMUSG00000046245	PILRA
ENSMUSG00000051748	WFDC21
ENSMUSG00000114980	AC102815.1
ENSMUSG00000018648	DUSP14
ENSMUSG00000018906	P4HA2
ENSMUSG00000025746	IL6
ENSMUSG00000054008	NDST1
ENSMUSG00000001473	TUBB6
ENSMUSG00000021477	CTSL
ENSMUSG00000025779	LY96
ENSMUSG00000022867	USP25
ENSMUSG00000038127	CCDC50
ENSMUSG00000001156	MXD1
ENSMUSG00000040489	SOX30
ENSMUSG00000024277	MAPRE2
ENSMUSG00000050967	CREG2
ENSMUSG00000054215	SPRR2K
ENSMUSG00000024014	PIM1
ENSMUSG00000045211	NUDT18
ENSMUSG00000025576	RBFOX3
ENSMUSG00000097111	PEAK1OS
ENSMUSG00000028525	PDE4B
ENSMUSG00000043336	FILIP1L
ENSMUSG00000004791	PGF
ENSMUSG00000056501	CEBPB
ENSMUSG00000032231	ANXA2

ENSMUSG00000060594	LAYN
ENSMUSG00000029103	LRPAP1
ENSMUSG00000034731	DGKH
ENSMUSG00000024736	TMEM132A
ENSMUSG00000020010	VNN3
ENSMUSG00000091955	GM9844
ENSMUSG00000031278	ACSL4
ENSMUSG00000069662	MARCKS
ENSMUSG00000048752	PRSS50
ENSMUSG00000022707	GBE1
ENSMUSG00000024109	NRXN1
ENSMUSG00000040264	GBP2B
ENSMUSG00000095304	PLAC9A
ENSMUSG00000023845	LNPEP
ENSMUSG00000042613	PBXIP1
ENSMUSG00000027398	IL1B
ENSMUSG00000072620	SLFN2
ENSMUSG00000037280	GALNT6
ENSMUSG00000019929	DCN
ENSMUSG00000025481	URAH
ENSMUSG00000027340	SLC23A2
ENSMUSG00000020407	UPP1
ENSMUSG00000042302	EHBP1
ENSMUSG00000031444	F10
ENSMUSG00000044098	RSBN1
ENSMUSG00000046805	MPEG1
ENSMUSG00000038400	PMEPA1
ENSMUSG00000003949	HLF
ENSMUSG00000029108	PCDH7
ENSMUSG00000016524	IL19
ENSMUSG00000055202	ZFP811
ENSMUSG00000062210	TNFAIP8
ENSMUSG00000028965	TNFRSF9
ENSMUSG00000106847	PEG13
ENSMUSG00000004535	TAX1BP1
ENSMUSG00000040511	PVR
ENSMUSG00000075015	GM10801
ENSMUSG00000020205	PHLDA1
ENSMUSG00000037411	SERPINE1
ENSMUSG00000051379	FLRT3
ENSMUSG00000024691	FAM111A
ENSMUSG00000028967	ERRFI1
ENSMUSG00000112023	LILR4B
ENSMUSG00000050549	FAM241A
ENSMUSG00000044117	2900011O08RIK
ENSMUSG00000027210	MEIS2
ENSMUSG00000021831	ERO1L
ENSMUSG00000022876	SAMSN1
ENSMUSG00000040026	SAA3
ENSMUSG00000052477	C130026I21RIK
ENSMUSG00000068566	MYADM
ENSMUSG00000029840	MTPN

ENSMUSG00000052727	MAP1B
ENSMUSG00000040430	PITPNC1
ENSMUSG00000031425	PLP1
ENSMUSG00000010406	MRPL52
ENSMUSG00000027580	HELZ2
ENSMUSG00000029409	U90926
ENSMUSG00000098557	KCTD12
ENSMUSG00000043670	DIRAS1
ENSMUSG00000075014	GM10800
ENSMUSG00000021701	PLK2
ENSMUSG00000015149	SIRT2
ENSMUSG00000011179	ODC1
ENSMUSG00000050092	SPRR2B
ENSMUSG00000051439	CD14
ENSMUSG00000094530	GM21399
ENSMUSG00000041754	TREM3
ENSMUSG00000020220	VPS13D
ENSMUSG00000030748	IL4RA
ENSMUSG00000089647	GM2245
ENSMUSG00000022488	NCKAP1L
ENSMUSG00000032412	ATP1B3
ENSMUSG00000016529	IL10
ENSMUSG00000042212	SPRR2D
ENSMUSG00000004267	ENO2
ENSMUSG00000038037	SOCS1
ENSMUSG00000020431	ADCY1
ENSMUSG00000020400	TNIP1
ENSMUSG00000030406	GIPR
ENSMUSG00000038587	AKAP12
ENSMUSG00000046157	TMEM229B
ENSMUSG00000049985	ANKRD55
ENSMUSG00000029379	CXCL3
ENSMUSG00000037706	CD81
ENSMUSG00000057135	SCIMP
ENSMUSG00000019943	ATP2B1
ENSMUSG00000020176	GRB10
ENSMUSG00000079597	GM5483
ENSMUSG00000040260	DAAM2
ENSMUSG00000074657	KIF5A
ENSMUSG00000029207	APBB2
ENSMUSG00000027639	SAMHD1
ENSMUSG00000056054	S100A8
ENSMUSG00000026786	APBB1IP
ENSMUSG00000028645	SLC2A1
ENSMUSG00000035356	NFKBIZ
ENSMUSG00000031955	BCAR1
ENSMUSG00000049988	LRRC25
ENSMUSG00000020868	XYLT2
ENSMUSG00000027646	SRC
ENSMUSG00000027907	S100A11
ENSMUSG00000025804	CCR1
ENSMUSG00000030717	NUPR1

ENSMUSG00000050737	PTGES
ENSMUSG00000030861	ACADSB
ENSMUSG00000056429	TGOLN1
ENSMUSG00000024539	PTPN2
ENSMUSG00000031227	MAGEE1
ENSMUSG00000032786	ALAS1
ENSMUSG00000031596	SLC7A2
ENSMUSG00000020023	TMCC3
ENSMUSG00000037820	TGM2
ENSMUSG00000027737	SLC7A11
ENSMUSG00000005533	IGF1R
ENSMUSG00000031155	PIM2
ENSMUSG00000109297	GM31522
ENSMUSG00000021367	EDN1
ENSMUSG00000104268	GM37750
ENSMUSG00000006818	SOD2
ENSMUSG00000052837	JUNB
ENSMUSG00000078763	SLFN1
ENSMUSG00000003863	PPFIA3
ENSMUSG00000008475	ARPC5
ENSMUSG00000004558	NDRG2
ENSMUSG00000008658	RBFOX1
ENSMUSG00000046223	PLAUR
ENSMUSG00000050953	GJA1
ENSMUSG00000035385	CCL2
ENSMUSG00000018102	HIST1H2BC
ENSMUSG00000023951	VEGFA
ENSMUSG00000011008	MCOLN2
ENSMUSG00000034300	FAM53C
ENSMUSG00000027878	NOTCH2
ENSMUSG00000019726	LYST
ENSMUSG00000030249	ABCC9
ENSMUSG00000028268	GBP3
ENSMUSG00000020641	RSAD2
ENSMUSG00000037887	DUSP8
ENSMUSG00000026773	PFKFB3
ENSMUSG00000038412	HIGD1A
ENSMUSG00000026875	TRAF1
ENSMUSG00000030718	PPME1
ENSMUSG00000047884	KLK9
ENSMUSG00000018217	PMP22
ENSMUSG00000045551	FPR1
ENSMUSG00000018927	CCL6
ENSMUSG00000025907	RB1CC1
ENSMUSG00000021457	SYK
ENSMUSG00000045763	BASP1
ENSMUSG00000005087	CD44
ENSMUSG00000053175	BCL3
ENSMUSG00000059588	CALCRL
ENSMUSG00000007872	ID3
ENSMUSG00000036099	VEZT
ENSMUSG00000042622	MAFF

ENSMUSG00000029249	REST
ENSMUSG00000039323	IGFBP2
ENSMUSG00000026185	IGFBP5
ENSMUSG00000027598	ITCH

Appendix 2 Signature 2 genes list

ID	Symbol
ENSMUSG00000064373	SELENOP
ENSMUSG00000027293	EHD4
ENSMUSG00000020377	LTC4S
ENSMUSG00000056305	USP39
ENSMUSG00000040234	TM7SF3
ENSMUSG00000047260	EMC6
ENSMUSG00000029177	CENPA
ENSMUSG00000066724	GM10175
ENSMUSG00000028972	CAR6
ENSMUSG00000021266	WARS
ENSMUSG00000028633	CTPS
ENSMUSG00000036781	RPS27L
ENSMUSG00000037966	NINJ1
ENSMUSG00000011148	ADSSL1
ENSMUSG00000086290	SNHG12
ENSMUSG00000015176	NOLC1
ENSMUSG00000080242	GM15487
ENSMUSG00000029763	EXOC4
ENSMUSG00000019689	FMC1
ENSMUSG00000025580	EIF4A3
ENSMUSG00000039680	MRPS6
ENSMUSG00000028066	PMF1
ENSMUSG00000043510	HSCB
ENSMUSG00000020307	CDC34
ENSMUSG00000057497	FAM136A
ENSMUSG00000032715	TRIB3
ENSMUSG00000032875	ARHGEF17
ENSMUSG00000024925	RNASEH2C
ENSMUSG00000022033	PBK
ENSMUSG00000081604	GM11518
ENSMUSG00000038845	PHB
ENSMUSG00000017716	BIRC5
ENSMUSG00000006442	SRM
ENSMUSG00000056666	RETSAT
ENSMUSG00000027698	NCEH1
ENSMUSG00000031388	NAA10
ENSMUSG00000047676	RPSA-PS10
ENSMUSG00000070713	GM10282
ENSMUSG00000054612	MGMT
ENSMUSG00000021258	CCNK
ENSMUSG00000024359	HSPA9
ENSMUSG00000022698	NAA50
ENSMUSG00000026127	IMP4

ENSMUSG00000046756	MRPS7
ENSMUSG00000058624	GDA
ENSMUSG00000054766	SET
ENSMUSG00000086841	2410006H16RIK
ENSMUSG00000026864	HSPA5
ENSMUSG00000025068	GSTO1
ENSMUSG00000033685	UCP2
ENSMUSG00000020328	NUDCD2
ENSMUSG00000026355	MCM6
ENSMUSG00000021811	DNAJC9
ENSMUSG00000019132	BC005537
ENSMUSG00000055660	METTL4
ENSMUSG00000032215	RSL24D1
ENSMUSG00000115497	AC131033.1
ENSMUSG00000102145	GM38056
ENSMUSG00000071041	IMPDH2-PS
ENSMUSG00000031730	DHODH
ENSMUSG00000003970	RPL8
ENSMUSG00000025732	MCRIP2
ENSMUSG00000026895	NDUFA8
ENSMUSG00000023505	CDCA3
ENSMUSG00000032279	IDH3A
ENSMUSG00000021474	SFXN1
ENSMUSG00000025232	HEXA
ENSMUSG00000021660	BTF3
ENSMUSG00000107383	GM4366
ENSMUSG00000032288	IMP3
ENSMUSG00000030867	PLK1
ENSMUSG00000004264	PHB2
ENSMUSG00000040658	DNPH1
ENSMUSG00000001020	S100A4
ENSMUSG00000026755	ARPC5L
ENSMUSG00000075279	MRPL23-PS1
ENSMUSG00000030007	CCT7
ENSMUSG00000042842	SERPINB6B
ENSMUSG00000055148	KLF2
ENSMUSG00000031921	TERF2
ENSMUSG00000007739	CCT4
ENSMUSG00000028560	USP1
ENSMUSG00000021967	MRPL57
ENSMUSG00000022437	SAMM50
ENSMUSG00000054428	ATPIF1
ENSMUSG00000030763	LCMT1
ENSMUSG00000006289	OSGEP
ENSMUSG00000018585	ATOX1
ENSMUSG00000101939	GM28438
ENSMUSG00000069516	LYZ2
ENSMUSG00000020741	CLUH
ENSMUSG00000023015	RACGAP1
ENSMUSG00000035443	THYN1
ENSMUSG00000034906	NCAPH
ENSMUSG00000037625	CLDN11

ENSMUSG00000002733	PLEKHA3
ENSMUSG00000039656	RXRB
ENSMUSG00000032121	TMEM218
ENSMUSG00000026939	TMEM141
ENSMUSG00000023992	TREM2
ENSMUSG00000038510	RPF2
ENSMUSG00000112099	GM8960
ENSMUSG00000035885	COX8A
ENSMUSG00000091478	GM10039
ENSMUSG00000025574	TK1
ENSMUSG00000026192	ATIC
ENSMUSG00000018446	C1QBP
ENSMUSG00000020150	GAMT
ENSMUSG00000033918	PARL
ENSMUSG00000024621	CSF1R
ENSMUSG00000026126	PTPN18
ENSMUSG00000023262	ACY1
ENSMUSG00000029802	ABCG2
ENSMUSG00000035754	WDR18
ENSMUSG00000019838	SLC16A10
ENSMUSG00000053801	GRWD1
ENSMUSG00000039001	RPS21
ENSMUSG00000020561	TWISTNB
ENSMUSG00000007029	VARS
ENSMUSG00000028010	GAR1
ENSMUSG00000036768	KIF15
ENSMUSG00000064326	SIVA1
ENSMUSG00000022474	PMM1
ENSMUSG00000061613	U2AF1
ENSMUSG00000022433	CSNK1E
ENSMUSG00000071042	RASGRP3
ENSMUSG00000036138	ACAA1A
ENSMUSG00000081992	GM13408
ENSMUSG00000021606	NDUFS6
ENSMUSG00000029836	CBX3
ENSMUSG00000027715	CCNA2
ENSMUSG00000068101	CENPM
ENSMUSG00000109324	PRMT1
ENSMUSG00000021607	MRPL36
ENSMUSG00000027330	CDC25B
ENSMUSG00000027168	PAX6
ENSMUSG00000025962	FASTKD2
ENSMUSG00000021427	SSR1
ENSMUSG00000041801	PHLDA3
ENSMUSG00000071655	UBXN1
ENSMUSG00000004996	MRI1
ENSMUSG00000020053	IGF1
ENSMUSG00000031029	EIF3F
ENSMUSG00000039105	ATP6V1G1
ENSMUSG00000038252	NCAPD2
ENSMUSG00000037805	RPL10A
ENSMUSG00000020321	MDH1

ENSMUSG00000059734	NDUFS8
ENSMUSG00000026374	TSN
ENSMUSG00000063856	GPX1
ENSMUSG00000004100	PPAN
ENSMUSG00000034424	GCSH
ENSMUSG00000041064	PIF1
ENSMUSG00000083011	GM12816
ENSMUSG00000022571	PYCRL
ENSMUSG00000028333	ANP32B
ENSMUSG00000069744	PSMB3
ENSMUSG00000036918	TTC7
ENSMUSG00000024369	NELFE
ENSMUSG00000024590	LMNB1
ENSMUSG00000031807	PGLS
ENSMUSG00000026019	WDR12
ENSMUSG00000079419	MS4A6C
ENSMUSG00000060419	RPS16-PS2
ENSMUSG00000101892	9130401M01RIK
ENSMUSG00000088252	SNORD13
ENSMUSG00000042462	DCTPP1
ENSMUSG00000021326	TRIM27
ENSMUSG00000025503	TALDO1
ENSMUSG00000066026	DHRS3
ENSMUSG00000021250	FOS
ENSMUSG00000015568	LPL
ENSMUSG00000024660	INCENP
ENSMUSG00000009647	MCU
ENSMUSG00000049932	H2AFX
ENSMUSG00000019961	TMPO
ENSMUSG00000028069	GPATCH4
ENSMUSG00000026955	SAPCD2
ENSMUSG00000041057	WDR43
ENSMUSG00000014633	CMC2
ENSMUSG00000018669	CDK5RAP3
ENSMUSG00000041881	NDUFA7
ENSMUSG00000025980	HSPD1
ENSMUSG00000057113	NPM1
ENSMUSG00000057863	RPL36
ENSMUSG00000030189	YBX3
ENSMUSG00000068744	PSRC1
ENSMUSG00000031826	USP10
ENSMUSG00000063888	RPL7L1
ENSMUSG00000040681	HMGN1
ENSMUSG00000038697	TAF5L
ENSMUSG00000021102	GLRX5
ENSMUSG00000110126	GM9347
ENSMUSG00000022673	MCM4
ENSMUSG00000108366	GM5586
ENSMUSG00000033735	SPR
ENSMUSG00000036678	AAAS
ENSMUSG00000027133	NOP10
ENSMUSG00000002395	USE1

ENSMUSG00000025742	PRPS2
ENSMUSG00000015961	ADSS
ENSMUSG00000017861	MYBL2
ENSMUSG00000075232	AMD1
ENSMUSG00000063457	RPS15
ENSMUSG00000022667	CD200R1
ENSMUSG00000034880	MRPL34
ENSMUSG00000078713	TOMM5
ENSMUSG00000029910	MAD2L1
ENSMUSG00000060377	RPL36A-PS1
ENSMUSG00000002083	BBC3
ENSMUSG00000042354	GNL3
ENSMUSG00000110841	GPX4-PS2
ENSMUSG00000040713	CREG1
ENSMUSG00000059108	IFITM6
ENSMUSG00000039660	SPOUT1
ENSMUSG00000063480	SNU13
ENSMUSG00000006315	TMEM147
ENSMUSG00000017999	DDX27
ENSMUSG00000066232	IPO7
ENSMUSG00000036371	SERBP1
ENSMUSG00000066878	GM10184
ENSMUSG00000029471	CAMKK2

Appendix 3 Signature 1 GO_bp enrichment

node	log2fold	enrichment_p_value	node_size
GO_REGULATION_OF_NITRIC_OXIDE_BIOSYNTHETIC_PROCESS	3.07584998	9.14E-09	12
GO_MODIFICATION_BY_SYMBIONT_OF_HOST_MORPHOLOGY_OR_PHYSIOLOGY	2.02962696	0.00707825	5
GO_REGULATION_OF_CELL_CELL_ADHESION	1.67836537	3.02E-07	25
GO_REGULATION_OF_LEUKOCYTE_PROLIFERATION	1.66339564	0.00023594	13
GO_RECEPTOR_INTERNALIZATION	2.70769886	2.26E-05	8
GO_REGULATION_OF_CYCLIC_NUCLEOTIDE_METABOLIC_PROCESS	2.18018664	1.18E-05	12
GO_LYMPHOCYTE_DIFFERENTIATION	1.62437048	0.00010881	15
GO_REGULATION_OF_PROTEIN_KINASE_B_SIGNALING	1.66081248	0.00212874	9
GO_POSITIVE_REGULATION_OF_VASCULATURE_DEVELOPMENT	1.97855278	4.96E-05	12
GO_REGULATION_OF_CALCIUM_ION_TRANSPORT	1.77964871	3.12E-05	15
GO_TYROSINE_PHOSPHORYLATION_OF_STAT_PROTEIN	3.50211473	0.00178234	3
GO_NEGATIVE_REGULATION_OF_INTERLEUKIN_6_PRODUCTION	2.97855278	7.97E-05	6
GO_EPITHELIAL_CELL_DEVELOPMENT	1.60636469	0.00034857	13
GO_EXOCYTOSIS	1.92964317	6.16E-10	29
GO_REGULATION_OF_CELLULAR_RESPONSE_TO_GROWTH_FACTOR_STIMULUS	1.34146754	0.00194409	13
GO_IN_UTERO_EMBRYONIC_DEVELOPMENT	1.22289109	0.00076915	18
GO_ACUTE_PHASE_RESPONSE	3.10979731	4.53E-05	6
GO_POSITIVE_REGULATION_OF_CALCIUM_ION_TRANSPORT	2.04268311	0.00030673	9
GO_PHAGOCYTOSIS	1.90658299	2.82E-06	17

GO_POSITIVE_REGULATION_OF_LEUKOCYTE_PROLIFERATION	1.74722723	0.00139635	9
GO_REGULATION_OF_PRODUCTION_OF_MOLECULAR_MEDIATOR_OF_IMMUNE_RESPONSE	2.04268311	0.00030673	9
GO_POSITIVE_REGULATION_OF_ENDOTHELIAL_CELL_MIGRATION	2.27972231	8.41E-05	9
GO_SODIUM_ION_EXPORT	3.33218973	0.00260808	3
GO_REGULATION_OF_FATTY_ACID_TRANSPORT	3.15161748	0.00017317	5
GO_REGULATION_OF_SMOOTH_MUSCLE_CELL_PROLIFERATION	2.05465575	6.22E-05	11
GO_REGULATION_OF_WOUND_HEALING	2.18018664	1.18E-05	12
GO_POSITIVE_REGULATION_OF_INFLAMMATORY_RESPONSE	2.91715223	4.97E-11	17
GO_NEGATIVE_REGULATION_OF_DEFENSE_RESPONSE	1.77667101	0.00035669	11
GO_REGULATION_OF_SMOOTH_MUSCLE_CONTRACTION	2.87275811	9.11E-06	8
GO_REGULATION_OF_CARDIAC_CONDUCTION	2.33218973	6.26E-05	9
GO_REGULATION_OF_COAGULATION	2.69475981	2.25E-07	12
GO_NEGATIVE_REGULATION_OF_NF_KAPPAB_IMPORT_INTO_NUCLEUS	3.4317254	6.08E-05	5
GO_T_CELL_ACTIVATION_INVOLVED_IN_IMMUNE_RESPONSE	2.63704431	0.00010324	7
GO_SUPEROXIDE_ANION_GENERATION	3.50211473	0.00178234	3
GO_REGULATION_OF_HEMOPOIESIS	1.9104885	3.26E-09	27
GO_MORPHOGENESIS_OF_A_BRANCHING_STRUCTURE	2.0166879	4.17E-06	15
GO_REGULATION_OF_CELL_COMMUNICATION_BY_ELECTRICAL_COUPLING	2.91715223	0.00634289	3
GO_HEART_PROCESS	1.63704431	0.00708641	7
GO_REGULATION_OF_CYTOKINE_BIOSYNTHETIC_PROCESS	2.39930393	6.07E-06	11
GO_LYMPHOCYTE_ACTIVATION	1.58896515	2.63E-06	23
GO_REGULATION_OF_INTERFERON_GAMMA_PRODUCTION	2.64413374	3.38E-07	12
GO_POSITIVE_REGULATION_OF_I_KAPPAB_KINASE_NF_KAPPAB_SIGNALING	1.2370325	0.00721639	11
GO_NEGATIVE_REGULATION_OF_HEMOPOIESIS	1.61337148	0.0045358	8
GO_PROTEIN_IMPORT_INTO_NUCLEUS_TRANSLOCATION	2.45772061	0.00539807	4
GO_MODIFICATION_OF_MORPHOLOGY_OR_PHYSIOLOGY_OF_OTHER_ORGANISM	1.99961439	0.0003852	9
GO_NEGATIVE_REGULATION_OF_VIRAL_TRANSCRIPTION	2.66922472	0.00309364	4
GO_CHRONIC_INFLAMMATORY_RESPONSE	3.91715223	9.95E-07	6
GO_GRANULOCYTE_MIGRATION	3.23265406	1.03E-10	14
GO_NEGATIVE_REGULATION_OF_VIRAL_PROCESS	2.64031203	1.13E-07	13
GO_RESPONSE_TO_CARBOHYDRATE	1.39359027	0.00482971	10
GO_RESPONSE_TO_RETINOIC_ACID	1.76740511	0.00232599	8
GO_NEGATIVE_REGULATION_OF_MAP_KINASE_ACTIVITY	2.17299113	6.57E-05	10
GO_NEGATIVE_REGULATION_OF_REACTIVE_OXYGEN_SPECIES_BIOSYNTHETIC_PROCESS	3.21671251	0.00066816	4
GO_REGULATION_OF_HOMOTYPIC_CELL_CELL_ADHESION	1.70955681	1.89E-06	21
GO_POSITIVE_REGULATION_OF_ALPHA_BETA_T_CELL_ACTIVATION	2.19468621	0.00429386	5
GO_SUBSTANTIA_NIGRA_DEVELOPMENT	2.66922472	2.78E-05	8
GO_BRANCHING_INVOLVED_IN_LABYRINTHINE_LAYER_MORPHOGENESIS	3.33218973	0.00260808	3
GO_PLASMA_MEMBRANE_ORGANIZATION	1.2982424	0.00176049	14
GO_REGULATION_OF_INTERLEUKIN_5_PRODUCTION	3.18018664	0.00363478	3
GO_REGULATION_OF_CELL_KILLING	2.06915532	0.00628917	5
GO_RESPONSE_TO_TYPE_I_INTERFERON	2.07584998	0.00274904	6
GO_REGULATION_OF_PROTEIN_BINDING	1.35236761	0.00268506	12
GO_REGULATION_OF_RESPONSE_TO_CYTOKINE_STIMULUS	2.18443611	1.76E-07	17

GO_REGULATION_OF_PLATELET_ACTIVATION	2.77964871	0.00064264	5
GO_ASTROCYTE_DIFFERENTIATION	2.64413374	0.00031673	6
GO_REGULATION_OF_SENSORY_PERCEPTION	2.66922472	0.00309364	4
GO_NEGATIVE_REGULATION_OF_TOLL_LIKE_RECEPTOR_SIGNALING_PATHWAY	2.8467629	0.00051035	5
GO_POSITIVE_REGULATION_OF_CD4_POSITIVE_ALPHA_BETA_T_CELL_ACTIVATION	2.74722723	0.0025072	4
GO_NEGATIVE_REGULATION_OF_CYTOPLASMIC_TRANSPORT	1.73128569	0.00084006	10
GO_PLATELET_DERIVED_GROWTH_FACTOR_RECEPTOR_SIGNALING_PATHWAY	2.45772061	0.00066016	6
GO_REGULATION_OF_LIPID_KINASE_ACTIVITY	2.29266137	0.00123906	6
GO_ACTIN_FILAMENT_ORGANIZATION	1.31049466	0.0049518	11
GO_REGULATION_OF_OXIDATIVE_STRESS_INDUCED_INTRINSIC_APOPTOTIC_SIGNALING_PATHWAY	2.39359027	0.00636629	4
GO_NEGATIVE_REGULATION_OF_MAPK_CASCADE	2.05041876	6.88E-07	17
GO_IMMUNE_RESPONSE_REGULATING_CELL_SURFACE_RECEPTOR_SIGNALING_PATHWAY	1.37066388	0.0001518	19
GO_CELLULAR_POTASSIUM_ION_HOMEOSTASIS	3.50211473	0.00178234	3
GO_LEUKOCYTE_CHEMOTAXIS	3.10979731	5.99E-14	20
GO_PHOSPHATIDYLINOSITOL_3_KINASE_SIGNALING	2.45772061	0.00539807	4
GO_NEGATIVE_REGULATION_OF_MUSCLE_CONTRACTION	3.41465189	1.16E-05	6
GO_POSITIVE_REGULATION_OF_OXIDOREDUCTASE_ACTIVITY	2.41465189	0.0007795	6
GO_LABYRINTHINE_LAYER_DEVELOPMENT	2.45772061	0.00066016	6
GO_REGULATION_OF_B_CELL_PROLIFERATION	2.14456273	0.00214356	6
GO_POSITIVE_REGULATION_OF_PROTEIN_AUTOPHOSPHORYLATION	2.59522414	0.00376714	4
GO_MULTI_MULTICELLULAR_ORGANISM_PROCESS	2.10979731	1.72E-07	18
GO_NEGATIVE_REGULATION_OF_PRODUCTION_OF_MOLECULAR_MEDIATOR_OF_IMMUNE_RESPONSE	2.77964871	0.00064264	5
GO_POSITIVE_REGULATION_OF_ADAPTIVE_IMMUNE_RESPONSE	2.05208181	0.00136819	7
GO_REGULATION_OF_NEUTROPHIL_MIGRATION	2.82968939	0.00200189	4
GO_REGULATION_OF_T_CELL_PROLIFERATION	1.6776863	0.00196206	9
GO_CELLULAR_RESPONSE_TO_LIPOPROTEIN_PARTICLE_STIMULUS	3.65411782	2.54E-05	5
GO_RESPONSE_TO_OXYGEN_LEVELS	1.54791842	2.64E-06	24
GO_POSITIVE_REGULATION_OF_ORGANELLE_ASSEMBLY	2.25418722	0.00143089	6
GO_VASCULAR_PROCESS_IN_CIRCULATORY_SYSTEM	2.1699183	2.43E-06	14
GO_RESPONSE_TO_DEXAMETHASONE	2.80167501	0.00016701	6
GO_LEUKOCYTE_MIGRATION	2.7349489	1.64E-21	39
GO_REGULATION_OF_MUSCLE_SYSTEM_PROCESS	1.97855278	6.88E-07	18
GO_REGULATION_OF_ENDOTHELIAL_CELL_MIGRATION	2.04268311	3.16E-05	12
GO_RESPONSE_TO_METAL_ION	1.63175001	9.39E-07	24
GO_POSITIVE_REGULATION_OF_NEUTROPHIL_MIGRATION	2.91715223	0.0015716	4
GO_POSITIVE_REGULATION_OF_CHEMOKINE_PRODUCTION	2.63704431	0.00010324	7
GO_POSITIVE_REGULATION_OF_EPITHELIAL_CELL_MIGRATION	2.31511622	6.96E-07	14
GO_ERYTHROCYTE_HOMEOSTASIS	1.89161714	0.00263574	7
GO_NEGATIVE_REGULATION_OF_BIOMINERAL_TISSUE_DEVELOPMENT	3.33218973	0.00047495	4
GO_RESPONSE_TO_TOXIC_SUBSTANCE	1.40145239	0.00038997	16
GO_NEGATIVE_REGULATION_OF_PROTEIN_CATABOLIC_PROCESS	1.57928259	0.00313884	9
GO_INTERLEUKIN_1_PRODUCTION	3.33218973	0.00047495	4
GO_NEURAL_NUCLEUS_DEVELOPMENT	2.41465189	3.91E-05	9

GO_LIPOPOLYSACCHARIDE_MEDIATED_SIGNALING_PATHWAY	3.27972231	1.75E-07	9
GO_LEUKOCYTE_MIGRATION_INVOLVED_IN_INFLAMMATORY_RESPONSE	3.69475981	0.00114196	3
GO_REGULATION_OF_BONE_REMODELING	2.59522414	0.0011946	5
GO_CELLULAR_RESPONSE_TO_ACID_CHEMICAL	1.81761656	4.25E-05	14
GO_NEGATIVE_REGULATION_OF_VIRAL_GENOME_REPLICATION	2.91715223	1.88E-06	9
GO_PARTURITION	3.33218973	0.00260808	3
GO_ADP_METABOLIC_PROCESS	2.33218973	0.00106754	6
GO_RESPONSE_TO_PROGESTERONE	2.41465189	0.0007795	6
GO_REGULATION_OF_EPITHELIAL_CELL_MIGRATION	2.10979731	1.72E-07	18
GO_CELLULAR_RESPONSE_TO_STEROID_HORMONE_STIMULUS	1.65036569	5.20E-05	16
GO_RESPONSE_TO_HEPATOCYTE_GROWTH_FACTOR	3.59522414	0.00021243	4
GO_CELLULAR_CARBOHYDRATE_CATABOLIC_PROCESS	2.45772061	0.00539807	4
GO_NEGATIVE_REGULATION_OF_EXTRINSIC_APOPTOTIC_SIGNALING_PATHWAY	1.83914972	0.0008819	9
GO_REGULATION_OF_STRESS_ACTIVATED_PROTEIN_KINASE_SIGNALING_CASCADE	1.38877326	0.00144728	13
GO_MAINTENANCE_OF_LOCATION_IN_CELL	1.96719291	0.00010924	11
GO_POSITIVE_REGULATION_OF_PROTEIN_SERINE_THREONINE_KINASE_ACTIVITY	1.67916295	8.92E-07	23
GO_POSITIVE_REGULATION_OF_STAT_CASCADE	2.81281557	1.04E-06	10
GO_NEGATIVE_REGULATION_OF_B_CELL_PROLIFERATION	2.91715223	0.00634289	3
GO_POSITIVE_REGULATION_OF_BLOOD_CIRCULATION	1.85825854	0.005901	6
GO_REGULATION_OF_CHEMOTAXIS	2.37873232	5.03E-10	21
GO_REGULATION_OF_ION_HOMEOSTASIS	1.57319783	0.00043599	13
GO_NEGATIVE_REGULATION_OF_SEQUENCE_SPECIFIC_DNA_BINDING_TRANSCRIPTION_FACTOR_ACTIVITY	1.50211473	0.00449345	9
GO_REGULATION_OF_BINDING	1.47657964	2.35E-05	21
GO_REGULATION_OF_ALPHA_BETA_T_CELL_DIFFERENTIATION	2.19468621	0.00429386	5
GO_MYELOID_CELL_ACTIVATION_INVOLVED_IN_IMMUNE_RESPONSE	2.28488401	0.0032452	5
GO_POSITIVE_REGULATION_OF_AUTOPHAGY	1.72450715	0.00508217	7
GO_CELLULAR_RESPONSE_TO_INTERLEUKIN_1	2.61947168	4.12E-07	12
GO_RESPONSE_TO_PURINE_CONTAINING_COMPOUND	2.14896791	5.71E-07	16
GO_ORGAN_OR_TISSUE_SPECIFIC_IMMUNE_RESPONSE	3.04268311	0.00487591	3
GO_REGULATION_OF_MYELOID_LEUKOCYTE_DIFFERENTIATION	2.16713048	2.97E-05	11
GO_NEGATIVE_REGULATION_OF_ERK1_AND_ERK2_CASCADE	2.88152832	6.43E-07	10
GO_CELLULAR_RESPONSE_TO_OXYGEN_LEVELS	1.64413374	0.00045916	12
GO_POSITIVE_REGULATION_OF_T_CELL_CYTOKINE_PRODUCTION	3.04268311	0.00487591	3
GO_REGULATION_OF_LEUKOCYTE_MIGRATION	2.57928259	8.49E-10	18
GO_NEGATIVE_REGULATION_OF_MYELOID_CELL_DIFFERENTIATION	2.16226473	0.00037119	8
GO_CELLULAR_RESPONSE_TO_FATTY_ACID	2.02962696	0.00707825	5
GO_REGULATION_OF_T_CELL_DIFFERENTIATION	1.74722723	0.00254273	8
GO_REGULATION_OF_CELL_JUNCTION_ASSEMBLY	1.91715223	0.00237844	7
GO_POSITIVE_REGULATION_OF_CELL_ADHESION	1.73540179	4.45E-08	27
GO_POSITIVE_REGULATION_OF_CYTOPLASMIC_TRANSPORT	1.10294364	0.00452059	15
GO_INTRACELLULAR_RECEPTOR_SIGNALING_PATHWAY	1.50211473	0.00110862	12
GO_TOLL_LIKE_RECEPTOR_SIGNALING_PATHWAY	1.70769886	0.00302342	8

GO_POSITIVE_REGULATION_OF_LIPID_TRANSPORT	2.19468621	0.00429386	5
GO_NEGATIVE_REGULATION_OF_KINASE_ACTIVITY	1.62998955	4.57E-06	21
GO_CELL_GROWTH	1.63511686	0.00082647	11
GO_REGULATION_OF_PEPTIDE_TRANSPORT	2.01903184	2.39E-08	22
GO_RESPONSE_TO_FATTY_ACID	1.81761656	0.00353708	7
GO_POSITIVE_REGULATION_OF_PROTEIN_LOCALIZATION_TO_NUCLEUS	1.56665498	0.002017	10
GO_NEGATIVE_REGULATION_OF_BINDING	1.44322104	0.00587381	9
GO_REGULATION_OF_MONOOXYGENASE_ACTIVITY	2.08065096	0.00121441	7
GO_NEGATIVE_REGULATION_OF_NEURON_DEATH	1.49088748	0.00118657	12
GO_REGULATION_OF_THE_FORCE_OF_HEART_CONTRACTION	2.33218973	0.00744313	4
GO_REGULATION_OF_CARDIAC_MUSCLE_CONTRACTION_BY_CALCIUM_ION_SIGNALING	2.45772061	0.00539807	4
GO_LENS_FIBER_CELL_DIFFERENTIATION	2.99115281	0.00030805	5
GO_NEGATIVE_REGULATION_OF_PROTEOLYSIS	1.5096484	6.61E-05	18
GO_REGULATION_OF_EPITHELIAL_CELL_PROLIFERATION	1.06629567	0.00742531	14
GO_COPPER_ION_HOMEOSTASIS	2.91715223	0.00634289	3
GO_POSITIVE_REGULATION_OF_NUCLEOCYTOPLASMIC_TRANSPORT	1.51722162	0.00419156	9
GO_CELLULAR_RESPONSE_TO_ETHANOL	3.33218973	0.00260808	3
GO_NEGATIVE_REGULATION_OF_NERVOUS_SYSTEM_DEVELOPMENT	1.13205012	0.00501485	14
GO_POSITIVE_REGULATION_OF_PROTEIN_SECRETION	1.97855278	6.88E-07	18
GO_CELLULAR_RESPONSE_TO_BIOTIC_STIMULUS	2.87275811	3.48E-19	32
GO_NEGATIVE_REGULATION_OF_CELL_DEVELOPMENT	1.21671251	0.00154679	16
GO_RESPIRATORY_BURST	3.77964871	1.53E-05	5
GO_REGULATION_OF_PROSTAGLANDIN_SECRETION	3.74722723	0.00013088	4
GO_REGULATION_OF_PHAGOCYTOSIS	2.88740489	4.59E-08	12
GO_NEGATIVE_REGULATION_OF_PROTEIN_COMPLEX_ASSEMBLY	1.59522414	0.0048978	8
GO_NEGATIVE_REGULATION_OF_CELL_ACTIVATION	2.03800663	7.31E-06	14
GO_CYTOKINE_PRODUCTION	2.19132719	4.69E-06	13
GO_REGULATION_OF_MAST_CELL_ACTIVATION	2.28488401	0.0032452	5
GO_NEGATIVE_REGULATION_OF_CELL_CELL_ADHESION	1.66081248	0.00212874	9
GO_REGULATION_OF_MUSCLE_HYPERTROPHY	2.15161748	0.00489979	5
GO_POSITIVE_REGULATION_OF_INTERFERON_GAMMA_PRODUCTION	2.14456273	0.00214356	6
GO_NECROPTOTIC_PROCESS	2.91715223	0.00039963	5
GO_POSITIVE_REGULATION_OF_MONOOXYGENASE_ACTIVITY	2.71551837	0.00079902	5
GO_REGULATION_OF_LEUKOCYTE_DIFFERENTIATION	1.93529958	2.73E-07	20
GO_REGULATION_OF_MACROPHAGE_DERIVED_FOAM_CELL_DIFFERENTIATION	2.8467629	0.00051035	5
GO_REGULATION_OF_METAL_ION_TRANSPORT	1.39689542	0.00011959	19
GO_POSITIVE_REGULATION_OF_RESPONSE_TO_EXTERNAL_STIMULUS	2.22749235	6.59E-13	31
GO_REGULATION_OF_NEURON_DEATH	1.45002622	0.00017331	17
GO_REGULATION_OF_CELL_SIZE	1.56230951	0.00046899	13
GO_ASTROCYTE_DEVELOPMENT	3.21671251	0.00066816	4
GO_NEGATIVE_REGULATION_OF_LEUKOCYTE_PROLIFERATION	2.07584998	0.00274904	6
GO_ADAPTIVE_IMMUNE_RESPONSE	1.36256338	0.00253197	12
GO_MAMMARY_GLAND_EPITHELIUM_DEVELOPMENT	2.37283171	0.00091483	6
GO_POSITIVE_REGULATION_OF_LEUKOCYTE_MIGRATION	2.68011303	2.52E-08	14
GO_ACTIVATION_OF_PROTEIN_KINASE_ACTIVITY	1.5525798	1.71E-05	20

GO_ENDODERM_DEVELOPMENT	1.82968939	0.00650537	6
GO_NEGATIVE_REGULATION_OF_NITRIC_OXIDE_METABOLIC_PROCESS	3.74722723	0.00013088	4
GO_CELLULAR_SODIUM_ION_HOMEOSTASIS	2.91715223	0.00634289	3
GO_POSITIVE_REGULATION_OF_INTERLEUKIN_13_PRODUCTION	3.50211473	0.00178234	3
GO_NEGATIVE_REGULATION_OF_PROTEIN_TYROSINE_KINASE_ACTIVITY	2.74722723	0.0025072	4
GO_REGULATION_OF_SYMBIOSIS_ENCOMPASSING_MUTUALISM_THROUGH_PARASITISM	1.79516171	8.13E-06	17
GO_REGULATION_OF_CYTOSOLIC_CALCIUM_ION_CONCENTRATION	1.95367811	7.21E-06	15
GO_POSITIVE_REGULATION_OF_PROTEIN_COMPLEX_DISASSEMBLY	2.82968939	0.00200189	4
GO_NEGATIVE_REGULATION_OF_COAGULATION	3.16226473	1.74E-06	8
GO_REGULATION_OF_CATION_TRANSMEMBRANE_TRANSPORT	1.39842343	0.00136184	13
GO_POSITIVE_REGULATION_OF_NUCLEOTIDE_METABOLIC_PROCESS	2.14776516	3.38E-05	11
GO_DEFENSE_RESPONSE_TO_VIRUS	2.25894075	1.96E-07	16
GO_RESPONSE_TO_ACID_CHEMICAL	1.68833354	4.59E-07	24
GO_NEGATIVE_REGULATION_OF_WOUND_HEALING	2.78786921	1.46E-05	8
GO_CELL_CHEMOTAXIS	2.7825027	1.61E-13	23
GO_ALPHA_BETA_T_CELL_DIFFERENTIATION	2.19468621	0.00429386	5
GO_NEGATIVE_REGULATION_OF_NUCLEOCYTOPLASMIC_TRANSPORT	2.13579252	0.00042199	8
GO_REGULATED_EXOCYTOSIS	2.39591533	1.22E-12	27
GO_ORGAN_REGENERATION	1.93987231	0.00106565	8
GO_REGULATION_OF_CHEMOKINE_PRODUCTION	2.49088748	7.12E-05	8
GO_ACTIVATION_OF_MAPKKK_ACTIVITY	3.04268311	0.00487591	3
GO_REGULATION_OF_ACTIN_FILAMENT_LENGTH	1.58325149	0.00067329	12
GO_MAMMARY_GLAND_MORPHOGENESIS	2.53864061	0.00143926	5
GO_REGULATION_OF_REACTIVE_OXYGEN_SPECIES_BIOSYNTHETIC_PROCESS	2.77419428	1.18E-07	12
GO_NEGATIVE_REGULATION_OF_RESPONSE_TO_EXTERNAL_STIMULUS	2.01411396	2.83E-09	25
GO_POSITIVE_REGULATION_OF_LYMPHOCYTE_MEDIATED_IMMUNITY	1.97855278	0.00388603	6
GO_REGULATION_OF_ENDOTHELIAL_CELL_PROLIFERATION	1.68833354	0.00328886	8
GO_REGULATION_OF_INTERLEUKIN_12_PRODUCTION	2.10979731	0.00556395	5
GO_REGULATION_OF_IMMUNOGLOBULIN_PRODUCTION	2.28488401	0.0032452	5
GO_REGULATION_OF_OSSIFICATION	1.91715223	1.94E-05	14
GO_CELLULAR_RESPONSE_TO_INTERFERON_GAMMA	2.13055587	8.50E-05	10
GO_REGULATION_OF_VASCULATURE_DEVELOPMENT	1.89035217	4.54E-07	20
GO_REGULATION_OF_TUMOR_NECROSIS_FACTOR_MEDIATED_SIGNALING_PATHWAY	2.14456273	0.00214356	6
GO_REGULATION_OF_VASOCONSTRICTION	2.91715223	7.11E-06	8
GO_NEGATIVE_REGULATION_OF_B_CELL_ACTIVATION	2.45772061	0.00539807	4
GO_NEGATIVE_REGULATION_OF_INTRINSIC_APOPTOTIC_SIGNALING_PATHWAY	1.85106304	0.00159955	8
GO_NEGATIVE_REGULATION_OF_RESPONSE_TO_CYTOKINE_STIMULUS	2.37283171	0.00091483	6
GO_POSITIVE_REGULATION_OF_P38MAPK_CASCADE	3.18018664	0.00363478	3
GO_CYTOKINE_SECRETION	2.85825854	0.00013213	6
GO_MAMMARY_GLAND_DEVELOPMENT	2.03673385	6.99E-05	11
GO_REGULATION_OF_PEPTIDASE_ACTIVITY	1.25818915	0.00041028	19

GO_POSITIVE_REGULATION_OF_PEPTIDYL_TYROSINE_PHOSPHORYLATION	1.94314744	1.58E-05	14
GO_REGULATION_OF_CELLULAR_RESPONSE_TO_INSULIN_STIMULUS	2.26507553	0.00055265	7
GO_REGULATION_OF_RECEPTOR_BIOSYNTHETIC_PROCESS	2.66922472	0.00309364	4
GO_REGULATION_OF_PODOSOME_ASSEMBLY	3.59522414	0.00021243	4
GO_NEGATIVE_REGULATION_OF_CATABOLIC_PROCESS	1.39359027	0.00093366	14
GO_RESPONSE_TO_CORTICOSTEROID	2.5837285	4.00E-13	25
GO_CELL_ACTIVATION_INVOLVED_IN_IMMUNE_RESPONSE	2.1699183	2.43E-06	14
GO_NEGATIVE_REGULATION_OF_NEURON_APOPTOTIC_PROCESS	1.41465189	0.00667628	9
GO_B_CELL_DIFFERENTIATION	2.08426222	0.00054055	8
GO_REGULATION_OF_REACTIVE_OXYGEN_SPECIES_METABOLIC_PROCESS	2.13425035	2.95E-07	17
GO_LENS_DEVELOPMENT_IN_CAMERA_TYPE_EYE	2.07584998	0.00274904	6
GO_NEGATIVE_REGULATION_OF_CATION_TRANSMEMBRANE_TRANSPORT	2.10979731	0.00243217	6
GO_NEGATIVE_REGULATION_OF_ESTABLISHMENT_OF_PROTEIN_LOCALIZATION	1.77579638	9.73E-06	17
GO_DIVALENT_INORGANIC_CATION_TRANSPORT	1.16638084	0.00552441	13
GO_MATURE_B_CELL_DIFFERENTIATION	3.01026163	0.00121011	4
GO_REGULATION_OF_INTERLEUKIN_4_PRODUCTION	2.82968939	0.00200189	4
GO_REGULATION_OF_CYSTEINE_TYPE_ENDOPEPTIDASE_ACTIVITY	1.18923178	0.00665456	12
GO_REGENERATION	1.75961095	0.00012028	13
GO_POSITIVE_REGULATION_OF_MYELOID_LEUKOCYTE_DIFFERENTIATION	2.10979731	0.00556395	5
GO_NEGATIVE_REGULATION_OF_CYTOKINE_SECRETION	3.16226473	1.74E-06	8
GO_POSITIVE_REGULATION_OF_T_CELL_MEDIATED_IMMUNITY	2.8467629	0.00051035	5
GO_TOLL_LIKE_RECEPTOR_4_SIGNALING_PATHWAY	3.4317254	6.08E-05	5
GO_NEGATIVE_REGULATION_OF_INTERLEUKIN_1_PRODUCTION	3.65411782	2.54E-05	5
GO_REGULATION_OF_OXIDATIVE_STRESS_INDUCED_CELL_DEATH	2.15161748	0.00489979	5
GO_POSITIVE_REGULATION_OF_MEMBRANE_PROTEIN_ECTODOMAIN_PROTEOLYSIS	3.21671251	0.00066816	4
GO_REGULATION_OF_PROTEIN_TARGETING	1.23532819	0.0006956	18
GO_RESPONSE_TO_INSULIN	1.4116242	0.00082593	14
GO_NEGATIVE_REGULATION_OF_TUMOR_NECROSIS_FACTOR_SUPERFAMILY_CYTOKINE_PRODUCTION	3.22909624	2.46E-07	9
GO_POSITIVE_REGULATION_OF_SEQUENCE_SPECIFIC_DNA_BINDING_TRANSCRIPTION_FACTOR_ACTIVITY	1.65588692	2.91E-05	17
GO_POSITIVE_REGULATION_OF_ENDOTHELIAL_CELL_PROLIFERATION	1.96961965	0.00192215	7
GO_POSITIVE_REGULATION_OF_LEUKOCYTE_DIFFERENTIATION	2.18534834	2.13E-06	14
GO_ESTABLISHMENT_OR_MAINTENANCE_OF_TRANSMEMBRANE_ELECTROCHEMICAL_GRADIENT	3.18018664	0.00363478	3
GO_ANTIMICROBIAL_HUMORAL_RESPONSE	2.99115281	0.00030805	5
GO_REGULATION_OF_NEUTROPHIL_CHEMOTAXIS	3.10979731	0.00091109	4
GO_PEPTIDYL_TYROSINE_MODIFICATION	1.87275811	7.49E-06	16
GO_CELLULAR_RESPONSE_TO_ALCOHOL	2.20820101	4.10E-06	13
GO_NEGATIVE_REGULATION_OF_CATION_CHANNEL_ACTIVITY	2.65411782	0.0009821	5
GO_POSITIVE_REGULATION_OF_PROTEIN_CATABOLIC_PROCESS	1.24787344	0.00062818	18
GO_REGULATION_OF_INFLAMMATORY_RESPONSE	2.32445408	1.02E-13	31

GO_REGULATION_OF_PEPTIDYL_SERINE_PHOSPHORYLATION	2.00154442	8.77E-05	11
GO_PRODUCTION_OF_MOLECULAR_MEDIATOR_INVOLVED_IN_INFLAMMATORY_RESPONSE	3.50211473	0.00178234	3
GO_POSITIVE_REGULATION_OF_PEPTIDYL_SERINE_PHOSPHORYLATION	2.35643728	2.11E-05	10
GO_POSITIVE_REGULATION_OF_MYELOID_CELL_DIFFERENTIATION	2.15633989	0.00016633	9
GO_LEUKOCYTE_CELL_CELL_ADHESION	1.96719291	4.63E-08	22
GO_B_CELL_ACTIVATION	1.6113438	0.00269734	9
GO_POSITIVE_REGULATION_OF_CYTOKINE_SECRETION	2.52483481	8.71E-07	12
GO_REGULATION_OF_TYROSINE_PHOSPHORYLATION_OF_STAT1_PROTEIN	3.18018664	0.00363478	3
GO_REGULATION_OF_TOLL_LIKE_RECEPTOR_SIGNALING_PATHWAY	2.47657964	0.00021601	7
GO_REGULATION_OF_INTERLEUKIN_1_PRODUCTION	2.63175001	3.39E-05	8
GO_REGULATION_OF_CELLULAR_RESPONSE_TO_VASCULAR_ENDOTHELIAL_GROWTH_FACTOR_STIMULUS	3.33218973	0.00260808	3
GO_MACROPHAGE_ACTIVATION	2.71551837	0.00079902	5
GO_POSITIVE_REGULATION_OF_ERK1_AND_ERK2_CASCADE	1.85825854	0.00011301	12
GO_REGULATION_OF_PEPTIDE_SECRETION	1.75795364	3.73E-05	15
GO_NEGATIVE_REGULATION_OF_INTERLEUKIN_1_BETA_PRODUCTION	3.74722723	0.00013088	4
GO_PEPTIDYL_TYROSINE_AUTOPHOSPHORYLATION	2.68011303	8.44E-05	7
GO_MODULATION_BY_SYMBIONT_OF_HOST_CELLULAR_PROCESS	2.71551837	0.00079902	5
GO_ATP_GENERATION_FROM_ADP	2.4317254	0.00203643	5
GO_REGULATION_OF_CELL_SHAPE	1.8790171	2.63E-05	14
GO_ENERGY_RESERVE_METABOLIC_PROCESS	1.82968939	0.00650537	6
GO_REGULATION_OF_RECEPTOR_MEDIATED_ENDOCYTOSIS	1.93987231	0.00106565	8
GO_RESPONSE_TO_ELECTRICAL_STIMULUS	2.96961965	2.08E-05	7
GO_POSITIVE_REGULATION_OF_LYASE_ACTIVITY	2.15161748	0.00489979	5
GO_NEGATIVE_REGULATION_OF_NF_KAPPAB_TRANSCRIPTION_FACTOR_ACTIVITY	1.91715223	0.00481647	6
GO_REGULATION_OF_ANTIGEN_RECEPTOR_MEDIATED_SIGNALING_PATHWAY	2.15161748	0.00489979	5
GO_ANGIOGENESIS	1.52156709	1.47E-05	21
GO_EMBRYO_IMPLANTATION	2.48419282	0.00171891	5
GO_RESPONSE_TO_COLD	2.19468621	0.00429386	5
GO_REGULATION_OF_INTERLEUKIN_2_PRODUCTION	2.45772061	0.00066016	6
GO_GLIAL_CELL_DEVELOPMENT	2.25418722	9.70E-05	9
GO_RESPONSE_TO_TEMPERATURE_STIMULUS	1.98823533	2.25E-05	13
GO_REGULATION_OF_CYTOKINE_PRODUCTION_INVOLVED_IN_INFLAMMATORY_RESPONSE	2.91715223	0.00634289	3
GO_MIDBRAIN_DEVELOPMENT	2.27972231	8.41E-05	9
GO_RESPONSE_TO_CORTICOSTERONE	2.99115281	0.00030805	5
GO_POSITIVE_REGULATION_OF_SMOOTH_MUSCLE_CELL_PROLIFERATION	2.30244239	0.00018594	8
GO_IRON_ION_HOMEOSTASIS	1.85825854	0.005901	6
GO_POSITIVE_REGULATION_OF_TYROSINE_PHOSPHORYLATION_OF_STAT3_PROTEIN	2.91715223	0.00010329	6
GO_MYELOID_LEUKOCYTE_MEDIATED_IMMUNITY	2.38109933	0.0023947	5
GO_MYELOID_LEUKOCYTE_ACTIVATION	2.08933321	0.00010876	10
GO_RECEPTOR_METABOLIC_PROCESS	2.23908033	4.39E-05	10
GO_CYTOPLASMIC_SEQUESTERING_OF_PROTEIN	2.02962696	0.00707825	5
GO_ACTIVATION_OF_ADENYLATE_CYCLASE_ACTIVITY	2.33218973	0.00744313	4

GO_REGULATION_OF_HETEROTYPIC_CELL_CELL_ADHESIO N	3.53864061	4.02E-05	5
GO_REGULATION_OF_CHRONIC_INFLAMMATORY_RESPONS E	3.69475981	0.00114196	3
GO_NEGATIVE_REGULATION_OF_SECRETION	2.03883079	7.72E-07	17
GO_NEGATIVE_REGULATION_OF_MEIOTIC_CELL_CYCLE	3.04268311	0.00487591	3
GO_RESPONSE_TO_FUNGUS	3.33218973	1.22E-07	9
GO_REGULATION_OF_TRANSCRIPTION_FROM_RNA_POLYM ERASE_II_PROMOTER_IN_RESPONSE_TO_HYPOXIA	2.33218973	0.00744313	4
GO_RECEPTOR_MEDIATED_ENDOCYTOSIS	1.55458215	0.00030371	14
GO_SECOND_MESSENGER_MEDIATED_SIGNALING	1.39359027	0.00482971	10
GO_POTASSIUM_ION_IMPORT	3.01026163	0.00121011	4
GO_POSITIVE_REGULATION_OF_PHAGOCYTOSIS	2.82968939	1.16E-05	8
GO_NEGATIVE_REGULATION_OF_ION_TRANSPORT	1.74722723	0.00139635	9
GO_RESPONSE_TO_AMINO_ACID	1.66081248	0.00212874	9
GO_REGULATION_OF_FEVER_GENERATION	3.33218973	0.00260808	3
GO_NEGATIVE_REGULATION_OF_I_KAPPAB_KINASE_NF_K APPAB_SIGNALING	2.59522414	4.12E-05	8
GO_NEGATIVE_REGULATION_OF_CELL_ADHESION	1.35080541	0.00183485	13
GO_NEGATIVE_REGULATION_OF_PEPTIDASE_ACTIVITY	1.65180766	0.00025555	13
GO_REGULATION_OF_LIPID_STORAGE	2.82968939	1.16E-05	8
GO_RESPONSE_TO_CALCIUM_ION	1.81281557	0.00053607	10
GO_PROTEIN_KINASE_B_SIGNALING	2.64413374	0.00031673	6
GO_REGULATION_OF_MACROPHAGE_ACTIVATION	3.01026163	0.00121011	4
GO_REGULATION_OF_OSTEOBLAST_DIFFERENTIATION	1.85825854	0.00080044	9
GO_REGULATION_OF_MEMBRANE_PROTEIN_ECTODOMAIN _PROTEOLYSIS	2.99115281	0.00030805	5
GO_REGULATION_OF_CHEMOKINE_BIOSYNTHETIC_PROCES S	3.50211473	0.00178234	3
GO_RESPONSE_TO_CAMP	2.13055587	8.50E-05	10
GO_REGULATION_OF_MEIOTIC_CELL_CYCLE	2.45772061	0.00539807	4
GO_REGULATION_OF_TYPE_2_IMMUNE_RESPONSE	2.74722723	0.0025072	4
GO_PYRUVATE_METABOLIC_PROCESS	2.04268311	0.00309584	6
GO_POSITIVE_REGULATION_OF_LEUKOCYTE_CHEMOTAXIS	2.94516661	7.40E-09	13
GO_NEGATIVE_REGULATION_OF_INTRACELLULAR_TRANSP ORT	1.72075502	0.00028077	12
GO_REGULATION_OF_TUMOR_NECROSIS_FACTOR_BIOSYN THETIC_PROCESS	3.65411782	2.54E-05	5
GO_NEGATIVE_REGULATION_OF_APOPTOTIC_SIGNALING_ PATHWAY	1.57611531	0.00015845	15
GO_REGULATION_OF_T_CELL_MEDIATED_IMMUNITY	2.10979731	0.00556395	5
GO_ACTIVATION_OF_MAPK_ACTIVITY	1.91715223	7.57E-05	12
GO_REGULATION_OF_NEURON_APOPTOTIC_PROCESS	1.32220564	0.00319005	12
GO_T_CELL_DIFFERENTIATION_INVOLVED_IN_IMMUNE_RE SPONSE	2.33218973	0.00744313	4
GO_RESPONSE_TO_TUMOR_NECROSIS_FACTOR	1.55960023	0.00011064	16
GO_REGULATION_OF_SEQUESTERING_OF_CALCIUM_ION	1.68833354	0.00328886	8
GO_KERATINOCYTE_DIFFERENTIATION	2.1699183	0.00083273	7
GO_REGULATION_OF_CALCIUM_ION_IMPORT	1.65841796	0.00653825	7
GO_MYELOID_LEUKOCYTE_DIFFERENTIATION	1.89725267	0.00065584	9
GO_REGULATION_OF_CELL_MATRIX_ADHESION	1.76740511	0.00232599	8
GO_NEGATIVE_REGULATION_OF_SIGNAL_TRANSDUCTION_ IN_ABSENCE_OF_LIGAND	2.39359027	0.00636629	4
GO_POSITIVE_REGULATION_OF_CELL_ACTIVATION	1.96295592	1.20E-08	24
GO_REGULATION_OF_ERYTHROCYTE_DIFFERENTIATION	2.45772061	0.00066016	6
GO_REGULATION_OF_ACTIN_FILAMENT_BASED_PROCESS	1.52782485	5.39E-06	23

GO_AGING	1.82600434	1.43E-07	23
GO_REGULATION_OF_NITRIC_OXIDE_SYNTHASE_ACTIVITY	2.14456273	0.00214356	6
GO_REGULATION_OF_ADAPTIVE_IMMUNE_RESPONSE	1.77964871	0.00064433	10
GO_FC_GAMMA_RECEPTOR_SIGNALING_PATHWAY	1.97855278	0.00043023	9
GO_MYELOID_CELL_DIFFERENTIATION	1.52483481	0.00037553	14
GO_REGULATION_OF_STRIATED_MUSCLE_CONTRACTION	2.01026163	0.00076759	8
GO_REGULATION_OF_CYTOKINE_SECRETION	2.68449147	2.39E-11	20
GO_REGULATION_OF_MAST_CELL_ACTIVATION_INVOLVED_IN_IMMUNE_RESPONSE	2.33218973	0.00744313	4
GO_POSITIVE_REGULATION_OF_NF_KAPPAB_TRANSCRIPTION_FACTOR_ACTIVITY	1.98823533	2.25E-05	13
GO_APOPTOTIC_SIGNALING_PATHWAY	1.55640489	6.26E-06	22
GO_REGULATION_OF_MACROPHAGE_DIFFERENTIATION	2.82968939	0.00200189	4
GO_POSITIVE_REGULATION_OF_CYTOSKELETON_ORGANIZATION	1.63704431	0.00016679	14
GO_REGULATION_OF_LIPID_TRANSPORT	2.06470942	0.00027276	9
GO_POSITIVE_REGULATION_OF_CYTOKINE_BIOSYNTHETIC_PROCESS	2.18018664	0.00188156	6
GO_SUPEROXIDE_METABOLIC_PROCESS	3.10979731	4.53E-05	6
GO_REGULATION_OF_ICOSANOID_SECRETION	3.77964871	1.53E-05	5
GO_REGULATION_OF_PROTEIN_POLYMERIZATION	1.50906749	0.00066749	13
GO_ESTABLISHMENT_OR_MAINTENANCE_OF_MONOPOLAR_CELL_POLARITY	2.91715223	0.00634289	3
GO_GLUCAN_METABOLIC_PROCESS	2.01026163	0.00347427	6
GO_EMBRYONIC_PLACENTA_DEVELOPMENT	2.28488401	3.30E-05	10
GO_FIBRINOLYSIS	3.59522414	0.00021243	4
GO_LIPID_LOCALIZATION	1.12573885	0.00696138	13
GO_REGULATION_OF_IMMUNOGLOBULIN_SECRETION	3.04268311	0.00487591	3
GO_POSITIVE_REGULATION_OF_REACTIVE_OXYGEN_SPECIES_BIOSYNTHETIC_PROCESS	2.63175001	3.39E-05	8
GO_POSITIVE_REGULATION_OF_REACTIVE_OXYGEN_SPECIES_METABOLIC_PROCESS	2.10979731	0.00021411	9
GO_REGULATION_OF_ORGANELLE_ASSEMBLY	1.42238754	0.00273257	11
GO_ENDOCRINE_PANCREAS_DEVELOPMENT	2.33218973	0.00744313	4
GO_NEGATIVE_REGULATION_OF_TRANSPORTER_ACTIVITY	1.97855278	0.00388603	6
GO_POTASSIUM_ION_HOMEOSTASIS	3.04268311	0.00487591	3
GO_NEGATIVE_REGULATION_OF_BLOOD_CIRCULATION	2.69475981	0.00025835	6
GO_POSITIVE_REGULATION_OF_ENDOCYTOSIS	2.57835032	2.53E-09	17
GO_STAT_CASCADE	2.47657964	0.00021601	7
GO_RESPONSE_TO_ORGANOPHOSPHORUS	2.10979731	8.89E-06	13
GO_GLIAL_CELL_DIFFERENTIATION	1.74722723	0.00042601	11
GO_DEFENSE_RESPONSE_TO_BACTERIUM	2.6572851	1.07E-10	19
GO_REGULATION_OF_B_CELL_ACTIVATION	1.82029069	0.00096997	9
GO_POSITIVE_REGULATION_OF_CHEMOTAXIS	2.52483481	1.31E-08	16
GO_VASCULAR_ENDOTHELIAL_GROWTH_FACTOR_RECEPTOR_SIGNALING_PATHWAY	2.73657998	4.50E-09	15
GO_RIBONUCLEOSIDE_DIPHOSPHATE_METABOLIC_PROCESS	2.10979731	0.00107449	7
GO_REGULATION_OF_PLATELET_AGGREGATION	3.04268311	0.00487591	3
GO_BROWN_FAT_CELL_DIFFERENTIATION	2.59522414	0.00376714	4
GO_POSITIVE_REGULATION_OF_INNATE_IMMUNE_RESPONSE	1.47236739	9.24E-05	18
GO_POSITIVE_REGULATION_OF_MYELOID_LEUKOCYTE_MEDIATED_IMMUNITY	3.18018664	0.00363478	3
GO_REGULATION_OF_TYROSINE_PHOSPHORYLATION_OF_STAT_PROTEIN	2.98426643	7.92E-08	11

GO_NEGATIVE_REGULATION_OF_OSSIFICATION	2.95031909	1.03E-07	11
GO_POSITIVE_REGULATION_OF_ACUTE_INFLAMMATORY_RESPONSE	2.99115281	0.00030805	5
GO_NEGATIVE_REGULATION_OF_CELLULAR_RESPONSE_TO_INSULIN_STIMULUS	2.53864061	0.00143926	5
GO_REGULATION_OF_VASCULAR_ENDOTHELIAL_GROWTH_FACTOR_RECEPTOR_SIGNALING_PATHWAY	2.97855278	7.97E-05	6
GO_REGULATION_OF_LEUKOCYTE_APOPTOTIC_PROCESS	1.91715223	0.00237844	7
GO_NEGATIVE_REGULATION_OF_INTRACELLULAR_PROTEIN_TRANSPORT	1.72732767	0.00277497	8
GO_NEGATIVE_REGULATION_OF_INTERLEUKIN_12_PRODUCTION	3.45772061	0.00032511	4
GO_REGULATION_OF_PEPTIDYL_TYROSINE_PHOSPHORYLATION	2.11919601	6.51E-09	22
GO_POSITIVE_REGULATION_OF_LYMPHOCYTE_DIFFERENTIATION	2.27972231	8.41E-05	9
GO_MATERNAL_PLACENTA_DEVELOPMENT	2.45772061	0.00539807	4
GO_NEGATIVE_REGULATION_OF_HORMONE_SECRETION	1.97855278	0.00388603	6
GO_REGULATION_OF_MYELOID_CELL_DIFFERENTIATION	2.15385249	4.74E-08	19
GO_REGULATION_OF_OXIDOREDUCTASE_ACTIVITY	1.80862777	0.00193605	8
GO_RESPONSE_TO_MINERALOCORTICOID	3.02406743	1.59E-05	7
GO_CELLULAR_RESPONSE_TO_DRUG	2.10979731	0.00107449	7
GO_RESPONSE_TO_LOW_DENSITY_LIPOPROTEIN_PARTICLE	3.53864061	4.02E-05	5
GO_FC_RECEPTOR_SIGNALING_PATHWAY	1.44033853	0.00044176	15
GO_RESPONSE_TO_NUTRIENT	1.62647507	0.00018026	14
GO_NEGATIVE_REGULATION_OF_CELL_PROJECTION_ORGANIZATION	1.35643728	0.00578651	10
GO_POSITIVE_REGULATION_OF_ION_TRANSPORT	1.37918721	0.00153713	13
GO_NEGATIVE_REGULATION_OF_CYTOKINE_PRODUCTION	2.4317254	4.75E-12	25
GO_POSITIVE_REGULATION_OF_PHOSPHATASE_ACTIVITY	2.52483481	0.00453344	4
GO_SIGNAL_RELEASE	1.56922893	0.0012076	11
GO_INACTIVATION_OF_MAPK_ACTIVITY	2.91715223	0.00010329	6
GO_NEGATIVE_REGULATION_OF_VASCULATURE_DEVELOPMENT	1.89161714	0.00263574	7
GO_REGULATION_OF_LEUKOCYTE_MEDIATED_IMMUNITY	1.95632283	1.42E-05	14
GO_REGULATION_OF_TYROSINE_PHOSPHORYLATION_OF_STAT5_PROTEIN	3.18018664	0.00363478	3
GO_REGULATION_OF_RESPONSE_TO_INTERFERON_GAMMA	2.45772061	0.00539807	4
GO_PROTEIN_AUTOPHOSPHORYLATION	1.58623535	8.89E-05	16
GO_MATERNAL_PROCESS_INVOLVED_IN_FEMALE_PREGNANCY	2.33218973	0.00041191	7
GO_KERATINIZATION	3.15161748	0.00017317	5
GO_TROPHOBLAST_GIANT_CELL_DIFFERENTIATION	3.33218973	0.00260808	3
GO_NEGATIVE_REGULATION_OF_HYDROLASE_ACTIVITY	1.09772448	0.00269454	17
GO_NEGATIVE_REGULATION_OF_INFLAMMATORY_RESPONSE	1.85106304	0.00159955	8
GO_REGULATION_OF_TRANSPORTER_ACTIVITY	1.2370325	0.00721639	11
GO_CELLULAR_COPPER_ION_HOMEOSTASIS	3.33218973	0.00260808	3
GO_REGULATION_OF_PROTEIN_TYROSINE_KINASE_ACTIVITY	1.85825854	0.005901	6
GO_REGULATION_OF_PROTEIN_IMPORT	1.77760088	1.74E-05	16
GO_POSITIVE_REGULATION_OF_SPROUTING_ANGIOGENESIS	3.04268311	0.00487591	3
GO_GLUCOSE_CATABOLIC_PROCESS	2.39359027	0.00636629	4
GO_POSITIVE_REGULATION_OF_SECRETION	1.75961095	5.64E-08	26
GO_NEGATIVE_REGULATION_OF_INTERFERON_GAMMA_PRODUCTION	2.91715223	0.00039963	5

GO_REACTIVE_OXYGEN_SPECIES_METABOLIC_PROCESS	2.39930393	6.07E-06	11
GO_LEUKOCYTE_MEDIATED_IMMUNITY	1.85825854	0.00011301	12
GO_POSITIVE_REGULATION_OF_PROTEIN_KINASE_B_SIGNALING	2.30571752	7.27E-05	9
GO_TISSUE_REMODELING	2.44584651	4.38E-06	11
GO_CHEMOKINE_MEDIATED_SIGNALING_PATHWAY	3.05917124	3.17E-06	8
GO_POSITIVE_REGULATION_OF_MONOCYTE_CHEMOTAXIS	2.91715223	0.00634289	3
GO_TRANSITION_METAL_ION_HOMEOSTASIS	1.95367811	0.00024109	10
GO_RESPONSE_TO_HEAT	1.89161714	0.00263574	7
GO_CELLULAR_RESPONSE_TO_KETONE	1.98641489	0.00085835	8
GO_NUCLEOTIDE_PHOSPHORYLATION	2.07584998	0.00274904	6
GO_REGULATION_OF_MUSCLE_CONTRACTION	2.10979731	4.03E-06	14
GO_REGULATION_OF_BLOOD_CIRCULATION	1.7548808	1.13E-06	21
GO_REGULATION_OF_EXTRINSIC_APOPTOTIC_SIGNALING_PATHWAY	1.61947168	0.00053664	12
GO_MAINTENANCE_OF_LOCATION	1.8418641	3.52E-05	14
GO_REGULATION_OF_ERK1_AND_ERK2_CASCADE	2.2118955	8.12E-10	23
GO_ACTIVATION_OF_INNATE_IMMUNE_RESPONSE	1.62091078	3.97E-05	17
GO_NEGATIVE_REGULATION_OF_MULTI_ORGANISM_PROCESS	2.30417535	5.04E-08	17
GO_RESPONSE_TO_ETHANOL	1.50211473	0.00449345	9
GO_REGULATION_OF_NUCLEOCYTOPLASMIC_TRANSPORT	1.56167158	6.69E-05	17
GO_POSITIVE_REGULATION_OF_HEMOPOIESIS	2.10979731	3.78E-07	17
GO_POSITIVE_REGULATION_OF_ALPHA_BETA_T_CELL_DIFFERENTIATION	2.53864061	0.00143926	5
GO_POSITIVE_REGULATION_OF_CELL_KILLING	2.45772061	0.00539807	4
GO_REGULATION_OF_ACTIN_CYTOSKELETON_REORGANIZATION	2.74722723	0.00020878	6
GO_REGULATION_OF_EARLY_ENDOSOME_TO_LATE_ENDOSOME_TRANSPORT	2.91715223	0.0015716	4
GO_REGULATION_OF_ORGANIC_ACID_TRANSPORT	2.68011303	8.44E-05	7
GO_REGULATION_OF_STAT_CASCADE	2.52483481	1.31E-08	16
GO_NEGATIVE_REGULATION_OF_PROTEIN_SECRETION	2.37283171	2.81E-06	12
GO_REGULATION_OF_CYTOKINE_PRODUCTION_INVOLVED_IN_IMMUNE_RESPONSE	2.18018664	0.00188156	6
GO_REGULATION_OF_PROTEIN_LOCALIZATION_TO_NUCLEUS	1.59522414	4.99E-05	17
GO_INTERACTION_WITH_HOST	1.60972371	0.0016106	10
GO_ACUTE_INFLAMMATORY_RESPONSE	2.80167501	3.88E-06	9
GO_REGULATION_OF_HORMONE_SECRETION	1.72952523	8.41E-06	18
GO_RESPONSE_TO_MECHANICAL_STIMULUS	2.09118163	9.40E-09	22
GO_CELL_REDOX_HOMEOSTASIS	2.33218973	6.26E-05	9
GO_LEUKOCYTE_DIFFERENTIATION	1.78101554	1.39E-07	24
GO_EXTRINSIC_APOPTOTIC_SIGNALING_PATHWAY	1.85825854	0.00080044	9
GO_RESPONSE_TO_LIPOPROTEIN_PARTICLE	3.25418722	2.40E-05	6
GO_NEGATIVE_REGULATION_OF_CYTOKINE_BIOSYNTHETIC_PROCESS	2.74722723	0.0025072	4
GO_CORTICAL_CYTOSKELETON_ORGANIZATION	2.23908033	0.0037433	5
GO_NEGATIVE_REGULATION_OF_GLUCOSE_TRANSPORT	3.04268311	0.00487591	3
GO_NEGATIVE_REGULATION_OF_CYSTEINE_TYPE_ENDOPEPTIDASE_ACTIVITY	1.72450715	0.00508217	7
GO_POSITIVE_REGULATION_OF_CELL_SIZE	3.04268311	0.00487591	3
GO_NEGATIVE_REGULATION_OF_IMMUNE_RESPONSE	1.5421128	0.00611741	8
GO_REGULATION_OF_RESPONSE_TO_OXIDATIVE_STRESS	1.97855278	0.00388603	6
GO_REGULATION_OF_MUSCLE_CELL_APOPTOTIC_PROCESS	2.15161748	0.00489979	5

GO_NEGATIVE_REGULATION_OF_LIPID_STORAGE	3.59522414	4.95E-06	6
GO_VASCULOGENESIS	2.1699183	0.00083273	7
GO_RESPONSE_TO_AXON_INJURY	2.25418722	0.00143089	6
GO_REGULATION_OF_GRANULOCYTE_CHEMOTAXIS	2.8467629	0.00051035	5
GO_NEGATIVE_REGULATION_OF_STAT_CASCADE	2.50211473	0.00055547	6
GO_POSITIVE_REGULATION_OF_MAP_KINASE_ACTIVITY	1.67874749	4.09E-05	16
GO_REGULATION_OF_CAMP_METABOLIC_PROCESS	2.19468621	5.76E-05	10
GO_REGULATION_OF_NUCLEOTIDE_METABOLIC_PROCESS	1.77031084	6.13E-05	14
GO_GLAND_MORPHOGENESIS	2.33218973	9.69E-06	11
GO_REGULATION_OF_P38MAPK_CASCADE	2.8467629	0.00051035	5
GO_REGULATION_OF_INTERLEUKIN_13_PRODUCTION	3.33218973	0.00260808	3
GO_MEMBRANE_REPOLARIZATION	3.18018664	0.00363478	3
GO_MYELOID_LEUKOCYTE_MIGRATION	3.05917124	3.64E-11	16
GO_NEGATIVE_REGULATION_OF_SMOOTH_MUSCLE_CONTRACTION	3.45772061	0.00032511	4
GO_CELLULAR_RESPONSE_TO_VASCULAR_ENDOTHELIAL_GROWTH_FACTOR_STIMULUS	2.48419282	0.00171891	5
GO_EXTRACELLULAR_MATRIX_DISASSEMBLY	1.91715223	0.00481647	6
GO_REGULATION_OF_CELLULAR_PROTEIN_CATABOLIC_PROCESS	0.99828899	0.00683992	16
GO_POSITIVE_REGULATION_OF_BINDING	1.53864061	0.00233113	10
GO_CELLULAR_IRON_ION_HOMEOSTASIS	2.23908033	0.0037433	5
GO_PROTEIN_SECRETION	1.85825854	0.00080044	9
GO_POSITIVE_REGULATION_OF_LEUKOCYTE_MEDIATED_IMMUNITY	2.56922893	1.81E-06	11
GO_LEUKOCYTE_DEGRANULATION	2.71551837	0.00079902	5
GO_NUCLEOSIDE_DIPHOSPHATE_METABOLIC_PROCESS	1.79376981	0.00388433	7
GO_CIRCULATORY_SYSTEM_PROCESS	1.17172506	0.00156816	17
GO_POSITIVE_REGULATION_OF_MACROPHAGE_DIFFERENTIATION	2.91715223	0.00634289	3
GO_PATTERN_RECOGNITION_RECEPTOR_SIGNALING_PATHWAY	1.79613683	0.00058814	10
GO_REGULATION_OF_INTRINSIC_APOPTOTIC_SIGNALING_PATHWAY	1.83623224	6.94E-05	13
GO_NEGATIVE_REGULATION_OF_OSTEOBLAST_DIFFERENTIATION	2.80167501	0.00016701	6
GO_POSITIVE_REGULATION_OF_RESPONSE_TO_WOUNDING	2.60972371	6.51E-11	20
GO_POSITIVE_REGULATION_OF_IMMUNE_EFFECTOR_PROCESS	2.12360311	1.62E-06	15
GO_TUBE_MORPHOGENESIS	1.17172506	0.00156816	17
GO_PLATELET_ACTIVATION	2.12360311	1.62E-06	15
GO_NEGATIVE_REGULATION_OF_PEPTIDYL_TYROSINE_PHOSPHORYLATION	2.45772061	0.00066016	6
GO_CELLULAR_RESPONSE_TO_CORTICOSTEROID_STIMULUS	2.36695515	0.00035319	7
GO_NEGATIVE_REGULATION_OF_IMMUNE_SYSTEM_PROCESS	1.77031084	1.47E-08	28
GO_REGULATION_OF_INTERLEUKIN_1_BETA_PRODUCTION	2.77031084	5.50E-05	7
GO_REGULATION_OF_LYMPHOCYTE_DIFFERENTIATION	1.74722723	0.00077003	10
GO_HEMOSTASIS	1.6159827	5.33E-06	21
GO_MONOCYTE_CHEMOTAXIS	3.33218973	1.69E-05	6
GO_REGULATION_OF_PROTEIN_KINASE_C_SIGNALING	3.04268311	0.00487591	3
GO_DIVALENT_INORGANIC_CATION_HOMEOSTASIS	1.78786921	1.27E-07	24
GO_REGULATION_OF_TRANSCRIPTION_FACTOR_IMPORT_INTO_NUCLEUS	2.25418722	6.85E-06	12
GO_REGULATION_OF_VIRAL_GENOME_REPLICATION	2.22909624	0.00011152	9

GO_REGULATION_OF_I_KAPPAB_KINASE_NF_KAPPAB_SIGNALING	1.63369828	1.25E-05	19
GO_CELLULAR_RESPONSE_TO_EXTERNAL_STIMULUS	1.59522414	6.68E-06	21
GO_CELLULAR_TRANSITION_METAL_ION_HOMEOSTASIS	2.30571752	7.27E-05	9
GO_POSITIVE_REGULATION_OF_TYPE_2_IMMUNE_RESPONSE	3.59522414	0.00021243	4
GO_DEFENSE_RESPONSE_TO_FUNGUS	3.15161748	0.00017317	5
GO_REGULATION_OF_CARDIAC_MUSCLE_CONTRACTION	2.02406743	0.00153677	7
GO_NEGATIVE_REGULATION_BY_HOST_OF_VIRAL_TRANSCRIPTION	3.18018664	0.00363478	3
GO_MONOSACCHARIDE_TRANSPORT	2.41465189	0.0007795	6
GO_POSITIVE_REGULATION_OF_RECEPTOR_MEDIATED_ENDOCYTOSIS	2.02962696	0.00707825	5
GO_POSITIVE_REGULATION_OF_TUMOR_NECROSIS_FACTOR_SUPERFAMILY_CYTOKINE_PRODUCTION	2.59522414	1.36E-05	9
GO_HUMORAL_IMMUNE_RESPONSE	2.37283171	2.81E-06	12
GO_CELLULAR_RESPONSE_TO_MECHANICAL_STIMULUS	2.43602554	1.73E-06	12
GO_RESPONSE_TO_VIRUS	2.168691	2.86E-10	25
GO_POSITIVE_REGULATION_OF_INTERLEUKIN_2_PRODUCTION	2.33218973	0.00744313	4
GO_REGULATION_OF_TUMOR_NECROSIS_FACTOR_SUPERFAMILY_CYTOKINE_PRODUCTION	2.99115281	3.36E-13	20
GO_RESPONSE_TO_VITAMIN_D	2.59522414	0.00376714	4
GO_PLACENTA_DEVELOPMENT	1.85825854	0.00011301	12
GO_MODULATION_OF_TRANSCRIPTION_IN_OTHER_ORGANISM_INVOLVED_IN_SYMBIOTIC_INTERACTION	2.66922472	0.00309364	4
GO_REGULATION_OF_LEUKOCYTE_CHEMOTAXIS	2.99115281	3.13E-10	15
GO_REGULATION_OF_HEART_CONTRACTION	1.67874749	4.09E-05	16
GO_POSITIVE_REGULATION_OF_PROTEIN_IMPORT	1.76514914	0.00127781	9
GO_REGULATION_OF_TYROSINE_PHOSPHORYLATION_OF_STAT3_PROTEIN	3.01026163	4.19E-06	8
GO_PATTERNING_OF_BLOOD_VESSELS	2.52483481	0.00453344	4
GO_REGULATION_OF_INTERLEUKIN_1_SECRETION	2.52483481	0.00453344	4
GO_CD4_POSITIVE_ALPHA_BETA_T_CELL_ACTIVATION	2.65411782	0.0009821	5
GO_POSITIVE_REGULATION_OF_CAMP_METABOLIC_PROCESS	2.50211473	2.36E-05	9
GO_REGULATION_OF_DNA_BINDING	2.08933321	0.00010876	10
GO_OSTEOCLAST_DIFFERENTIATION	2.74722723	0.00020878	6
GO_NEGATIVE_REGULATION_OF_PEPTIDYL_THREONINE_PHOSPHORYLATION	3.10979731	0.00091109	4
GO_DEFENSE_RESPONSE_TO_GRAM_NEGATIVE_BACTERIUM	3.04268311	6.06E-05	6
GO_REGULATION_OF_ENDOCYTOSIS	2.16458978	1.57E-09	23
GO_CELLULAR_RESPONSE_TO_DEXAMETHASONE_STIMULUS	2.45772061	0.00539807	4
GO_NEUROTROPHIN_SIGNALING_PATHWAY	2.52483481	0.00453344	4
GO_POSITIVE_REGULATION_OF_B_CELL_DIFFERENTIATION	2.91715223	0.00634289	3
GO_RESPONSE_TO_REACTIVE_OXYGEN_SPECIES	1.68833354	3.77E-05	16
GO_SPROUTING_ANGIOGENESIS	2.23908033	0.0037433	5
GO_SPONGIOTROPHOBLAST_LAYER_DEVELOPMENT	3.59522414	0.00021243	4
GO_RESPONSE_TO_INTERFERON_GAMMA	2.14456273	1.53E-05	12
GO_POSITIVE_REGULATION_OF_INTRINSIC_APOPTOTIC_SIGNALING_PATHWAY	2.04268311	0.00309584	6
GO_REGULATION_OF_LYMPHOCYTE_MIGRATION	2.71551837	0.00079902	5
GO_REGULATION_OF_VASCULAR_ENDOTHELIAL_GROWTH_FACTOR_PRODUCTION	3.27329604	8.97E-07	8
GO_ALPHA_BETA_T_CELL_ACTIVATION	2.25418722	0.00143089	6

GO_RESPONSE_TO_YEAST	3.33218973	0.00260808	3
GO_REGULATION_OF_PHOSPHOPROTEIN_PHOSPHATASE_ACTIVITY	1.80167501	0.00715345	6
GO_REGULATION_OF_INTERLEUKIN_6_PRODUCTION	2.33218973	3.82E-06	12
GO_NEGATIVE_REGULATION_OF_REACTIVE_OXYGEN_SPECIES_METABOLIC_PROCESS	2.78786921	1.46E-05	8
GO_RESPONSE_TO_KETONE	1.98904515	6.17E-07	18
GO_POSITIVE_REGULATION_OF_LIPID_KINASE_ACTIVITY	2.71551837	0.00079902	5
GO_REGULATION_OF_PROTEIN_AUTOPHOSPHORYLATION	2.54791842	0.00046415	6
GO_MAST_CELL_MEDIATED_IMMUNITY	2.91715223	0.00634289	3
GO_REGULATION_OF_MONOCYTE_CHEMOTAXIS	3.01026163	0.00121011	4
GO_POSITIVE_REGULATION_OF_CYCLIC_NUCLEOTIDE_METABOLIC_PROCESS	2.4317254	1.31E-05	10
GO_ENDODERM_FORMATION	2.21671251	0.00164453	6
GO_POSITIVE_REGULATION_OF_VASCULAR_ENDOTHELIAL_GROWTH_FACTOR_RECEPTOR_SIGNALING_PATHWAY	3.4317254	6.08E-05	5
GO_POSITIVE_REGULATION_OF_ACTIN_CYTOSKELETON_REORGANIZATION	3.53864061	4.02E-05	5
GO_POSITIVE_REGULATION_OF_STRESS_ACTIVATED_PROTEIN_KINASE_SIGNALING_CASCADE	1.62437048	0.00149094	10
GO_POLYSACCHARIDE_METABOLIC_PROCESS	1.8418641	0.00321398	7
GO_NECROTIC_CELL_DEATH	2.48419282	0.00171891	5
GO_BONE_REMODELING	2.39359027	0.00636629	4
GO_MYELOID_CELL_HOMEOSTASIS	1.95779421	0.00047951	9
GO_NEGATIVE_REGULATION_OF_TRANSCRIPTION_FACTOR_IMPORT_INTO_NUCLEUS	2.41465189	0.0007795	6
GO_CARBOHYDRATE_CATABOLIC_PROCESS	1.76514914	0.00127781	9
GO_LYMPHOCYTE_ACTIVATION_INVOLVED_IN_IMMUNE_RESPONSE	1.91715223	0.00118331	8
GO_RESPONSE_TO_INTERLEUKIN_1	2.43910493	2.32E-07	14
GO_REGULATION_OF_NEUROLOGICAL_SYSTEM_PROCESS	2.02962696	0.00707825	5
GO_REGULATION_OF_ACUTE_INFLAMMATORY_RESPONSE	1.94752588	0.00433286	6
GO_POSITIVE_REGULATION_OF_APOPTOTIC_SIGNALING_PATHWAY	1.53012911	0.00058094	13
GO_RESPONSE_TO_MOLECULE_OF_BACTERIAL_ORIGIN	2.82029069	8.01E-31	54
GO_NEGATIVE_REGULATION_OF_CHEMOTAXIS	2.19468621	0.00429386	5
GO_RESPONSE_TO_HYDROGEN_PEROXIDE	1.71551837	0.00091524	10
GO_POSITIVE_REGULATION_OF_VASCULAR_ENDOTHELIAL_GROWTH_FACTOR_PRODUCTION	2.91715223	0.00039963	5
GO_POSITIVE_REGULATION_OF_DNA_BINDING	2.37283171	0.00091483	6
GO_POSITIVE_REGULATION_OF_CALCIUM_MEDIATED_SIGNALING	2.4317254	0.00203643	5
GO_DEFENSE_RESPONSE_TO_GRAM_POSITIVE_BACTERIUM	2.37283171	0.00091483	6
GO_HEXOSE_CATABOLIC_PROCESS	2.02962696	0.00707825	5
GO_REGULATION_OF_LYMPHOCYTE_CHEMOTAXIS	3.33218973	0.00047495	4
GO_PLATELET_DEGRANULATION	2.93626105	2.77E-12	19
GO_NEGATIVE_REGULATION_OF_RESPONSE_TO_WOUNDING	2.21671251	2.96E-07	16
GO_RESPONSE_TO_VITAMIN	1.6159827	0.0076679	7
GO_MAST_CELL_ACTIVATION	3.01026163	0.00121011	4
GO_RESPONSE_TO_PROTOZOAN	3.59522414	4.95E-06	6
GO_INTEGRIN_MEDIATED_SIGNALING_PATHWAY	2.15161748	7.48E-05	10
GO_CELLULAR_RESPONSE_TO_ABIOTIC_STIMULUS	1.18018664	0.00273456	15
GO_BODY_FLUID_SECRETION	2.04268311	0.00309584	6
GO_NEGATIVE_REGULATION_OF_MACROPHAGE_DERIVED_FOAM_CELL_DIFFERENTIATION	3.04268311	0.00487591	3
GO_CELLULAR_CARBOHYDRATE_METABOLIC_PROCESS	1.73393041	0.00025771	12

GO_POSITIVE_REGULATION_OF_CELL_CELL_ADHESION	1.82470598	6.16E-06	17
GO_NEGATIVE_REGULATION_OF_PROTEIN_SERINE_THREONINE_KINASE_ACTIVITY	1.44466446	0.00375234	10
GO_BRANCHING_MORPHOGENESIS_OF_AN_EPITHELIAL_TUBE	1.64413374	0.0023065	9
GO_GLIOGENESIS	1.8467629	1.79E-05	15
GO_REGULATION_OF_INSULIN_RECEPTOR_SIGNALING_PATHWAY	2.45772061	0.00066016	6
GO_PEPTIDE_CROSS_LINKING	3.40257906	2.22E-06	7
GO_REGULATION_OF_NF_KAPPAB_IMPORT_INTO_NUCLEUS	3.08707723	6.31E-07	9
GO_EXTRACELLULAR_STRUCTURE_ORGANIZATION	1.45117777	4.71E-05	20
GO_INTRINSIC_APOPTOTIC_SIGNALING_PATHWAY	1.53633045	0.00089982	12

Appendix 4 Signature 2 GO_bp enrichment

node	log2fold	enrichment_p_value	node_size
GO_NUCLEAR_CHROMOSOME_SEGREGATION	2.36177962	1.58E-06	13
GO_NUCLEOSIDE_MONOPHOSPHATE_METABOLIC_PROCESS	1.95815132	0.00013302	11
GO_CELLULAR_AMINO_ACID_METABOLIC_PROCESS	1.8612093	6.56E-05	13
GO_DNA_CONFORMATION_CHANGE	2.12830519	2.08E-05	12
GO_CHROMOSOME_SEGREGATION	2.05302691	1.64E-05	13
GO_RIBOSOME_ASSEMBLY	3.70573402	2.29E-08	9
GO_SISTER_CHROMATID_COHESION	2.69078368	1.06E-05	9
GO_DNA_PACKAGING	2.38380592	5.84E-05	9
GO_ALPHA_AMINO_ACID_METABOLIC_PROCESS	2.08514761	0.00013094	10
GO_RRNA_METABOLIC_PROCESS	2.52949524	8.30E-10	19
GO_RIBONUCLEOPROTEIN_COMPLEX_SUBUNIT_ORGANIZATION	2.16235062	3.71E-05	11
GO_MITOTIC_SISTER_CHROMATID_SEGREGATION	2.60619834	0.00015021	7
GO_SISTER_CHROMATID_SEGREGATION	2.56382339	3.19E-07	13
GO_RIBOSOMAL_LARGE_SUBUNIT_BIOGENESIS	3.21388092	4.20E-05	6